The Impact of Preeclampsia on Fetal Nutrition and Offspring Metabolism and Cardiovascular Function

Sol Olivera

BSc (Hons), MRes

Thesis submitted in fulfilment of the requirements for the degree of Doctor of Philosophy (PhD)

School of Cardiovascular and Metabolic Health
College of Medical, Veterinary and Life Sciences
University of Glasgow

November 2024

Abstract

The incidence of pregnancy complications, including preeclampsia (PE), is increasing nowadays. PE is one of the main causes of maternal and fetal morbidity and mortality worldwide. PE can also affect the later-life health of both mother and baby by increasing the risk for the development of CVD, although the mechanisms for this remain unknown.

The development of an insulin-resistant state is a normal adaptation during late pregnancy which leads to increased adipose tissue lipolysis and presents a source of both short chain saturated fatty acids as an energy source and long-chain polyunsaturated fatty acids (LC-PUFAs) as a key nutrient for the fetus. LC-PUFAs are essential for fetal neural development and their supply depends on the delivery from the mother through the placenta. Mothers with PE have exacerbated levels of insulin resistance that lead to increased maternal adipose tissue lipolysis leading to maternal excess of plasma non-esterified fatty acids (NEFAs) and triglycerides (TGs) as well as reduced maternal and fetal levels of LC-PUFAs. There is preliminary evidence for ectopic fat accumulation in the PE placenta which may affect LC-PUFA transport to the baby, although the presence of placental lipid droplets is yet to be confirmed. Reduced LC-PUFA transport may also impact the cardiovascular development of the offspring and, consequently, increase the risk of later-life CVD. Therefore, it was hypothesised that PE impairs essential fatty acid transfer by the placenta to the growing fetus thereby limiting cardiac and vascular development in the offspring.

Firstly, this thesis aimed to investigate the cardiovascular impact on the offspring of pregnancies complicated by PE in a rat model of superimposed PE. Pregnant stroke-prone spontaneously hypertensive rats (SHRSP) were implanted with osmotic minipumps for the continuous delivery of 0.9 % saline (vehicle control) or 700 ng/kg/min angiotensin II (ANGII). Wistar Kyoto (WKY) rats were also implanted with vehicle minipumps and used as a normotensive control. Fetal growth restriction (FGR) was observed in the ANGII neonates which were significantly smaller than the SHRSP vehicle control neonates (birth weight: 5.11 ± 0.05 vs 6.00 ± 0.12 g; mean ± SEM, $P<0.001$). Phenotyping of the offspring by echocardiography and tail-cuff plethysmography between week 5 and 17 of age showed that ANGII-exposed offspring present a worsened cardiovascular phenotype compared to

controls, but without an impact on their systolic blood pressure. Fractional shortening (FS) was significantly lower in the ANGII offspring compared to vehicle controls (ANGII: 48.51 ± 0.97 ± Control: 52.12 ± 0.95; mean ± SEM, P<0.001). Relative wall thickness (RWT) was also smaller in the ANGII offspring compared to vehicle controls (ANGII: 0.51 ± 0.04 vs Control: 0.58 ± 0.03 mm; mean ± SEM, P=0.024). Lower FS and RWT in the ANGII are signs of systolic dysfunction. Additionally, the early to late mitral valve flow velocity ratio (E/A) was significantly higher in the ANGII offspring compared to SHRSP vehicle control (ANGII: 1.94 ± 0.06 vs Control: 1.53 ± 0.04; mean ± SEM, P<0.001), which is evidence of diastolic dysfunction.

A lipidomics analysis of human and rat placentas was carried out to investigate the potential lipid dysregulation in PE and to further validate the ANGII animal model. Placental samples were collected at Caesarean section from women with PE and healthy pregnancies. Placental lipids were extracted and analysed via shotgun lipidomic techniques using high-resolution mass spectrometry. Lipid droplets from PE and healthy human placental cryosections were stained with Oil red O and quantitated by image analysis. TGs and cholesteryl esters (CEs) concentrations were significantly higher in PE placentas compared to controls (TG: PE 453.6 ± 262.1 vs healthy 129.3 ± 109.4; P<0.001; CE: PE 1063 ± 1004 vs healthy 425.9 ± 432.7 nmol/g; median ±IQR, P<0.001), which is evidence of neutral lipid accumulation. PE placentas had a significantly higher lipid droplet area compared to healthy controls (5.56 ± 5.15 vs 1.94 ± 1.70 %; median ±IQR, P=0.009). Gene expression of lipid-droplet associated proteins perilipin 4 and 5 (*PLIN4* and *PLIN5*) were also significantly higher in PE compared to healthy placentas, which further corroborated the presence of ectopic fat in the PE placenta. Lipidomic analyses of placentas from ANGII-treated dams and vehicle controls did not show any differences in lipid content between groups. Therefore, the ANGII model of superimposed PE does not mimic the elevated placental lipid storage accumulation observed in human PE pregnancies.

Gene expression of placental markers of fatty acid transport, lipolysis and synthesis were examined in PE in order to obtain further insights into impaired placental lipid metabolism. PE placentas had higher expression of genes involved in *de novo* lipogenesis (*DGAT2*, *FASN* and *SREBF-1*) compared to healthy controls

which suggests that the elevated ectopic placental fat presence in PE is due to greater lipid synthesis. Elevated angiopoietin-like 4 (*Angptl4*) expression in the PE placenta was also observed, which may indicate decreased fatty acid uptake by the placenta through the inhibition of lipoprotein lipase (LPL), consequently contributing to the lower LC-PUFA status in PE. *LIPE* expression was higher in the PE placenta compared to controls, which may be a reflection of the elevated TG stored in intracellular lipid droplets. This dysregulated fatty acid homeostasis in the PE placenta may be caused by increased fatty acid supply due to severe insulin resistance in the mother.

Another condition characterised by elevated maternal insulin resistance during pregnancy, namely gestational diabetes mellitus (GDM), was used as a comparator to PE. GDM pregnancy did not demonstrate ectopic fat accumulation on the placenta. Placental neutral lipid content, *PLIN* expression and lipid droplet content were not different between healthy and GDM women, although several differences in other lipid species were identified and warrant further investigation.

Overall, the data presented in this thesis indicated that impaired placental fatty acid metabolism and storage may contribute to the pathology of PE. Despite some phenotypic similarities with PE, GDM did not have elevated ectopic fat storage in the placenta, which suggests excess fatty acids may be stored elsewhere. Due to the role of hyperlipidaemia and insulin resistance in the aetiology of PE, reducing lipid levels in the mother could potentially improve neonatal and offspring later-life outcomes. The offspring of a model of superimposed PE showed impaired cardiovascular development after ANGII intrauterine exposure, which suggests that PE offspring may benefit from long-term monitoring to ameliorate CVD risk.

Table of Contents

List of Tables

List of Figures

Publications and conference presentations

Publications

Olivera, S., Graham, D. Sex differences in preclinical models of hypertension. *J Hum Hypertens* (2022).

Olivera, S., Graham, D. Modelling pre-eclampsia and its cardiovascular effects. *Nat Rev Cardiol* (2024).

Conference presentations

S. Olivera, T. Mitchell, B. Meyer, D. Graham, D. Freeman (2023). Poster presentation: Investigation of the placental gene expression of fatty acid regulators as evidence of ectopic fat storage and essential fatty acid transport. International Federation of Placental Associations (IFPA) meeting, Rotorua (New Zealand).

S. Olivera, D. Graham, D. Freeman (2023). Oral presentation: Cardiovascular effects of in utero Angiotensin II exposure in a rat model of superimposed preeclampsia. Physiological Society meeting, Harrogate.

S. Olivera, H. Fulton, D. Freeman, D. Graham (2022). Poster presentation: Sex differences on the offspring exposed to in-utero angiotensin II in a model of superimposed preeclampsia. Early Career Cardiovascular Symposium, University of Manchester. Top scoring abstract, awarded with £250 for travel expenses.

S. Olivera, D. Freeman and D. Graham (2022). Poster presentation: Investigation of the cardiovascular impact of a model of superimposed preeclampsia on the offspring. Online poster presentation at the Glasgow Paediatric Research Day, University of Glasgow. Awarded Poster Presentation Runner-Up prize.

Acknowledgement

Firstly, I would like to thank my supervisors Dr Delyth Graham and Dr Dilys Freeman for allowing me to carry out this amazing research and for being part of my PhD journey. I am extremely grateful for all your advice, support and encouragement. I appreciate all the opportunities you have provided me with that have made me the scientist I am today. You have inspired me both in a personal and professional way. I would also like to thank our collaborators in Australia Professor Barbara Meyer and Professor Todd Mitchell for allowing me to visit your lab and for your support with the lipidomics data, and Dr Helen Barrett for allowing me to use your human placental samples. Extended thanks to Dr Celine Kelso and Dr Alan Maccarone, for all your technical help with the very temperamental mass spectrometer, and to Luke Bale for sharing your extensive lipidomics knowledge with me.

Thank you to all the SCMH technical staff that have helped me along the way, your extensive knowledge and ability is inspiring. I am also grateful to Dr Dawn Kernaghan and Dr Alan Mathers for all your help with patient recruitment and sample collection at the GRI. Special mention to all the undergraduate and postgraduate students who have helped with my research and have allowed me to mentor them, I wish you all the best in your future careers.

I owe a great part of the good times during my PhD to the Freeman lab. Zoe, the tissue collection days and our night shift would have not been possible (and as fun) without you. Jack, I am extremely grateful for your endless help and support and for always making me laugh. Max, it has been fun to have another “last” Freeman PhD student and I always enjoy sharing the rather discouraging patient recruitment process with you. Fiona, I am sad you were only part of the lab briefly during my PhD but you were always there to provide knowledge, support and a good laugh; thank you for being the best lab mum. Each and every one of you have had a major impact on me during these past 3 years and I am sure you will continue to do so in the future. Also, to the lab 535 crew, especially Tom, Elaine, Michael and Joyce, for all the good times in and out of the lab, and to Eleanor, for being my gym buddy and believing in me even when I didn’t. I would also like to acknowledge my recently acquired lab family at the University of Edinburgh,

especially Carolynn, David and Cora, who have supported me during these rather tough last few weeks of my writing process. Thank you for keeping me “sane”.

To my parents Cynthia and Washington, I would not be where I am today if it wasn’t for your constant love and encouragement. I hope you feel as proud of me as I am to be your daughter. I promise I am done with school now.

To my partner Pati, thank you for being the greatest cheerleader. I am extremely grateful for all your love and support throughout this experience. I could not have done it without you.

Finally, thank you to the BHF for investing in me and giving me the opportunity to be part of their meaningful research, and thank you to all the mothers at the PRMU who kindly donated their placentas for this study. Our research would not be possible without you.

Author's Declaration

I declare that this thesis is my own composition and has not been submitted elsewhere for any other degree, diploma or professional qualification. This document has not previously been submitted in any form to the University of Glasgow for assessment or any other purpose. The work presented in this thesis has been carried out by me except where otherwise acknowledged.

Sol Olivera
November 2024

Abbreviations

AA	Arachidonic acid
ACAT	Acyl-CoA:cholesterol acyltransferase
ACE	Angiotensin-converting-enzyme
Ach	Acetylcholine
ACSL	Fatty acyl-CoA synthetase
ADHD	Attention deficit hyperactivity disorder
ALA	α-linolenic acid
ANGII	Angiotensin II
ANOVA	Analysis of variance
Apo-AI	Apolipoprotein AI
AT1	Angiotensin receptor 1
ATGL	Adipose triglyceride lipase
AUC	Area under the curve
AWERB	Animal Welfare Ethical Review Body
AWT	Anterior wall thickness
BAT	Brown adipose tissue
BHT	Butylated hydroxytoluene
BMI	Body mass index
BSA	Bovine serum albumin
C-section	Caesarean section
Cch	Carbachol
CD68	Cluster of differentiation 68
cDNA	complementary DNA
CE	Cholesteryl ester
CETP	Cholesteryl ester transfer protein

CSF1R	Colony stimulating factor 1 receptor
CO	Cardiac output
CoA	Coenzyme A
C_T	Cycle threshold
CVD	Cardiovascular disease
DG	Diacylglycerol
DHA	Docosahexaenoic acid
DNL	*de novo* lipogenesis
DSS rat	Dahl salt-sensitive rat
DTT	Dithiothreitol
E/A	Early to late wave velocity ratio
EC_{50}	Half maximal effective concentration
EDD	End diastolic diameter
EDTA	Ethylenediaminetetraacetic acid
EF	Ejection fraction
ESD	End systolic diameter
ET	Ejection time
FA-CoA	Fatty-acyl CoA
FABP	Fatty acid binding protein
FABPpm	Plasma membrane fatty acid-binding protein
FAM	Fluorescein amidite
FAT	Fatty acid translocase
FATP	Fatty acid transport protein
FFA	Free fatty acid
FGR	Fetal growth restriction
FS	Fractional shortening

FATP	Fatty acid transport protein
GD	Gestational day
GDM	Gestational diabetes mellitus
HDL	High-density lipoprotein
HMVECn	Human neonatal microvascular endothelial cells
HR	Heart rate
HRP	Horseradish peroxidase
HSL	Hormone sensitive lipase
HUVEC	Human umbilical vein endothelial cells
ICAM-1	Intercellular adhesion molecule 1
IgG	Immunoglobulin G
IHC	Immunohistochemistry
IL-6	Interleukin 6
IQR	Interquartile range
IRK	Insulin receptor kinase
IVCT	Isovolumetric constriction time
IVRT	Isovolumetric relaxation time
KPSS	High potassium physiological salt solution
LA	Linoleic acid
LCAT	Lecithin–cholesterol acyltransferase
LC-PUFA	Long-chain polyunsaturated fatty acids
LGA	Large-for-gestational age
LDL	Low-density lipoprotein
LDLR	Low-density lipoprotein receptor
LDS	Lithium dodecyl sulfate
LNF	Lane Normalisation Factor

LPL	Lipoprotein lipase
LV	Left ventricle
LVM	Left ventricular mass
LVMI	Left ventricular mass index
MASLD	Metabolic dysfunction-associated steatotic liver disease
MFSD2a	Major facilitator superfamily domain containing 2a
MG	Monoacylglycerol
MPI	Myocardial performance index
MTBE	Methyl tert-butyl ether
MTHRF	Methylenetetrahydrofolate reductase
mTOR	Mammalian target of rapamycin
MUFA	Monounsaturated fatty acid
NA	Noradrenaline
NEFA	Non-esterified fatty acids
NICE	National Institute for Health and Care Excellence
OCT	Optimal cutting temperature
ORO	Oil red O
PAGE	Polyacrylamide gel electrophoresis
PBS	Phosphate-buffered saline
PC	Phosphatidylcholine
PC1	Principal component 1
PC2	Principal component 2
PCA	Principal component analysis
PE	Preeclampsia
PEMT	Phosphatidylethanolamine-N-methyltransferase
PhE	Phosphatidylethanolamine

PG	Phosphatidylglycerol
PI	Phosphatidylinositol
PIH	Pregnancy-induced hypertension
PKC	Protein kinase C
PP	Pre-pregnancy
PPAR	Peroxisome proliferator-activated receptor
PRMU	Princess Royal Maternity Unit
PS	Phosphatidylserine
PSS	Physiological salt solution
PWT	Posterior wall thickness
QC	Quality control
QQ plot	Quantile-quantile plot
qPCR	Quantitative polymerase chain reaction
qRT-PCR	Quantitative reverse transcription polymerase chain reaction
RA	Retinoic acid
RAAS	Renin-angiotensin-aldosterone system
RIPA	Radioimmunoprecipitation lysis buffer
RNA	Ribonucleic acid
ROS	Reactive oxygen species
RT	Reverse transcription
RUPP	Reduced uterine perfusion pressure
SA-FA	Saturated fatty acid
SAT	Subcutaneous adipose tissue
SBP	Systolic blood pressure
SD	Standard deviation
SDS	Sodium dodecyl sulfate

SDS-PAGE	Sodium dodecyl sulfate–polyacrylamide gel electrophoresis
SEM	Standard error of the mean
SGA	Small for gestational age
SHHF rat	Spontaneous hypertension and heart failure rat
SHR	Spontaneously hypertensive rats
SHRSP	Stroke-prone spontaneously hypertensive rat
SM	Sphingomyelin
SNP	Sodium nitroprusside
SOAT	Sterol *O*-acyl-transferase
SR-BI	Scavenger receptor class B type I
SRE-1	Sterol regulatory element-1
SV	Stroke volume
T2DM	Type 2 diabetes mellitus
TBS	Tris-buffered saline
TBS-T	Tris-buffered saline with Tween 20
TG	Triacylglycerol
THF	Tetrahydrofolate
TNF-α	Tumour necrosis factor alpha
VAT	Visceral adipose tissue
VCAM-1	Vascular cell adhesion protein 1
VIP	Variable importance plot
VLDL	Very low-density lipoprotein
VLDLR	Very low-density lipoprotein receptor
W1P	Week 1 of pregnancy
W3P	Week 3 of pregnancy
W5	5 weeks of age in the animal offspring study

W13	13 weeks of age in the animal offspring study
W17	17 weeks of age in the animal offspring study
W18	18 weeks of age in the animal offspring study
WAT	White adipose tissue
WKY	Wistar Kyoto

1 Introduction

1.1 Global burden of cardiovascular disease

Cardiovascular disease (CVD) is the leading cause of global mortality which has doubled since 1990 with over 500 million cases worldwide in 2019 (Roth et al., 2020). In the UK, there are over 7 million people (around 700,000 people in Scotland) living with heart disease and over 5 million people with diabetes (British Heart Foundation, 2024). Lifestyle factors affecting this increase include unhealthy diet, obesity, smoking and physical inactivity, as well as aging (Reynolds et al., 2019). Similarly, the prevalence of acquired CVD among the pregnant population is also increasing due to the rising numbers of older mothers with preexisting obesity, diabetes and hypertension (Ramlakhan et al., 2020). Hence, CVD complicates up to 4 % of the pregnancies in the world and it is the main cause of maternal death (Ramlakhan et al., 2020), however, management of these conditions is challenging due to the potential impact on the growing fetus.

1.2 Maternal cardiovascular adaptations during pregnancy

Cardiovascular and metabolic adaptations take place in the mother during pregnancy in order to supply the needs of the growing fetus and developing placenta. Pregnancy has a profound effect on the cardiovascular physiology of the mother and it is considered a cardiovascular stress test that may elucidate the susceptibility of women to later-life CVD. This adaptation to pregnancy begins after embryonic implantation into the decidua (Boeldt and Bird, 2017). The normal adaptation to pregnancy involves the increase in maternal blood volume, cardiac output, stroke volume and heart rate of up to 50 % compared to pre-pregnancy levels from as early as 6 weeks of gestation (Boeldt and Bird, 2017). This is accompanied by a decrease in systemic artery resistance achieved through pregnancy hormone-triggered vascular remodelling and vasodilation, which is the reason why blood pressure decreases or remains unchanged during healthy pregnancies despite the increase in stroke volume.

The elevated stroke volume is achieved through an increase in left ventricular mass, ventricular wall thickness and end-diastolic volume (Soma-Pillay et al.,

2016). In addition, the remodelling of the uterine spiral arteries by trophoblast invasion converts these vessels to low resistance dilated vessels to allow for the increase in perfusion towards the placenta. The vascular remodelling, alongside the drop in resistance, allows an increase of blood flow toward the uterus and the placenta. These changes in the maternal vasculature are triggered by pregnancy hormones including estrogen and progesterone, which assist the development of the placenta and help maintain the pregnancy.

Other haemodynamic changes occur during healthy pregnancies, including elevated renal blood flow and water retention (Sanghavi et al., 2014). The changes in systemic vascularity and cardiac output result in a 50 % increase in renal plasma flow and glomerular filtration rate (GFR) (Sanghavi et al., 2014). Renal vascular resistance decreases which allows the maintenance of glomerular hydrostatic pressure despite an increase in renal flow (Soma-Pillay et al., 2016). Additionally, there is an elevated minute ventilation and tidal volume during pregnancy that lead to an increase in oxygen consumption and an up to 15 % increase in the metabolic rate (Soma-Pillay et al., 2016). Oxygen arterial partial pressure is increased while carbon dioxide arterial pressure is decreased due to the elevated ventilation rate which, paired with greater red blood cell mass, favours oxygen dissociation from haemoglobin and promotes placental oxygen transfer to the fetus (Hegewald and Crapo, 2011).

Estrogen contributes to the activation of the renin-angiotensin-aldosterone system (RAAS), which increases plasma volume and maintains maternal blood pressure. This is achieved by an increase in the levels of the components of the RAAS, including renin and angiotensinogen (Irani and Xia, 2011). Angiotensin II (ANGII), one of the main components of the pathway, is normally elevated in response to low blood pressure in order to increase it, however, during normotensive pregnancies the ANGII sensitivity decreases, thereby preventing an exaggerated increase in blood pressure (Shah, 2005). This decrease in the sensitivity to RAAS-triggered blood pressure increase occurs due to the inactivation of the of the angiotensin receptor 1 (AT1) that, interestingly, takes place to a lesser extent in hypertensive disorders of pregnancy such as preeclampsia (PE) (AbdAlla et al., 2001). In addition, RAAS activation contributes to the increase in plasma volume through the action on the kidney to increase water retention (Rizi et al., 2024).

Overall, these orchestrated haemodynamic changes sustain fetal growth and placental development.

1.3 Hypertensive disorders of pregnancy

Hypertensive disorders of pregnancy, such as gestational hypertension and preeclampsia (PE), are commonly occurring high blood pressure disorders in pregnant women which increase the risk of maternal and fetal morbidity and mortality. PE is a severe manifestation of gestational hypertension that involves organ dysfunction. PE is responsible for up to 8 % of maternal complications worldwide and is characterised by the presence of one or more diagnostic features including new onset of hypertension, kidney dysfunction and/or fetal growth restriction (Brown et al., 2018). Mothers with PE can develop additional adverse conditions affecting the brain (eclampsia), the kidney (acute kidney injury) and the liver (HELLP syndrome) that require the immediate delivery of the baby, which usually leads to premature birth. In addition to being one of the major cause of maternal and perinatal mortality, it is known to be a risk factor for the development of CVD later in life in both mother and offspring. The maternal CVD risk is found to be over 10 % higher in women with early-onset PE (appearance before 34 weeks of gestation) compared to late-onset PE (appearance on or after the 34th week of gestation) (Veerbeek et al., 2015). Additionally, early-onset PE appears to be correlated with increased neonatal adverse outcomes such as FGR and preterm delivery (Rahman et al., 2024), which are known to be risk factors for adult offspring later-life CVD development.

The causes of PE are unknown, although impaired adaptation to pregnancy is believed to play a major role. Women presenting comorbidities, including chronic hypertension and obesity, are at increased risk of pregnancy complications (Paré et al., 2014), possibly due to the inability of the mother to undergo the essential adaptations to pregnancy, including placental development. Therefore, it has women with cardiometabolic dysfunctions pre-pregnancy are more prone to develop PE. Furthermore, a recent study has found that pregnancies where mothers present with comorbidities are not only correlated with an increased risk of PE but are also associated with preterm delivery and poorer neonatal outcome (Tanner et al., 2022). This evidence highlights the importance of investigating pregnancy complications in mothers with a CVD background, which is relevant as

there is an elevated number of older and obese mothers with pre-existing cardiovascular conditions with elevated prevalence of PE and deleterious impacts on the offspring.

1.3.1 Management of PE

The only definitive cure for PE is delivery of the baby and the placenta. Most drugs that are used in the non-pregnant population must be reconsidered when treating pregnant women due to their possible adverse effects in the fetus (Braunthal and Brateanu, 2019) and their altered pharmacokinetics during pregnancy (Koren and Pariente, 2018) which may affect the effectiveness of the drug. Antihypertensive medication for women with PE may be administered to manage the symptoms, however, there are no guidelines on which drugs are better to treat these women. Drugs commonly used to treat hypertension in the non-pregnant population, including angiotensin-converting-enzyme (ACE) inhibitors and angiotensin receptor blockers, have a negative impact on the fetus and therefore cannot be used for PE treatment (Smith, et al., 2022). Women at high risk of developing PE are recommended to take low-dose acetylsalicylic acid (aspirin) from mid to late pregnancy (Smith, et al., 2022), however, it is not known whether this has a positive impact on the offspring.

Magnesium sulfate is a calcium channel blocker commonly used as an anticonvulsant during eclampsia and it has shown beneficial effects on PE in humans (Coetzee et al., 1998), although limited information is available regarding the impact on the offspring. Nifedipine, also a calcium channel blocker, is one of the few oral anti-hypertensive drugs that has shown to be well tolerated in pregnant women (Firoz et al., 2014). In addition, β-adrenoreceptor blockers are commonly used for treating hypertensive disorders of pregnancy and deemed safe in pregnancy, although the effect on the fetus is unclear (Katsi et al., 2023). Labetalol is a β- and α-adrenergic receptor blocker safe to use during pregnancy which has shown to relieve hypertension and improve uteroplacental blood flow during PE (Odigboegwu et al., 2018). However, despite the alleviation of the symptoms in the mother, anti-hypertensive drugs have not demonstrated a beneficial impact on the baby and offspring outcome. In fact, certain β-blockers including labetalol may increase the risk for small for gestational age (SGA) babies and the rates of caesarean section (C-section) (Bellos et al., 2020) and may have

an additional impact on the baby as these drugs are known to cross the placenta (Lennestål and Olausson, 2009). Additionally, the use of antihypertensive medication during early pregnancy has been associated with increased risk of cardiac defects in the offspring, although it is not clear whether this effect is due to the drug or the impact of the severe hypertension (Caton et al., 2009). Therefore, current antihypertensive medication may not improve or even worsen offspring outcomes, and future studies should investigate other alternatives to improve the phenotype of both mother and baby.

1.4 The development of the placenta

Placentation begins shortly after the fertilisation of the egg, whereby the blastocyst attaches to the surface of the uterus (recently reviewed in Cindrova-Davies and Sferruzzi-Perri, 2022). The blastocyst is formed of two different cell types: the trophectoderm (single layer of cytotrophoblasts) which later develops onto the placenta and the inner cell mass which gives rise to the embryo (Maltepe and Fisher, 2015). Upon attachment to the uterine wall, the cytotrophoblasts from the trophectoderm proliferate and form syncytiotrophoblasts that penetrate the endometrial cells at around day 8 post-fertilisation (Cindrova-Davies and Sferruzzi-Perri, 2022). This leads to the transformation of the endometrium into a primitive decidua (Sandra Schlafke, 1975). The cytotrophoblast and syncytiotrophoblast cells derived from the blastocyst form the chorionic plate which covers the gestational sac that surrounds the embryo and, at day 12 post-fertilisation, start releasing pregnancy hormones to promote the development of the full placenta (West et al., 2019). Once it is fully developed, the syncytiotrophoblast layer acts as a barrier between the maternal and fetal blood with the cytotrophoblast layer underneath, which forms the placental chorionic villi (O'Brien and Wang, 2023). Importantly, the trophoblasts from the early placenta (around 10 weeks) invade the spiral arteries of the uterus that leads to artery remodelling for vasodilation, which allows an increase in placental perfusion. Placental development is completed at 12 weeks of gestation, but it continues to grow until the third trimester.

The placenta plays an essential role in the success of pregnancy, as it facilitates the delivery of oxygen and nutrients to the fetus and removes waste products. The placenta is responsible for the delivery of nutrients to the fetus, therefore it

can affect its nutritional status. The placenta presents a maximal surface area to facilitate molecule exchange and its trophoblast cells contain selective transporters for the transport of carbohydrates, lipids and amino acids which are essential for fetal growth. Humans have a hemochorial placenta that is characterised by a thin cellular barrier that separates maternal and fetal blood (Furukawa et al., 2014). The cellular placental barrier is comprised of three components: the trophoblast layer (cytotrophoblasts and syncytiotrophoblast cells), connective tissue, and the fetal vascular endothelium (Kulvietis et al., 2011). The cell layers of the trophoblast membrane form the chorionic villi that are in contact with the maternal blood and these cells have important roles in pregnancy ranging from initiating vascular remodelling to regulation of substance exchange to and from the fetal blood (Saunders, 2009). The syncytiotrophoblast barrier in particular has several functions including transport, hormone production, neutralisation of toxic compounds and interaction with the maternal immune system (Soares et al., 2018). Thus, alterations affecting trophoblast cell organisation are associated with disease states in pregnancy such as PE (Kaufmann et al., 2003).

The development of the placenta is an essential adaptation to pregnancy and shallow transformation of the spiral arteries may lead to pregnancy complications, such as PE and fetal growth restriction (FGR). Insufficient spiral artery remodelling is associated with the development of PE (Khong et al., 1986) which leads to placental hypoxia during the first weeks of gestation. Placental ischemia and hypoxia lead to placental and systemic endothelial dysfunction due to the release of antiangiogenic and inflammatory factors caused by the oxidative stress (reviewed in Ramlakhan et al., 2020). Endothelial dysfunction is responsible for the development of the symptoms of PE, including hypertension, kidney and liver malfunction, which are predisposing factors for the reduced uteroplacental blood flow during pregnancy and, consequently, FGR. In addition, the alteration of the RAAS may also partly explain reduced uteroplacental blood flow in PE. Pregnancies complicated by PE are characterised by an elevated ANGII reactivity (Irani and Xia, 2011) as well as high expression levels of the AT1 receptor together with elevated presence of the agonist AT1 autoantibodies (Herse et al., 2007). Altogether, this abnormal response to pregnancy may culminate in elevated maternal blood pressure and reduced placental perfusion.

1.5 Metabolic adaptations to pregnancy: adipose tissue, lipids and insulin resistance

1.5.1 Adipose tissue function and lipid metabolism

Adipose tissue is not only a fat storage depot, but it serves a wide variety of metabolic functions in both pregnant and non-pregnant individuals through the secretion of adipokines and cytokines. Adipose tissue is able to "respond" to the environment by secreting adipokines that regulate inflammation and insulin sensitivity, which promotes fat storage when elevated and lipolysis (fatty acid release) when decreased. This is particularly relevant during pregnancy as the maternal environment adapts the sensitivity to insulin, and therefore fatty acid turnover in adipose tissue, in order to regulate fat storage/release according to the needs of the baby.

The two main adipose tissue depots in humans are subcutaneous adipose tissue (SAT) and visceral adipose tissue (VAT). SAT is the main fat storage depot whereas VAT storage is associated with cardiometabolic disease. In fact, waist-to-hip ratio (a marker of visceral fat accumulation) is a stronger predictor of metabolic alterations including T2DM and CVD compared to BMI (Coutinho et al., 2011; Bray et al., 2008). VAT fat comprises up to 20 % total body fat weight in men and up to 10 % in women, and this difference in fat distribution is believed to be one of the main causes of higher cardiometabolic risk in men (Guglielmi and Sbraccia, 2018). Additionally, individuals with elevated visceral fat content e.g. South Asians are at elevated risk of developing T2DM at a lower BMI compared to Caucasians (Sattar and Freeman, 2012). However, a causative role of visceral fat accumulation and cardiometabolic disease remains to be determined and increasing literature is reporting the important role of insulin resistance, adipose tissue plasticity and ectopic fat accumulation, as important predictors of cardiometabolic health.

Excess fatty acids are generally stored in SAT, however, the storage capacity of this depot depends on the number of adipocytes and the ability to generate newly mature adipocytes, known as adipogenesis. The process of the healthy physiological fat storage mechanism in adipose tissue by adipogenesis is known as hyperplasia. Generally, SAT adipocytes have a greater capacity for adipogenesis compared to VAT adipocytes (Tchkonia et al., 2005), however, certain individuals

(from different ethnicities, genders, etc) have a limited capacity for adipogenesis. If adipogenesis is limited, subcutaneous adipocytes expand, forming hypertrophic adipocytes which are insulin resistant. In addition, hypertrophic adipocytes exhibit inflammation due to immune cell infiltration which further contributes to their insulin resistant status. Overspill of the excess fatty acids from hypertrophic adipocytes or as a consequence of the failure of adipocyte to undergo hyperplasia leads to their accumulation in ectopic sites including the liver, which contributes to the development of systemic insulin resistance (Krahmer et al., 2013). Sex differences in CVD incidence may partly be explained by the impact of sex steroids on adipogenesis where oestrogen promotes preadipocyte differentiation whereas testosterone impairs adipogenesis (Guglielmi and Sbraccia, 2018). South Asians have a limited adipose tissue plasticity which is believed to play an important role in the development of T2DM in this population (McLaren et al., 2024). Moreover, studies investigating the impact of omentectomy (procedure that removes part of the VAT) in obese individuals have reported a lack of improvement in insulin sensitivity and hyperlipidaemia (Karastergiou and Fried, 2013). Thus, it appears that ectopic fat accumulation in the liver, rather than fat storage in VAT, is responsible for the insulin resistance status during obesity (Fabbrini et al., 2009). This association is evident in patients with lipodystrophy (diseases involving the partial or total lack of adipose tissue) who develop severe insulin resistance due to the accumulation of hepatic lipids despite the lack of VAT (Perry et al., 2014). Hence, in individuals without lipodystrophy, an impairment of adipogenesis and consequent ectopic fat accumulation contributes to cardiometabolic risk. There is evidence that ectopic fat deposition, particularly in the liver and pancreas, contributes to the development of T2DM due to the inability of insulin to inhibit glucose production in the liver (hepatic insulin resistance) alongside the impairment of pancreatic ß-cells in the islets of Langerhans. Interestingly, a calorie restricted diet is able to normalise ß-cell function and increase hepatic insulin sensitivity by reducing fat storage in these organs (Lim et al., 2011), which further provides evidence for the link between ectopic fat accumulation and insulin resistance.

1.5.2 Insulin resistance

Changes in adipose tissue, lipid homeostasis and insulin resistance are an essential metabolic adaptation in healthy pregnancy. The main maternal metabolic

adaptation during pregnancy is the increase in insulin sensitivity during early gestation followed by an increase in insulin resistance as the pregnancy progresses. Insulin sensitivity is elevated during early pregnancy in order to store lipids in adipose tissue (anabolic state) through elevated lipogenesis to sustain the high demand of the fetus and the pregnancy itself. Elevated activity of adipose tissue lipoprotein lipase (LPL) allows for the incorporation of circulating lipids into this depot. Adipose tissue expansion during pregnancy occurs by both adipocyte hyperplasia and hypertrophy. This remodelling results from a crosstalk between adipose tissue and inflammatory cytokines, extracellular matrix and angiogenic factors (Resi et al., 2012). Proinflammatory cytokine recruitment by the maternal adipose tissue also contributes to the development of the insulin resistant state for later gestation.

During the late stages of the pregnancy, there is a development of an insulin resistant state. This phenotype is similar to the development of an insulin resistant state in non-pregnant individuals with T2DM, leading to elevated lipolysis and ectopic fat accumulation. The late pregnancy period is characterised by a decrease in peripheral insulin sensitivity by more than 50 % and an increase in insulin release which is over 3-fold higher at 36 weeks of gestation compared to the early gestational period (Catalano et al., 1991). The responsible mechanism triggering insulin resistance during pregnancy is the release of placental hormones, thereby implicating this organ in the metabolic state of the mother during pregnancy. Insulin resistance promotes the breakdown of the maternal fat stores (catabolic state) as insulin is unable to suppress lipolysis, which elevates circulating lipids that further contribute to the peripheral insulin resistance (Sivan and Boden, 2003). Thus, maternal adiposity is increased until mid-late pregnancy and decreases after this point due to the elevated lipid mobilisation from these stores. Under this state, hormone sensitive lipase (HSL) activity is elevated to increase adipose tissue lipolysis, while LPL function is decreased (Laitinen, 2021). Consequently, plasma TG concentrations increase up to four times and plasma cholesterol increase up to 50 % in the last trimester of pregnancy compared to pre-pregnancy levels (Lau, 2020). Plasma free fatty acids (FFAs) are directed to the maternal liver where they are esterified and released into the circulation as very low-density lipoproteins (VLDL)-TG. The TG in VLDL is hydrolysed by the

placental LPL and transported to the fetus as non-esterified fatty acids (NEFAs) (Figure 1-1).

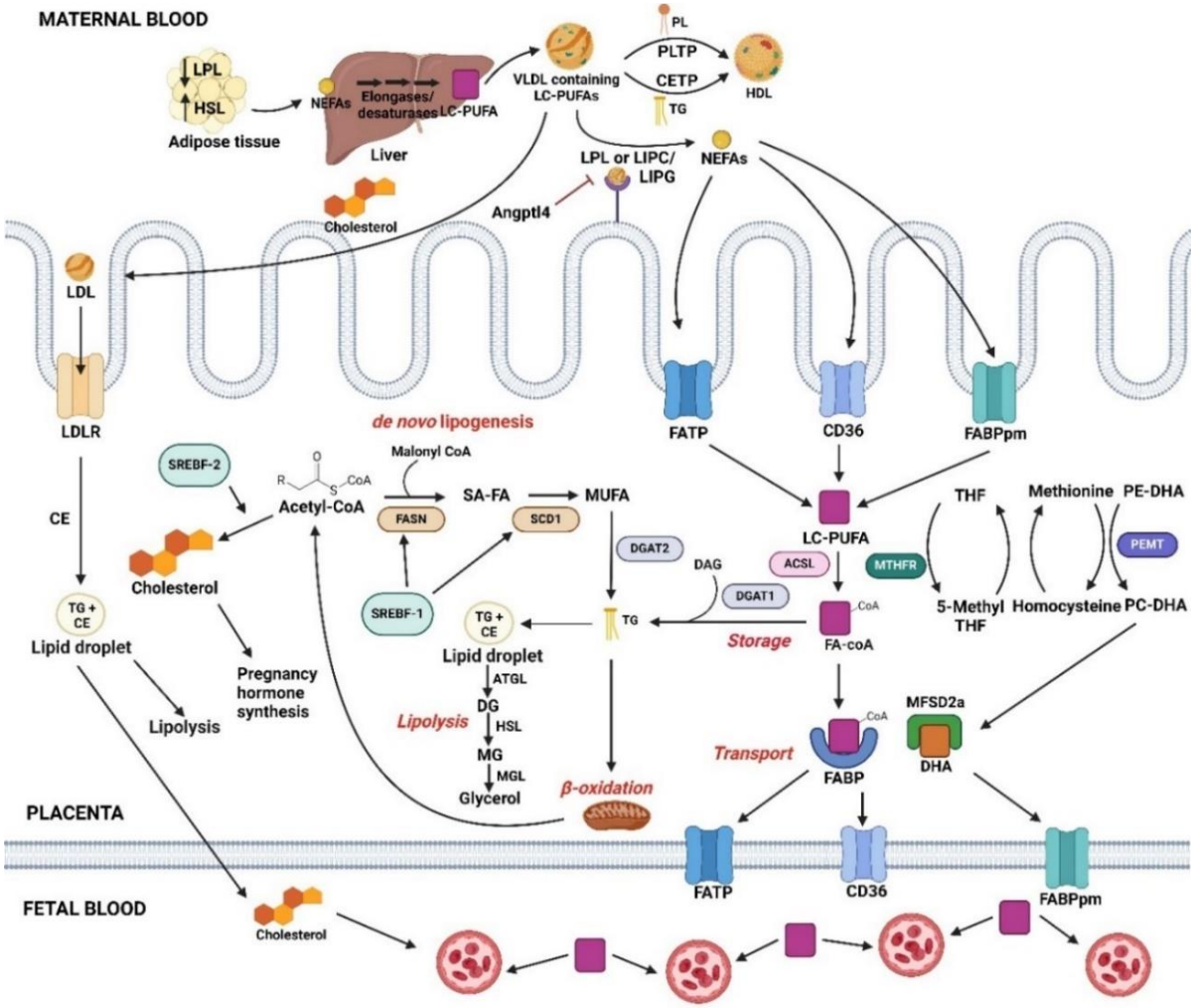

Figure 1-1. Lipid metabolism and transport in the healthy placenta. NEFAs are released into the maternal circulation through lipolysis of fat stores in the adipose tissue. Essential fatty acids are converted into LC PUFAs through a series of steps involving elongases (ELOVL2/5) and desaturases (FASD1/2) in the liver. LC-PUFAs are released to the maternal circulation in VLDL, which transfers PLs and TGs to HDL via PLTP and CETP, respectively, and is converted to LDL via shrinkage due to lipolysis of core lipids. LDL is transported into the placenta by LDLR and CE is stored in lipid droplets as a storage for the baby and the placenta. TGs from VLDL are released by LPL, LIPG or LIPE and hydrolysed to NEFAs. Angptl4 suppresses TG release from VLDL by inhibiting LPL. NEFAs (including LC-PUFAs) can cross the placenta via fatty acid transporters FATPs, FABPpm and FATPs and enter different pathways. A coenzyme A (CoA) is added to a fatty acid by ACSL to form a fatty acyl CoA (FA-CoA) molecule which can be esterified and stored in lipid droplets or transported to the baby. TGs contained within lipid droplets are hydrolysed and NEFAs and glycerol are released by several lipases (ATGL, HSL and MGL). New lipids, including cholesterol, SA-FAs and MUFAs are synthesised via cholesterol synthesis and *de novo* lipogenesis and stored or used for lipid signalling or energy production via β-oxidation of the SA-FA. While PC synthesis by PEMT is important for the transport of DHA in the liver, we hypothesise that a similar mechanism may take place in the placenta to allow the transport of DHA to the baby via the specific transporter MFSD2a. ACSL: Acyl-CoA Synthetase Long Chain; Angptl4: angiopoietin like 4; ATGL: adipose triglyceride lipase; CD36: fatty acid translocase; CE: cholesteryl ester; CETP: cholesteryl ester transfer protein; DGAT1/2: diacylglycerol O-acyltransferase 1/2; DG: diacylglycerol; DHA: docosahexaenoic acid; FA: fatty acid: FABP: fatty acid binding protein; FABPpm: plasma membrane-associated fatty acid-binding protein; FASN: fatty acid synthase; FATP: fatty acid transport protein; HSL: hormone sensitive lipase; LC-PUFA: long chain polyunsaturated fatty acid; LDL: low-density lipoprotein; LDLR: low-density lipoprotein receptor; LPL: lipoprotein lipase; MFSD2a: Major facilitator superfamily domain-containing protein 2; MG: monoacylglycerol MGL: monoglyceride lipase MUFA: monounsaturated fatty acid; NEFA: non-esterified fatty acid; PC: phosphatidylcholine; PE: phosphatidylethanolamine; PL: phospholipid; PLTP: phospholipid transfer protein; SA-FA: saturated fatty acids; SCD1: stearoyl-CoA desaturase 1; SREBF-1/2: sterol regulatory element binding transcription factor 1/2; TG: triglyceride; THF: tetrahydrofolate; VLDL: very low-density lipoprotein. Figure created with Biorender.com.

This insulin resistant state also promotes hepatic glucose production which, alongside fatty acids, act as fuel for the growing fetus. The increase in glucose production by the liver occurs in parallel with the decline in the maternal blood glucose levels (explained by the elevated utilisation) as well as an increase in insulin (Lain and Catalano, 2007). Maternal sensitivity of the ß-cells in the islets of Langerhans in the pancreas to glucose increases during the late gestational stages (stimulated by prolactin and placental lactogen), thereby promoting insulin secretion to manage the elevated glucose production (Clark et al., 1992). The lack of suppression of hepatic gluconeogenesis by insulin is evidence of the insulin resistant state during late pregnancy (Lau, 2020). In addition, the maternal skeletal muscle utilises less glucose in order to allow for fetal transport (Resi et al., 2012). This healthy adaptation of the maternal insulin sensitivity returns to normal after the delivery of the baby.

In contrast to healthy pregnancies, PE is characterised by exhacerbated insulin resistance, dyslipidaemia and potentially ectopic fat accumulation in humans. Elevated levels of TGs, total cholesterol, LDL and low levels of HDL have been associated with PE pregnancies (Stadler et al., 2023). It has been hypothesised that women with PE may have an innate insulin resistance that becomes higher than normal during pregnancy, potentially due to the hormones released by the abnormal placenta (Trivett et al., 2021). Maternal adipocytes during PE are resistant to lipolysis inhibition by insulin (Huda et al., 2014). This causes a dysregulation of fatty acid metabolism in pregnant women with PE which leads to elevated plasma TGs and NEFAs compared to women with healthy pregnancies (MacKay et al., 2012), which can contribute to vascular dysfunction and insulin resistance.

Furthermore, there is evidence of a heightened inflammatory status during PE pregnancies which may further contribute to the systemic insulin resistance. Maternal systemic inflammation is part of healthy pregnancy but it is exaggerated in PE which contributes to endothelial dysfunction. Freeman et al. (2004) have found that the release of proinflammatory markers (including interleukin 6 (IL-6)) is elevated in PE which may potentiate other phenotypes including insulin resistance and endothelial dysfunction. VAT adipocytes from women with PE have shown higher macrophage infiltration and release of proinflammatory cytokines

(Huda et al., 2014) which may contribute to the systemic insulin resistance. In addition, there is evidence of elevated macrophage activation in PE placentas compared to controls (Hayashi et al., 2002), however, cytokine release does not differ (Benyo et al., 2001). Thus, this exacerbated maternal inflammation may originate from the inflammatory response to the impaired placentation and placental function, although causality is yet to be confirmed. Interestingly, this proinflammatory profile is retained in women with previous PE after 20 years post pregnancy (Freeman et al., 2004), which may contribute to the long-term consequences of PE.

1.5.3 Lipoprotein metabolism during pregnancy

Due to increased supply of fatty acids to the liver resulting from increased lipolysis during pregnancy, there is an increase of VLDL production and VLDL-TG release from the maternal liver which is promoted by oestrogen (Herrera, 2002). The elevated maternal VLDL pool is also attributed to the decreased utilisation by the mother by decreased activity of hepatic LPL (Alvarez et al., 1996). TGs also accumulate in other higher-density lipoproteins during pregnancy, including high-density lipoprotein (HDL) and low-density lipoprotein (LDL), which normally contain low TG content. This is due to an increase in cholesteryl ester transfer protein (CETP) activity (Alvarez et al., 1996) which transfers TGs from VLDL to LDL and HDL. Increase in TG-rich LDL leads to elevated small dense LDL formation. In addition, both HDL and LDL levels are increased during the pregnant state. Due to the elevated lipid levels in PE, there is an increase in the concentration of small dense LDL which is more prone to oxidation and may contribute further to vascular endothelial dysfunction (Sattar et al., 1998). Oestrogen drives the formation of HDL by increasing the hepatic apolipoprotein AI (apo-AI) levels which facilitate lecithin–cholesterol acyltransferase (LCAT) expression for HDL synthesis (Alvarez et al., 1996). The TG content of these TG-rich lipoproteins is available to the fetus via lipoprotein receptors present in the trophoblast cells of the placenta (Figure 1-1).

1.6 Lipid droplets

Lipid droplets are lipid-containing cellular organelles that store neutral lipids and are found in almost all cell types. Excess lipids in the body are stored in lipid

droplets, forming an important energy reservoir. Lipid droplets are mainly accumulated in adipose tissue, however, energy imbalances and limited adipose tissue storage capacity can lead to the accumulation of ectopic lipid droplets in other organs and cause lipotoxicity.

1.6.1 Lipid droplets in white adipose tissue

Adipose tissue mainly stores fat in the form of TG. TGs are stored in cytosolic lipid droplets in adipose tissue that are formed by a neutral-lipid core (cholesteryl esters (CEs) and TGs) surrounded by a phospholipid monolayer. Unlike other cell types which contain several small lipid droplets (up to 5 μm), adipocytes in white adipose tissue (WAT) comprise one large lipid droplet of up to 100 μm in size (Krahmer et al., 2013). CEs are formed by a molecule of cholesterol bound to a fatty acid chain which is synthesised by acyl-CoA:cholesterol acyltransferase (ACAT) or sterol *O*-acyl-transferase (SOAT) enzymes. TGs are synthesised using fatty acids derived from different sources, including the esterification from circulating FFAs and *de novo* lipogenesis (DNL) from carbohydrates. Circulating FFAs are incorporated into a molecule of glycerol to form monoacylglycerols (MG), which are then converted to diacylglycerols (DGs) and triglycerides (TGs) by the addition of one or two FFAs, respectively. Esterification of TGs from DGs occurs through the action of diacylglycerol acyltransferases (DGAT1 and DGAT2). DNL-derived TGs are synthesised from acetyl-CoA sourced from carbohydrates, amino acids and other carbon sources (Figure 1-1). DNL mainly takes place in the liver and it is tightly regulated by insulin as it promotes the clearance of excess carbohydrates as fatty acids which are esterified into TGs and secreted in VLDL or stored in lipid droplets. DNL also takes place in adipocytes, although it only accounts for a small proportion of the adipose tissue TG content as most FFAs in TG are obtained from circulating TG in lipoproteins. Fatty acid uptake by the adipocytes takes place by the action of LPL, which hydrolyses the TG core in the lipoprotein and releases FFAs and glycerol which enter the cell. LPL is also upregulated by insulin, which facilitates the clearance of circulating TGs.

Lipid droplets are surrounded by peripheral associated proteins that regulate lipid release and storage in the droplet. Lipid droplets expand to accommodate the excess of fatty acids in the environment and degrade when lipid mobilisation is needed. Fatty acid release from the TG and CE core in the lipid droplet occurs via

lipolysis or lipid droplet degradation by autophagy, which has recently been summarised in (Mathiowetz and Olzmann, 2024). Lipolysis is mediated by lipases that interact with the proteins within the lipid droplet monolayer, including perilipin proteins (PLINs). In adipose tissue, sequential reactions by adipose triglyceride lipase (ATGL), hormone sensitive lipase (HSL) and monoacylglycerol lipase (MAG) convert TGs into DGs and MGs, respectively, releasing FFAs and glycerol from the lipid droplets. HSL hydrolases CEs to release cholesterol and a FFA. The process of lipolysis is regulated by hormones including adrenaline, which promotes lipolysis, and insulin, which inhibits lipolysis, in order to respond to specific needs.

1.6.2 Ectopic fat storage in lipid droplets

Dysregulated accumulation and impaired lipid storage in lipid droplets can have an impact on health and disease in the non-pregnant population, including obesity, lipodystrophy, fatty liver disease and cardiovascular disease among others, recently summarised in Zadoorian et al., (2023). As mentioned previously, excess lipid accumulation and lipid droplet formation is associated with metabolic disease. Accumulation of lipid droplets in ectopic sites due to limited adipose tissue storage capacity is associated with lipotoxicity and insulin resistance (Krahmer et al., 2013). This can contribute to the development of metabolic complications such as T2DM as lipid droplet accumulation in the pancreas can interfere with its endocrine function leading to hyperglycaemia and ß-cell dysfunction. Elevated lipid droplet content in the liver, known as metabolic dysfunction-associated steatotic liver disease (MASLD), interferes with signalling pathways and leads to hepatic insulin resistance (Seebacher et al., 2020). In contrast, some authors believe that MASLD is a consequence, rather than a cause, of adipose tissue dysfunction, inflammation and insulin resistance which leads to exacerbated lipolysis and ectopic fat accumulation (Parker, 2018). In this instance, insulin is unable to suppress hepatic glucose production but continues to stimulate DNL, which is known as selective insulin resistance (Brown and Goldstein, 2008). This condition leads to both hyperglycaemia and hypertriglyceridemia, which further contributes to the accumulation of hepatic lipid droplets.

Additionally, ectopic fat storage may be associated with pregnancy complications such as PE. The increased adipose tissue lipolysis may lead to the accumulation of ectopic fat in non-adipose tissue organs, comparable to the pathology of T2DM in non-pregnant individuals. There is preliminary evidence of elevated placental neutral lipid content in the PE placenta compared to healthy controls (Brown et al., 2016), which may indicate the presence of ectopic fat storage which further contributes to the insulin resistant state, although this remains to be confirmed. Similar to non-pregnant individuals, the accumulation of fat in non-adipose tissue depots can increase tissue-specific insulin resistance and further contribute to the pathology of PE. Patients with PE are characterised by spiral artery atheroma caused by the accumulation of lipid droplet containing macrophages (foam cells), thereby causing necrosis and vessel lesion (Sattar and Greer, 1999). This may also contribute to the vascular injury observed in PE.

1.7 Long chain polyunsaturated fatty acids and their importance in pregnancy

Lipids play an important role in the development of the fetus during pregnancy. In particular, long-chain polyunsaturated fatty acids (LC-PUFAs) are essential for the human fetal brain and retina development. LC-PUFAs are 18-20 carbon chain fatty acids that contain two or more double bonds. The fetus is able to synthesise LC-PUFAs from essential fatty acids but this production is suboptimal for its demand and therefore there is a high dependency for placental transfer from the mother. LC-PUFAs have shown to be important in normal fetal development as enzyme and membrane precursors and have been correlated with pregnancy outcomes (Al et al., 2000). Furthermore, specific LC-PUFAs including arachidonic acid (AA) and docosahexaenoic acid (DHA) are important in neurodevelopment especially during brain tissue synthesis (Al et al., 2000). Inadequate supply of these essential fatty acids during pregnancy have a long-term impact including increased incidence of mental disorders such as attention deficit hyperactivity disorder (ADHD) and depression (Horrocks and Yeo, 1999). Early pregnancy is a crucial stage for the accumulation of essential LC-PUFAs where essential fatty acid dietary consumption plays an important role in maternal storage.

The mother synthesises LC-PUFAs, including AA (20:4 n-6) and DHA (22:6 n-3), from the unsaturated fatty acid precursors α-linolenic acid (ALA, 18:3 n-3) and

linoleic acid (LA, 18:2 n-6) obtained from diet sources (Figure 1-2). DHA and AA are synthesised by the mother in the liver (and adipose tissue to a lesser degree) via Δ5 and Δ6 desaturase and very long chain fatty acid elongase enzymes that convert dietary unsaturated fatty acids to LC-PUFAs. Therefore, maternal dietary intake of the essential fatty acids AA and ALA is crucial for fetal growth and their deficiency can lead to fetal underdevelopment (Heath and Klevebro, 2022) which usually occurs in babies born prematurely. This is supported by cohort studies looking at the impact of essential LC-PUFA intake in pregnant women on the offspring's development. Hibbeln et al. (2007) reported that the children born from mothers who consumed low seafood quantities (main source of LC-PUFAs) during the third trimester presented substandard behavioural and cognitive abilities compared to children born from mothers with high seafood intake. Additionally, high maternal intake of fish and seafood has been associated with a reduced risk of congenic heart disease in the offspring (Obermann-Borst et al., 2011). These studies suggest the importance of LC-PUFA in the maternal diet and propose that impaired lipid profile present in mothers from early pregnancy is a determinant factor in the delivery of essential fatty acids and, consequently, fetal development. Interestingly, omega-3 fatty acid supplementation during pregnancy has shown to reduce the incidence of preterm birth (Middleton et al., 2018) although the impact on fetal outcome is conflicting. Some studies have also reported that omega-3 PUFA supplementation does not affect maternal lipid pools (Colombo et al., 2004) and it is associated with reduced fetal weight and growth (Oken et al., 2004), suggesting null or negative effects of the elevated LC-PUFA intake. Additionally, there is insufficient evidence on the benefits of LC-PUFA on improving neonatal neurodevelopmental outcomes and studies do not provide consistent results (De Giuseppe et al., 2014). The reason behind this inconclusive evidence may be the baseline maternal omega-3 fatty acid pool and maternal lipid homeostasis, as well as the lack of agreement on dosage and best period for supplementation during gestation.

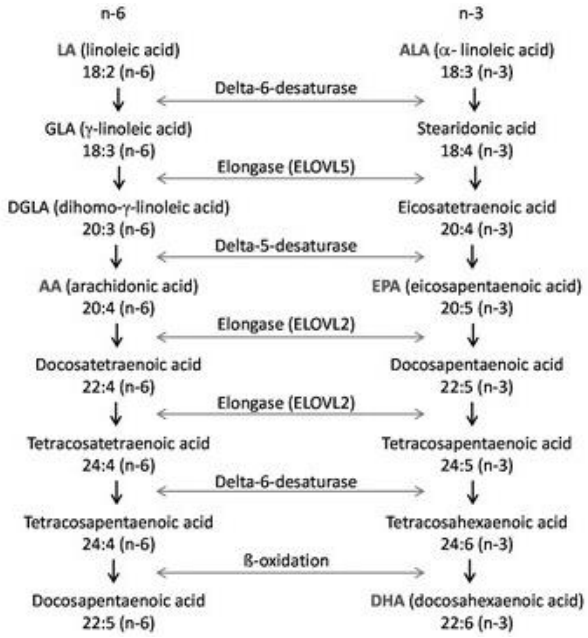

Figure 1-2. Synthesis of LC-PUFAs in humans. Diagram shows the biosynthesis of the essential LC-PUFAs from dietary n-6 and n-3 fatty acids. Figure was adapted from Marventano et al. (2015).

There is a high accretion of AA and DHA in the developing fetal brain which results from the preferential placental transport of these fatty acids from the maternal circulation. This causes an elevated accumulation of LC-PUFAs and a lower concentration of non-essential fatty acids in the fetus compared to the mother, which favours neurological development. Therefore, placental function is important for the delivery of LC-PUFAs, and pregnancy complications affecting the health of the placenta, such as PE, may impede their delivery.

Interestingly, MacKay et al. (2012) have shown indirect evidence of ectopic liver fat as reduced LC-PUFA synthesis. The elevated state of insulin resistance in PE that leads to elevated maternal plasma NEFAs and TGs may cause ectopic lipid droplet storage in the placenta, analogous to what occurs in MASLD. In MASLD, the liver uptakes circulating fatty acids released by the increased lipolysis as a consequence of insulin resistance, leading to ectopic fat accumulation in this organ (Gaggini et al., 2013). In addition, it has been suggested that there is a reduction in the synthesis of hepatic LC-PUFAs during MASLD due to the impaired action of fatty acid desaturases (Videla et al., 2004). MacKay et al. (2012) have found lower maternal adipose tissue expression of fatty acid desaturases in PE pregnancies, which suggests an analogous mechanism to MASLD which may contribute to the low LC-PUFA status in both mother and baby.

Additionally, cholesterol is also essential for pregnancy and fetal development due to its important role as a building block for pregnancy hormones as well as a component of cellular membranes and signalling pathways (Woollett, 2011). The source of cholesterol for the baby is endogenous (fetal synthesis) or exogenous (transported from the mother), and both sources have shown to be important. Exogenous cholesterol is particularly important during the first weeks of pregnancy when most organs are being formed (Kallol and Albrecht, 2020).

1.8 Placental lipid transfer

The human placenta is responsible for the transport of maternal fatty acids to the fetus through selective uptake and delivery on both fetal and maternal sites. Impaired placentation may affect the expression of placental fatty acid transport proteins necessary for nutrient delivery, although this has not been extensively investigated and the results are ambiguous. Placental transfer of LC-PUFAs occurs as both NEFAs and fatty acids released from lipoprotein TGs. The transport of LC-PUFAs involves the uptake and transport by specialised placental proteins that favour the delivery of LC-PUFA fatty acids to the baby over other non-essential fatty acids (Haggarty, 2004). LC-PUFA uptake by the placenta is carried out by specific membrane-associated fatty acid transporters including the placental plasma membrane fatty acid-binding protein (FABPpm), fatty acid transport protein (FATP) and fatty acid translocase (FAT/*CD36*) (Duttaroy and Basak, 2022) (Figure 1-1). These fatty acids are transported within the cytoplasm of the placental villi by fatty acid binding proteins (FABPs) and delivered into the fetal circulation by the above-mentioned transport proteins.

Additionally, the DHA transporter major facilitator superfamily domain containing 2A (MFSD2a) is believed to play an important role in the placental delivery of DHA to the fetus (Prieto-Sánchez et al., 2017). It has been suggested that DHA levels may be correlated with folate plasma concentration status in humans and animals (Umhau et al., 2006), which may also take place in the placenta (Figure 1-1). The mechanism of action that relates plasma folate and DHA levels may rely on the provision of methyl groups from folate needed for the conversion between phosphatidylethanolamine (PE) and phosphatidylcholine (PC) in the liver, which is a critical step in the release of DHA (Umhau et al., 2006). This is supported by animal studies whereby mice deficient in phosphatidylethanolamine-N-

methyltransferase (*PEMT*) expression, which is involved in PC biosynthesis, are also deficient in plasma DHA concentrations (Watkins et al., 2003). Another gene involved in the conversion of folate to 5-methyl tetrahydrofolate (THF), which is the methyl donor in the intermediate reaction above that allows the PE to PC conversion, known as methylenetetrahydrofolate reductase (*MTHRF*), may also play an important role in DHA mobilisation, although this has not been confirmed.

Once the fatty acids enter the cellular cytoplasm of the placental villi, fatty acyl-CoA synthetases (ACSLs) can link coenzyme A (CoA) to the fatty acid which fixes it into the cell by stopping their efflux (Duttaroy and Basak, 2020). The resulting fatty-acyl CoA (FA-CoA) acts as a substrate and/or intermediate for other intracellular processes including esterification and storage in lipid droplets (Figure 1-1). Lipid droplet storage of NEFAs within the placenta prevents lipotoxicity and provides a reservoir of lipids for the fetus. Interestingly, some authors have hypothesised that DHA may evade the coenzyme A (CoA) thioester formation to avoid storage and favour transport (Tobin et al., 2009), although this requires further study.

The delivery of maternal cholesterol to the fetus is also carried out by the placenta. Cholesterol can be transferred through the placenta by selective transport proteins. Cholesterol uptake by the placenta from HDL, LDL and VLDL takes place via specific lipoprotein receptors, including the scavenger receptor class B type I (SR-BI), the LDLR and the VLDLR, respectively. Once in the trophoblast layer of the placenta, the cholesteryl esters inside the lipoproteins can be stored in lipid droplets and hydrolysed into free cholesterol for transport to the baby (Figure 1-2). Cholesterol efflux to the fetal endothelium occurs through the membrane proteins SR-BI and ATP-binding cassette transporters ABCA1 and ABCG1. Notably, the specific contribution of these placental cholesterol transporters to cholesterol metabolism and fetal transport remains unknown (Kallol and Albrecht, 2020).

1.8.1 Impact of PE on LC-PUFA transport

Nutrient transfer may be affected in PE due to the deleterious effect on the placenta, which may impact the offspring's health long-term. Offspring from PE pregnancies have been shown to have lower levels of LC-PUFAs compared to

healthy pregnancies (Kulkarni et al., 2010; MacKay et al. 2012). Interestingly, PE is associated with an increased risk of neurodevelopmental disorders in the offspring (Koulouraki et al., 2023) which may be due to the low LC-PUFA supply during pregnancy.

PE pregnancies are characterised by significantly lower essential fatty acid levels in maternal serum, placenta and umbilical cord (Kulkarni et al., 2010). In addition, it has been shown that the adipose tissue of mothers with PE have lower expression of Δ5- and Δ6-desaturase and very long chain fatty acid elongase (*ELOVL2*) (MacKay et al., 2012), which are needed for the synthesis of LC-PUFAs from maternal dietary LA and ALA (Figure 1-1). Therefore, it is unclear whether low maternal levels, impaired placental transport, or both, are responsible for the deficiency in the offspring. Some studies have reported that omega-3 fatty acid supplementation has beneficial effects on late-onset PE and not on early-onset PE in rat models of PE (Kasture et al., 2020) but, interestingly, the data on humans is mainly negative (Burchakov et al., 2017). Therefore, the lipid profile of mother and baby is an important determinant of later-life disease but understanding essential fatty acid transport across the placenta may also be relevant to devising approaches to mitigate adverse pregnancies.

1.9 Fetal lipid metabolism

Fatty acid synthesis in the fetus begins around 10 weeks of gestation when the levels of TGs and insulin start increasing (Dunlop and Court, 1978). Despite this, the majority of fatty acids are derived from the mother until 6 months of gestation (Desoye and Herrera, 2021). At this point, the fetus becomes less dependent on the transfer of non-essential fatty acids from the mother and, instead, TGs are derived from the fetal *de novo* lipogenesis (Dancis et al., 1973). Transported maternal NEFAs through the placenta are incorporated in the fetal liver or adipose tissue for esterification into TGs and released to the fetal circulation in lipoproteins (mainly VLDL). The TG core can be released into extrahepatic tissues by the action of LPL, which is abundant in the fetal adipose tissue (Desoye and Herrera, 2021). Additionally, there is a high esterification of fatty acids in rat fetal adipose tissue compared to adults which diminishes the levels of circulating NEFAs that inhibit lipogenesis (Nikawa et al., 1979), thereby favouring elevated rates of fatty acid synthesis necessary for growth.

Fetal fat accumulation during development occurs in WAT and brown adipose tissue (BAT). Similar to adults, fetal WAT is involved in energy storage, metabolism and homeostasis. In contrast, BAT is important maintaining the body's temperature by thermogenesis. The human fetus has the ability to generate *de novo* fatty acids from glucose that accumulate as TG in adipose tissue. Fetal adipogenesis begins during the second trimester in order to store these TGs (Ailhaud et al., 1992). There is a rapid accumulation of fat in the fetus during the last stages of pregnancy mainly in SAT depots, at which point the progenitor and adipocyte populations are established for later postnatal development (Scheidl et al., 2023). Interestingly, fetal adiposity is associated with children adiposity which, in conditions of high fat accretion *in utero*, can contribute to childhood obesity (Gluckman et al., 2008).

1.10 Cardiovascular development in the fetus

The heart is the first organ to form during embryonic development which starts as a primitive heart tube formed with cardiac progenitor cells prior to the development of a heart segmented into four chambers (Buckingham et al., 2005). This is in parallel with the formation of the coronary vasculature which ensures the delivery of nutrients to the developing heart (Patterson and Zhang, 2010). Cardiac progenitor cells proliferate rapidly during the early stages of cardiogenesis but, in contrast, they become differentiated cardiomyocytes unable to propagate during later stages of gestation. Importantly, cardiac development occurs under hypoxic conditions which are needed for heart growth and cardiomyocyte differentiation, however, conditions of chronic hypoxia e.g. caused by abnormal placentation can be detrimental and cause impaired cardiogenesis (Patterson and Zhang, 2010).

Gas exchange occurs via the placenta, whereby oxygenated blood reaches the fetal organs, preferentially heart and brain, via the fetal vascular system. After birth, the neonatal cardiovascular system becomes independent from the mother and therefore functionally different from the fetal circulation. Glycolysis of glucose and lactate substrates is the main energy source for the developing fetal heart (mainly due to the relatively low oxygen environment), whereas fatty acid β-oxidation is the main energy source in adults. The switch from glycolysis to fatty acid oxidation is needed to meet the energy demands of the differentiating

cardiomyocytes in the developing heart (Chung et al., 2007) because fatty acid oxidation generates a higher ATP yield. As oxygen is needed for fatty acid oxidation, hypoxic *in utero* environments e.g. PE or FGR pregnancies may affect this transition and consequently full cardiac development. Interestingly, it has been suggested that offspring born preterm have an immature cardiovascular system which may impair the transition from fetal to neonatal heart (Tan and Lewandowski, 2020), thereby affecting long-term cardiovascular health.

LC-PUFAs play an important role in the development of the fetal heart. For instance, AA is an important component of cardiomyocytes and it regulates the expression of growth factors needed for the fetal cardiovascular development (Collins et al., 2020). There is evidence for the association between low maternal seafood intake and the increased risk of congenital heart defects in the offspring (Obermann-Borst et al., 2011), perhaps linking low maternal LC-PUFA status with poor cardiac development in the fetus. In addition, FGR has been associated with impaired offspring cardiac remodelling which was independent of birthweight and ameliorated with a high PUFA dietary intake (Rodriguez-Lopez et al., 2016). LC-PUFA supplementation improved cardiovascular health in growth restricted offspring compared to their growth-restricted counterparts with low LC-PUFA intake (Skilton and Phang, 2016; Skilton et al., 2012). The authors hypothesised that the reason behind this beneficial effect on FGR offspring may be due to the compensation of the offspring's impaired fatty acid metabolism or the anti-inflammatory profile of LC-PUFAs improving endothelial function, although this remains to be confirmed.

1.11 Developmental programming

Offspring exposed to adverse intrauterine environments are programmed for later-life CVD. This hypothesis is known as Barker's theory, or the updated Developmental Origins of Health and Disease (DOHaD), which states that adverse early-life exposures (first 1000 days, from conception to 2 years old) can lead to adult disease in humans (Barker, 1998). The DOHaD theory originates from the observations that low birth weight babies are more prevalent to suffer from ischemic heart disease in adulthood (Barker et al., 1989) but now incorporates a wider body of evidence. This theory originated from studies carried out in England and Wales which found a correlation between coronary heart disease and infant

birthweight, which led to the hypothesis that *in utero* undernutrition was responsible for long-lasting structural and metabolic changes in the offspring, thereby increasing their susceptibility to heart disease later in life (Barker, 2007). Further studies by Barker and Osmond (1988) have found an inverse relationship between elevated diastolic blood pressure in adults with low birth weight for gestational age at birth, suggesting that the establishment of this increased risk of hypertension occurs *in utero*. Barker also observed that reduced glucose tolerance was another impairment associated with low birth weight, which was strongly associated with the onset of T2DM (Hales and Barker, 1992). These observations were confirmed in other longitudinal studies in Europe and the US whereby correlations between poor early life conditions and later-life disease have been made (Forsdahl, 1977; Buck and Simpson, 1982).

In addition, observations on the impact of maternal undernutrition during the Dutch famine during World War II on the offspring's early onset of CVD provided further evidence for offspring programming after adverse intrauterine conditions (Painter et al., 2006). Interestingly, the timing of the nutritional perturbation due to the Dutch famine determined the organ affected by this insult: early gestation exposure was associated with cardiovascular and metabolic disease, whereas mid gestation exposure affected the lungs and kidneys and late gestation exposure impacted glucose homeostasis (Painter et al., 2006). Additionally, young adults exposed to the Dutch famine during early pregnancy (and not late pregnancy) had elevated rates of obesity, possibly due to an alteration of food intake regulation and excess fat accumulation (Ravelli et al., 1976). Thus, the differences in the impact of the timing of the undernutrition on the offspring suggest that it is dependent on the development of the different organs in the fetus (Roseboom et al., 2006).

Therefore, it was hypothesised that the exposure to maternal undernutrition programmed babies to survive under this environment which predisposed them to metabolic disease (Hales and Barker, 1992). This was termed "programming" which is described as the adaptive responses from the fetus to an adverse *in utero* environment that result in the permanent adverse consequences of the offspring (Lucas, 1991). Further research led to the establishment of the developmental plasticity concept, which states that the prenatal environment is able to

determine the developmental pathway of the offspring later in life (Bateson et al., 2004). In contrast to previous theories, developmental plasticity programmes the offspring to survive in an environment similar to *in utero*, however, if this changes later in life, this adaptation can confer a disadvantage. Even though these theories were developed focusing on fetal undernutrition, they still have relevance in the light of the current obesity and cardiometabolic disease epidemic. In this context, maternal complications during pregnancy including PE and GDM may programme the offspring for later-life disease that is affected by their environment and lifestyle, although the specific mechanisms remain unknown.

1.11.1 Mechanisms of fetal programming

1.11.1.1 Maternal nutrition and metabolic status

Experimental animal models have provided mechanistic evidence of the impact of adverse intrauterine environments on programming CVD in the offspring. Offspring from obese rats have shown impaired regulation of leptin and other key appetite regulators from early postnatal life (Morris and Chen, 2009). Rodent offspring from mothers under high fat diet show hyperlipidaemia and greater adiposity and blood pressure compared to controls (Elahi et al., 2009). Interestingly, there is evidence that an *in utero* environment of hyperlipidaemia in a mouse model led to compromised vessel walls and elevated atherogenic risk in the offspring (Alkemade et al., 2007). Additionally, insulin resistance has been observed in offspring from high fat diet fed rats, despite the offspring having a normal diet (J.F. Martin et al., 2000). Importantly, fetal adipogenesis and adiposity can be influenced by the *in utero* environment which can have consequences for the development of metabolic disease later in life, possibly due to the programming of dysregulated transcription factor activation and hormonal release (Joss-Moore et al., 2010). Pregnant animal models on a low protein diet have shown fetal growth restriction and offspring obesity and elevated WAT content (Sarr et al., 2012). In addition, reduced placental perfusion in rats leads to an elevated VAT content in the offspring (Joss-Moore et al., 2010), suggesting that the placenta and nutrient delivery to the offspring is important in determining fetal adiposity.

Similarly, humans exposed to obese and diabetic pregnancies have also been shown to develop detrimental phenotypes that increase the risk for later-life CVD (Palinski et al., 2009), although the mechanisms are not clear. Obesity during pregnancy may programme the offspring to obesity and later-life CVD through alterations in body composition (mainly fat mass), adipocyte function, insulin resistance, increased inflammation and hyperphagia (Inzani and Ozanne, 2022). Similar mechanisms are believed to take place in pregnancies affected by GDM (Scheidl et al., 2023) (discussed further in section 1.12.1.1). Additionally, there is evidence that, in humans, atherogenic lesions (including fat accumulation and oxidised LDL recruitment) occur during fetal development in pregnancies where the mothers are affected by hypercholesterolemia (Napoli et al., 1997), suggesting a link between compromised maternal lipid metabolism and vascular complications in the offspring.

1.11.1.2 Epigenetics

Epigenetics is a potential mechanism to explain offspring programming after adverse intrauterine environment exposure. Epigenetics involves the changes in gene function without interfering with the coding sequence but can affect the resulting phenotype. The establishment of epigenetic patterns e.g. via DNA methylation takes place during early development whereby the maternal and paternal DNA marks are partly erased to allow for *de novo* modifications (Godfrey et al., 2015). Epigenetic changes are involved in tissue-specific gene expression and can be affected by detrimental *in utero* environments, such as pregnancy complications. Studies from animal models have provided strong evidence for the impact of epigenetics in the programming theory, which provide a useful tool when attempting to identify effects of the *in utero* environment independent of genetics. Maternal nutrition has shown to independently affect site-specific methylation patterns during early development in the offspring which impacts adult phenotypes (Waterland and Jirtle, 2003). The authors from the Waterland and Jirtle (2003) study in mice showed that maternal intake of methyl donors (including folic acid) altered the DNA methylation of the *Agouti* gene which induced coat colour changes in the offspring. Interestingly, epigenetic changes affect multiple generations after the exposure, as it has been shown that the third offspring generation after intrauterine maternal undernutrition (grand-offspring

of fetally malnourished females) is also detrimentally affected despite having normal nutrition (Benyshek et al., 2006), thus perpetuating the phenotype.

In addition, human data also provide evidence of the impact of the *in utero* environment on epigenetic patterns. Offspring from mothers exposed to Dutch famine showed changes in DNA methylation tags in genes involved in growth and metabolic disease nearly 60 years after birth (Tobi et al., 2009). Godfrey and colleagues reported that methylation of specific transcription factors contribute to 25 % of the offspring adiposity in healthy pregnancies after adjusting for sex and age (Godfrey et al., 2011). Epigenetic changes have also been found in cord blood DNA from obese pregnancies which are associated with offspring adiposity and, interestingly, these methylation patterns changed after maternal lifestyle interventions (Jönsson et al., 2021). Additionally, differential DNA methylation in offspring born after maternal bariatric gastrointestinal bypass surgery compared to their siblings born before the surgery affected the predisposition for improved metabolic homeostasis in the former, which were correlated with the gene methylation levels (Guénard et al., 2013).

However, it is important to note that these epigenetic changes may not always have long-lasting effects depending on the lifestyle of the offspring, thus showing the importance of the environment and lifestyle. For example, adult offspring from a mouse animal model born after intrauterine hyperglycaemic exposure only exhibited elevated adiposity under a high fat diet but not under control diet (Talton et al., 2019). Epigenetics can also be highly influenced by the environmental stimuli and therefore the utility of epigenetic marks to predict offspring disease is controversial although it may be useful for early intervention. In the context of pregnancy, identifying the key developmental stages in the fetus susceptible to the maternal environment may help prevent epigenomic alterations that affect the offspring long-term and may provide insight for developing effective interventions for both mother and baby.

1.11.1.3 Oxidative stress

Oxidative stress caused by fetal and placental stress may also programme the offspring for CVD later in life. Pregnancy complications (including PE), environmental factors and toxic substances (e.g. tobacco) can impact placental

function thereby limiting nutrient and oxygen delivery to the baby (Rodríguez-Rodríguez et al., 2018). Elevated ROS production and lipid peroxidation have been found in women with PE, mainly caused by the poor placental perfusion (Raijmakers et al., 2004). In addition, placental oxidative stress in PE has been associated with FGR in humans (Fujimaki et al., 2011). Similarly, animal models of PE have shown elevated superoxide production which contributes to maternal vascular dysfunction (Bridges et al., 2009) and oxidative stress has been suggested as one of the main contributors to hypertension development in animal models of FGR (Rodríguez-Rodríguez et al., 2015). Altogether, this environment leads to fetal stress and elevated ROS production thereby causing systemic damage which may impact long-term health.

1.11.2 Impact of PE on offspring programming

Offspring from PE pregnancies have short and long-term neurodevelopmental, cardiovascular, immunological, respiratory, metabolic and gastrointestinal issues (Figure 1-3). The most documented impact of PE on the offspring is the elevated blood pressure and cardiac malfunction later in life. The reason behind this phenomenon remains unknown, but it is believed fetal programming may play an important role. This means that fetal development is impaired due to the detrimental intrauterine environment, which may program the offspring for later-life CVD. Animal models of placental dysfunction and maternal undernutrition provide evidence of *in utero* programming in the offspring. In contrast, humans appear to also be influenced by genetics and environmental factors, as it has been observed that siblings from both normotensive and hypertensive pregnancies present similar risk of later-life CVD (Alsnes et al., 2017).

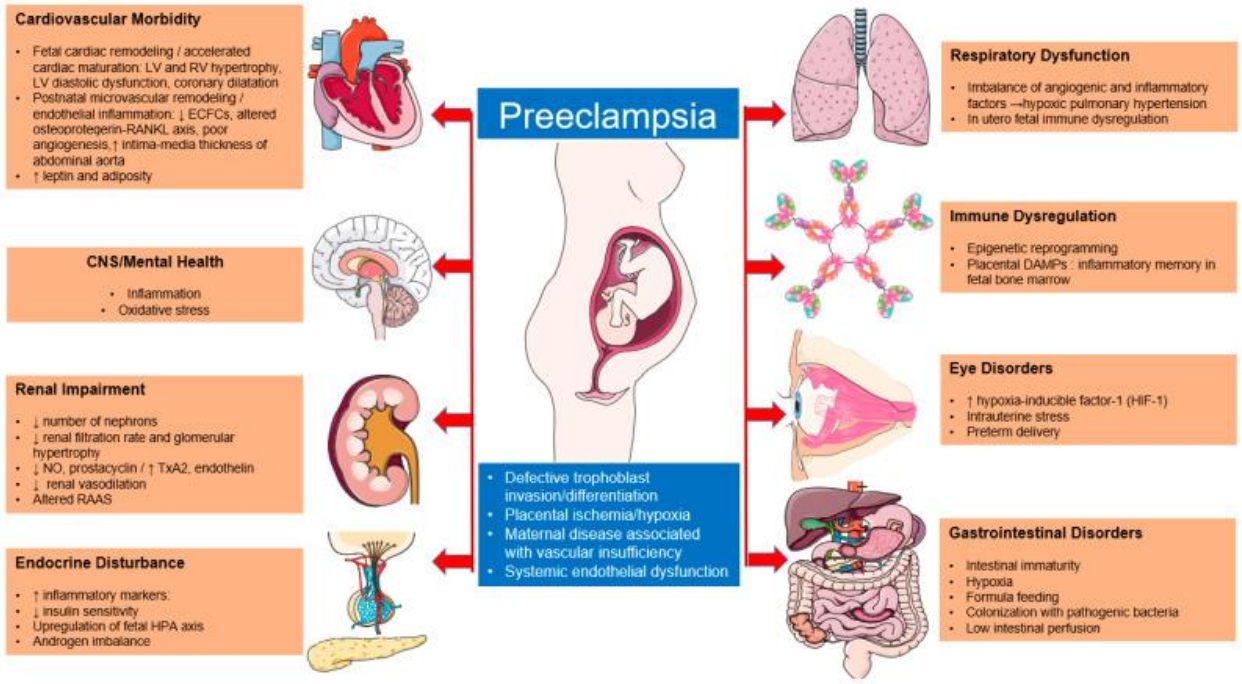

Figure 1-3. Consequences of PE exposure during pregnancy in the offspring. Impaired vascular, placental and endothelial function in the mother causes PE which leads to short- and long-term systemic consequences in the offspring. Figure from Koulouraki et al. (2023).

Structural and functional cardiovascular changes occur in offspring of PE pregnancies, recently summarised in Yang et al. (2023). Elevated umbilical cord artery inflammation and enlarged coronary arteries have been found in babies born after PE pregnancies compared to healthy controls (Lin et al., 2021). Offspring from hypertensive pregnancies present higher ventricular mass at 3 months of age (Aye et al., 2020) and diastolic dysfunction between 5 and 8 years of age (Fugelseth et al., 2011). Adolescents born after PE pregnancies have elevated relative ventricular wall thickness and lower left ventricular end-diastolic volume (Timpka et al., 2016), which may be an early sign of left ventricular hypertrophy. Additionally, PE is associated with higher blood pressure and serum lipids in young adult offspring (Alsnes et al., 2017). The causes that lead to these cardiovascular and metabolic alterations remain to be elucidated and it is unknown whether these cardiovascular changes in the offspring of PE pregnancies resolve or remain and contribute to later-life CVD.

1.12 Gestational diabetes mellitus (GDM)

Gestational diabetes mellitus (GDM) is characterised by gestational hyperglycaemia diagnosed around 24–28 weeks of pregnancy and has a global prevalence of 14 % of pregnancies worldwide (Wang et al., 2022). The GDM

prevalence in the UK is estimated to be up to 24 % (Farrar et al., 2016). GDM pregnancies are increasing due to the elevated rates of obesity and lack of physical activity in women of childbearing age, similar to the increase in T2DM in the non-pregnant population. This elevated prevalence is concerning due to the association of GDM with later-life T2DM and CVD in the mothers, as approximately 60 % of women with a history of GDM develop cardiometabolic disease later in life (Plows et al., 2018).

GDM is believed to develop in women with a prior chronic insulin resistance background to which the insulin resistance from the pregnancy is added. This causes an even greater level of maternal insulin resistance which leads to reduced glucose uptake/utilisation and reduced suppression of glucose production in response to insulin (Buchanan and Xiang, 2005). In fact, glucose uptake triggered by insulin is reduced by over 50 % in GDM compared to pregnant women with normal glucose tolerance (Catalano, 2013). Consequently, pancreatic β-cells deteriorate in this chronic insulin resistant state and have reduced plasticity and adaptation to pregnancy.

In addition, GDM is also a risk factor for the development of PE and caesarean delivery (Catalano, 2010). The reason behind the risk of PE in women with GDM may be associated with the increase in fat deposition and insulin resistance which may affect endothelial function and vasodilation. This is supported by studies showing that the incidence of PE in women with GDM is associated with hyperglycaemia (poorly controlled GDM) and pregravid BMI (Yogev et al., 2004). Elevated BMI and blood glucose may be signs of more severe insulin resistance which can impact vessel function and contribute to the onset of hypertension.

In addition, there is some evidence of an inflammatory component in GDM that may participate in the phenotype. Obesity is associated with a low-grade chronic inflammation status that consists of the release of proinflammatory cytokines from adipocytes, which is believed to contribute to insulin resistance, as reviewed in Shoelson et al. (2007). Inflammation is also believed to contribute to the development of T2DM in obese individuals due to its impact on insulin signalling leading to insulin resistance. Similarly, obesity during pregnancy is characterised by adipose tissue and placental inflammation, which contributes to systemic inflammation (Challier et al., 2008). Due to the interaction between the maternal

adipose tissue and placenta with the immune response, it has been hypothesised that the diabetic and/or obesogenic environment during pregnancy may contribute to inflammation, insulin resistance and fetal adiposity (Catalano and Hauguel-De Mouzon, 2011).

There is no widely accepted treatment for GDM, but it usually resolves after the delivery of the baby and the placenta. Women with GDM are often treated with lifestyle interventions (diet and exercise) and insulin, although this has limited effect due to the insulin resistance associated with this condition. Management of GDM can also involve oral antidiabetics such as metformin, however, the impact of these drugs on the fetus and the later life of the offspring is still in question as they have been observed to cross the placenta (Feig and Moses, 2011).

1.12.1.1 Impact of GDM on the offspring

Given the importance of adipose tissue expandability in adult metabolic disease establishment, it has been hypothesised that the adverse intrauterine environment caused by maternal metabolic perturbations (such as GDM and obesity) during pregnancy may programme impaired adipose tissue development in the offspring. The critical timepoint for preadipocyte and adipocyte population development occurs *in utero* and adverse alterations can therefore affect this and later life. It has been hypothesised that overnutrition during pregnancy may programme accelerated adipogenesis during childhood, thereby exhausting the progenitor pool prematurely leading to limited adipose tissue plasticity later in life (Scheidl et al., 2023).

There is an elevation in glucose and fatty acid transport to the baby during GDM, which often results in fetal overgrowth (leading to large-for-gestational age (LGA)) babies, macrosomia and elevated fetal adiposity. It is known that maternal hyperglycaemia causes fetal hyperglycaemia, ß-cell stress and exacerbated insulin production that contributes to fetal macrosomia, which is known as the Pedersen hypothesis (Pedersen, 1955). This *in utero* exposure may also be responsible for programming the increased long-term risk of cardiovascular and metabolic disease in offspring born after GDM pregnancies. In fact, there is an association between maternal GDM with excessive fetal insulin release and later-life impaired glucose regulation in the offspring (Silverman et al., 1995). In addition, maternal

hyperglycaemia during pregnancy has been associated with offspring obesity during early childhood (Hillier et al., 2007).

However, Pedersen's hypothesis was developed observing pregnant women with type 1 diabetes which does not represent the majority of hyperglycaemic pregnancies in the present pregnant population which involve women with T2DM and GDM, where there is an effect of insulin resistance. Well-controlled GDM pregnancies still deliver babies with macrosomia despite regulated blood glucose levels, perhaps due to the impaired maternal lipid metabolism caused by the insulin resistance (Catalano et al., 2003). This means that despite glucose being an important factor in fetal weight and overgrowth, there are other contributing factors, including lipids, in pregnancies affected by insulin resistance. Thus, as GDM management does not reduce the levels of FFAs that are available to cross the placenta, the baby still receives large amounts of lipids thereby affecting fetal nutrition and growth. Babies from well-controlled GDM pregnancies have an elevated proportion of fat mass, even when born at a normal birthweight (Catalano et al., 2003) which can be risk factor for later-life elevated adiposity and obesity in the offspring. In addition, women with GDM have demonstrated elevated circulating plasma TG levels which correlate with the incidence of LGA babies (Cianni et al., 2005). This may be because the elevated maternal plasma TG can also increase delivery of FFA to the baby as these can be hydrolysed by the action of placental LPL and transported by the placenta. However, due to the independent lipogenesis (from carbohydrate sources) in the fetus during late pregnancy, it may be hypothesised that glucose excess during GDM pregnancies, rather than FFAs, mainly contributes to lipid synthesis in the fetus, while both glucose and FFAs have an impact during early gestation. The hyperglycaemic environment may stimulate insulin release which promotes DNL in fetal adipose tissue and liver (Desoye and Herrera, 2021) (Figure 1-4). In addition, fetal adipose tissue LPL may also be upregulated by insulin which facilitates the uptake of FFAs by fetal adipocytes which further contributes to TG formation and storage (Desoye and Herrera, 2021) (Figure 1-4).

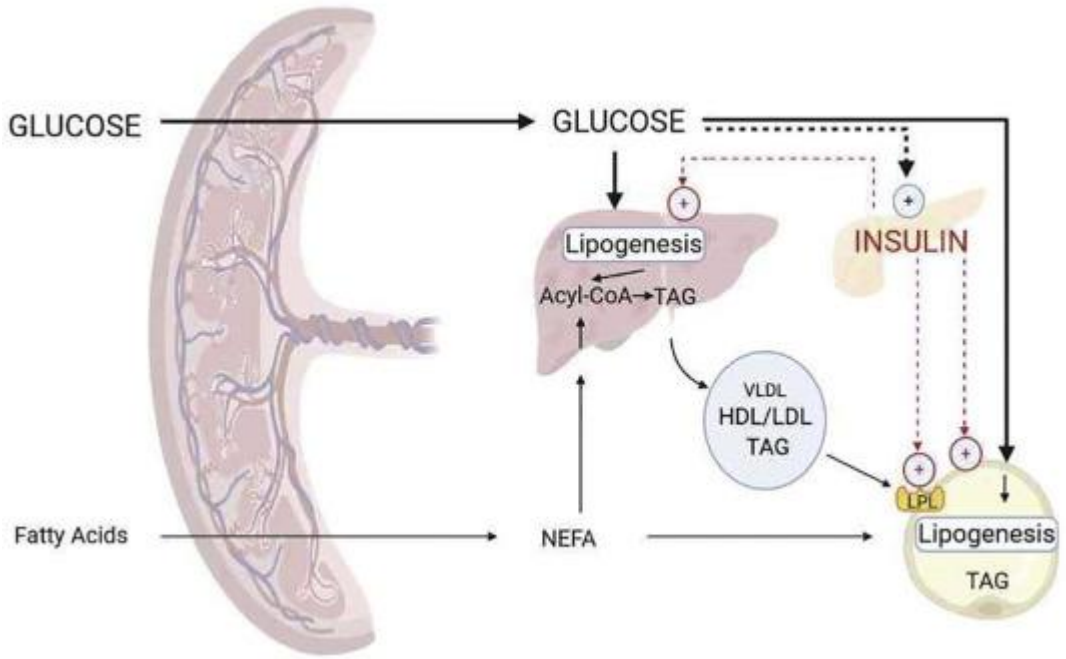

Figure 1-4. Hypothesised mechanism of elevated fetal lipogenesis in GDM pregnancies. High glucose transport to the fetus stimulates DNL in the fetal liver via insulin secretion. TGs are transported to the fetal adipose tissue via lipoproteins for storage. This increases adiposity in the fetus. To a lesser extent, NEFAs also contribute to the new TG formation. Figure from Desoye and Herrera (2021).

The programming of the GDM offspring for CVD and T2DM later in life may also rely on the epigenetic changes that take place *in utero*. There are studies showing that the placenta adapts to the hyperglycaemic environment through DNA methylation of genes involved in metabolic homeostasis, and there is evidence of epigenetic changes in the embryo as well (summarised in Słupecka-Ziemilska et al. (2020)). Investigations on children born after GDM pregnancies have identified DNA methylation profiles independently associated with maternal BMI and GDM status (Hjort et al., 2018). Importantly, these methylation patterns have been shown to affect genes associated with insulin secretion, β-cell function and diabetes risk (Chen et al., 2017). Animal models have corroborated these findings and shown similar epigenetic tags in the pancreas from offspring exposed to intrauterine hyperglycaemia thereby affecting glucose homeostasis and susceptibility to T2DM (Zhu et al., 2019). Therefore, identification of epigenetic marks in the offspring may help identify future-life CVD and T2DM risk and aid prevention. Additionally, due to the increasing awareness of the importance of lipids in GDM, it has been proposed that cord blood lipidome may provide insights into the specific lipid changes in the offspring that may serve as biomarkers of future metabolic disease (Desoye and Herrera, 2021). This has proven beneficial in identifying lipid signatures of relevance in predicting the development of type

1 diabetes in children (Lamichhane et al., 2018), and may be relevant to determine susceptibility to other metabolic conditions.

1.13 Animal models of pregnancy

Animal models are essential for the study of pregnancy and pregnancy complications due to ethical considerations which preclude placing mother and baby under any risk. Selecting animal models to investigate pregnancy *in vivo* must take into consideration the type of placentation they undergo as it varies across different species and this can have an impact when attempting to translate the results to humans. Humans present haemochorial placentas, as do other non-human primates, guinea pigs and rodents, which are characterised by a thin trophoblast layer separating the maternal and fetal bloods. Rodents present an excellent model of pregnancy due to their short pregnancy period (22 days), ease of use and high reproducibility, however, only rats undergo a profound trophoblast invasion that causes a spiral artery vasodilation similar to humans (Soares et al., 2017). This blood flow increase takes place gradually in humans from embryo implantation, whereas in rats this adaptation takes place mid-to-late pregnancy in normotensive rats (Buelke-Sam et al., 1982). Additionally, rats present some similarities with human lipid metabolism, including the response to insulin from adipose tissue and the process of DNL in the liver, although the proportion of cholesterol-containing lipoproteins differs between these two species (Bergen and Mersmann, 2005). Similar to humans, rats experience a period of insulin sensitivity and anabolism to accumulate lipids during early pregnancy that is followed by insulin resistance and a catabolic state during late pregnancy (Ramos et al., 2003). Therefore, the rat presents analogous features to humans that make it a suitable model to study pregnancy and placentation *in vivo*.

1.13.1 Rat models of PE

There is a wide variety of rat models of PE which has been summarised in Gatford et al. (2020). It is important to note that pregnancy-induced hypertension is a human exclusive condition which needs to be artificially induced in other mammals. The lack of spontaneous hypertension presents a challenge when trying to imitate PE in humans and often different animal models present different phenotypes of this multifactorial condition. Nevertheless, the availability of

genetic and non-genetic rodent models allows the study of vascular, environmental and genetic factors that lead to the development of PE. Several animal models have been developed based on the knowledge of the factors leading to PE in humans, including hypoxia, inflammation and RAAS dysregulation. Importantly, most interventions to induce PE in animal models occur after full placental development, which presents a limitation when comparing results to humans (McCarthy et al., 2011).

1.13.1.1 Surgical models

The reduced uterine perfusion pressure (RUPP) model, commonly used in the Sprague Dawley rat, involves clipping the ovarian arteries on gestational day (GD) 14 (Soares M.J. and Hunt, 2006). This model imitates the human PE phenotype in several aspects including reduced uteroplacental blood flow, proteinuria, endothelial dysfunction and elevated maternal blood pressure. The phenotype is analogous to humans, however, similar to other models of PE, it does not allow the study of the mechanisms that lead to the formation of the dysfunctional placenta as the reduced perfusion takes place after this organ is formed. Additionally, the lipid, glucose and insulin abnormalities are not observed between the RUPP model vs controls (Gilbert et al., 2007). Nevertheless, the offspring of the RUPP rodent model present similar cardiovascular effects observed in PE offspring, including hypertension and arterial dysfunction (Alexander, 2003; Anderson et al., 2006).

1.13.1.2 Genetic models

The spontaneous hypertension and heart failure (SHHF) rat is genetically predisposed to chronic hypertension, insulin resistance and cardiomyopathy. Pregnant SHHF rats develop spontaneous pregnancy-induced hypertension with SGA offspring, however, they do not present maternal proteinuria or placental histological abruption (Sharkey et al., 2001). Alternatively, the Dahl salt-sensitive (DSS) rat develops hypertension with endothelial dysfunction and kidney disease under a high-salt diet. This strain has been proposed as a potential model of spontaneous superimposed PE as pregnant dams present high blood pressure, proteinuria, placental hypoxia and FGR (Gillis et al., 2015). However, this rat colony was under a normal salt diet and therefore did not exhibit the normal characteristics of the female DSS rat which are normotensive and do not show

signs of superimposed PE when pregnant (West, 2023). This raises concerns about reproducibility of the model moving forward.

1.13.1.3 Pharmacological models

Infusion of the antiangiogenic factor sFLT1 in Sprague Dawley rats at GD 13 increases maternal blood pressure, endothelial dysfunction and leads to FGR, however it does not induce proteinuria (Bridges et al., 2009). Treatment of pregnant rats with the nitric oxide inhibitor L-NAME caused hypertension, proteinuria and FGR, although these investigations were carried out in late pregnancy (GD 17-18) (Molnár et al., 1994; Yallampalli and Garfield, 1993). Notably, these approaches trigger PE with known consequences of the PE phenotype in humans, such as elevated antiangiogenic factors and reduced NO production, and may not be useful to determine the causes that lead to the development of the symptoms.

1.13.1.4 Genetic and pharmacological models

The stroke-prone spontaneously hypertensive rat (SHRSP) has a genetically determined predisposition to hypertension which makes it an ideal model to study pregnancy on a hypertensive background. SHRSP does not spontaneously develop PE and therefore an extra stimulus needs to be given with a pharmacological agent, such as angiotensin II (ANGII). A model of superimposed PE in the pregnant SHRSP rat has been previously published by our group (Morgan et al., 2018). Continuous infusion of ANGII (500 ng/kg/min dose) from GD 10.5 causes maternal increase in blood pressure and proteinuria, whereas a higher dose (1000 ng/kg/min) leads to blood pressure increase, proteinuria, lower uterine artery diameter and fetal growth restriction (Morgan et al., 2018). The low and high ANGII doses mimic mild and extreme PE phenotypes respectively, however, there are welfare concerns on the animals associated with the higher dose. An optimised ANGII dosage has been developed by Dr Kayley Scott using 750 ng/kg/min which imitates the maternal high blood pressure and cardiovascular impairment, proteinuria, impaired uterine artery remodelling and fetal growth restriction (personal communication). These results may indicate a promising animal model that imitates the full human PE phenotype, however, the metabolic changes in this model have not been investigated. Additionally, the impact of intrauterine ANGII environment on the offspring is unknown.

1.14 Hypothesis and aims

Knowledge of the importance of lipids in pregnancy complications is growing, however, key questions on the impact of these on the offspring remain unanswered. This may be because of the limited pregnancy research in humans due to ethical considerations and the limited appropriate animal models that mimic a full PE phenotype. PE is associated with a maternal dysregulation of lipid homeostasis which may be responsible for ectopic fat accumulation on the placenta, thereby affecting placental lipid metabolism and transport of essential fatty acids needed for fetal development. This may be linked with the offspring's cardiovascular underdevelopment during PE pregnancies and later-life impact. Therefore, it was hypothesised that PE impairs essential fatty acid transfer by the placenta to the growing fetus thereby adversely affecting cardiac and vascular development in the offspring. The main aims were:

1.- To investigate the cardiovascular defects in the offspring of an animal model of superimposed PE.

2.- To quantify plasma lipids and lipid composition of rat placentas from an animal model of superimposed PE.

3.- To quantify ectopic fat accumulation, lipid composition and inflammation in placenta from healthy pregnancies and pregnancies complicated by PE.

4.- To investigate expression of genes involved in lipid synthesis, transport and hydrolysis in healthy, PE and FGR placentas.

5.- To quantify ectopic fat accumulation and lipid composition in placental sections from healthy and GDM pregnancies.

2 Materials and methods

2.1 *In vivo* procedures

2.1.1 Animal maintenance and mating

Stroke-prone spontaneously hypertensive (SHRSP) rats and Wistar Kyoto (WKY) rats were obtained from inbred colonies from the University of Glasgow. Animals were kept under strict 12 h light/dark conditions at 21±3 °C. Water and standard diet (rat and mouse No.1 maintenance diet, Special Diet Services) were provided *ad libitum*. Animal procedures were performed following the regulations established in the Animals (Scientific Procedures) Act 1986, under the Home Office approval of Project Licence PP0895181 and local Animal Welfare Ethical Review Body (AWERB) approval.

Adult SHRSP and WKY females (10-26 weeks-old) were time-mated with stud males from the same strain and were kept in the same cage for a maximum of 72 h. Successful mating and pregnancy were confirmed by the presence of a copulation plug, denoted as gestational day (GD) 0.5. Only pregnant females were allowed to continue in the study. Pregnant SHRSP were randomly assigned into control (0.9 % saline infusion) or treated (700 ng/kg/min angiotensin II (ANGII) infusion) groups. Pregnant WKY females were treated with 0.9 % saline only. Dams that lost ≥20 % body weight post-surgery for minipump implantation were removed from the study and humanely culled.

2.1.2 Minipump implantation

Subcutaneous minipump implantations were performed aseptically on pregnant dams (GD 10.5) under general anaesthesia. Rats were anaesthetised in an induction box with 5 % isoflurane in 1.5 l/min oxygen and maintained with 2.5 % on mask. Anaesthetised rats were placed in prone position on a heating blanket with nose and mouth inside the anaesthetic mask. A toe “pinch” reflex was used to check that they were fully under anaesthesia before the start of any procedure. Analgesia (dose of 5 mg/kg Rimadyl) was injected subcutaneously immediately before the surgical procedure. An osmotic minipump (ALZET 2002) containing either 0.9 % saline or 700 ng/kg/min ANGII (SigmaAldrich) was implanted in the unconscious rats. Continuous dosage of saline or ANGII was maintained up to 2

days after parturition (14 days in total). Pups were weighed 1-7 days after birth at which point litters were reduced to n=4 (2 males and 2 females if possible) or n=6 (3 males and 3 females if possible). The rest of the pups were sacrificed for tissue collection as described in section 2.1.7.2. Mothers were sacrificed after weaning for tissue harvesting as described in section 2.1.7.1.

2.1.3 Tail-cuff plethysmography

Systolic blood pressure (SBP), measured by the tail-cuff plethysmography method, was recorded in conscious SHRSP and WKY rats. Blood pressure in male and female offspring was recorded biweekly from 5 to 17 weeks of age (7 times in total). Maternal blood pressure was recorded pre-pregnancy, at week 1 of pregnancy (W1P) and at week 3 of pregnancy (W3P).

Rats were placed in heat boxes (at 30°C) for 10 min to allow vasodilation of the tail arteries. Once vasodilated, rats were restrained in a soft cloth towel exposing the tail and placed on a heating blanket. An occlusion and a detector cuff were placed on the tail of the prewarmed animal. The occlusion cuff was inflated by "in-house" developed software until the blood flow through from the tail artery was occluded indicating SBP. SBP was recorded a minimum of six times in order to provide the average SBP of the animal per sitting. The average and standard deviation were automatically generated by the software.

2.1.4 Echocardiography

Echocardiography of the heart (M-mode) and mitral valve (Doppler) were performed on the offspring at 5, 9, 13 and 17 weeks of age using an Acuson Sequoia c256 ultrasound with an array transducer (frequency = 14 MHz). M-mode images were obtained from the mothers at pre-pregnancy and at W3P.

Both techniques were performed under anaesthesia (isoflurane, 5% for induction, 2.0% for maintenance on mask in 1.5 L/min oxygen) with animals placed in supine position on a heating blanket with nose and mouth inside the anaesthetic mask. Before the start of the procedure, a toe "pinch" reflex was used to check that they were fully under anaesthesia and the animal's chest was shaved. Images were collected for at least 3 cardiac cycles and 3 representative images were selected and analysed on ImageJ software (Figure 2-1).

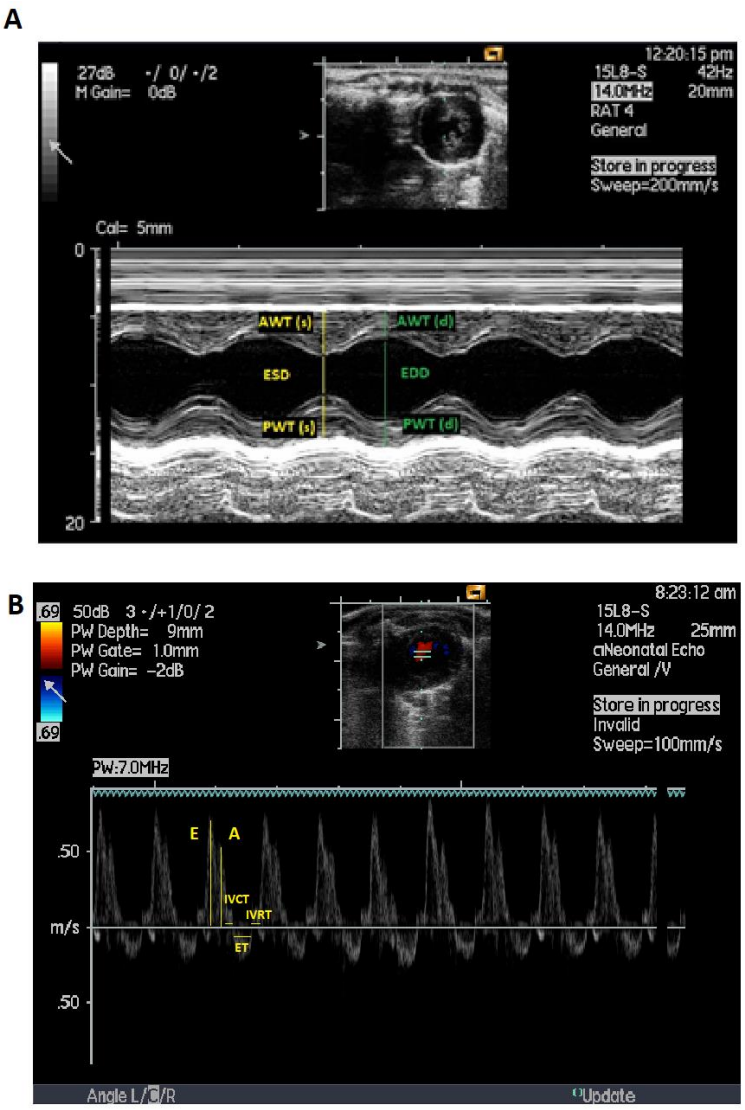

Figure 2-1. Example of M-mode and Doppler image analysis on Image J. (A) Waveforms represent anterior (AWT) and posterior (PWT) wall thickness in systole (peaks) and diastole (troughs). Length between cardiac walls represents end systolic diameter (ESD) (yellow lines) and end diastolic diameter (EDD) (green lines). (B) Long and short peaks represent early (E) and late (A) wave velocities, respectively. Waves in between peaks represent the isovolumetric constriction time (IVCT), LV ejection time (ET) and isovolumetric relaxation time (IVRT).

2.1.4.1 VEVO F2 system

Echocardiography and doppler ultrasounds were also performed with the VEVO F2 system with an array transducer (frequency = 15.0-29.0 MHz). Ultrasound procedures were performed under anaesthesia (isoflurane, 5 % for induction, 2 % for maintenance on mask in 1.5 l/min oxygen) and animals were placed in supine position on a heating pad with nose and mouth inside the anaesthetic mask. Front and rear paws were taped to electrodes on the heating pad in order to record respiratory rate and heart rate. Hair from the echoed area was shaved and completely removed with shaving cream. Internal body temperature was recorded by the insertion of a rectal probe. Cardiac M-mode short-axis images were taken

for all the animals. Transmitral doppler images were obtained in the offspring only. Image analysis was performed by the Vevo Lab software (version 5.7.1) in order to obtain AWT, PWT, ESD, EDD, E, A, IVRT, IVCT and ET measurements.

2.1.4.2 Echocardiography calculations and formulae

Measurements obtained from echocardiograms were used to calculate the left ventricular mass (LVM), cardiac output (CO), fraction shortening (FS), ejection fraction (EF) and stroke volume (SV) of the animals, according to the formulae:

Stroke volume (ml) = EDV/ESV

Cardiac output (ml/min) = $SV \times HR$

Ejection Fraction (%) = $(SV/EDVol) \times 100$

Fractional shortening (%) = $(EDD-ESD/EDD) \times 100$

Left ventricular mass (g) = $(0.8 \times ASEcube) + 0.6/1000$, where ASEcube = $1.04 \times (IVSTd+LVIDd+PWTd)3 - LVIDd3$

LVIDd = average EDD × 10

IVSTd = average AWTd × 10

APWTd = average PWTd × 10

EDVol = $1.047 \times LVIDd^3$

ESV = $1.047 \times (Average\ EDDs)^3$

HR = Calculated from number of peaks (beats/min): (60/(1286.67/# of peaks))*1000

Measurements obtained from the transmitral doppler images were used to calculate E/A index and myocardial performance index (Tei index) from the following formulae:

E/A index = E/A

Tei index = (IVRT+IVCT)/ET

2.1.5 Blood collection

Blood samples were collected from the tail vein of male and female offspring at 9 and 13 weeks of age. Rats were anaesthetised in an induction box with 5 % isoflurane in 1.5 l/min oxygen and maintained with 2.5 % on mask. Anaesthetised rats were placed on a right lateral recumbent position on a heating blanket with nose and mouth inside the anaesthetic mask. A toe “pinch” reflex was used to check that they were fully under anaesthesia before the start of any procedure.

A small incision was made on the tail with a sterile scalpel blade in order to extract no more than 10% of total circulating blood volume. Blood samples were kept in heparin on ice. At sacrifice, blood was collected via cardiac puncture. In this case, 5 ml of blood were drawn directly from the left ventricle into a lithium heparin and an ethylenediaminetetraacetic acid (EDTA) blood tube (approximately 2.5 ml on each). Blood samples were centrifuged at 1200 g at 4 °C for 15 min. Plasma was separated and stored at -80 °C.

2.1.6 Metabolic cages

Offspring and mothers were placed in metabolic cages in pairs for an acclimatisation period of at least 1 h a week prior to the start of the formal phenotyping period. Urine and faeces were collected from the offspring at 5, 9, 13 and 17 weeks of age and from the mothers at pre-pregnancy and W3P. For sample collection, animals were placed individually in metabolic cages for a 24 h period. A total volume of 200 ml of water was provided and the amount consumed after 24 h was recorded. Urine volume was also recorded after 24 h. Food was provided *ad libitum*. Urine and faecal samples were collected and stored at -80 °C.

2.1.7 Sacrifice procedure

2.1.7.1 Offspring and mothers

Juvenile (6-weeks old) and adult rats (17-26 weeks old) were sacrificed by exsanguination. These rats were anaesthetised in an induction box with 5 % isoflurane in 1.5 l/min oxygen which was maintained on the mask for the duration of the procedure. Rats were placed in supine position and exsanguination was performed by making an incision to open the thoracic cavity, cutting the rib cage and exposing the heart. Cardiac puncture was performed for blood sampling at this point. The thoracic aorta and heart were subsequently removed. Death was confirmed before proceeding with tissue harvesting.

2.1.7.2 Neonates

Neonates (1-7 days old) were sacrificed by anaesthesia overdose (0.5 ml of Dolethal). Dolethal was applied by intraperitoneal injection and neonates were decapitated once death was confirmed. Tissues including heart, thoracic aorta,

lungs, liver, kidneys, gonadal and retroperitoneal fat pads were harvested at this point.

2.2 Mesenteric artery wire myography

Mesenteric arteries supplying the intestines were isolated from rats at 18 weeks of age. Four vessel segments from each animal were mounted on 40 µm wire on a multi wire myograph system (Multi Myograph 610M DMT Model 4 Channel Interface & Four Vessel Chambers Lab) in physiological salt solution (PSS) (120 mM NaCl, 4.7 mM KCl, 1.2 mM $MgSO_4$, 25 mM $NaHCO_3$, 1.2 mM KH_2PO_4, 10 mM glucose, 2.5 mM $CaCl_2$). After mounting, the vessels were equilibrated for 30 min at 37 °C and gassed with 5 % O_2 and 5 % CO_2 prior to the normalisation procedure from the DMT system, which was used to determine the optimal tension for maximal active force production and sensitivity to agonists. The vessels at normalised tension were equilibrated for another 10 min in order to reach a stable baseline tension before the addition of 5 ml high potassium PSS (KPSS) (120 mM KCl, 1.2 mM $MgSO_4$, 25 mM $NaHCO_3$, 1.2 mM KH_2PO_4, 10 mM glucose, 2.5 mM $CaCl_2$) to the bath for "waking up" the vessels. After this, the vessels were washed three times with 5ml PSS and were allowed to return to the baseline. These steps were repeated to obtain a total of two KPSS curves. It is important to note that vessels that did not react to KPSS were not used in experiments. After this, an "endothelium check" was performed by contracting the vessels with $1x10^{-7}$ M U46610 prior to relaxation with $1x10^{-6}$ M acetylcholine (ACh). The contractile response to noradrenaline (NA) was observed by adding increasing concentrations at 2 min intervals ($1x10^{-10}$ M, $3x10^{-10}$ M, $1x9^{-10}$ M, $3x9^{-10}$ M, $1x8^{-10}$ M, $3x8^{-10}$ M, $1x7^{-10}$ M, $3x7^{-10}$ M, $1x6^{-10}$ M, $3x6^{-10}$ M and $1x5^{-10}$ M). The vessels were returned to baseline with 3 x PSS washes before pre-constriction with U46610. The relaxation response to carbachol (Cch) was observed by adding increasing concentrations at 2 min intervals ($1x10^{-10}$ M, $3x10^{-10}$ M, $1x9^{-10}$ M, $3x9^{-10}$ M, $1x8^{-10}$ M, $3x8^{-10}$ M, $1x7^{-10}$ M, $3x7^{-10}$ M, $1x6^{-10}$ M and $3x6^{-10}$ M). Vessels were washed and pre-constricted as before and the relaxation response to sodium nitroprusside (SNP) was observed by adding increasing concentrations at 2 min intervals ($1x10^{-10}$ M, $3x10^{-10}$ M, $1x9^{-10}$ M, $3x9^{-10}$ M, $1x8^{-10}$ M, $3x8^{-10}$ M, $1x7^{-10}$ M, $3x7^{-10}$ M, $1x6^{-10}$ M and $3x6^{-10}$ M).

LabChart software (ADInstruments) was used to record vessel responses, including baseline tension before agonist addition and maximal contraction and relaxation

responses post-agonist addition. Vessel responses were analysed on Excel and GraphPad Prism. The vessels response to noradrenaline was expressed as a percentage of KPSS constriction, where 100 % was the maximal constriction achieved after KPSS addition. Vasodilation curves were expressed as a percentage of relaxation after U46610 constriction. The dose responses were log_{10} transformed in order to obtain the area under the curve (AUC) from each agonist. A non-linear regression analysis was performed to obtain the half maximal effective concentration (EC_{50}). The AUC and EC50 values were subject to further statistical analysis on GraphPad Prism.

2.3 Lipidomics

Lipids were extracted from rat and human placentas following an methyl tert-butyl ether (MTBE)-based isolation protocol. Lipids from human PE and control placental samples were extracted by Professor Barbara Meyer (University of Wollongong). Lipids from some human GDM and control placental samples were extracted by Honours student Luke Bale (University of Wollongong). Human frozen placentas were cut with a scalpel (10-40 mg) and placed in a 2 ml homogenisation tube (FastPrep-24 Lysing Matrix D Tubes) containing 270 µl methanol (with 0.01 % w/v butylated hydroxytoluene (BHT)) and 30 µl of SPLASH LIPIDOMIX internal standard (Avanti Polar Lipids). Rat frozen placentas were cut with a scalpel (10-40 mg) and placed in a 2 ml homogenisation tube containing 270 µl methanol (with 0.01 % w/v BHT) and 30 µl of internal standard EquiSPLASH (Avanti Polar Lipids). Lipid concentrations from the internal standards can be found in Table 1. Samples were homogenised with a tissue homogeniser (QIAGEN) 2 x 30 s at 25 kHz. Homogenates were transferred to a 2 ml glass vial and washed with an additional 100 µl methanol. MTBE (920 µl) was added to the homogenates and mixed in a Roller Mixer Spiramix for 1 h at room temperature. Phase separation was induced by adding 230 µl of 0.15 M ammonium acetate solution (Scientific Laboratory Supplies) to each sample. Samples were then centrifuged for 5 min at 2000 g at room temperature. Upper phase was transferred to a new 2 ml glass tube and stored at -20 °C until use. A quality control (QC) sample and a blank extract were added to each extraction batch to ensure batch to batch consistency and to assess internal standard detection and possible presence of contamination.

Table 1. Lipid concentrations from SPLASH LIPIDOMIX and EquiSPLASH lipid standards used for lipidomics. PC, phosphatidylcholine; PhE, phosphatidylethanolamine; PG, phosphatidylglycerol; PI, phosphatidylinositol; PS, phosphatidylserine; TG, triacylglycerol; DG, diacylglycerol; MG, monoacylglycerol; Chol Ester, cholesteryl ester; SM, sphingomyelin.

SPLASH LIPIDOMIX			EquiSPLASH		
Lipid components	**Concentration (µg/ml)**	**Molecular weight (mg/mmol)**	**Lipid components**	**Concentration (µg/ml)**	**Molecular weight (mg/mmol)**
15:0-18:1(d7) PC	150.6	752.6	15:0-18:1(d7) PC	100	752.6
18:1 (d7) Lyso PC	23.8	529.4	18:1 (d7) Lyso PC	100	529.4
15:0-18:1 (d7) PhE	5.3	710.6	15:0-18:1 (d7) PhE	100	710.6
18:1(d7) Lyso PhE	4.9	487.4	18:1(d7) Lyso PhE	100	487.4
15:0-18:1(d7) PG (Na salt)	26.7	741.6	15:0-18:1(d7) PG (Na salt)	100	741.6
15:0-18:1(d7) PI (NH4 salt)	8.5	829.6	15:0-18:1(d7) PI (NH4 salt)	100	829.6
15:0-18:1(d7) PS (Na salt)	3.9	777.0	15:0-18:1(d7) PS (Na salt)	100	777.0
15:0-18:1(d7)-15:0 TG	52.8	811.8	15:0-18:1(d7)-15:0 TG	100	811.8
15:0-18:1(d7) DG	8.8	587.6	15:0-18:1(d7) DG	100	587.6
18:1(d7) MG	1.8	363.3	18:1(d7) MG	100	363.3
18:1(d7) Chol Ester	329.1	657.6	18:1(d7) Chol Ester	100	657.6
d18:1-18:1(d9) SM	29.6	737.6	d18:1-18:1(d9) SM	100	737.6
Cholesterol (d7)	98.4	393.4	C15 Ceramide-d7	100	393.4

Lipidomics analysis of the extracted lipid samples was obtained using a chip-based nano-electrospray ionisation source (TriVersa NanoMate, Advion) coupled with an Orbitrap Fusion mass spectrometer (Orbitrap Fusion Tribrid, ThermoFisher Scientific). Prior to analysis, samples were diluted 1 in 50 in methanol:chloroform (2:1 v/v) with 5 mM ammonium acetate and loaded onto a 96-well plate. A non-targeted approach was used to obtain a full lipidomics spectrum ranging from 200 to 1200 m/z. Each sample was analysed in duplicate in MS (MS^1) and MS/MS (MS^2) acquisition by individual automatic direct infusion with a gas pressure and ionisation voltage of 0.35 psi and 1.45 kV in both positive and negative ionization modes. Qual browser (Xcalibur software, ThermoFisher Scientific) was used to export the results from the total ion chromatogram for each sample. Lipid results (MS^1) were normalised to each individual internal lipid standard and their wet tissue weight appropriately. MS^2 data was not analysed in this project.

2.4 Human tissue collection

2.4.1 Patient recruitment

Patients with healthy, PE and GDM pregnancies were recruited for the study at the Princess Royal Maternity Unit (PRMU), Glasgow Royal Infirmary, Glasgow. Patient characteristics were retrospectively acquired from Badgernet electronic maternity notes via Mr Paul Burton. PE was defined according to the diagnostic criteria established by the International Society for the Study of Hypertension in Pregnancy: gestational hypertension presented together with one or more new-onset conditions including proteinuria, end-organ dysfunction e.g. pulmonary oedema, haematological and liver complications, etc. and/or uteroplacental dysfunction (Magee et al., 2022). GDM was defined according to the diagnostic criteria established by the National Institute for Health and Care Excellence (NICE): a fasting plasma glucose level of 5.6 mmol/l or above or a 2-hour plasma glucose level of 7.8 mmol/l or above (National Institute for Health and Care Excellence, 2015). The study was approved by the West of Scotland Research Ethics Service (ethics approval: 11/AL/0017 Glasgow Royal Infirmary REC AM12) and all recruited patients gave their informed voluntary written consent.

2.4.2 Archival placental collection

Paraffin-embedded placental blocks and slides, as well as frozen tissue from healthy pregnancies and pregnancies complicated by FGR and PE were obtained from an available archival placental collection. These samples were collected from pregnant women at Caesarean delivery at Glasgow Royal Infirmary, after giving their written and informed consent, and stored at the University of Glasgow. The samples were collected by Dr Shahzya Huda (ethics approval: 06/S070/14 Glasgow Royal Infirmary LREC1), Dr Vanessa Mackay and Dr Frances Stewart (ethics approval: 01OB007 Glasgow Royal Infirmary REC). Placental biopsies were processed and flash-frozen in liquid nitrogen and stored at -80 °C or preserved in 10 % formalin prior to paraffin embedding. Paraffin blocks were sectioned into 5 µm slices and mounted on slides with coverslips.

Frozen placental biopsies from GDM (n=31) and age and BMI-matched healthy control (n=1) for lipidomics studies were obtained from an available archival placental collection at the University of Queensland. These samples were collected from pregnant women at delivery at the Royal Brisbane and Women's Hospital (Queensland, Australia) by Dr Helen Barrett. Additional age and BMI-matched healthy controls (n=17) for lipidomics studies were obtained from an available archival placental collection at the University of Glasgow. These samples were collected from pregnant women at delivery at the National Health Service Greater Glasgow and Clyde maternity units by Dr Eleanor Jarvie. The studies were performed under the approval from the Royal Brisbane and Women's Human Research Ethics Committee (HREC/11/QRBW/427), the University of Queensland Human Research Ethics Committee (2011/HE001301) and the West of Scotland Research Ethics Committee (09/S0701/105). All women gave their informed and voluntary written consent.

2.4.3 Tissue and blood sampling

2.4.3.1 Placenta

Placental biopsies were sampled from women with healthy pregnancies and pregnancies complicated by GDM and PE at Caesarean delivery in the third trimester. Maternal blood was collected prior to delivery. Samples were obtained at the Glasgow Royal Infirmary by myself and Dr Zoe Lees.

Placentas were immediately processed after delivery or transferred to the lab on ice. Two ~1 cm strips (full thickness) were cut from each half of the placenta (left and right) with scissors. Four random blocks (~5 g each) were further cut (labelled 1-4) and snap frozen in liquid nitrogen. Four random thinly cut samples were also obtained and placed on clear based moulds covered by optimal cutting temperature (OCT) medium (Sakura) for cryosectioning. These samples were frozen by placing them directly above liquid nitrogen for approximately 10 min or until the OCT medium turned white. Frozen samples were stored at -80 °C.

2.4.3.2 Maternal bloods

Twenty millilitres of blood were collected from the antecubital fossa or foot prior to delivery into K_2EDTA, lithium heparin, fluoride oxalate and serum tubes. Blood tubes were kept on ice before centrifuging for 15 min (1200 g, 4 °C). Plasma was aliquoted and stored at -80 °C until use.

2.5 Plasma and urine analyses

Plasma and urine analyses of rat and human samples were performed by research technicians Ellen Macdonald and Elaine Butler on an automated Cobas c analyser. Plasma from rat blood was used to measure total cholesterol and triglycerides. Rat urines were used to quantify albumin and creatinine. Human plasma samples were used to measure total cholesterol, HDL, glucose, insulin and triglycerides. All the measurements were determined using enzymatic colorimetric assays (Roche) compatible with the automated analyser: total cholesterol (cholesterol Gen.2), triglycerides (TRIGL), albumin (ALBT2, Tina-quant Albumin Gen.2), creatinine (CREP2, Creatinine plus ver.2), HDL (HDLC4, HDL-Cholesterol Gen.4), glucose (GLUC3, Glucose HK Gen.3) and insulin (Elecsys® Insulin).

2.6 Histology

2.6.1 Lipid preservation on paraffin sections

Placental paraffin sections (5 µm) were cut using a Leica RM 2135 rotary microtome (Leica Biosystems) and mounted on slides. Lipid preservation on paraffin-embedded sections was carried out by following a method to fix lipids for

staining fat droplets from Tracy and Walia, (2002). Briefly, slides were treated in three different solutions (70 % ethylene glycol with 1v/w % linoleic acid and 0.4 v/w% lecithin, 2 % chromic acid and 5 % sodium bicarbonate) for 72 h (at 56 °C), 24 h (at 4 °C) and 24 h (at room temperature), respectively, with 70 % ethanol or water washes in between.

2.6.2 Oil red O staining

Oil red O (ORO) staining (SigmaAldrich) with haematoxylin counterstain was performed by following the manufacturer's instructions optimised for paraffin sections. Briefly, slides were deparaffinised in two 10 min immersions in HistoChoice Clearing Agent (Sigma-Aldrich) (xylene substitute) and rehydrated in decreasing concentrations of ethanol (100 %, 90 % and 70 %, 2 min each). Slides were immersed in 60 % 2-propanol (20 sec) prior to ORO stain for 30 min. Excess stain was washed in 60 % 2-propanol (30 s) and distilled water (20 s) before staining with haematoxylin (SigmaAldrich) for 30 min. Dehydration was performed by a 100 % ethanol wash (2 min) prior to two 10 min immersions in HistoChoice Clearing Agent. Slides were mounted with an aqueous mounting medium (Aquatex, SigmaAldrich) and a cover glass and left to dry overnight before imaging.

Representative ORO images were captured with a Nikon Eclipse Ts2 microscope using NIS-Element software. Image analysis was randomised and blinded. ORO paraffin images were analysed in ImageJ with the colour deconvolution setting. Briefly, three region of interest (ROI) sections were selected in order to separate the placental tissue, lipid droplets and background into different images. The threshold tool was used in the separate images to calculate the area in pixels^2. Lipid droplets were quantified with the analyse particles tool (settings: size 20-infinity and circularity to 0.5-1.00). Units were converted from pixels to µm with a granular ruler using a ratio of 1 pixel:0.40317378 µm. ORO imaging and analysis was performed by undergraduate student Sophia Stavrides.

Placental cryosections (5 µm) were cut by technical staff Fiona McMonagle and Tyler Shaw and stored at -80 °C until use. Cryosections were fixed in 10 % formalin for 15 min and washed in PBS for 5 min. Fixed cryosections were stained with ORO following optimised manufacturer's instructions. Briefly, sections were washed in distilled water (5 s) and stained in ORO (0.6 % v/v) for 15 min. Stained ORO slides

were washed in water (30 s) and 60 % isopropanol (30 s) before counter-staining with haematoxylin for 30 s. Slides were washed in running tap water (10 min) and mounted with an aqueous mounting medium and a cover glass and left to dry overnight. Slides were stored at -20 °C until use.

Whole cryosections were imaged using a Hamamatsu NanoZoomer® slide scanner (x40). Scanned cryosections were uploaded to QuPath for analysis. Stain vectors were selected for ORO and haematoxylin-stained areas for automated analysis and repeated for each individual scanned slide if needed. Scans were divided into different regions (depending on the size of the tissue) covering the entire tissue area, and then analysed individually. ORO and haematoxylin areas were calculated using the pixel classification function (parameters: Resolution: Full, Prefilter: Gaussian, Smoothing sigma: 1.5). Threshold parameter was changed appropriately for each slide. Automatic pixel classification was carried out for each region and data was averaged to obtain whole-scan ORO and haematoxylin areas.

2.6.3 LDLR, CSF1R and CD68 immunostaining

Placental paraffin sections were stained with low-density lipoprotein receptor (LDLR) (Santa Cruz, SC11822), polyclonal anti-human colony stimulating factor 1 receptor (CSF1R) (Chemicon, CBL776) and monoclonal anti-human macrophage cluster of differentiation 68 (CD68) (Dakoytomation, PG-M1 M0876) antibodies by Christopher Onyiaodike (LDLR) and Jack Bray (CSF1R and CD68).

The placental paraffin slides were incubated at 60 °C for 35 min and deparaffinised in xylene (2 x 10 min) and decreased concentrations of ethanol 100 %, 90 % and 70 % (2 min each). Slides were washed once in phosphate-buffered saline (PBS) (5 min) before quenching the peroxidase activity in 0.5 % H_2O_2 (Sigma) in methanol for 30 min. The slides were pretreated with 0.1 % trypsin in Tris buffer containing 0.1 % $CaCl_2$ at 37 °C for 15 min and washed in water and twice in PBS (5 min) prior to incubation with blocking agent (20 % human/20 % horse serum) in humidified box at room temperature for 30 min. Blocking serum was removed and the slides were incubated in the appropriate primary antibody (LDLR (1:10000 dilution in 3 % non-fat milk in PBS, CSF1R (1:25 dilution) in 2 % goat serum in PBS and CD68 (1:50 dilution) in 2 % horse serum in PBS) overnight at 4 °C. LDLR slides were washed in 0.05 % PBS-Tween (PBST) (6 x 10 min) and incubated in goat

polyclonal rabbit immunoglobulin G (IgG) horseradish peroxidase (HRP) conjugated secondary antibody (Abcam, Ab6721) (1:6000 dilution). CSF1R and CD68 slides were washed in PBS (2 x 5 min) and incubated in the appropriate secondary antibody (biotinylated anti-rabbit (1:200 dilution) in 2 % goat serum with 5 % human serum (PBS) for CSF1R, biotinylated anti-mouse IgG (1:200 dilution) (BA200, Vector Laboratories) in 2 % horse serum with 5 % human serum (PBS) for CD68) for 30 min at room temperature in a humidified box. After this, samples were incubated in Avidin-Biotin complex (in PBS) at room temperature for 30 min, washed in PBS (2 x 5 min) and incubated in 3,3′-diaminobenzidine (DAB) stain for 10 min at room temperature in the dark. After washing in PBS and water (5 min each), the slides were incubated in haematoxylin (15-20 s) and washed in running water. Samples were dehydrated through alcohols (70 %, 90 %, 95 %, 100 %) and xylene (5 min each) and mounted with DPX.

LDLR, CSF1R and CD68 paraffin slides were imaged by the Tissue Research Facility (Queen Elizabeth University Hospital) with a slide scanner (x40) and analysed by undergraduate student Chelsea Corney. CSF1R and CD68 whole-tissue scans were uploaded and analysed in QuPath 0.5.0 software. Stain vectors (haematoxylin and positive stain) were selected and random regions (1 mm^2) were generated automatically for individual analysis. Stained CD68 area was detected with the positive cell detection function with parameters optimised for each image. Due to the complexity of the CSF1R stain in placenta, the QuPath object classifier was trained for accurate stain detection in each scanned image. Training was performed by the observer by selecting positive and negative stain areas in the scans. LDLR scans were analysed manually by standard weighted immunohistoscoring (protocol from the Edwards lab, University of Glasgow) by one observer (with a 10 % quality check from a second observer). Briefly, the whole scan was examined by eye and areas with no staining, weak staining, moderate staining and strong staining were determined as a percentage (maximum total 100 % per image). Total score was calculated by multiplying the percentage of unstained area by 0, weak stain by 1, moderate stain by 2 and strong stain by 3. Total scores were added up for the final result, with a maximum score of 300 %.

2.7 RNA isolation and RT-qPCR

Ribonucleic acid (RNA) was extracted from placental tissue with Trizol (Life Technologies) for quantitative reverse transcription polymerase chain reaction (RT-qPCR) (details on specific volumes described in each chapter). After RNA dissociation, homogenates were combined with 0.2 ml chloroform and centrifuged at 16,200 g for 15 min at 4 ˚C to induce phase separation. The upper phase was transferred to a new tube and combined with 0.5 ml 100% isopropanol to precipitate the RNA. After a 10 min incubation, samples were centrifuged at 16,200 g for 10 min at 4 ˚C. Supernatant was decanted and the pellet was resuspended with 1 ml 70 % ethanol. Samples were centrifuged at 9,600 g for 10 min at 4 ˚C, supernatant was decanted and pellets were dried at room temperature for 10 min. Pellets were resuspended with nuclease-free water (QIAGEN) (15 µl for small pellets or 40 µl for large pellets) and incubated twice at 65 ˚C for 5 min.

RNA concentrations and purities were calculated using a NanoDrop spectrophotometer (Thermo Scientific) which read absorbance at 260 nm and 280 nm to detect nucleic acids and proteins, respectively. An absorbance ratio (260/280) of 1.7 to 2.1 was deemed sufficiently pure for experiments. RNA concentrations were used to work out dilutions needed for complementary deoxyribonucleic acid (cDNA) synthesis, a process known as reverse transcription (RT). Prior to the RT step, RNA was treated with a DNase treatment kit (Thermo Fisher Scientific) to remove DNA contamination from the samples according to manufacturer's instructions. DNase-treated RNA was used for RT reactions, which were set up in a total volume of 25 µl with 5000 ng RNA input using a cDNA Reverse Transcriptase Kit (Applied Biosystems) (reaction volumes used according to manufacturer's instructions). RT reactions were carried out in a SimpliAmp Thermal Cycler (AppliedBiosystems), following manufacturer's instructions (25 ºC for 10 min, 37 ºC for 120 min and 85 ºC for 5 s).

TaqMan quantitative polymerase chain reaction (qPCR) was carried out to quantitate expression results in RNA samples. Expression of the genes of interest was normalised to the expression of the housekeeping gene topoisomerase 1 (*TOP1*) (Cleal et al., 2009). qPCR was performed in a 96-well format and each sample was assayed in duplicate and a water and no RT control were included in

each plate as negative controls. Reactions were set up with 12.5 µl TaqMan Universal PCR Master Mix (Applied Biosystems), 10.25 µl nuclease-free water, 1.25 µl 20x TaqMan assay and 1 µl cDNA. qPCR was performed on StepOnePlus Real-Time PCR System (AppliedBiosystems) under standard TaqMan RT-qPCR thermal cycling conditions (50 °C 2 min, 95 °C 10 min then 40 cycles of 95 °C 15 s and 60 °C 1 min). TaqMan probes (Table 2) were acquired from Thermo Fisher Scientific and had a fluorescein amidite (FAM) dye label. All reactions were carried out on ice and in a RNAse-free environment.

Several RNA isolations and RT-qPCR experiments were performed by students in the Freeman lab: Louise McKenna (*GOT2*, *FABP7*, *FADS2*), Angelos Alexandropoulos (*MTHFR*, *PEMT*, *LPL*), Katie Cruikshank (*Angptl4*, *LIPC*, *LIPE*, *LIPG*), Samantha Cheng (*ELOVL2*, *ELOVL6*, *FADS1*, *SCD1*), Brecken Calhoon (*DGAT1*, *DGAT2*), Elli McMillan (*PLIN2*, *27A1*, *27A4*, *MFSD2a*), Andrew McNair (*SCD1*, *FASN*, *SREBF-1*, *SREBF-2*), Rachel Thompson (*FABP3*, *FABP4*, *FATP2*, *PLTP*, *CD36*) and Charlene Lau (*FABP2*, *FABP5*, *FABP6*, *ACSL1*, *ACSL3*, *ACSL5*, *ELOVL5*). Data from these experiments was compiled in this thesis.

Mean and standard deviation (SD) were calculated for all the cycle threshold (C_T) values from each duplicate. Assays were repeated if the SD was >1. Mean C_T values from the corresponding housekeeping genes were subtracted from the mean C_T values from the target gene. The fold change relative to the endogenous control was calculated with the $2^{-\Delta}$CT formula and expressed as a percentage.

Table 2. TaqMan probes used in RT-qPCR.

Gene symbol	Gene product	Assay ID
27A1	Solute Carrier Family 27 Member 1	Hs01587917_m1
27A4	Solute Carrier Family 27 Member 4	Hs00192700_m1
ACSL1	Acyl-CoA Synthetase Long Chain Family Member 1	Hs00960561_m1
ACSL3	Acyl-CoA Synthetase Long Chain Family Member 3	Hs00244853_m1
ACSL5	Acyl-CoA Synthetase Long Chain Family Member 5	Hs01061754_m1
ANGPTL4	Angiopoietin Like 4	Hs01101127_m1
CD36	Fatty acid translocase	Hs00354519_m1
DGAT1	Diacylglycerol O-Acyltransferase 1	Hs01017541_m1
DGAT2	Diacylglycerol O-Acyltransferase 2	Hs01045913_m1
ELOVL2	ELOVL Fatty Acid Elongase 2	Hs00214936_m1

Gene name	Gene product	Assay ID
ELOVL5	ELOVL Fatty Acid Elongase 5	Hs01094711_m1
ELOVL6	ELOVL Fatty Acid Elongase 6	Hs00225412_m1
FABP1	Fatty Acid Binding Protein 1	Hs00155026_m1
FABP2	Fatty Acid Binding Protein 2	Hs01573164_g1
FABP3	Fatty Acid Binding Protein 3	Hs00997360_m1
FABP4	Fatty Acid Binding Protein 4	Hs01086177_m1
FABP5	Fatty Acid Binding Protein 5	Hs02339439_g1
FABP6	Fatty Acid Binding Protein 6	Hs01031183_m1
FABP7	Fatty Acid Binding Protein 7	Hs00361426_m1
FADS1	Fatty Acid Desaturase 1	Hs00203685_m1
FADS2	Fatty Acid Desaturase 2	Hs00188654_m1
FASN	Fatty Acid Synthase	Hs01005622_m1
FATP2	Fatty acid transport protein 2	Hs00186324_m1
GADPH	Glyceraldehyde-3-Phosphate Dehydrogenase	Hs02786624_g1
GOT2	Glutamic-Oxaloacetic Transaminase 2	Hs00905827_g1
LIPC	Lipase C, Hepatic type	Hs00165106_m1
LIPE	Lipase E, Hormone Sensitive Type	Hs00193510_m1
LIPG	Lipase G, Endothelial Type	Hs00195812_m1
LPL	Lipoprotein lipase	Hs00173425-m1
MFSD2a	MFSD2 Lysolipid Transporter A	Hs00293017_m1
MTHFR	Methylenetetrahydrofolate Reductase	Hs00195560_m1
PEMT	Phosphatidylethanolamine N-Methyltransferase	Hs00540979-m1
PLIN1	Perilipin 1	Hs00160173_m1
PLIN2	Perilipin 2	Hs00605340_m1
PLIN3	Perilipin 3	Hs00998416_m1
PLIN4	Perilipin 4	Hs00287411_m1
PLIN5	Perilipin 5	Hs00965990_m1
PLTP	Phospholipid Transfer Protein	Hs01067287_m1
PNPLA2	Patatin Like Phospholipase Domain Containing 2	Hs00982042_m1
SCD1	Fatty Acid Desaturase	Hs01682761_m1
SREBF-1	Sterol Regulatory Element Binding Transcription Factor 1	Hs01088691_m1
SREBF-2	Sterol Regulatory Element Binding Transcription Factor 2	Hs01081784_m1
TOP1	DNA Topoisomerase I	Hs00243257_m1

2.8 Western blotting

2.8.1 Tissue lysis

Western blotting experiments were kindly performed and analysed by undergraduate student Chelsea Corney. Placental tissue (approximately 0.5 mg) was homogenised with an electric homogeniser in 300 µl lysis buffer, made up with radioimmunoprecipitation lysis buffer (RIPA) (50 mM Tris-HCl [pH 7.4], 150 mM NaCl, 1 % v/v Triton X-100, 0.5 % (m/v) sodium deoxycholate, 1 mM ethylenediaminetetraacetic acid (EDTA), 10 mM NaF in dH_2O, pH 7.4) containing a protease inhibitor cocktail tablet (Roche). Homogenisation probes were rinsed twice with 300 µl lysis buffer. Homogenates were placed on an orbital shaker at 4 °C for 2 h. Samples were centrifuged at 12,000 g for 10 min at 4 °C. Supernatants were transferred to a new tube.

2.8.2 Protein quantification

Protein content in the samples was determined with a Bradford assay in a 96-well plate format. A standard curve was generated with bovine serum albumin (BSA) (Sigma-Aldrich) standards with known concentrations ranging from 0.1 mg/ml to 1 mg/ml, with deionised water as a blank. Samples, blanks and standards (5 µl) were diluted as appropriate and added in duplicate. Bradford reagent (250 µl, Thermo Fisher Scientific) was added to each well and incubated at room temperature for 15 min. The plate was read at 595 nm in a Multiskan FC plate reader (Thermo Fisher Scientific). Protein concentrations were automatically calculated by the Multiskan software from the linear standard curve equation.

2.8.3 SDS-PAGE and blotting

Protein samples were combined with Bolt lithiumdodecylsulfate (LDS) sample buffer (Thermo Fisher Scientific) and diluted with dithiothreitol (DTT) (200 mM) at a ratio of 3:1 before heating at 70 °C for 10 min. Equal amounts of protein (15 µg) were loaded to a Bolt 12 % Bis-Tris Plus sodium dodecyl sulfate (SDS) polyacrylamide gel (15 well, Invitrogen). The Precision Plus Protein All Blue Standard (4 µl, BioRad) was used as a reference marker with known molecular weights. SDS–polyacrylamide gel electrophoresis (SDS-PAGE) was performed using the XCELL Surelock system (Thermo Fisher Scientific) with MES SDS Running Buffer

(Invitrogen). Running buffer (250 ml) with Bolt antioxidant (625 µl) were added to the inner chamber of the tank. Running buffer without antioxidant was added to the outer chamber of the tank, volume dependent on the amount of gels being run at the same time. Gel electrophoresis was performed for 40 min at 170 V.

Proteins on the gel were transferred to a nitrocellulose membrane (0.45 µm pore size, Invitrogen) sandwiched in between filter paper on a XCell II blot module (Life Technologies). The blot module was filled with Bis-Tris transfer buffer (Invitrogen) with 10% methanol and run for 1:30 h at 25 V.

After the transfer, the nitrocellulose membrane containing the proteins was incubated in 5 ml Revert 700 Total Protein Stain (LI-COR) for 5 min and washed twice briefly with LI-COR wash solution (6.7 % v/v glacial acetic acid, 30% methanol). Membranes were imaged using an Odyssey DLx Imaging System (LI-COR) at 700 nm (red channel) in order to quantify the total protein stain. The membranes were then incubated in blocking buffer (Tris-buffered saline (TBS): 2 mM Tris, 13.7 mM NaCl in dH_2O, pH 7.6, containing 5 % milk powder) for 30 min prior to overnight incubation with the human anti-FABP5 monoclonal antibody (66299-1-IG, Proteintech) diluted 1:8000 in TBS-T (TBS with 0.1 % v/v Tween 20) with 5 % BSA at 4 °C. Membranes were washed 3 x 5 min in TBS-T and incubated in 800cw donkey anti-mouse (926-68072, LI-COR) (1:10000) in 5 % BSA in TBS-T for 1 h at room temperature. The membranes were washed 3 x 5 min in TBS-T before imaging in the Odyssey Imaging System at 700 nm (red channel) and 800 nm (green channel).

Images were exported and loaded onto LI-COR Image Studio Lite software (version 5.2) for quantification. In the red channel, a rectangle was drawn around each lane in order to quantify the total protein signal. Each signal value was normalised to the highest total protein signal from the gel:

Lane Normalisation Factor (LNF) = Total protein signal from a particular lane/Lane with the highest total protein signal

In the green channel, a rectangle was drawn around the signal band from the protein of interest. Both the LNF and the target signal were used to calculate the normalised signal as:

Normalised signal = Target signal / LNF

Normalised signals were plotted and used for statistical analysis.

2.9 Statistical analysis

Statistical analyses were carried out on Minitab and/or GraphPad Prism. Data that followed a normal distribution after a Ryan-Joiner test for normality were presented as mean and standard deviation (SD) or standard error of the mean (SEM). Nonparametric data was log-transformed for analysis where possible and represented as median and interquartile range. P values were deemed significant if <0.05. Individual statistical analyses are described in each chapter.

3 Investigating the cardiovascular impact of a model of superimposed preeclampsia in the offspring

3.1 Introduction

Preeclampsia affects the later-life cardiovascular health of mothers. This is also observed in the offspring, as they are more likely to develop cardiovascular disease after being exposed to a pregnancy complicated by PE (Wojczakowski et al., 2021). This effect appears to be worsened in pregnancies where hypertension is present from an early gestational age, rather than late pregnancy (Staley et al., 2015). This highlights the importance of studying PE superimposed to a hypertension background (known as superimposed PE) in order to investigate the cardiovascular impact on the offspring, since it is associated with worsened outcomes for mother and baby (Boneh et al., 2022).

Determining the cause that leads to CVD in the offspring after a pregnancy complicated by PE remains a challenge due to the multifactorial nature of this pathology. It is likely that a combination of placental dysfunction and genetic/epigenetic factors are responsible for the phenotypes observed in the offspring. For the purposes of this study, the focus will be on discussing the developmental programming in the offspring due to exposure to the adverse intrauterine environment of a PE pregnancy. Despite the increasing incidence of PE, the short and long-term consequences of this adverse *in utero* environment remain unclear. PE is associated with FGR due to the limited nutrient delivery caused by the impaired placenta. Oxygen and nutrient deprivation lead to vascular underdevelopment, oxidative stress and adaptation in the fetus in order to direct the essential nutrients towards vital organs including the brain and heart. This is believed to “programme” the offspring for later-life cardiovascular complications (Cohen et al., 2016). This *in utero* programming has been observed in animal models and suggested in humans, which shows the relevance of animal models in the study of PE.

Meta-analysis studies investigating clinical CVD risk factors in children and young adults exposed to PE have reported an increase in blood pressure and BMI in offspring up to 30 years of age (Davis et al., 2012). Early echocardiography studies

performed on babies born at term after maternal hypertension have shown differences in cardiac development including reduced heart chamber volumes and increased right and left ventricular mass with no functional impact compared to babies born after healthy pregnancies after a 3-month follow-up (Aye et al., 2020). Adults born after PE pregnancies show early signs of left ventricular systolic dysfunction and heart failure compared to adults born after preterm normotensive pregnancies (Lewandowski et al., 2013). This evidence suggests that the unique *in utero* exposure to PE may programme the impaired development of the heart and consequently leading to cardiac dysfunction later in life.

The rat presents analogous pregnancy features to humans that make it an ideal model to study pregnancy and the development of the offspring *in vivo*. Offspring exposed to the placental insufficiency caused by the reduced uterine perfusion from the RUPP rodent model have been shown to develop hypertension and arterial dysfunction from an early age (Alexander, 2003; Anderson et al., 2006). This evidence is analogous to the phenotype observed in children born from pregnancies complicated by PE, however, this model does not allow the study of the mechanisms that lead to the formation of the dysfunctional placenta as the reduced perfusion takes place after this organ is formed. Other animal models of hypoxia (which has been shown to induce PE-like phenotypes) have produced offspring with altered vascular and cardiac phenotypes such as aortic wall thickening, increased cardiac mass and ventricular dilation (Davis et al., 2012).

A novel model of superimposed preeclampsia in the pregnant SHRSP rat has been previously published by our group (Morgan et al., 2018). Briefly, the infusion with 500ng/kg/min and 1000ng/kg/min of angiotensin II (ANGII) on GD 10.5 increases blood pressure in the pregnant SHRSP dam, which results in mild or extreme PE phenotypes, respectively. Further investigations performed by Dr Kayley Scott have shown that the infusion of 750ng/kg/min ANGII to the pregnant SHRSP rat is able to mimic the increase in blood pressure in the dam as well as growth restriction in the offspring, characteristic of the human PE phenotype (personal communication). This model presents advantages compared to other rodent models of PE because it allows the study of the development of PE on a hypertensive background and the investigation of the onset of the dysfunctional placenta. However, the impact of this uterine environment on the later-life

cardiovascular state of the offspring have not yet been studied. For this reason, this chapter will discuss the phenotypic characterisation of the offspring exposed to a hypertensive intrauterine environment using the ANGII rat model of superimposed PE.

It is important to note that the study of offspring up to 17/18 weeks of age is comparable to studying humans in their emerging adulthood stage (between 18 and 25 years old) (Ghasemi, Asghar; Sajad, 2021) and therefore strong indices of cardiovascular disease are not expected at this stage, regardless of their intrauterine environment. In addition, the study of offspring at 5/6 weeks would be equivalent to children between 11 and 14 years old (Ghasemi, Asghar; Sajad, 2021), which allows the study of different parameters prior to sexual maturity.

3.1.1 Hypothesis and aims

The main hypothesis was that dams treated with 700 ng/kg/min will have an elevated blood pressure and proteinuria compared to controls and that the offspring born after intrauterine ANGII exposure will show a decrease in cardiovascular function and elevated circulating lipids compared to untreated SHRSP and WKY. The main aims were:

-To confirm the “preeclampsia-like” phenotype exhibited by the ANGII-treated SHRSP dams through blood pressure measurements, proteinuria and gestation length.

-To carry out a long-term study on the offspring from ANGII-treated dams vs vehicle controls and WKY, which includes:

> -Investigating the cardiovascular function differences between offspring born after ANGII exposure compared to SHRSP controls and WKY offspring from the juvenile stage to adulthood.
>
> -Measuring the plasma lipids differences between offspring born after ANGII exposure compared to SHRSP controls and WKY offspring during development to adulthood.

-Assessing the organ weights and vascular function differences between offspring born after ANGII exposure compared to SHRSP controls and WKY offspring in adulthood.

-Should there be any differences between ANGII-exposed offspring and vehicle controls and WKY, a short-term study on cardiovascular function, plasma lipids and organ weights will be carried out in order to observe the effects in the juvenile stage only.

3.2 Materials and methods

SHRSP and WKY rats were maintained and time-mated as described in the materials and methods chapter (section 2.1.1). At pre-pregnancy (PP), SHRSP and WKY females were placed in metabolic cages in pairs for a 1-hour acclimatisation period. The following week, they underwent tail-cuff plethysmography and a 24h metabolic cage assessment, as described in sections 2.1.3 and 2.1.6. After pregnancy confirmation, the dams underwent tail-cuff plethysmography at week 1 of pregnancy (W1P). At GD 10.5, an osmotic minipump was implanted subcutaneously as in section 2.1.2. Dams were checked daily post-surgery for signs of pain and weight loss and were given soft and/or baby food during the first few days post-surgery. At week 3 of pregnancy (W3P), the dams underwent tail-cuff plethysmography and a 24h metabolic cage assessment. After birth, the litters were assigned to the short-term (sacrificed at 6 weeks of age) or the long-term study (sacrificed at 18 weeks of age) (Figure 3-1) and reduced to n=3/sex or n=2/sex, respectively. All the pups were weighed, and any extra ones were used for tissue collection as described in section 2.1.7.2.

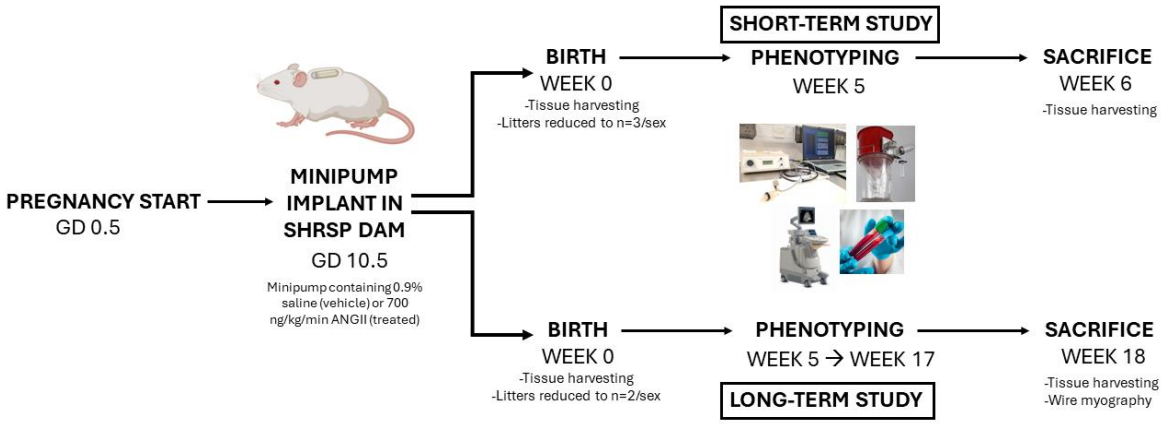

Figure 3-1. Study timeline for long and short-term experiments. Short-term study (top) consisted of offspring phenotyping including blood pressure measurements, metabolic cage collection and echocardiography at week 5 of age. Animals were sacrificed on week 6 of age, and tissues and blood samples were harvested. Long-term study (bottom) consisted of offspring phenotyping including blood pressure measurements, metabolic cage collection, echocardiography and blood sampling by venepuncture from week 5 to 17 of age. Animals were sacrificed on week 18 of age, and tissues and blood samples were harvested.

Offspring were kept with their mother until weaning (approximately at 4 weeks old). After weaning, offspring were placed in different cages separated by sex and the mothers were sacrificed for tissue collection as described in section 2.1.7.1. Juvenile offspring (post-weaning) were placed in metabolic cages in pairs for a 1-hour acclimatisation period. At 5 weeks of age (W5), offspring underwent tail-cuff plethysmography, cardiac and mitral valve echocardiography, and a 24h metabolic cage assessment, as described in sections 2.1.3, 2.1.4 and 2.1.6, respectively. It is important to note that in all of the SHRSP offspring echocardiography measurements were carried out with the Acuson Sequoia c256 system and analysed on ImageJ, whereas most of the WKY offspring measurements were carried out with the VEVO F2 system and analysed on the Vevo Lab Software. This is because the older Acuson Sequoia ultrasound machine stopped functioning before the completion of this study, and it was substituted for the newer VEVO F2 machine.

Animals in the short-term study group were sacrificed at 6 weeks of age (described in section 2.1.7.1) and heart, kidney, thoracic aorta and gonadal fat tissues were collected and weighed and flash frozen in liquid nitrogen. Lungs, liver and retroperitoneal fat were also dissected and discarded after weighing. Blood samples were also collected by cardiac puncture (described in section 2.1.7.1) and centrifuged for plasma separation. Tissue and plasma samples were stored at -80°C until use. Offspring in the long-term study group underwent tail-cuff plethysmography (biweekly), echocardiography (monthly), 24-hour metabolic

cage assessment (monthly) and tail vein blood sampling (only at weeks 9 and 13 of age). At W18, the offspring were sacrificed for tissue collection as described previously. Total fat pad weight was calculated by the addition of the gonadal and retroperitoneal fat weights. Rat intestines were also harvested at this point and placed in a sterile tube with PSS on ice for mesenteric artery isolation for wire myography (described in section 2.2).

3.2.1 Statistical analysis

Statistical analysis was performed using a mixed effects model or a general linear model, depending on whether age was included as a co-variate or not, respectively. Mixed effects models include random and fixed effects which address the statistical impact of individual animals through the repeated measurements. This avoids including bias that could be affecting the fixed variables of interest, such as sex or treatment group. In the offspring experiments, rat ID was included as a random factor to account for repeated measures and sex and age at sampling and treatment were inputted as fixed effects. In the mothers' experiments, rat ID was included as a random factor to account for repeated measures and gestation at sampling and treatment were inputted as fixed effects. As the outcome variables investigated in this study are known to be impacted by age and gestation at sampling e.g. BP is higher on older compared to younger rats, and this was not the primary focus of the current analysis, they were not reported in this chapter to allow better interpretation of the effects of interest. Results for treatment group effect (P_{GROUP}) and sex effect (P_{SEX}) were reported. These P values indicate whether there was a significant effect of treatment or sex overall. If there was a significant effect for treatment, *post hoc* testing was carried to identify between which groups the difference laid. Interactions between sex and treatment were also included in the model, which indicated specific sex differences within treatment groups. In this case, results for interaction effects were reported (P_{INTER}). If an interaction term was significant, *post hoc* testing was carried out to identify within which treatment group the sex difference laid. In addition, a mixed effects model does not require all groups to have the same sample number and it can handle missing data, as opposed to a repeated measures analysis of variance (ANOVA).

General linear models have the same assumptions as the mixed effect models, but they are not suitable for repeated measures, therefore these tests were used for analysing variables studied at one time-point only (including wire myography data and tissue weights) where the factors included were sex and treatment. If a sex difference was found, offspring groups were presented separately but if there was no sexual dimorphism, results were presented together. Importantly, both models operate under the assumption that the regression residuals are normally distributed, which can be examined by qualitative assessment of the quantile-quantile (QQ) plots. If residuals did not follow a normal distribution, a new analysis was performed on log-transformed data. Neonatal characteristics and body weights were analysed by a one-way ANOVA. All statistical tests were followed by *post hoc* Tukey test if significant. Statistical analyses were performed on Minitab software version 21.4.3. Statistical significance was assumed at $P<0.05$.

3.3 Results

3.3.1 Phenotypic characterisation of the PE phenotype in dams

Systolic blood pressure was measured in the SHRSP and WKY females at PP, W1P and W3P (Figure 3-2). No significant differences were found between groups.

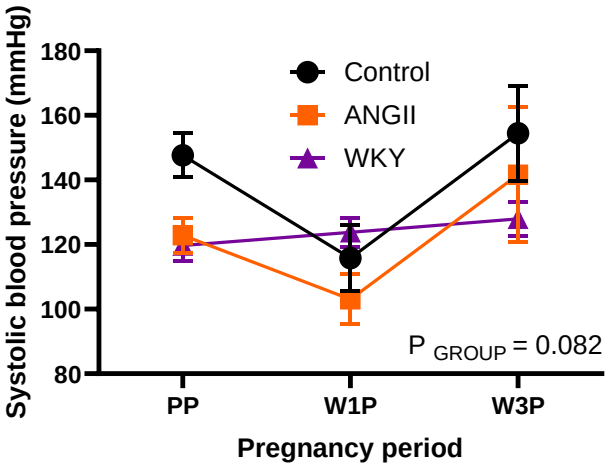

Figure 3-2. Systolic blood pressure in SHRSP ANGII, control and WKY females before and during pregnancy. Measurements obtained by tail-cuff plethysmography at PP, W1P and W3P. Data presented as mean ±SEM (n=5-8 per group) where individual females represent each data point. Analysis was carried out using a mixed effects model SBP vs treatment and pregnancy period with Tukey *post hoc* test; significance at $P<0.05$.

Urine albumin and creatinine concentrations were measured in SHRSP vehicle and ANGII and WKY females at PP and W3P (Figure 3-3). No significant differences were found between groups.

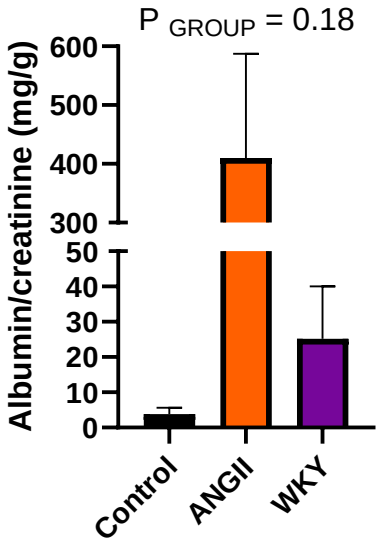

Figure 3-3. Albumin/creatinine ratios in the urine of the SHRSP control, ANGII and WKY females during pregnancy. Metabolic cages were used to collect urines for 24h at W3P. Albumin to creatinine ratios are presented in this figure. Data is shown as mean ±SEM (n=3-4 per group) where individual females represent each data point. Analysis was carried out using a Kruskal-Wallis test; significance at P<0.05.

Gestation duration (in days) in the SHRSP dams exposed to ANGII and vehicle control and WKY (Figure 3-4) was also investigated since pre-term delivery is common in the human PE phenotype. No significant differences were found between groups.

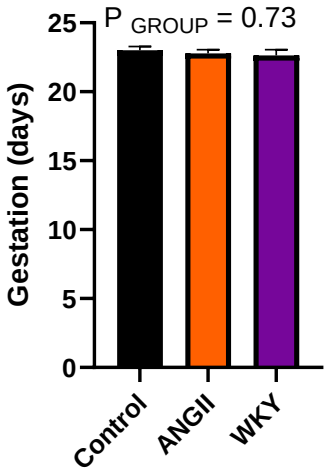

Figure 3-4. Length of gestation in the SHRSP ANGII, control and WKY pregnancies. Gestation (days) was calculated from the day when the copulation plug was found to the day when the litter was born. Data presented as mean ±SEM (n=8-9 per group) where individual pregnancies represent each data point. Analysis was carried out using a one-way ANOVA with Tukey *post hoc* test; significance at P<0.05.

3.3.2 Impact of the intrauterine environment on the neonates

After birth, neonates were weighed between 1 and 8 days of age and the litters were reduced to n = 2/sex or n = 3/sex for the long or short-term study, respectively. Results were separated into weights from 1 to 4 days of age (Figure 3-5A) and from 5 to 8 days of age (Figure 3-5B). At 1 to 4 days of age, ANGII neonates were significantly smaller than the SHRSP vehicle control and WKY neonates (5.11 ± 0.05 vs 6.00 ± 0.12 and 6.69 ± 0.38 g; P<0.001 for both) and SHRSP control were smaller than WKY neonates (P=0.014). In contrast, at 5 to 8 days of age ANGII neonates were significantly heavier than SHRSP vehicle control and WKY neonates (10.76 ± 0.40 vs 9.24 ± 0.41 and 7.83 ± 0.21 g; P=0.015 and P<0.001, respectively) and there were no differences between SHRSP control and WKY (P=0.081). Harvested heads from the sacrificed neonates were weighed and head to body ratios were calculated (Figure 3-6A). Original litter sizes were also recorded to investigate the impact of the ANGII treatment on the number of pups produced by the mothers (Figure 3-6B). No significant differences in either head to body ratio or litter size were found between groups.

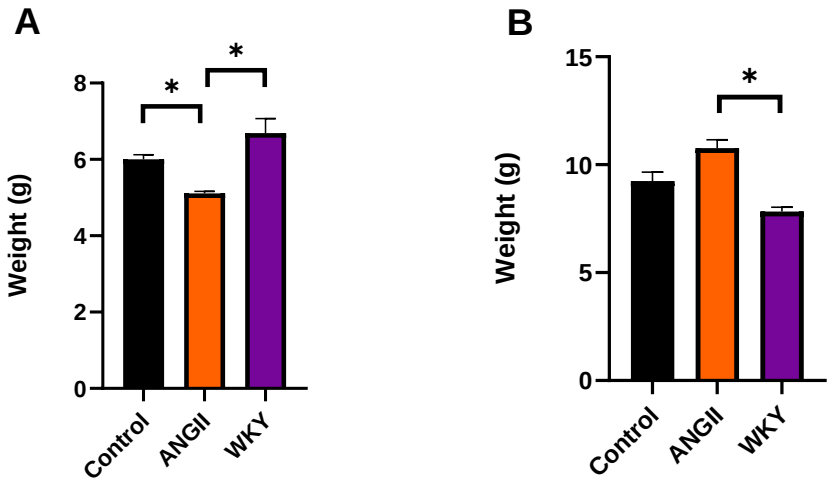

Figure 3-5. Neonatal weights from offspring born from SHRSP control, ANGII and WKY females. (A) Weights from 1–4-day-old offspring exposed to ANGII or vehicle control during pregnancy. (B) Weights from 5–8-day-old offspring exposed to ANGII or vehicle control during pregnancy. Data is shown as mean ±SEM where individual offspring represent each data point (n=13-114). Analysis was carried out using a one-way ANOVA with Tukey *post hoc* test; significance at *P<0.05.

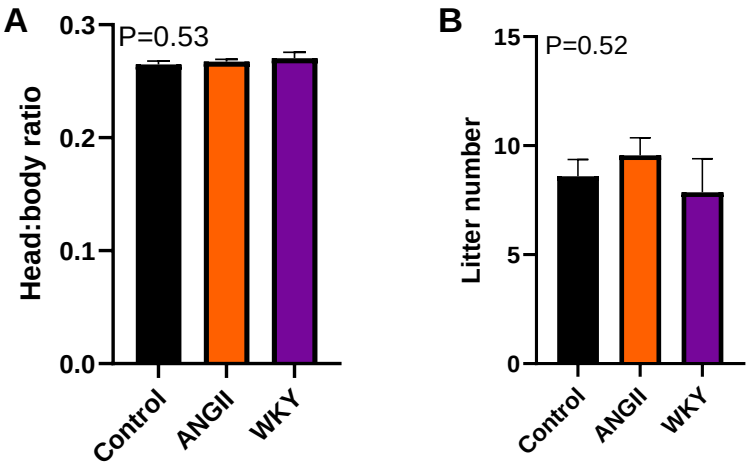

Figure 3-6. Neonatal characteristics from offspring born from SHRSP control, ANGII and WKY females. (A) Head to body ratio from offspring (1-8 days old) exposed to ANGII or vehicle control during pregnancy. (B) Litter size from dams exposed to ANGII or vehicle control during pregnancy. Data described as mean ±SEM where individual pups (n=21-44) or litter numbers (n=7-10) represent each data point. Analysis was carried out using a one-way ANOVA with Tukey *post hoc* test; significance at P<0.05.

3.3.3 Impact of the intrauterine environment on offspring body weight from the juvenile state to adulthood

Body weight was measured at the time of echocardiography measurements at weeks 5, 9, 13 and 17 of age (Figure 3-7). Average WKY offspring weight was significantly higher than SHRSP vehicle and ANGII (179.90 ± 10.70 vs 175.39 ± 9.32 and 176.46 ± 7.98 g; P=0.017 and 0.0080, respectively). There were no differences between SHRSP vehicle and ANGII offspring (P=0.98). Sex differences were observed as the average male body weight was higher than females (211.49 ± 8.57 vs 144.52 ± 4.50 g; P<0.001). There were no sex*treatment group interactions ($P_{INTER.}$=0.62).

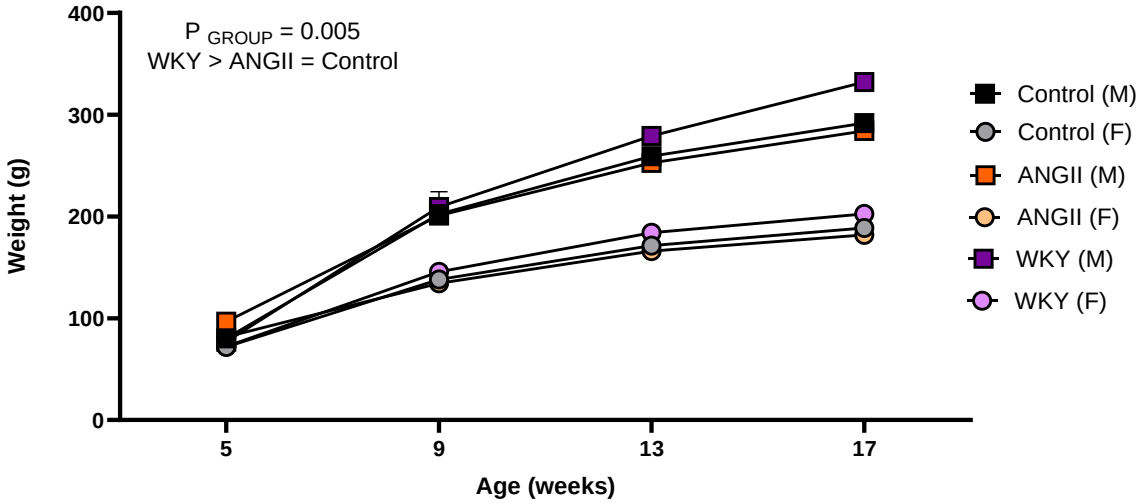

Figure 3-7. Body weight measurements in control, ANGII and WKY offspring. Measurements obtained at 5, 9, 13 and 17 weeks of age. Data presented as mean ±SEM (n=8-10 per group) where individual offspring represent each data point. Analysis was carried out using a mixed effects model body weight vs treatment, sex and age with Tukey *post hoc* test; significance at P<0.05.

3.3.4 Organ weights

Whole hearts, left ventricles (LVs), lungs, kidneys, livers and gonadal and retroperitoneal fat from the adult offspring were harvested and weighed and corrected to tibia length (Figure 3-8). Heart, LV, kidneys, gonadal fat and total fat mass indexes were significantly lower in the WKY offspring compared to both SHRSP offspring groups (Figure 3-8A). Sex differences were observed as males had larger organs compared to females (Figure 3-8B). There were no sex*treatment group interactions ($P_{INTER.} > 0.05$).

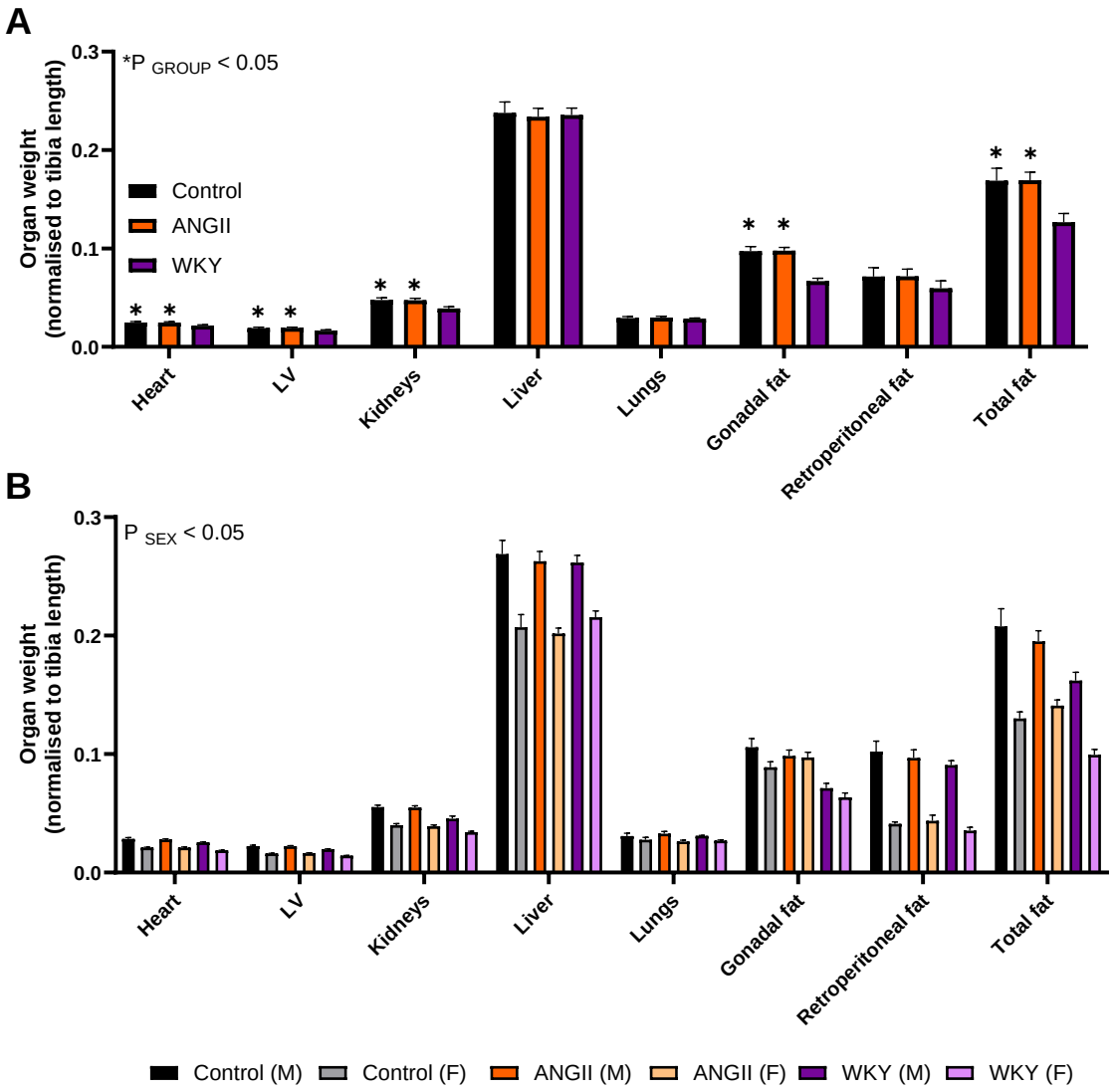

Figure 3-8. Dissected organ weights normalised to tibia length from WKY, and SHRSP control and ANGII-exposed offspring. Data is shown as all the offspring together (n=16-19 per group) (A) and separated by sex (n=7-10) (B). Data is shown as mean ±SEM where individual offspring represent each data point. Data was analysed by a general linear model organ weight:tibia length vs sex and treatment group. *P<0.05 (vs WKY) with Tukey *post hoc* test.

3.3.5 Systolic blood pressure measurements

Systolic blood pressure (SBP) was measured on the offspring born from WKY, SHRSP vehicle control and ANGII-treated mothers at 5, 7, 9, 11, 13, 15 and 17 weeks of age (Figure 3-9A). No significant differences were found between SHRSP vehicle control and ANGII offspring (149.0 ± 2.9 vs 147.2 ± 2.7 mmHg; P=0.9), however the BP measurements of both these groups were significantly higher compared to their normotensive WKY counterparts (130.7 ± 2.3 mmHg; P<0.001 for difference between both WKY and control, and WKY and ANGII groups). An overall sex effect was not observed when comparing the values between weeks 5 and 17 of age (144.15 ± 2.49 vs 141.05 ± 1.97 mmHg; P=0.37), however sex differences were

present when comparing the offspring groups at the adulthood stage after sexual maturity had taken place (week 17 of age) (males: 162.52 ± 4.89 vs females: 145.91 ± 5.73; P=0.026) (Figure 3-9B). There were no sex*treatment group interactions ($P_{INTER.}$=0.61).

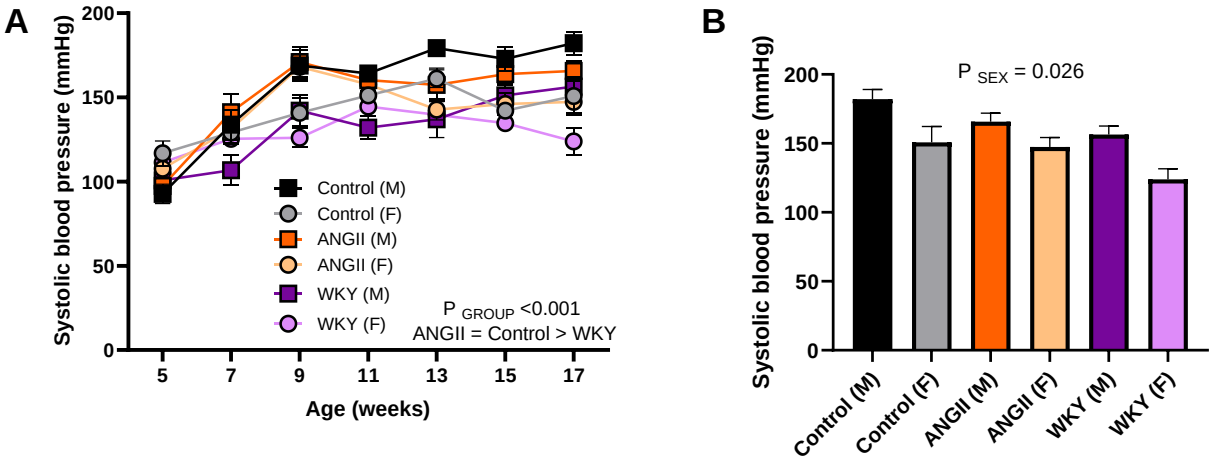

Figure 3-9. Systolic blood pressure in control, ANGII and WKY offspring. Measurements obtained by tail-cuff plethysmography at 5, 7, 9, 11, 13, 15 and 17 weeks of age. BP is presented from a juvenile stage until adulthood (**A**) and at adulthood only (**B**). Data presented as mean ±SEM (n=8-10 per group) where individual offspring represent each data point. Analysis was carried out using a mixed effects model SBP vs treatment, sex and age (A) and general linear model vs treatment and sex (B) with Tukey *post hoc* test; significance at P<0.05.

3.3.6 Cardiac function in the offspring

Echocardiography was performed on all the offspring groups at 5, 9, 13 and 17 weeks of age in order to investigate differences in cardiac function and blood flow. The images obtained were used to calculate the measurements shown in Figure 3-10 and Figure 3-11. Left ventricular mass index (LVMI, LVM:body weight) was not different between SHRSP ANGII and control (3.05 ± 0.08 vs 2.80 ± 0.13; P=0.14), but ANGII was different from WKY offspring (2.66 ± 0.09; P=0.004) (Figure 3-10A). Fractional shortening (FS) was significantly increased in the SHRSP vehicle control offspring compared to SHRSP ANGII and WKY (Control: 52.12 ± 0.95 vs ANGII: 48.51 ± 0.97 and WKY: 45.94 ± 1.09 %; P=0.027 and P<0.001, respectively) (Figure 3-10B). SHRSP vehicle control offspring showed the highest relative wall thickness (RWT), which was significantly different to SHRSP ANGII and WKY offspring (Control: 0.58 ± 0.025 vs ANGII: 0.51 ± 0.0038 vs WKY: 0.45 ± 0.0034 mm; Control vs ANGII, P=0.024; Control vs WKY, P<0.001; WKY vs ANGII, P=0.010) (Figure 3-10C). In addition, stroke volume (SV) was significantly increased in the ANGII offspring compared to WKY offspring (0.24 ± 0.040 vs 0.19 ± 0.030 ml; P=0.007), but not SHRSP vehicle control (0.20 ± 0.050 ml; P=0.051) (Figure 3-10D).

Cardiac output (CO) was significantly increased in the ANGII offspring compared to controls (61.43 ± 8.88 vs 53.15 ± 12.16 ml/min; P=0.044) but was not different from WKY (58.42 ± 9.76 ml/min; P=0.85) (Figure 3-10E). Males had a significantly higher SV (0.25 ± 0.012 vs 0.18 ± 0.0075 ml; P<0.001) and CO (65.06 ± 2.87 vs 51.48 ± 1.97 ml/min; P<0.001) compared to females, but they had smaller LVMI (2.67 ± 0.08 vs 0.84 ± 0.08; P<0.001). Ejection fraction (EF) was significantly lower in WKY compared to SHRSP ANGII and vehicle control (WKY: 79.44 ± 1.89 vs ANGII: 84.45 ± 1.48 and Control: 86.63 ± 1.27 %, P<0.001 for both) (Figure 3-10F). There were no sex*treatment group interactions ($P_{INTER.}$>0.05).

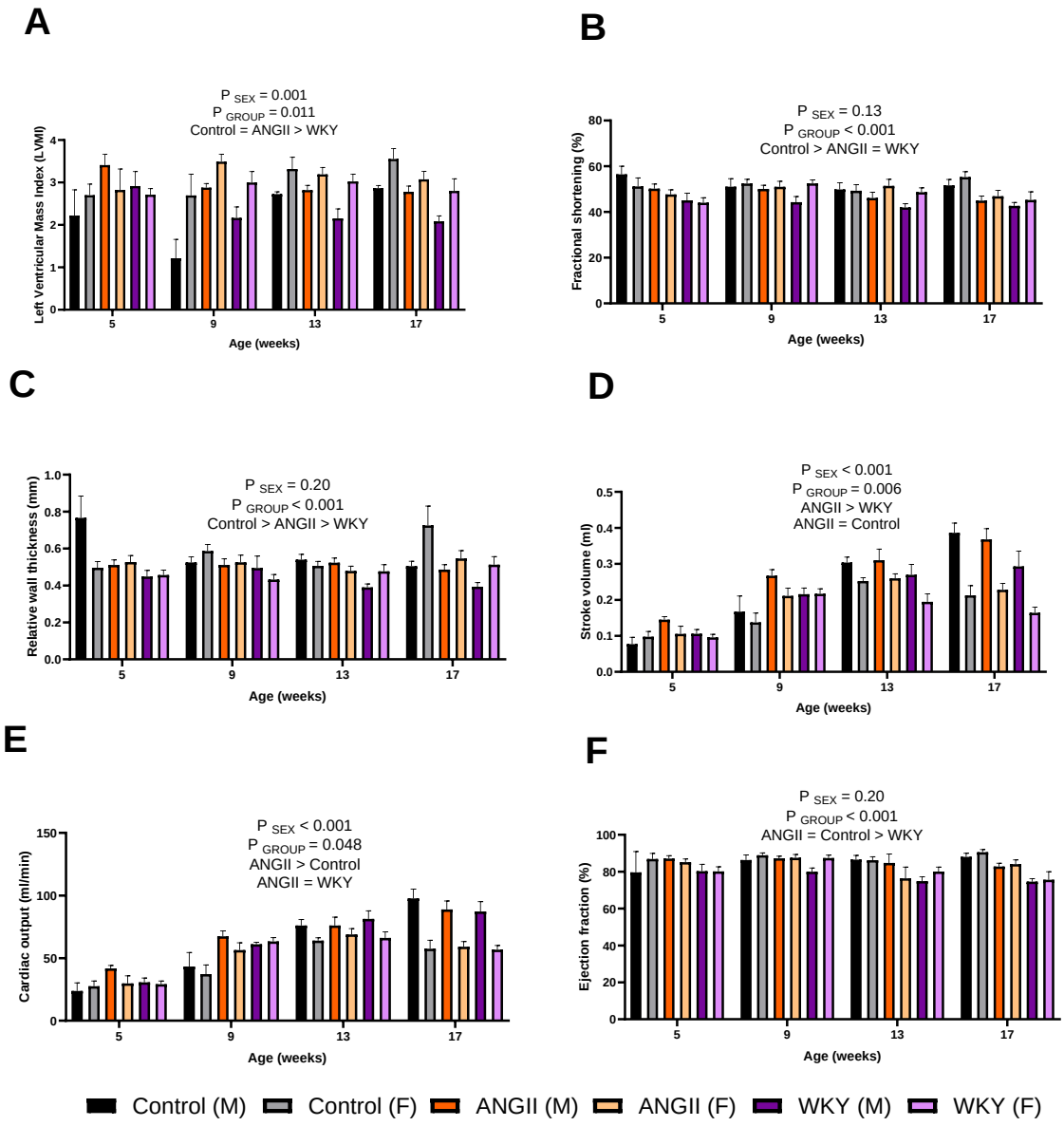

Figure 3-10. M-mode echocardiography measurements from SHRSP control, ANGII and WKY offspring. Data presented as left ventricular mass index normalised to body weight (A), FS (B), RWT (C), SV (D), CO (E) and EF (F). Data presented as mean ±SEM (n=8-10 per group) where individual offspring represent each data point. Data was analysed by a mixed effects model vs sex, age and treatment group with Tukey *post hoc* test; significance at P<0.05.

Mitral valve flow measurements including the early (E) to late (A) velocities ratio (E/A) and the myocardial performance index (MPI), which was calculated from the isovolumetric constriction time (IVCT), LV ejection time (ET) and isovolumetric relaxation time (IVRT), are represented in Figure 3-11. The E/A ratio was significantly increased in the ANGII offspring compared to SHRSP vehicle control and WKY (ANGII: 1.94 ± 0.055 vs Control: 1.53 ± 0.041 vs WKY: 1.40 ± 0.021; P<0.001 for both) (Figure 3-11A). No significant differences were observed in MPI between groups (Figure 3-11B). No sex differences were found in either of these parameters. There were no sex*treatment group interactions ($P_{INTER.}$>0.05).

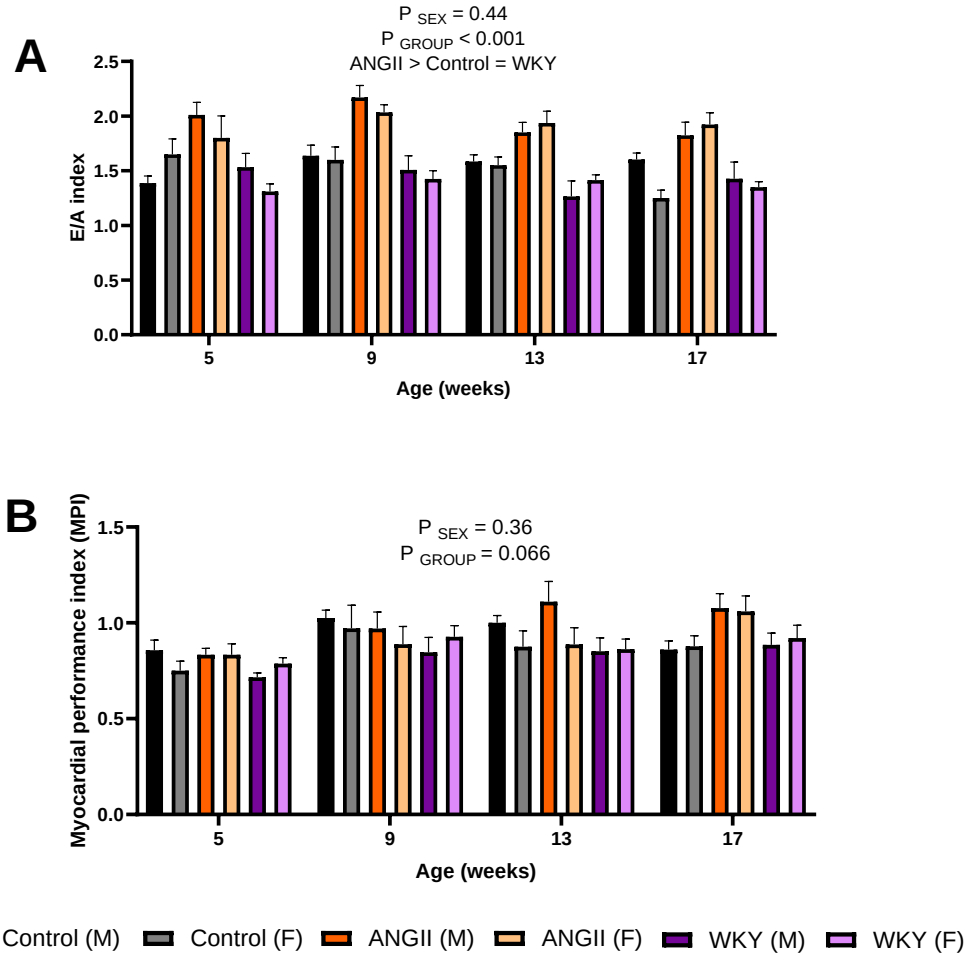

Figure 3-11. Doppler echocardiography measurements from SHRSP control, ANGII and WKY offspring. Data presented as E/A ratio (A) and MPI (B). Data presented as mean ±SEM (n=8-10 per group) where individual offspring represent each data point. Data was analysed by a mixed effects model vs sex, age and treatment group with Tukey *post hoc* test; significance at P<0.05.

3.3.7 Fluid homeostasis and proteinuria

Water intake and urine output were recorded after a 24h period on the offspring at 5, 9, 13 and 17 weeks of age (Figure 3-12). Water intake was significantly higher in the WKY offspring compared to the ANGII-exposed offspring (28.8 ± 1.5 vs 23.8

± 0.9 ml; P=0.006), but not the SHRSP vehicle group (26.7 ± 1.0 ml; P=0.10) (Figure 3-12A). Similarly, the urine output was significantly higher in the WKY offspring compared to the ANGII offspring (12.7 ± 1.3 vs 9.7 ± 0.7 ml; P=0.032), but not compared to the SHRSP control offspring (10.3 ± 0.8 ml; P=0.13) (Figure 3-12B). However, there were no significant differences in the urine excretion corrected for water intake (Figure 3-12C). Water intake was significantly higher in males compared to females (27.8 ± 1.0 vs 24.8 ± 0.9 ml; P=0.011), which consequently led to a decreased output:intake ratio in the males (34.6 ± 1.6 vs 41.4 ± 1.7 ml; P=0.001). There were no sex*treatment group interactions ($P_{INTER.}$>0.05).

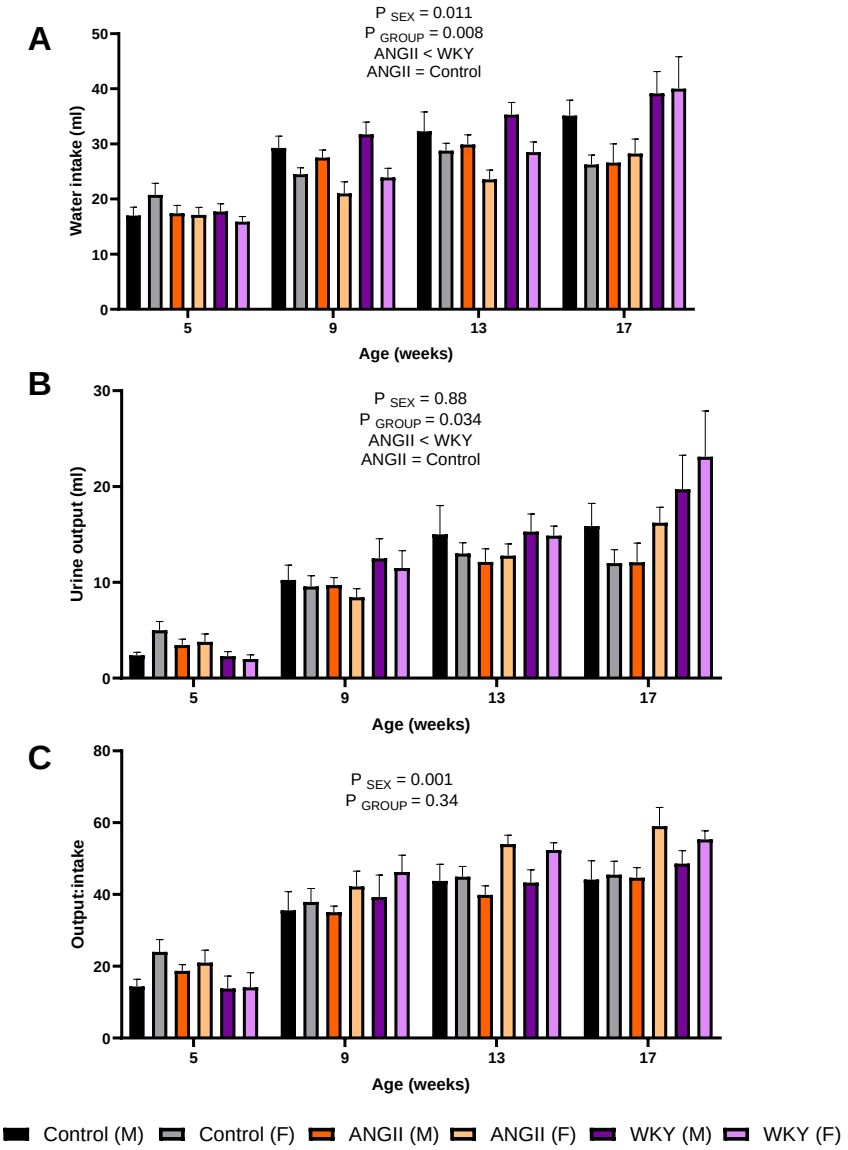

Figure 3-12. Fluid homeostasis of the SHRSP control, ANGII and WKY offspring. Metabolic cages were used to collect data on 24h water intake (A) and urine output (B) in the different offspring groups at 5, 9, 13 and 17 weeks of age. Urine output was corrected to water intake to give an estimation of fluid homeostasis (C). Data is shown as mean ±SEM (n=8-10 per group) where individual offspring represent each data point. Data was analysed by a mixed effect model water intake, urine output or output:intake percentage vs sex, age and treatment group with Tukey *post hoc* test; significance at P<0.05.

Urine output was collected at 5, 9, 13 and 17 weeks of age and it was used to measure the albumin/creatinine ratio which is a marker of kidney damage (Figure 3-13). No significant differences were observed between groups. Males showed significantly higher ratios compared to females (13.55 ± 1.64 vs 7.92 ± 0.99; P<0.001). A sex*treatment interaction was found ($P_{INTER.}$<0.001), where WKY females had significantly higher albumin/creatinine ratios compared to SHRSP control and ANGII females (10.32 ± 10.81 vs 3.46 ± 3.47 and 3.26 ± 2.84; P<0.001 for both) and SHRSP control males had significantly higher ratios compared to WKY males (15.62 ± 8.09 vs and 6.25 ± 5.83; P=0.037).

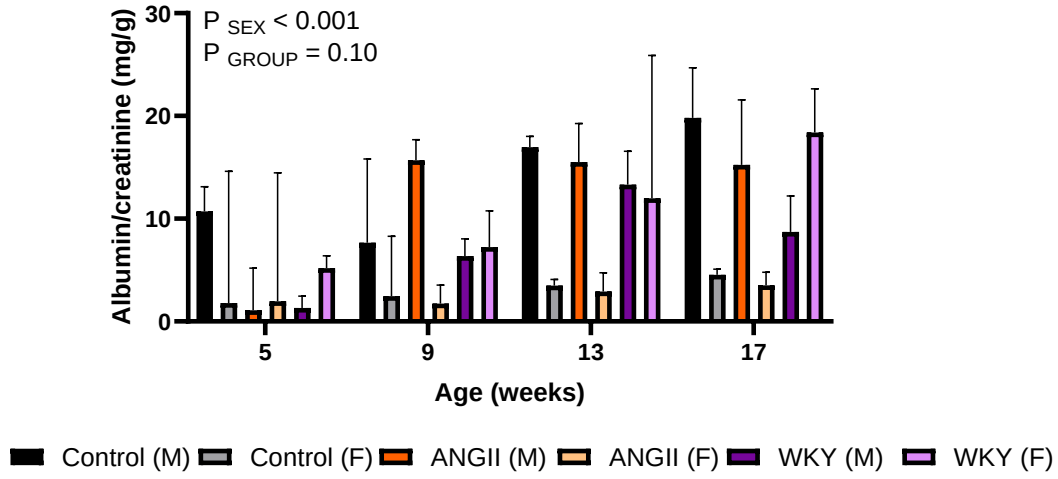

Figure 3-13. Urine albumin/creatinine ratios of the SHRSP control, ANGII and WKY offspring. Metabolic cages were used to collect the urine output of the offspring at 5, 9, 13 and 17 weeks of age for 24h. Data is shown as median ± interquartile range (IQR) (n=8-10 per group) where individual offspring represent each data point. Data was analysed on log-transformed data by a mixed effect model albumin/creatinine vs sex, age and treatment group with Tukey *post hoc* test; significance at P<0.05.

3.3.8 Mesenteric artery function

Mesenteric arteries were isolated from adult rat intestines and mounted onto myographs for functional assessment by wire myography (Figure 3-14). Mesenteric arteries from the offspring exposed *in utero* to ANGII showed a trend towards increased contraction in response to NA compared to the WKY group, which was not significant on *post hoc* Tukey comparisons testing (AUC = 173.4 ± 19.0 vs 118.8 ± 16.7 mN·M; P=0.084) (Figure 3-14A). The effect of NA at half maximal effective concentration (EC_{50}) was significantly lower in the ANGII offspring compared WKY ($7.36x10^{-7}$ ± $1.31x10^{-7}$ vs $1.85x10^{-6}$ ± $4.01x10^{-7}$; P=0.015) (Figure 3-14B), which indicates a faster contraction in response to NA. This higher vasocontraction reaction to NA was further confirmed by the significantly higher maximal response

to NA in the mesenteric vessels from ANGII offspring compared to WKY (156.7 ± 12.3 vs 116.6 ± 8.3 %; P=0.023) (Figure 3-14D). In contrast, vasodilation reactions to SNP and Cch did not differ between groups (Figures 3-14C, E-G). Both male and female offspring data are presented together as sex differences were not observed in any of the studied parameters ($P_{SEX.}$>0.05). There were no sex*treatment group interactions ($P_{INTER.}$>0.05).

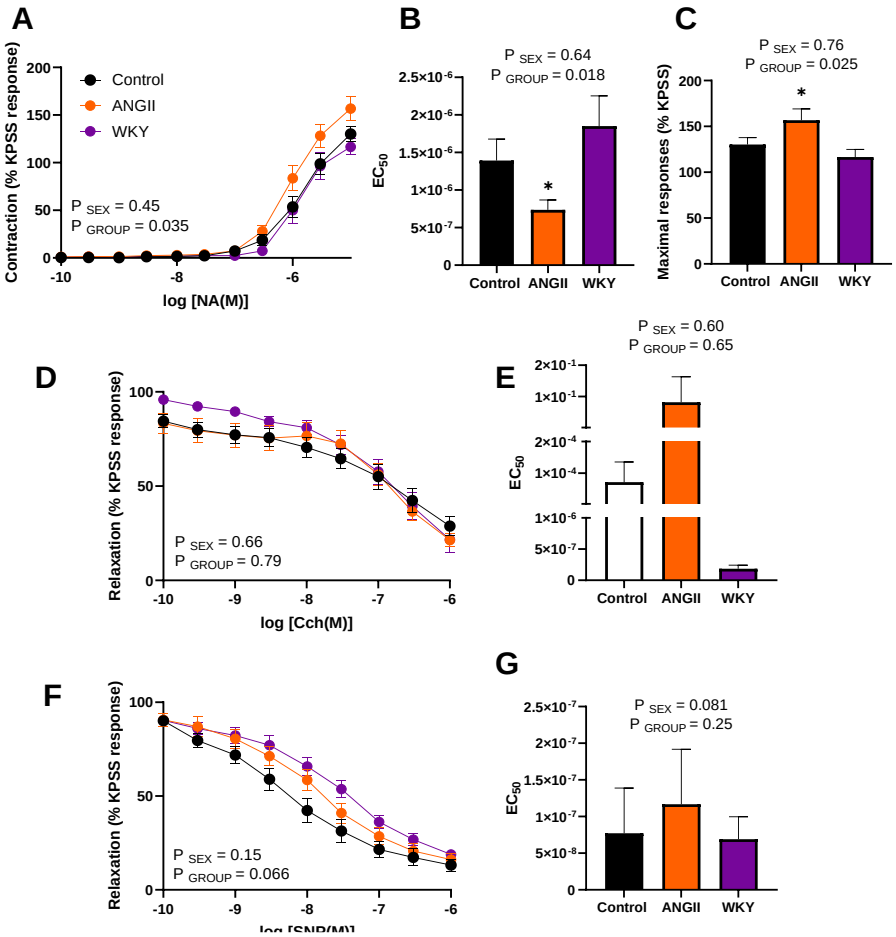

Figure 3-14. Vessel function wire myography analysis of mesenteric arteries from WKY and SHRSP control and ANGII-exposed offspring. Mesenteric artery response to NA is presented as area under the curve (A), half maximal effective concentration (EC_{50}) (B) and maximal responses (C). Mesenteric artery response to carbachol (CCh) is presented as area under the curve (D) and EC_{50} (E). Mesenteric artery response to sodium nitroprusside (SNP) is presented as area under the curve (F) and EC_{50} (G). Data is shown as mean ±SEM (n=12-18 per group) where individual offspring represent each data point. Data was analysed by a general linear model of AUC, EC_{50} and maximal responses vs sex and treatment group *(P<0.05 vs WKY) with Tukey *post hoc* test.

3.3.9 Plasma lipids

Plasma triglycerides and total cholesterol were measured in the offspring's plasma at weeks 9, 13 and 18 of age (Figure 3-15). WKY offspring had a significantly lower concentration of plasma triglycerides compared to their SHRSP control and ANGII counterparts (0.74 ± 0.035 vs 1.12 ± 0.059 and 1.03 ± 0.041 mmol/L respectively; P<0.001 and P=0.002) (Figure 3-15A). Interestingly, this effect was accompanied

by a higher value of total cholesterol in the plasma from WKY offspring compared to the SHRSP groups (WKY: 2.36 ± 0.055 vs control: 1.88 ± 0.051; P<0.001 and ANGII: 1.87 ± 0.041 mmmol/L; P<0.001) (Figure 3-15B). Triglycerides were higher in males compared to females (1.09 ± 0.041 vs 0.84 ± 0.035 mmol/L; P<0.001). In contrast, males had a lower plasma cholesterol content compared to females (1.89 ± 0.049 vs 2.19 ± 0.041 mmol/L; P<0.001). There were no sex*treatment group interactions ($P_{INTER.} > 0.05$).

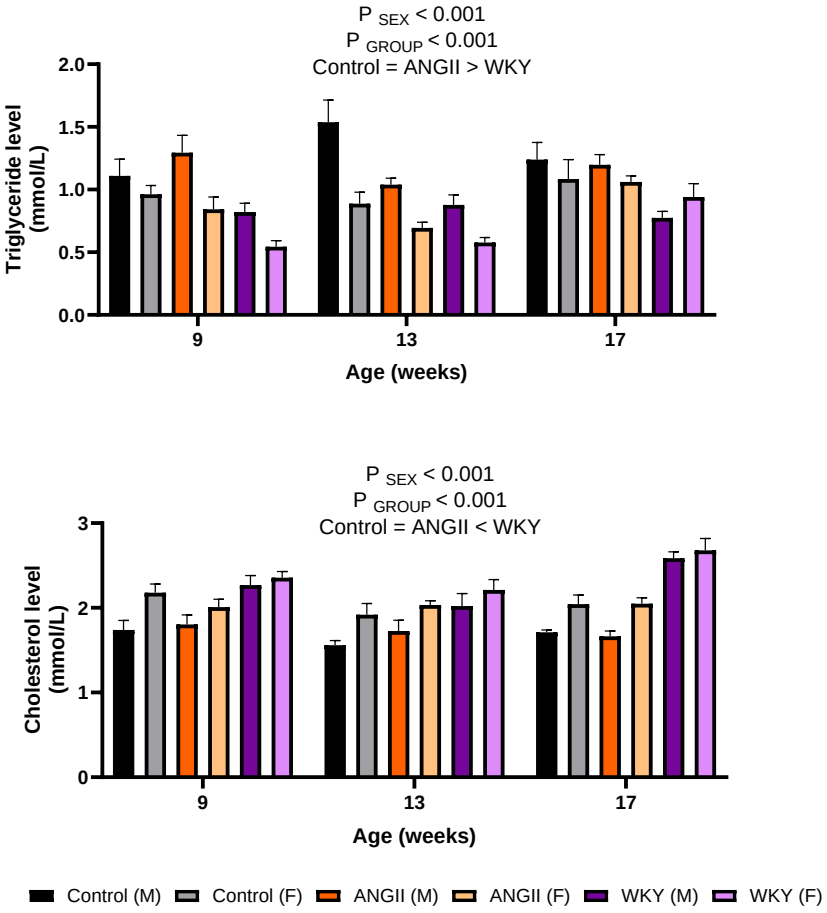

Figure 3-15. Plasma triglycerides and total cholesterol from WKY and SHRSP control and ANGII-exposed offspring. Triglyceride (A) and cholesterol (B) content was measured from plasma collected at week 9, 13 and 18 of age. Data is shown as mean ±SEM (n=7-10 per group) where individual offspring represent each data point. Data was analysed by a mixed effects model of lipid concentration vs sex, age and treatment group (P<0.05) with Tukey *post hoc* test.

3.3.10 Short-term experiment

In the short-term animal experiment, the offspring underwent echocardiography and blood pressure measurements at week 5 of age. Urine and faeces were also collected at this point through metabolic cage collections. Animals were sacrificed at 6 weeks of age and blood and tissues were collected. Due to the similarities with the long-term study, the short-term study results have been summarised in Table 3 and Table 4 in order to minimise repetition of the graphs. A summary of the results comparing the long and short-term studies are found in Table 5.

Blood pressure was found to be significantly increased in the ANGII offspring compared to vehicle controls and WKY offspring (131.23 ± 7.23 vs 110.54 ± 3.92 and 98.33 ± 4.22 mmHg; P=0.032 and P<0.001), but there were no differences between SHRSP vehicle control and WKY offspring (P=0.34). There were no significant differences in the fluid homeostasis or albumin/creatinine ratios between groups. The data obtained from the echocardiography experiments showed no significant differences in RWT, FS, SV, CO and MPI measurements between SHRSP control and ANGII offspring. In contrast, EF and E/A ratio were significantly increased in the ANGII group compared to the controls (EF: 86.08 ± 1.31 vs 81.46 ± 1.92 %; P=0.031 / E/A: 2.1 ± 0.11 vs 1.47 ± 0.067; P<0.001). Strain differences were only observed in FS and EF measurements. FS was significantly lower in WKY offspring compared to ANGII (40.02 ± 1.32 vs 49.15 ± 1.68 %; P<0.001) but not SHRSP vehicle control (45.89 ± 1.65 %; P=0.081). EF was significantly reduced in the WKY group compared to SHRSP control and ANGII (69.85 ± 1.58 vs 81.46 ± 1.92 and 86.08 ± 1.31 %; P<0.001 for both).

The *in utero* environment impacted the heart and lung mass indices, which were significantly higher in the ANGII offspring compared to SHRSP controls (heart: 0.014 ± 0.00031 vs 0.013 ± 0.00033; P=0.002 / lungs: 0.024 ± 0.00075 vs 0.021 ± 0.00065; P=0.036). Similar to the long-term study, heart, LV, kidneys and fat pads (gonadal, retroperitoneal and total) mass indices were significantly reduced in the WKY offspring compared to both SHRSP offspring groups. In contrast, liver mass index was significantly higher in the WKY offspring compared to SHRSP control and ANGII (0.050 ± 0.00095 vs 0.043 ± 0.00065 and 0.040 ± 0.00092; P<0.001 for both).

WKY offspring had a significantly lower concentration of plasma triglycerides compared to their SHRSP control and ANGII counterparts (0.77 ± 0.062 vs 1.16 ± 0.084 and 1.24 ± 0.095 mmol/L respectively; P=0.003 and P<0.001), which was also shown in the long-term study. Plasma cholesterol was also significantly decreased in the WKY offspring compared to SHRSP control and ANGII (2.24 ± 0.036 vs 2.73 ± 0.10 and 2.82 ± 0.083 mmol/L respectively; P<0.001 for both). In contrast to the results from the long-term study, sex differences were only observed in the offspring plasma triglycerides levels, but not plasma cholesterol levels, where females had significantly higher triglycerides compared to males (1.16 ± 0.076 vs 0.94 ± 0.072 mmol/L; P=0.029). There were no sex*treatment group interactions in any of the studied parameters ($P_{INTER.} > 0.05$) (Table 5).

Table 3. Summary of cardiovascular parameters, fluid homeostasis, organ weights and plasma lipids results in the offspring in the short-term study according to overall *in utero* environment and sex effect. Data was analysed by a general linear model of variable vs sex and treatment group (P<0.05) with Tukey *post hoc* test. n=17-19 per group (male and female together) and n=6-12 (male and female separate).

	Treatment effect				Sex effect		
	Control (mean ± SEM)	ANGII (mean ± SEM)	WKY (mean ± SEM)	P_{GROUP}	Male (mean ± SEM)	Female (mean ± SEM)	P_{SEX}
BP (mmHg)	110.54 ± 3.92	131.23 ± 7.23	98.33 ± 4.22	0.001	113.44 ± 6.27	113.30 ± 3.74	0.90
FS (%)	45.89 ± 1.65	49.15 ± 1.68	40.02 ± 1.32	<0.001	43.49 ± 1.51	46.70 ± 1.36	0.11
RWT (mm)	0.52 ± 0.038	0.56 ± 0.015	0.45 ± 0.033	0.036	0.49 ± 0.021	0.54 ± 0.028	0.25
SV (ml)	0.10 ± 0.010	0.096 ± 0.0037	0.089 ± 0.0051	0.37	0.097 ± 0.0045	0.095 ± 0.0064	0.69
CO (ml/min)	32.20 ± 2.30	28.40 ± 1.01	33.50 ± 1.83	0.14	32.29 ± 1.38	30.31 ± 1.54	0.34
EF (%)	81.46 ± 1.92	86.08 ± 1.31	69.85 ± 1.58	<0.001	77.36 ± 1.84	81.35 ± 1.82	0.11
E/A	1.47 ± 0.067	2.10 ± 0.11	1.43 ± 0.072	<0.001	1.74 ± 0.10	1.63 ± 0.089	0.40
MPI	0.72 ± 0.021	0.72 ± 0.048	0.67 ± 0.022	0.59	0.69 ± 0.027	0.71 ± 0.029	0.62
Water intake (ml)	17.6 ± 0.7	19.6 ± 0.9	16.0 ± 0.6	0.008	17.8 ± 0.7	17.7 ± 0.7	0.98
Urine output (ml)	2.3 ± 0.3	4.1 ± 0.6	3.1 ± 0.4	0.14	3.4 ± 0.4	2.9 ± 0.4	0.62
Output:intake	13.4 ± 1.7	19.79 ± 2.4	19.7 ± 2.4	0.14	18.9 ± 1.9	16.4 ± 1.9	0.59
Albumin/creatinine (mg/g)	1.90 ± 0.61	3.95 ± 1.30	1.80 ± 0.33	0.41	2.38 ± 0.68	2.51 ± 0.62	0.74
Heart mass index	0.013 ± 0.0003	0.014 ± 0.0003	0.012 ± 0.0002	<0.001	0.013 ± 0.00028	0.013 ± 0.00033	0.45
LV mass index	0.0093 ± 0.0002	0.010 ± 0.0004	0.0084 ± 0.0001	<0.001	0.0093 ± 0.00025	0.0093 ± 0.00024	0.95
Lungs mass index	0.021 ± 0.0007	0.024 ± 0.0008	0.021 ± 0.0006	0.014	0.023 ± 0.00062	0.021 ± 0.00052	0.15
Kidneys mass index	0.028 ± 0.0007	0.030 ± 0.0007	0.024 ± 0.0009	<0.001	0.028 ± 0.00065	0.027 ± 0.00091	0.080
Liver mass index	0.13 ± 0.005	0.14 ± 0.004	0.15 ± 0.003	0.005	0.14 ± 0.0028	0.14 ± 0.0045	0.81
Gonadal fat mass index	0.017 ± 0.002	0.021 ± 0.002	0.0086 ± 0.0005	<0.001	0.016 ± 0.0018	0.016 ± 0.0014	0.74
Retroperitoneal fat mass index	0.010 ± 0.0008	0.013 ± 0.001	0.0057 ± 0.0005	<0.001	0.011 ± 0.0010	0.0088 ± 0.00085	0.055
Total fat	0.028 ± 0.002	0.034 ± 0.003	0.014 ± 0.0007	<0.001	0.026 ± 0.0026	0.024 ± 0.0022	0.29
Triglycerides (mmol/L)	1.16 ± 0.084	1.24 ± 0.095	0.77 ± 0.062	<0.001	0.94 ± 0.072	1.16 ± 0.076	0.029
Total cholesterol (mmol/L)	2.73 ± 0.10	2.82 ± 0.083	2.24 ± 0.036	<0.001	2.51 ± 0.064	2.67 ± 0.094	0.20

Table 4. Summary of cardiovascular parameters, fluid homeostasis, organ weights and plasma lipids results in the offspring in the short-term study according to *in utero* environment by sex. Data was analysed by a general linear model of variable vs sex and treatment group (P<0.05) with Tukey *post hoc* test. n=6-12 per group.

	Males			Females			
	Control (mean ± SEM)	ANGII (mean ± SEM)	WKY (mean ± SEM)	Control (mean ± SEM)	ANGII (mean ± SEM)	WKY (mean ± SEM)	P INTER.
BP (mmHg)	108.45 ± 9.52	135.80 ± 11.40	94.12 ± 4.98	111.59 ± 3.83	125.58 ± 8.26	103.60 ± 7.08	0.43
FS (%)	41.31 ± 0.63	47.57 ± 2.85	40.73 ± 1.76	48.38 ± 1.75	50.91 ± 1.56	38.99 ± 2.11	0.16
RWT (mm)	0.48 ± 0.029	0.54 ± 0.024	0.45 ± 0.044	0.55 ± 0.056	0.59 ± 0.014	0.46 ± 0.055	0.78
SV (ml)	0.10 ± 0.014	0.098 ± 0.0059	0.093 ± 0.0069	0.11 ± 0.014	0.093 ± 0.0043	0.083 ± 0.0073	0.71
CO (ml/min)	32.49 ± 3.19	29.64 ± 1.49	34.81 ± 2.56	32.04 ± 3.21	27.19 ± 1.30	31.63 ± 2.58	0.87
EF (%)	76.61 ± 3.75	84.47 ± 2.20	70.72 ± 2.09	84.11 ± 1.81	87.88 ± 1.15	68.62	0.12
E/A	1.51 ± 0.10	2.16 ± 0.18	1.46 ± 0.081	1.44 ± 0.092	2.03 ± 0.14	1.40 ± 0.14	0.96
MPI	0.69 ± 0.040	0.73 ± 0.063	0.66 ± 0.025	0.74 ± 0.024	0.71 ± 0.076	0.69 ± 0.039	0.82
Water intake (ml)	17.0 ± 1.0	19.8 ± 1.2	16.2 ± 0.6	17.9 ± 1.0	19.3 ± 1.5	15.8 ± 1.0	0.77
Urine output (ml)	2.7 ± 0.8	4.1 ± 0.7	3.1 ± 0.5	2.2 ± 0.3	4.0 ± 1.2	3.1 ± 0.7	0.97
Output:intake	15.6 ± 4.6	20.6 ± 2.9	19.4 ± 2.9	12.3 ± 1.4	18.8 ± 4.2	20.1 ± 4.3	0.82
Albumin/creatinine (mg/g)	1.22 ± 0.51	3.43 ± 1.91	2.01 ± 0.50	2.13 ± 0.79	4.60 ± 1.95	1.5 ± 0.38	0.72
Heart mass index	0.013 ± 0.0003	0.014 ± 0.0004	0.012 ± 0.0002	0.013 ± 0.0005	0.011 ± 0.0003	0.014 ± 0.0005	0.80
LV mass index	0.0095 ± 0.0002	0.099 ± 0.0005	0.0085 ± 0.0002	0.0092 ± 0.0003	0.010 ± 0.0004	0.0082 ± 0.0002	0.35
Lungs mass index	0.022 ± 0.0005	0.024 ± 0.001	0.021 ± 0.0009	0.020 ± 0.0009	0.022 ± 0.0009	0.021 ± 0.0006	0.80
Kidneys mass index	0.028 ± 0.0004	0.031 ± 0.0007	0.024 ± 0.0007	0.028 ± 0.001	0.030 ± 0.001	0.022 ± 0.002	0.58
Liver mass index	0.13 ± 0.004	0.14 ± 0.005	0.15 ± 0.003	0.13 ± 0.007	0.14 ± 0.008	0.15 ± 0.006	0.87
Gonadal fat mass index	0.018 ± 0.003	0.022 ± 0.002	0.021 ± 0.0009	0.017 ± 0.002	0.020 ± 0.003	0.0093 ± 0.001	0.73
Retroperitoneal fat mass index	0.013 ± 0.0009	0.014 ± 0.002	0.0059 ± 0.0007	0.0094 ± 0.0009	0.011 ± 0.002	0.0054 ± 0.0006	0.52
Total fat	0.031 ± 0.003	0.036 ± 0.004	0.014 ± 0.0007	0.026 ± 0.003	0.031 ± 0.005	0.015 ± 0.001	0.59
Triglycerides (mmol/L)	1.23 ± 0.16	1.10 ± 0.076	0.63 ± 0.049	1.12 ± 0.10	1.45 ± 0.19	0.99 ± 0.081	0.052
Total cholesterol (mmol/L)	2.72 ± 0.14	2.69 ± 0.065	2.23 ± 0.052	2.74 ± 0.14	3.01 ± 0.16	2.26 ± 0.048	0.38

Table 5. Summary of cardiovascular parameters, fluid homeostasis, organ weights, vascular function and plasma lipids findings in the offspring in the short-term and long-term study according to *in utero* environment, strain and/or sex effect. In the parameters where an *in utero* environment difference was found, the strain difference was reported only if SHRSP control offspring were different from WKY. In the parameters where an *in utero* environment difference was not found, the strain difference was reported if SHRSP control offspring were different from WKY.

	Long-term study			Short-term study		
	***In utero* environment**	**Strain**	**Sex**	***In utero* environment**	**Strain**	**Sex**
BP	-	↑ SHRSP ↓ WKY	-	↓ Control ↑ ANGII	-	-
LVMI	-	-	↓ M ↑ F			
FS	↑ Control ↓ ANGII	↑ SHRSP ↓ WKY	-	-	-	-
RWT	↑ Control ↓ ANGII	↑ SHRSP ↓ WKY	-	-	-	-
SV	-	-	↑ M ↓ F	-	-	-
CO	↓ Control ↑ ANGII	-	↑ M ↓ F	-	-	-
EF	-	↑ SHRSP ↓ WKY	-	↓ Control ↑ ANGII	↑ SHRSP ↓ WKY	-
E/A	↓ Control ↑ ANGII	-	-	↓ Control ↑ ANGII	-	-
MPI	-	-	-	-	-	-
Water intake	-	↓ SHRSP ↑ WKY	↑ M ↓ F	-	-	-
Urine output	-	↓ SHRSP ↑ WKY	-	-	-	-
Output:intake	-	-	↑ M ↓ F	-	-	-
Albumin/creatinine	-	-	↑ M ↓ F	-	-	-
Heart	-	↑ SHRSP ↓ WKY	↑ M ↓ F	↓ Control ↑ ANGII	↑ SHRSP ↓ WKY	-
LV	-	↑ SHRSP ↓ WKY	↑ M ↓ F	-	↑ SHRSP ↓ WKY	-
Lungs	-	-	↑ M ↓ F	↓ Control ↑ ANGII	-	-
Kidneys	-	↑ SHRSP ↓ WKY	↑ M ↓ F	-	↑ SHRSP ↓ WKY	-
Liver	-	↑ SHRSP ↓ WKY	↑ M ↓ F	-	↓ SHRSP ↑ WKY	-
Gonadal fat	-	↑ SHRSP ↓ WKY	↑ M ↓ F	-	↑ SHRSP ↓ WKY	-
Retroperitoneal fat	-	↑ SHRSP ↓ WKY	↑ M ↓ F	-	↑ SHRSP ↓ WKY	-
Total fat	-	↑ SHRSP ↓ WKY	↑ M ↓ F	-	↑ SHRSP ↓ WKY	-
Wire myography	-	-	-			
Triglycerides	-	↑ SHRSP ↓ WKY	↑ M ↓ F	-	↑ SHRSP ↓ WKY	↓ M ↑ F
Total cholesterol	-	↓ SHRSP ↑ WKY	↓ M ↑ F	-	↑ SHRSP ↓ WKY	-

3.4 Discussion

This chapter aimed to investigate the developmental differences between offspring born after intrauterine ANGII exposure and controls, in terms of their cardiovascular and metabolic phenotype, between 5 and 18 weeks of age. The results from this study show that ANGII-exposed offspring present a worsened cardiac phenotype compared to their vehicle-treated counterparts, without changes in their blood pressure, fluid homeostasis, organ weights, mesenteric vascular function and circulating lipids. The short-term study investigating the impact of *in utero* ANGII exposure in the offspring at 5 weeks of age exclusively showed significant differences in blood pressure, EF and E/A ratios compared to controls. A summary of sex differences was also documented in this chapter.

The beginning of this chapter demonstrated the PE phenotype in the SHRSP dams after 700 ng/kg/min ANGII treatment. This effect has been previously shown by our lab with a dose of 500, 750 and 1000 ng/kg/min ANGII. Even though this model has been optimised for 750 ng/kg/min ANGII, the 700 ng/kg/min dose was used for the current experiments due to welfare concerns with the dams regarding excessive weight loss exceeding the limits of the project license at the higher dose. A possible explanation for this may be that the animal batches used for these experiments were more reactive to ANGII and led them to lose their appetite and weight. Since the main goal of this chapter was to investigate the impact on the offspring, the experiments were powered for the offspring but not for the mothers. These results did not show any significant BP, albumin/creatinine ratios or gestation length differences between SHRSP ANGII, control and WKY females, possibly due to the low n number. However, growth restriction in the ANGII-exposed offspring was observed, which is a common characteristic of the human PE phenotype. This effect was observed between 1 and 4 days of age but disappeared between 5 and 8 days of age. Juvenile to adult offspring did not show any significant differences in body weight, which indicates that the ANGII-exposed offspring underwent “catch up” growth to match their control counterparts.

Investigating offspring after PE pregnancies

The main challenge that affects the study of later-life consequences after hypertensive pregnancies is that many of the features of babies born to PE mothers

are shared with preterm normotensive pregnancies, therefore assigning the contribution of each pregnancy complication becomes an issue. Many studies on both humans and animals mainly focus on the impact of preterm birth on cardiac development, without separating hypertensive from normotensive pregnancies thereby affecting the interpretation of the data. PE is a complicated condition to study because it is usually accompanied by FGR and preterm birth, therefore attempting to determine the contribution of the PE environment only is challenging. A main strength of this study is that we have shown no differences in the length of gestation between ANGII-treated dams and controls, and therefore any impact observed in the offspring is caused by the *in utero* hypertensive environment.

The reason why offspring from mothers affected by PE are at increased risk of CVD later in life remains unknown. There are studies showing that an adverse intrauterine exposure can "programme" the offspring to later-life disease. In addition, growth-restricted babies (often as a consequence of PE) experience a "catch up" growth after birth that appears to also be detrimental thereby contributing to disease development later in life. This chapter has demonstrated a "catch up" growth in the ANGII-exposed offspring between 5 and 8 days of age. This compensatory growth was originally used to describe the increased developmental rate at which animals (including humans) exposed to undernutrition grow after normality is recovered (Wilson and Osbourn, 1960). This term has now been extended to children born after exposure to undernutrition *in utero*, also known as "catch up" growth. This seems to be an adaptive mechanism that ensures survival during the first stages of life, however, this benefit appears to be accompanied by negative later-life effects. In humans, babies exposed to intrauterine growth limitations have shown faster growth rates in early childhood which correlate with later-life likelihood of disease. Infants presenting catch up growth during early development (up to two years old) showed greater BMI, body fat mass and central body fat distribution at 5 years of age (Ong et al., 2000). This rapid growth and body fat deposition seem to correlate with insulin resistance present in 7-year-old children born with low birth weight (Crowther et al., 1998). Male babies who were born with lower birth weights and who caught up with their counterparts were more likely to die of coronary heart disease (Eriksson et al.,

1999). Growth-restricted males were also associated with an increase in high blood pressure at 50 years of age (Leon et al., 1996).

It is important to note that most of these studies have been performed in "well-nourished" populations, and therefore it has been hypothesised that the reason behind the small birth weight in babies is placental insufficiency, rather than maternal malnutrition (Henriksen and Clausen, 2008). Human studies have shown that the limited nutrient supply due to impaired placenta formation in PE may lead to the suboptimal development of the cardiovascular system and posterior CVD development. Low birth weight is negatively correlated with endothelial function and elevated blood vessel stiffness in humans, even from early life (Martin et al., 2000), which can lead to the onset of hypertension. Offspring from hypertensive pregnancies have been shown to develop high blood pressure even from a young age, especially when blood pressure was elevated at an early gestational stage (Staley et al., 2015). In addition, there is a positive correlation between maternal blood pressure, lower birth weight and increased pressure in children and adolescents between 5 and 15 years of age (Primatesta et al., 2005). Interestingly, a 20-year follow-up study comparing offspring from PE vs pregnancy-induced hypertension (PIH) showed that the risk of developing hypertension was three times higher in the PE offspring compared to PIH (Davis et al., 2015). Another study comparing premature babies born after hypertensive and normotensive pregnancies showed that, despite both groups having elevated blood pressure after a 20-year follow-up, the former presented increased endothelial dysfunction and atherosclerotic plaque formation whereas the latter showed evidence of increased arterial stiffness (Lazdam et al., 2010). It is important to note that in Lazdam et al. (2010) pregnancies complicated by PE and gestational hypertension were combined and that premature babies were not growth restricted. Regardless, these findings show that even if offspring born after different pregnancy challenges present similar phenotypes, the underlying mechanisms leading to these may be different, and highlights the need to investigate beyond the observed phenotypes.

Investigations carried out in animal models show similar results to human studies, which allow the study of the molecular mechanisms involved. The offspring exposed to limited nutrients during pregnancy in a model of maternal

undernutrition present impaired collagen and elastin composition, hypertrophy and deficient development of the aorta, and elevated blood pressure at 6 months of age (only in males), but not at an earlier time point (21 days of age) (Gutiérrez-Arzapalo et al., 2018). Similarly, the results presented in this chapter show no blood pressure differences up to 17 weeks of age. In contrast, other experiments with rodent models of reduced uterine perfusion during pregnancy have found no postnatal body weight "catch up" in growth-restricted offspring, although this group presented with a significantly elevated blood pressure compared to control offspring at 4 and 8 weeks of age (Alexander, 2003). These investigations suggest that growth-restricted offspring are born with cardiovascular defects that increase the risk of developing CVD later in life, even if they experience a "catch up" growth.

Cardiovascular, metabolic and renal changes in offspring exposed to PE pregnancies

The echocardiography results from this study showed no significant differences in LVMI, SV, EF and MPI between ANGII and vehicle control offspring. FS was significantly lower in the ANGII-exposed offspring, which is indicative of reduced left ventricular systolic function. Additionally, the E/A ratio was significantly elevated in these animals thereby showing signs of left ventricular diastolic dysfunction. The reduction in RWT in the ANGII group, in parallel with the loss of function, could indicate early remodelling changes that may lead to severe dysfunction and heart failure later in life. The observed increase in CO may signify that there is a pressure overload on the hearts of the ANGII offspring that might be leading to an eccentric-like hypertrophy phenotype. These animals were sacrificed at a relatively young age and, despite the fact that onset of hypertension had already taken place, some important later-life changes in cardiac shape and function might have been missed that would merit further study.

Similar to the results presented in this chapter, heart structure and functional defects have been observed in humans from an early age, as children born from pregnancies affected by PE or PIH present increased left and right ventricular mass at 3 months of age and diastolic dysfunction between 5 and 8 years old (Fugelseth et al., 2011). Moreover, reduced heart contractility (Iruretagoyena et al., 2014)

and vascular inflammation and vessel thickness (Lo Vasco et al., 2011) have been observed in infants born with FGR. Unlike the current data, pulse wave velocity has not been found to be different in children between 9 and 12 years old born after PE pregnancies (Lawlor et al., 2012).

Male and female offspring from obese PE-like BPH/5 mice show an impaired cardiometabolic profile compared to controls, evidenced as high blood pressure and elevated heart mass (Sutton et al., 2017) (Beckers et al., 2021). Interestingly, only males were found to have increased left ventricular mass (Beckers et al., 2021). Increased LVMI has been observed in aged Sprague-Dawley rat males (but not females) born under hypoxic conditions compared to controls, although both male and female offspring showed signs of left ventricular dysfunction with an increased mitral E/A index (Rueda-Clausen et al., 2009). In contrast, other echocardiographic measurements including FS, EF and CO did not show any differences amongst groups.

Fluid homeostasis, measured by the urine output to water intake ratio, has been previously observed to increase in dams treated with 1000 ng/kg/min ANGII due to an elevated water intake and urine output (performed by Dr Hannah Morgan at the University of Glasgow, data not published). The offspring of mothers treated with 700 ng/kg/min ANGII in the present study do not show an elevated output:input ratio or proteinuria (indicated by the albumin/creatinine ratio) up to 17 weeks of age. In contrast, previous models of offspring born after placental insufficiency have shown evidence of kidney damage in adult WKY females (Moritz et al., 2009). Similarly, FGR led to reduced nephron number in adult WKY males (Wlodek et al., 2008), which is associated with renal insufficiency. In humans, reduced nephron number has been observed in FGR babies (Hinchliffe et al., 1992).

Mesenteric artery contractility to NA in the ANGII SHRSP offspring was significantly higher compared to WKY offspring, but not SHRSP control. These results show that the ANGII-exposure not only has detrimental effects on the cardiac function of the offspring, but it also impairs the vascular reactivity of resistance arteries, despite the lack of increase in blood pressure. Coronary arteries, but not mesenteric arteries, from FGR Wistar rats were found to be hypercontractile to U46619 (Selivanova et al., 2021). Young and adult offspring from the Sprague Dawley RUPP

model show increased thoracic aorta contraction to phenylephrine and reduced relaxation response to Ach, but no differences were found in the relaxation response to SNP (Payne et al., 2003). Other investigations have found increased vasoconstriction in the mesenteric arteries after the addition of phenylephrine and potassium chloride, but not decreased relaxation to Ach and SNP (Anderson et al., 2006). Similarly, we did not find any significant differences in the relaxation reaction of the mesenteric arteries to Ach and SNP.

The current results did not show any differences in plasma lipids between ANGII and control offspring. It is important to note that insulin resistance would have been a valuable parameter to measure in this model, however the limits in the animal license prevented the collection of blood in a fasted state. The available publications discussing plasma cholesterol and triglyceride levels in offspring born after PE pregnancies are limited. Interestingly, FGR Sprague-Dawley offspring under a high-fat diet presented several metabolic abnormalities including elevated plasma triglycerides and insulin resistance, however this effect was not observed in hypoxia-induced IUGR offspring under a low-fat diet (Rueda-Clausen et al., 2011), which suggests that a PE-like environment alone does not contribute to this phenotype.

In humans, elevated total cholesterol and triglyceride levels have been found in cord blood in PE compared to controls, even after adjusting for mode of delivery (Rodie et al., 2004). Interestingly, these results were not correlated with maternal plasma lipids, which suggests that it is the *in utero* environment affecting the lipid metabolism of the offspring, rather than the maternal dyslipidaemia. Early childhood studies have shown elevated total cholesterol but not triglycerides in children between 5 and 8 years old after PE pregnancies (Kvehaugen et al., 2011). Serum lipids were not found to be different in children born after maternal PE compared to healthy controls at 12 years of age (Tenhola et al., 2003). A similar study investigating the impact of PE pregnancies on children between 9 and 12 years old also found no significant differences in offspring lipids when comparing PE and healthy pregnancies (Lawlor et al., 2012). It is possible that acute transient changes in cord blood occur without having an impact in the offspring in later life, and therefore expanding the present findings with cord blood lipid analyses would be beneficial.

Strain differences: SHRSP vs WKY

Similar to the present findings, previous studies have demonstrated that SHRSP rats show an increase in BP compared to WKY between 12 and 17 weeks of age, although it is important to note that these experiments were only conducted in males (Koh-Tan et al., 2013). In addition, they also showed elevated heart, LV and kidney weights in SHRSP at 17 weeks of age compared to WKY. Left ventricular hypertrophy in the male SHRSP has been shown to be maintained up to 9 months of age (Amann et al., 1995). The presence of left ventricular hypertrophy in the SHRSP strain is not limited to males, although published papers on females are scarce. This phenotype is observed due to the additional effort exerted by the heart during hypertension in these animals as well as due to genetic predisposition in this strain. Thus, the lack of LVMI difference between SHRSP and WKY in this study is surprising, however, we found an elevated whole heart and LV wet weight at sacrifice which could indicate that the echocardiography results are imprecise. This may be due to the issues encountered during the experiments, such as echocardiography-derived LV mass being an estimated measurement which could introduce errors, as well as the issues of being forced to use two different echo machines when one failed before the study was completed. This latter issue may also be the reason why we observed higher EF in the ANGII offspring in the short-term study, in contrast with the long-term study where EF was elevated in the control offspring.

In terms of cardiac function, previous investigations have shown an elevated SV and CO in 16-week old SHRSP males, without changes in E/A ratios (Tada et al., 2010). In contrast, the current study did not show any differences between SHRSP and WKY on these cardiac parameters. Usually, reduced EF can be evidence of a cardiomyopathy as the heart is not pumping blood out adequately, however, high EF values could be indicative of hypertrophic cardiomyopathy which is characterised by increased heart muscle thickness. The results presented here indicating that SHRSP have increased RWT and EF compared to normotensive WKY rats would support the hypothesis of a hypertrophic heart in this strain.

Despite the lack of strain differences in our experiments (SHRSP control vs WKY offspring), vascular reactivity has been found to be impaired in male spontaneously hypertensive rats (SHR) vs WKY at 12 weeks of age, which was

characterised by hypercontractility to the vasoconstrictor agent NA and reduced relaxation to the vasodilating agent Ach (Rizzoni et al., 1994). Interestingly, the increased reactivity to NA was also observed in these animals at 4 weeks of age, prior to the onset of hypertension and cardiac hypertrophy, which could indicate that the vascular dysfunction in this strain may contribute to the development of later-life hypertension. This theory is supported by other studies where mesenteric artery wall thickness and vascular reactivity to NA were increased in male SHR at 6, 11 and 18 weeks of age (Inoue et al., 1989).

Gonadal fat, retroperitoneal fat and fat pads were significantly increased in SHRSP compared to WKY. As these are VAT depots, it is not unexpected to observe that SHRSP present with high amounts as this strain is more insulin resistant compared to WKY (Swislocki and Tsuzuki, 1993). This might contribute to the elevated triglyceride content also observed in the offspring from this strain. In contrast, plasma cholesterol and triglycerides have not previously been found to be different between male SHRSP and WKY (Tada et al., 2010), but the reason behind this may be the inclusion of both male and females in our study.

Sex differences

Sex differences were observed in the long-term study, but not in the short-term study, independent of their strain and *in utero* environment. Sex differences in preclinical models of hypertension has recently been reviewed by our group (Olivera and Graham, 2023). Males had increased blood pressure compared to females at 17 weeks of age, which is in agreement with previous studies in SHRSP, although this effect was observed at 6 months of age (Maris et al., 2005). CO and SV were significantly lower in males compared to females, which is also observed in humans (Patel et al., 2021). Hypertensive women demonstrated higher prevalence of left ventricular hypertrophy compared to men (Gerdts et al., 2018), which supports the present finding of elevated LVMI in females, although the hypertensive patients also presented with elevated EF which was not observed in the animal data shown in this chapter. Analogous to the present results, these women also had elevated serum total cholesterol and reduced triglycerides compared to men (Gerdts et al., 2018). Additionally, all the wet tissue weights normalised to tibia length were significantly increased in males compared to

females. This finding may be an inherent characteristic in males, although there have not been any published studies reporting sex differences in organ weights.

Interestingly, differences in sex appear to be evident even from the *in utero* stage, where males and females are affected differently after the same adverse pregnancy insult. The current study did not find any interactions between sex and treatment, suggesting that the intrauterine exposure to ANGII did not have a sex-specific effect. In contrast, other studies investigating the impact of FGR in the RUPP Sprague-Dawley model showed that both male and female offspring developed hypertension during early stages of their life, but it was only maintained into adulthood (12 weeks of age) in males (Alexander, 2003). Thus, female offspring appear to be at a lower risk, which may be due to an oestrogen-associated protection (Ojeda et al., 2007). In humans, studies comparing the sex-specific effects of maternal undernutrition showed that men were more affected by this environment than women, and only men developed hypertension later in life which the authors attributed to changes in the placenta (Van Abeelen et al., 2011).

Short-term vs long-term study

It is important to note that the results from the long and short-term studies are not directly comparable as they were performed under different conditions. The main difference between these two studies (apart from when the animals were culled) is the number of offspring kept after birth as four pups (two per sex) were kept for the long-term study whereas six pups (three per sex) were kept for the short study. The rate of development of the pups after birth is known to be associated with the number of pups available during the suckling period as well as the litter size, where the higher the litter size the slower the developmental rate of the offspring (Chahoud and Paumgartten, 2009). Therefore, differences between both long and short-term studies may be expected and are representative of other offspring developmental studies. Moreover, the analysis carried out in the long-term study allows investigation of the overall effect of intrauterine ANGII on the development of offspring from early life up to adulthood while the short-term study focuses on the 5 week of age timepoint exclusively, which was conducted as part of a MSc project with the main goal of generating tissues at this earlier timepoint. While some subtle phenotyping differences were found between both

studies e.g. BP effect, the observed impact on the diastolic function of the offspring remained consistent.

Systolic blood pressure was significantly higher in the ANGII offspring compared to controls only in the short-term study offspring. The blood pressure differences observed at 5 weeks of age in contrast with the long-term experiment may be attributable to errors introduced because the measurements on smaller rats were being used at the limits of the equipment and it may affect the results. Although less likely, litter size may contribute to this result, which would match previous investigations where growth-restricted offspring from a RUPP model showed elevated blood pressure compared to controls at 4 and 8 weeks of age (Alexander, 2003). Similarly, offspring from Dahl Salt-Sensitive dams showed increased blood pressure between 5 and 20 weeks of age (Terstappen et al., 2019). Interestingly, in both studies a litter size of eight or more was used, which could suggest that higher litter sizes tend to have more impact on offspring blood pressure. The lack of blood pressure difference between control SHRSP and WKY offspring is observed because the onset of hypertension in the SHRSP strain does not take place until eight weeks of age (Yamori and Horie, 1977). In addition, left ventricular mass is not different before this age either (Rizzoni et al., 1994), suggesting that the left ventricular hypertrophy takes place after this timepoint and possibly after the development of hypertension.

In contrast with the long-term study, 6-week-old females had elevated triglycerides compared to males and no significant differences in their total cholesterol content were found. In humans, girls have more plasma triglycerides and cholesterol compared to boys at 12 months of age (Ellul et al., 2020), but interestingly only triglycerides remain different in childhood at 11/12 years of age (Ellul et al., 2019).

In summary, the results presented in this study show the consequences of a hypertensive intrauterine environment on an aberrant cardiovascular phenotype in the offspring. ANGII-exposed offspring presented signs of systolic and diastolic dysfunction that are comparable to the human data on offspring from human PE pregnancies and other animal models. This chapter elucidates the consequences of a hypertensive environment on the offspring's development and cardiometabolic health and highlights the need to follow up these individuals in

more detail throughout their lives. Animal models generate invaluable data that allow us to understand the phenotype that may translate to humans. In addition, these experiments provided the opportunity for carrying out *omics* experiments to further understand the molecular mechanisms behind these phenotypes. For this reason, the next chapter will focus on the lipidomics analysis of the human and rat placentas to investigate the potential lipid dysregulation in PE and to further validate our animal model.

4 Placental lipid storage and inflammation in pregnancies complicated by preeclampsia

4.1 Introduction

Cardiovascular and metabolic adaptations take place in the mother during pregnancy in order to supply the needs of the growing fetus and developing placenta. PE is associated with a limited maternal vascular adaptation that leads to widespread endothelial dysfunction, which causes hypertension, and restricted transmission of oxygen and nutrients to the fetus (Boeldt and Bird, 2017). Moreover, there is increasing evidence of the role of impaired adipose tissue expansion in PE (Trivett et al., 2021). The versatility of this endocrine organ is essential for the accumulation and delivery of lipids that sustain gestation. Healthy pregnancies consist of an early increased insulin sensitivity phase followed by elevated insulin resistance and lipolysis towards the late gestational period. Adipocyte dysfunction and increased insulin resistance during PE may exacerbate fatty acid release during late pregnancy (Trivett et al., 2021), alongside ectopic fat accumulation, lipotoxicity and limited nutrient transfer across the placenta.

Nutrient transfer to the fetus is affected during PE due to the deleterious effect of the condition on the placenta. Abnormal placental transport not only affects the development of the fetus in the womb, but it can also have consequences later in life. The best example of this is the dysregulation of placental fatty acid transfer. Essential polyunsaturated fatty acids, including LC-PUFAs, are needed for brain development in the fetus and their inadequate supply during pregnancy is associated with long-term impacts including increased incidence of mental disorders such as ADHD and depression (Horrocks and Yeo, 1999). PE pregnancies are characterised by significantly lower LC-PUFAs in maternal serum, placenta and umbilical cord (Kulkarni et al., 2010). Moreover, fetal levels of LC-PUFAs have been shown to be significantly reduced in PE (MacKay et al., 2012) and correlated with insulin sensitivity in the offspring (Lewis et al., 2018), thereby suggesting a link between the LC-PUFAs supply and metabolic disorders in the offspring. Overall, these data provide evidence of the importance of placental fatty acid transport in fetal development.

The causes of the reduced LC-PUFA levels in PE are not clear, although it has been hypothesised that, similar to what happens during MASLD, the elevated maternal NEFAs during PE may interfere with LC-PUFA synthesis. This raises the question of the benefits of maternal fatty acid supplementation to increase fatty acid delivery and improvement of pregnancy outcome. However, there is limited evidence that increased dietary or supplemental LC-PUFAs aids successful fetal development in humans (Hadders-algra, 2008) as the mechanism of LC-PUFA delivery to the fetus is yet to be elucidated.

The synthesis and delivery of LC-PUFAs to the fetus may be impaired due to the increased insulin resistance during PE. In humans, maternal insulin resistance has been associated with PE (Hauth et al., 2011) and maternal SAT lipolysis has been shown to be resistant to insulin suppression (Huda et al., 2014). Consequently, pregnant women affected by PE have been found to have higher plasma TGs and NEFAs than healthy controls (MacKay et al., 2012). This increase in maternal lipid concentrations may lead to ectopic storage in the placenta and the liver that may affect nutrient transfer to the fetus and synthesis of LC-PUFAs. However, despite the increasing evidence of higher placental fat content in PE, the presence of lipid droplets on the placenta has not been confirmed. There is evidence of ectopic fat accumulation in the placenta of a rodent model of PE (Sun et al., 2012) as well as increased neutral lipid in the human PE placenta compared to normotensive pregnancies (Brown et al., 2016), suggesting the presence of ectopic lipid droplets. MacKay et al. (2012) have reported an excess of plasma TGs as well as lower LC-PUFAs concentrations in erythrocytes from both mothers and babies in PE and FGR pregnancies, thereby potentially linking neutral lipids and impaired fetal nutrition.

In addition, other lipid alterations have been observed in PE including elevated plasma levels of diacylglycerols (DGs) (Hong et al., 2020). DGs are products and/or precursors of TGs and have been associated with insulin resistance in T2DM (Erion and Shulman, 2010) and GDM (Furse et al., 2022). Elevated levels of DGs activate protein kinase C (PKC) which phosphorylates and inhibits the insulin receptor kinase (IRK) which then fails activate the insulin receptor, thereby causing insulin resistance. It is unknown whether this mechanism contributes to the insulin resistance observed in PE. DGs have not previously been investigated in the PE

placenta, which is needed to further elucidate the role of DGs in this pathology and to complement previous findings on neutral lipid content.

Animal models have shown inconsistent results in placental lipid storage and LC-PUFAs availability in PE-induced dams. The RUPP Sprague-Dawley dams have not shown elevated plasma TG and cholesterol compared to controls (Gilbert et al., 2007). In contrast, female C57BL/6 mice treated with L-NAME showed higher TGs, cholesterol and NEFAs compared to controls, together with ectopic fat infiltration in liver and placenta (Sun et al., 2012). No differences in erythrocyte essential fatty acid levels were found between PE and controls in L-NAME Wistar treated dams, despite mimicking other human PE features including high blood pressure and low fetal birth weight (Kasture et al., 2020). In contrast, a PE model on testosterone-treated Sprague-Dawley rats caused FGR and reduced maternal and fetal LC-PUFAs content (Gopalakrishnan et al., 2022), however the study did not report blood pressure effects and/or insulin resistance in this study. Interestingly, LC-PUFA supplementation in the testosterone-treated dams led to increased placental but not fetal LC-PUFAs, suggesting that these essential fatty acids are being diverted towards storage in the placenta rather than transport to the fetus (Gopalakrishnan et al., 2022).

Apart from lipid abnormalities, PE pregnancies have also been associated with increased inflammation which has been suggested to be one of the main causes of endothelial dysfunction (Redman et al., 1999). Our group has previously shown that the serum cytokine interleukin 6 (IL-6) is higher in women with PE in the third trimester, even after accounting for BMI (Freeman et al., 2004). Pregnant women with PE have also shown elevated serum and adipose tissue tumour necrosis factor alpha (TNF-α) and intercellular adhesion molecule 1 (ICAM-1) presence compared to controls (Zhao et al., 2016), indicating increased inflammation. In addition, positive colony stimulating factor 1 receptor (CSF1R) cells (a marker of activated macrophages) in VAT were higher in PE compared to healthy pregnancies (Huda et al., 2017). Adipose tissue production of inflammatory factors and macrophage presence may reflect or contribute to the insulin resistance and increased lipolysis in PE, although this is yet to be confirmed.

Immune cells are involved in the normal development of the placenta in both humans and rodents (Faas and De Vos, 2018). In humans, dysregulation of the

inflammatory response in the placental bed has been linked to pregnancy disorders, including PE. The study of the inflammatory response in rodent models of PE is challenging as most investigations on this topic induce the PE phenotypes with proinflammatory agents and therefore the impact of PE alone cannot be determined. In contrast with the results from adipose tissue, cytokines including TNFα and interleukin 6 (IL-6) are not different between PE and healthy placentas in humans (Benyo et al., 2001). Total serum and placental CSF1R protein levels have been shown to be higher in women with PE compared to controls (Hayashi et al., 2002). However, to our knowledge, there have not been previous studies investigating the localisation of these activated macrophages, which has been proven to be of importance (Reister et al., 1999), and therefore immunohistochemistry (IHC) investigations need to be carried out.

Altogether, previous data suggest a link between insulin resistance, lipid accumulation and proinflammatory macrophage presence in human PE. For this reason, this chapter will further explore lipid composition and lipid droplet presence as well as macrophage presence and activation in PE placentas. Moreover, a lipidomic analysis of the placentas from our rat model of superimposed PE will be carried out in order to explore neutral lipid composition and to further validate the model. In addition, FGR samples were included in the analysis because it can be used as a comparator group that displays similar placental abnormalities to PE without the lipid abnormalities allowing separation of the effects specific to PE.

4.2 Hypothesis and aims

It was hypothesised that the placentas from pregnancies affected by PE will have higher lipid contents and macrophage counts and activation compared to healthy placentas. Similar to previous observations in humans, it was hypothesised that the placentas from SHRSP dams infused with ANGII will have a higher neutral lipid content compared to vehicle controls. The main aims were:

-To quantify the lipid droplet content in placentas from healthy and PE human pregnancies and to confirm the neutral lipid content by an improved lipidomics analysis.

-To investigate the expression of genes coding for proteins involved in the structure and function of lipid droplets in PE and healthy human placentas.

-To quantitate the DG content in PE and healthy human placentas.

-To quantitate the presence and activation of macrophages in placentas from PE and healthy human pregnancies.

-To investigate circulating plasma lipids and lipid composition of rat placentas from WKY, SHRSP ANGII and SHRSP vehicle control females.

4.3 Materials and methods

4.3.1 Patient recruitment

Patient recruitment of pregnant women with healthy, GDM and PE pregnancies for Oil red O (ORO) staining was carried out at the PRMU under the West of Scotland Research Ethics Service (ethics approval: 11/AL/0017 Glasgow Royal Infirmary REC AM12) (details in section 2.4.1). The archival placental tissue from PE, FGR and healthy pregnancies used for gene expression analysis and CD68 and CSF1R IHC was obtained from recruited patients at the PRMU under ethics approval 06/S070/14 Glasgow Royal Infirmary LREC1 and 01OB007 Glasgow Royal Infirmary REC (details in section 2.4.2). All recruited patients gave their informed voluntary consent.

4.3.2 Oil red O staining

Archival placental paraffin sections were initially used for ORO staining after lipid preservation (summarised in section 2.6.2), however this method was not optimised during the duration of the project and cryosections (gold-standard for ORO staining) were used instead. Placental biopsies were collected from pregnant women with healthy and PE pregnancies at Caesarean delivery, as described in section 2.4.3.1. Samples from each quarter of the placenta were sampled (four samples per placenta) due to the heterogeneity of this tissue. These samples were stored at -80 ºC in moulds with OCT and cryosectioned at 5 µm. Placental cryosections were fixed in 10 % formalin and stained with ORO with haematoxylin counterstain (detailed in section 2.6.2). Whole stained cryosections were imaged

on a slide scanner (X40) and uploaded to QuPath for automated pixel classification analysis. Results for each sample were calculated as a percentage of ORO staining by haematoxylin staining and an average from the four placental quarters was reported.

4.3.3 Expression analysis of genes coding for lipid droplet associated proteins with qRT-PCR

RNA was extracted from frozen archival placental tissue for qRT-PCR analysis. Placentas from healthy, FGR and PE pregnancies were used for these experiments, which were collected as described in section 2.4.2. Frozen placental sections were broken down with a mortar and pestle (up to 0.1g) and placed in 1 ml of Trizol for RNA extraction. RNA isolation, reverse transcription and qPCR were performed as described in section 2.7. Taqman gene expression assays *PLIN1*, *PLIN2*, *PLIN3*, *PLIN4* and *PLIN5* (assay IDs and gene descriptions in Table 1 section 2.8) were used for qPCR analysis on the extracted placental RNA using *TOP1* as the housekeeping gene. The fold change relative to *TOP1* was calculated with the $2^{-\Delta}$CT formula and expressed as a percentage.

4.3.4 Rat maternal plasma lipid quantification

Plasma was collected by Dr Kayley Scott from pregnant WKY and SHRSP dams treated with 750 ng/kg/min ANGII or vehicle control at PP and GD 6.5, 13.5 and 18.5 and stored at -80 ºC until use. Blood was collected by tail venepuncture at PP and GD 6.5 and 13.5 and cardiac puncture at sacrifice at GD 18.5. Plasma triglycerides and total cholesterol were measured as described in section 2.5.

4.3.5 MTBE lipid extraction and lipidomic analysis

Rat placental samples were harvested by Dr Kayley Scott from pregnant WKY and SHRSP dams treated with 750 ng/kg/min ANGII or vehicle control and stored at -80 ºC until use. Lipids were extracted with the MTBE-based isolation protocol described in section 2.3 using 30 µl of internal standard (EquiSPLASH, Avanti Polar Lipids). Lipid extractions from frozen archival human placental tissue from healthy and PE patients were performed by Professor Barbara Meyer at the University of Wollongong. Lipids were extracted with the MTBE-based isolation protocol described in section 2.3 using 30 µl of internal standard (SPLASH® LIPIDOMIX®,

Avanti Polar Lipids). Extracted lipid samples were diluted in methanol:chloroform (2:1 v/v) with 5 mM ammonium acetate and analysed in duplicate. Lipid peak areas from the obtained spectra were normalised to the appropriate lipid standard and their wet tissue weight. Even though a full dataset of lipids was obtained, issues with the MS machine led to internal standard peak shifting and misinterpretation of the results in the negative ionisation mode. Phospholipids including phosphatidylethanolamine (PhE), phosphatidylglycerol (PG), phosphatidylserine (PS) and phosphatidylinositol (PI) are identified in the negative ionisation mode and therefore could not be correctly quantified for these experiments. To aid interpretation of the main relevant lipids for this study, only neutral lipids (triacylglycerols (TG) and cholesteryl esters (CE)) and diacylglycerols (DG) were included in this chapter. It is important to note that only MS1 data was included in this chapter due to difficulties in analysing MS2 data, and therefore the individual fatty acyl groups making up the different lipids could not be investigated.

4.3.6 CSF1R and CD68 staining on placental paraffin sections

Archival placental paraffin sections were stained with CD68 and CSF1R antibodies as markers of macrophage infiltration and activation, respectively, as described in section 2.6.3. Whole stained slides were imaged with a slide scanner (x40) and analysed on QuPath to automatically detect positively stained cells (method in section 2.6.3). Ten and fifteen regions per slide were used to count positive CD68 and CSF1R cells, respectively, which were averaged to provide a mean cell count per mm^2. Analysed regions were randomly selected and analysed blindly by one observer.

4.3.7 Statistical analysis

GDM samples were included in the analysis of gene expression and ORO area results because the same healthy placental samples were used as control for both groups. However, to aid the interpretation of the current chapter, only PE (and FGR) data will be presented in this chapter and GDM data will be presented in Chapter 6. ORO area was log-transformed and analysed by a mixed effects model which included the patient ID as a random factor and placental section and patient group as fixed factors. Since placental sections were not found to be significantly

different, an average of the ORO area was taken from all the sections from each patient and the average was used for statistical analysis. Data was presented as an average of the ORO areas normalised to haematoxylin-stained areas from the sections of the same placenta and represented as an individual data point. Data analysis of the averaged ORO area was performed by a one-way ANOVA with Tukey *post hoc* test. Gene expression data was also analysed by a one-way ANOVA.

Positive CSF1R staining data was imputed by adding 0.01 to all data points before log transformation for statistical analysis due to the large number of zeroes in the dataset (West, 2022). Imputed log transformed data was analysed by an unpaired t-test. CD68 data was analysed by an unpaired t-test on log transformed data.

Due to the large number of missing values in the lipidomics results, originating from the lack of presence in the sample and/or limits of detection from the mass spectrometry method, a "clean-up" method was carried out. Lipid species that were not detected in more than 20 % of the samples were removed from the analysis. It is important to note that only even-chain fatty acids were considered in this thesis as these are the ones found in animals, while odd chain fatty acids are from dietary sources. Before clean-up, 196 and 226 even-chain lipid species from the TG, DG and CE families were detected in total in the human and rat samples respectively, but only 66 and 175 remained after removing the lipids undetected in more than 20 % of the samples. Additionally, the missing values for the remaining lipid species were imputed by adding the lowest value detected, which was used as a reasonable estimation for the detection limit of the machine (Wehrens et al., 2016). Total TG, DG and CEs were calculated from the sum of the individual species after the clean-up and imputed values.

Statistical analysis of the TG, DG and CE sum composition was carried out in Minitab on log transformed data. Statistical analysis of the individual species from lipidomics data was carried out with the web-based platform MetaboAnalyst, which generated the principal component analysis (PCA) and the statistical tests between groups. A PCA allows for the visualisation and the distribution of multivariate data by separating it into new dimensions derived from the original variables, known as principal components. However, a PCA does not provide information on what the differences between groups are, and therefore a PCA loadings plot and variable importance plot (VIP) are needed to provide insights

into the nature of the PCA. Lipidomics data was log transformed and auto-scaled (each value was divided by the standard deviation) by the software before analysis, as suggested suitable for other *omics* data analysis (van den Berg et al., 2006). Human lipidomics data was analysed by a t-test (healthy vs PE) and rat lipidomics data was analysed by a one-way ANOVA (Control vs ANGII vs WKY).

Patient characteristics are presented as mean ± SD for continuous variables and number (percent) for primiparous and fetal sex. Differences between continuous variables was carried out by an unpaired t-test or one-way ANOVA, depending on the number of groups analysed. Differences between proportions was carried out by a Fisher's exact test. Plasma rat lipids results were analysed using a mixed effects model with Tukey *post hoc* test. Statistical analyses were performed on Minitab software version 21.4.3. Statistical significance was assumed at $P<0.05$ for all experiments apart from lipidomics results, where statistical significance was assumed at $P<0.01$ to account for multiple testing.

4.4 Results

4.4.1 Patient demographics

Patient demographics used for the ORO analysis are summarised in Table 6. Age, BMI, SBP, DBP, smoking status and fetal sex were not significantly different between groups, however, gestational age and birthweight were significantly lower in the PE group compared to controls. This is expected as a consequence of common preterm emergency C-sections performed in PE. There was also a significantly higher number of primiparous pregnancies in the PE group compared to controls.

Table 6. Maternal characteristics at booking and delivery. Blood pressure at PE diagnosis is only presented in the PE group and therefore no statistical analysis was carried out. Data analysed with an unpaired t-test (*on log-transformed data). BMI: Body mass Index. Significance at P<0.05.

	Healthy (n=14)	PE (n=9)	P-value
Age (years)	32.4 ± 3.2	29.3 ± 5.4	0.16
***Booking BMI (kg/m^2)**	25.8 ± 4.8	28.5 ± 7.1	0.36
***Booking systolic blood pressure (mmHg)**	112.4 ± 11.1	121.7 ± 13.2	0.17
***Booking diastolic blood pressure (mmHg)**	66.6 ± 9.7	76.8 ± 10.2	0.054
Systolic blood pressure at diagnosis (mmHg)	-	145.4 ± 5.0	-
Diastolic blood pressure at diagnosis (mmHg)	-	86.3 ± 10.9	-
Gestational age at delivery (days)	270 ± 10	240 ± 26	0.013
Birthweight (g)	3525 ± 469	2371 ± 832	0.006
Primiparous (n, %)	0 (0)	5 (55.6)	0.001
Fetal sex (male, %)	8 (57.1)	4 (44.4)	0.75
Smoker n (%)	2 (14.3)	0 (0)	0.24

Patient demographics used for the gene expression analysis and CD68 and CSF1R are summarised in Table 7. Note that for some experiments only a subset of samples was used, which will be indicated in each section as required. Age, smoking status and BMI were not significantly different between groups, however, systolic and diastolic blood pressure were significantly higher in PE patients. In addition, gestational age at delivery and birthweight were significantly lower in PE patients compared to healthy controls. This is expected as a consequence of common preterm emergency C-sections performed in patients with PE. There were no differences in percent primiparous pregnancies or fetal sex distribution between groups.

Table 7. Maternal characteristics at booking. Data analysed with a one-way ANOVA (*on log-transformed data). BMI: Body mass Index. Values with different superscript letters indicate significant differences after Tukey *post hoc* test. Significance at P<0.05.

	Healthy (n=68)	PE (n=23)	FGR (n=10)	P-value
Age (years)	30.4 ± 5.1	29.8 ± 5.8	29.7 ± 4.9	0.84
***Booking BMI (kg/m^2)**	28.9 ± 6.4	30.1 ± 7.4	24.7 ± 5.5	0.068
***Systolic blood pressure (mmHg)**	121 ± 15^a	144 ± 25^b	113 ± 4^a	P<0.001
***Diastolic blood pressure (mmHg)**	71 ± 10^a	90 ± 16^b	72 ± 3^{a,b}	P<0.001
Gestational age at delivery (days)	275 ± 9^a	253 ± 21^b	253 ± 21^b	P<0.001
Birthweight (g)	3538 ± 576^a	2434 ± 805^b	1969 ± 478^b	P<0.001
Primiparous (n, %)	27 (39.7)	14 (60.8)	4 (40.0)	0.21
Fetal sex (male, %)	32 (47.1)	13 (56.5)	3 (30.0)	0.54
Smoker n (%)	14 (21)	4 (17)	5 (50)	0.5

4.4.2 Placental lipid droplet quantification

ORO area was quantified as a percentage of haematoxylin area on placental tissue from women with PE and healthy pregnancies (Figure 4-1). PE placentas had

significantly higher ORO area compared to healthy controls (5.56 ± 5.15 vs 1.94 ± 1.70 %; P=0.009).

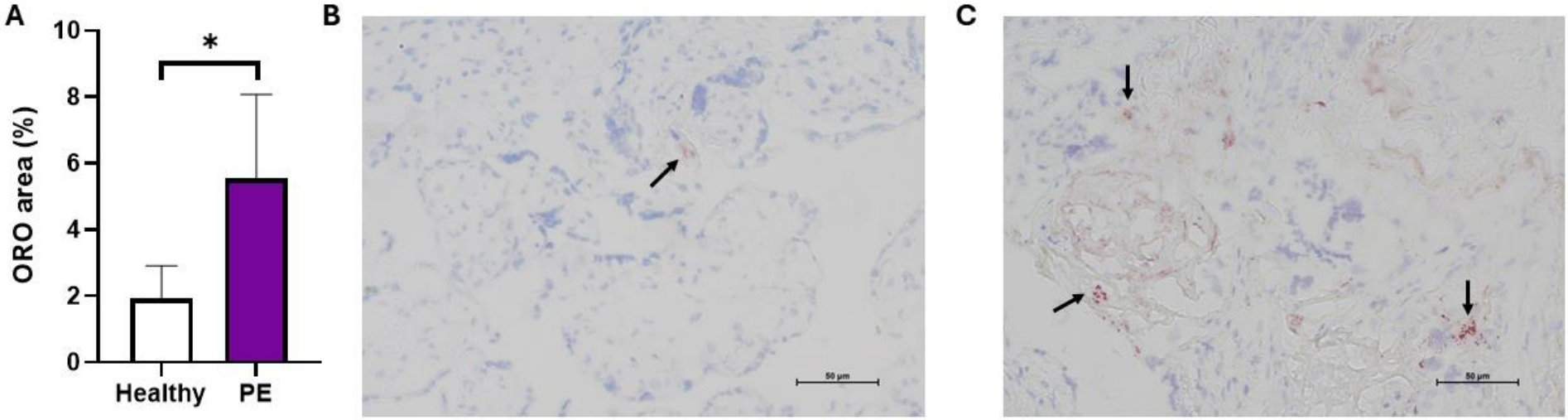

Figure 4-1. Lipid droplet quantification in healthy and PE placentas. (A) Lipid droplet by haematoxylin area in healthy and PE placentas. **(B)** Representative ORO image from a healthy placenta. **(C)** Representative ORO image from a PE placenta. Data is shown as median ±IQR where individual samples represent each data point (Healthy: n=14 and PE: n=9). Data was analysed by a one-way ANOVA (including GDM group) with Tukey *post hoc* test (reported here) on log-transformed data; significance at *P<0.05.

4.4.3 Placental expression of genes coding for lipid droplet associated proteins

Several perilipin genes were investigated in healthy, PE and FGR placentas (Figure 4-2) as markers of lipid droplet presence as they are found in the surface of lipid droplets and are involved in the mobilisation of lipids in adipose tissue. There were no significant differences between groups in placental *PLIN1*, *PLIN2* and *PLIN3* expression. PE placentas had a significantly higher expression of *PLIN4* compared to healthy and FGR (0.51 ± 0.92 vs 0.23 ± 0.22 and 0.17 ± 0.35 %; P<0.001 and P=0.007, respectively). PE placentas also had a significantly higher expression of *PLIN5* compared to healthy (0.24 ± 0.29 vs 0.096 ± 0.16 %; P=0.003) but not FGR placentas (0.089 ± 0.19 %; P=0.088).

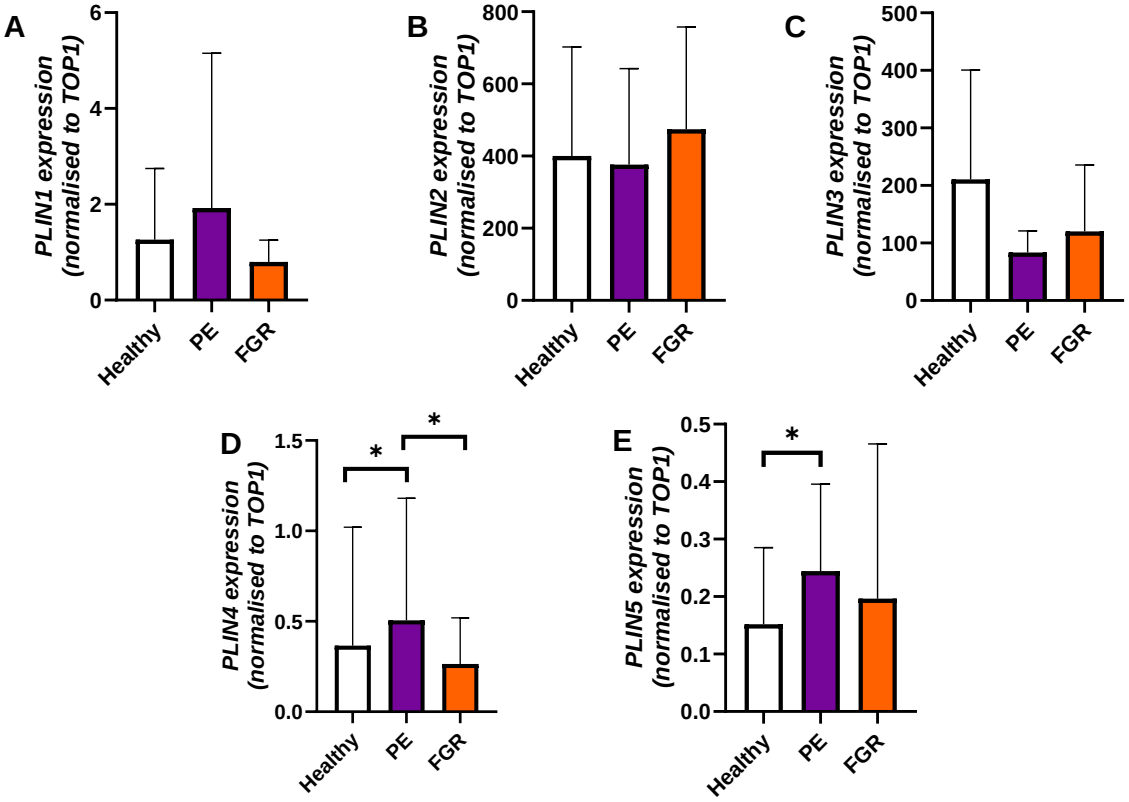

Figure 4-2.Gene expression of lipid droplet associated genes. Gene expression of *PLIN1* (A), *PLIN2* (B), *PLIN3* (C), *PLIN4* (D) and *PLIN5* (E) were analysed by qRT-PCR and are presented as a percentage of the expression of the housekeeping gene *TOP1*. Data is shown as median ±IQR where individual samples represent each data point (Healthy: n=68, PE: n=23, FGR: n=10). Data was analysed by a one-way ANOVA (including GDM group) with Tukey *post hoc* test (reporter here) on log transformed data; significance at *P<0.05.

4.4.4 Lipid composition in the PE placenta

A lipidomic analysis of healthy and PE placentas was performed on a subset of samples (healthy (n=10) and PE (n=16)) from the patients in Table 7. It is important to note that there were no differences in demographics compared to the full dataset, and PE and healthy samples were still BMI and age matched.

The PCA scores, loading and VIP plots are presented in Figure 4-3. PCA scores plot show clear separation between healthy (left-hand side) and PE (right-hand side) groups with minimal overlap. The PCA loadings plot and VIP plot show the variables that drive the separation of the groups: TG and CE species heavily contribute to the separation of the groups with VIP scores greater than 1 (considered of important contribution to the model) and are higher in PE. Only three DG species were identified as contributors to the group separation within the 30 top variables in the VIP plot and these are lower in PE.

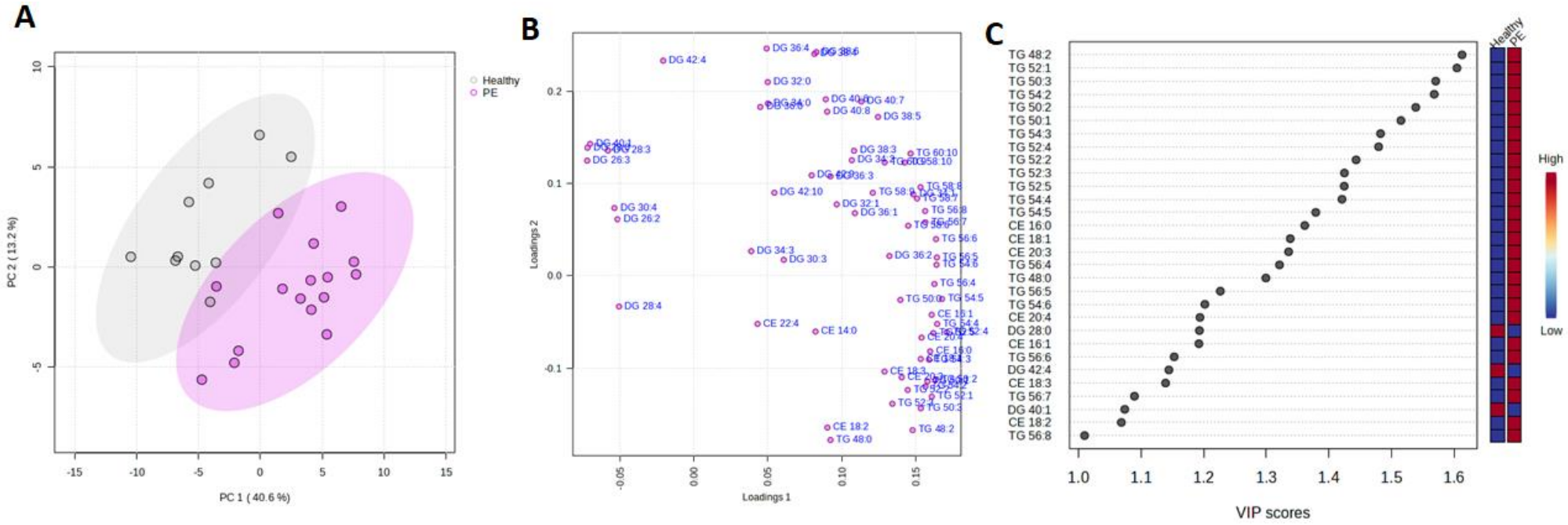

Figure 4-3. Distribution of human lipidomics data by PCA scores and loadings plot and VIP plot of the individual contribution to group differences. (A) PCA scores plot of the healthy (n=10) and PE (n=16) groups. Each data point represents each individual sample and the ellipses indicate the 95 % confidence intervals. **(B)** PCA loadings plot of the different variables contributing to the differences between healthy and PE groups. Variables on the x axis extreme are correlated to the principal component 1 (PC1) and variables on the y axis extreme are correlated with the principal component 2 (PC2). **(C)** VIP plot of the top 30 contributors of the differences between groups with indication of whether these were higher or lower.

Total TG, DG and CEs were calculated from the sum of the individual lipid species from healthy and PE placentas and represented in Figure 4-4. TGs and CEs were significantly higher in PE placentas compared to controls (TG: PE 453.6 ± 262.1 vs healthy 129.3 ± 109.4; P<0.001; CE: PE 1063 ± 1004 vs healthy 425.9 ± 432.7 nmol/g; P<0.001). In contrast, DG were not significantly different between groups (PE 60.69 ± 63.64 vs healthy 71.7 ± 82.6 nmol/g; P=0.48).

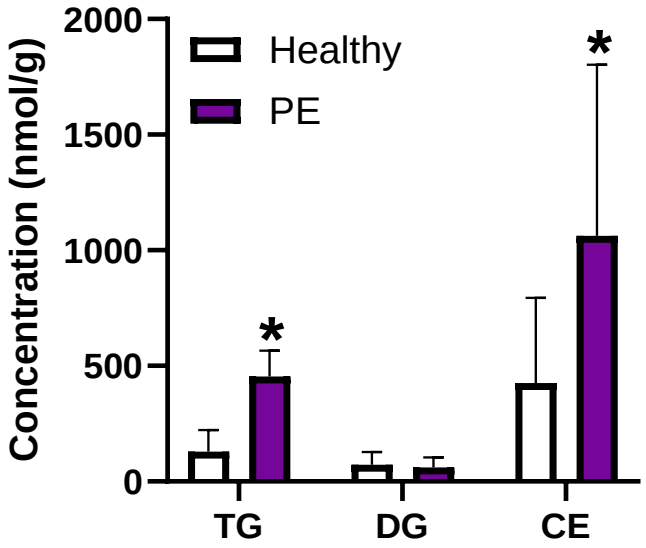

Figure 4-4. Placental composition of TG, DG and CE in healthy and PE pregnancies. Lipid concentration of the total TG, DG and CE in healthy (n=10) and PE (n=16) placentas. Data is presented as median ±IQR where individual samples represent each datapoint. Data was analysed by an unpaired t-test on log transformed data, significance at *P<0.05.

Since the present study confirmed the observations in our previous study (Brown et al., 2016), only DG individual lipid species were investigated as these have not been studied in PE before (Figure 4-5). Three lipid species (DG 28:0, DG 40:1 and DG 42:4) were found to be significantly lower in PE placentas compared to controls (P<0.01). The other 26 detected DG species were not found to be significantly different between groups.

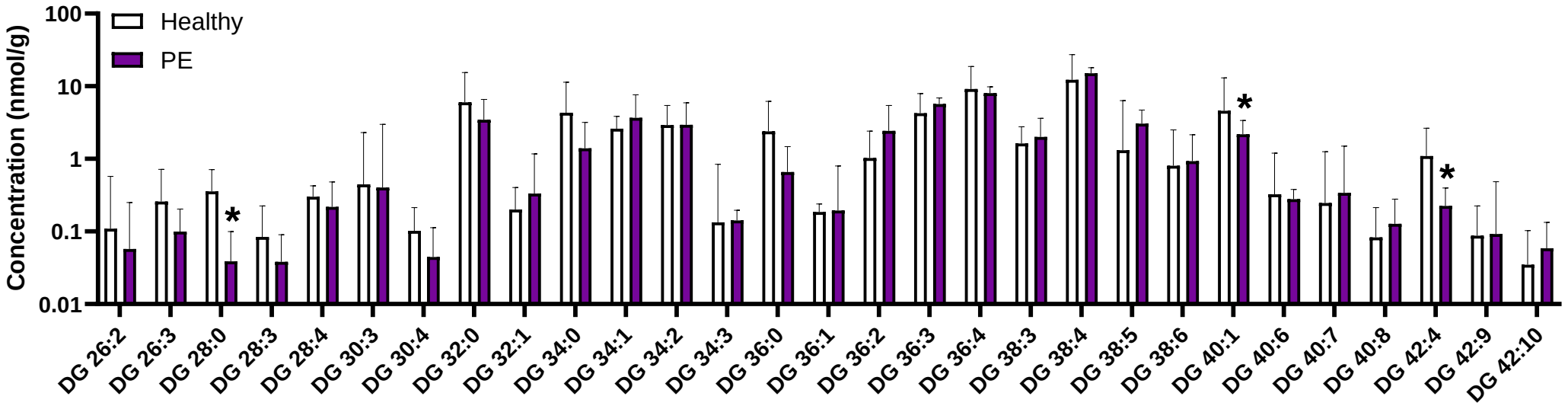

Figure 4-5. Placental composition of individual DG species in healthy and PE pregnancies. Lipid concentration of different detected DG species in healthy (n=10) and PE (n=16) placentas. Data is shown on a logarithmic scale to aid interpretation. Data is presented as median ±IQR where individual samples represent each datapoint. Data was analysed by an unpaired t-test on log transformed data, significance at *P<0.01.

4.4.5 Macrophage infiltration and activation in the placenta

Healthy and PE placentas were stained using CD68 (marker of total macrophages) and CSF1R (marker of activated macrophages) antibodies and positive cells were quantified (Figure 6-6). There were no significant differences between healthy and PE placental CD68 and CSF1R positive cells. Data was presented as individual datapoints to highlight the variability and trends of the data.

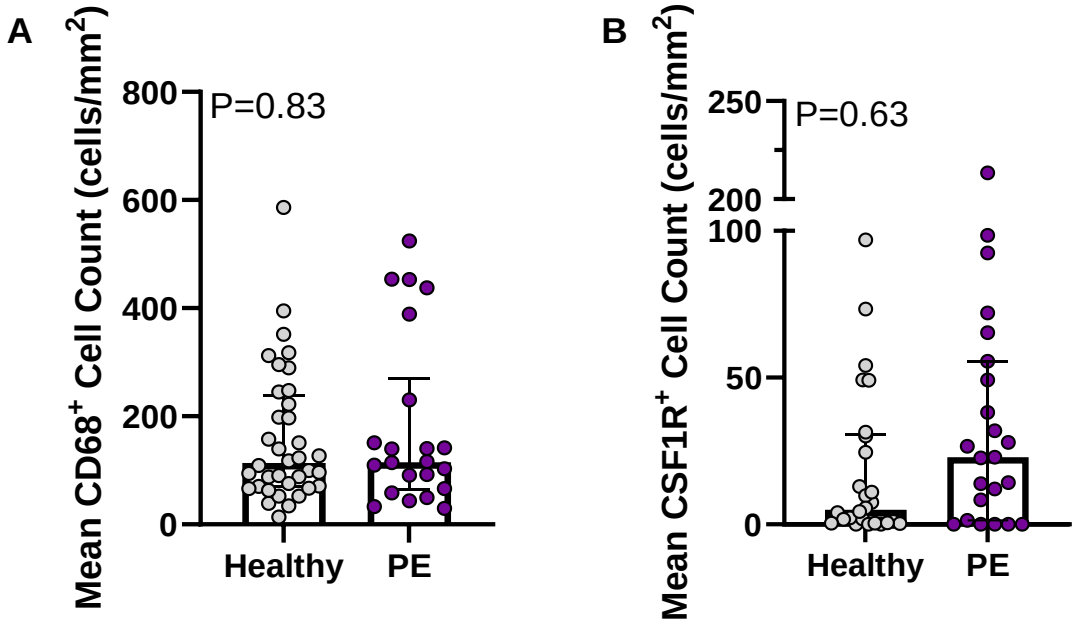

Figure 4-6. CD68 and CSF1R positive cells in PE and healthy placentas. Positive CD68 (A) and CSF1R (B) counts are presented by tissue area. Data is shown as median ±IQR where individual samples represent each data point (CD68 - Healthy: n=36 and PE: n=22; CSF1R - Healthy: n=26 and PE: n=23). Data was analysed by an unpaired t-test on log-transformed data; significance at P<0.05.

4.4.6 Lipid metabolism in an animal model of superimposed preeclampsia

4.4.6.1 Plasma lipids in the mother and the offspring

Total cholesterol and triglycerides were measured in plasma from SHRSP and WKY females at PP and GD 6.5, 13.5 and 18.5 (Figure 4-7) in order to look for lipid abnormalities in circulating lipids after ANGII treatment. WKY females had significantly lower plasma triglycerides on average across all time periods compared to SHRSP vehicle control and ANGII (0.80 ± 0.070 vs 2.10 ± 0.36 and 1.92 ± 0.23 mmol/l; P=0.001 and P<0.001). In contrast, WKY females had significantly higher total plasma cholesterol on average across all time periods compared to SHRSP vehicle control and ANGII (2.42 ± 0.079 vs 2.01 ± 0.10 and 2.13 ± 0.082 mmol/l; P=0.006 and P=0.019). There were no significant differences in circulating plasma lipids between SHRSP vehicle control and ANGII females (P>0.05). There

was an effect of gestational day on both TG and cholesterol (P<0.001) as expected for pregnancy lipids.

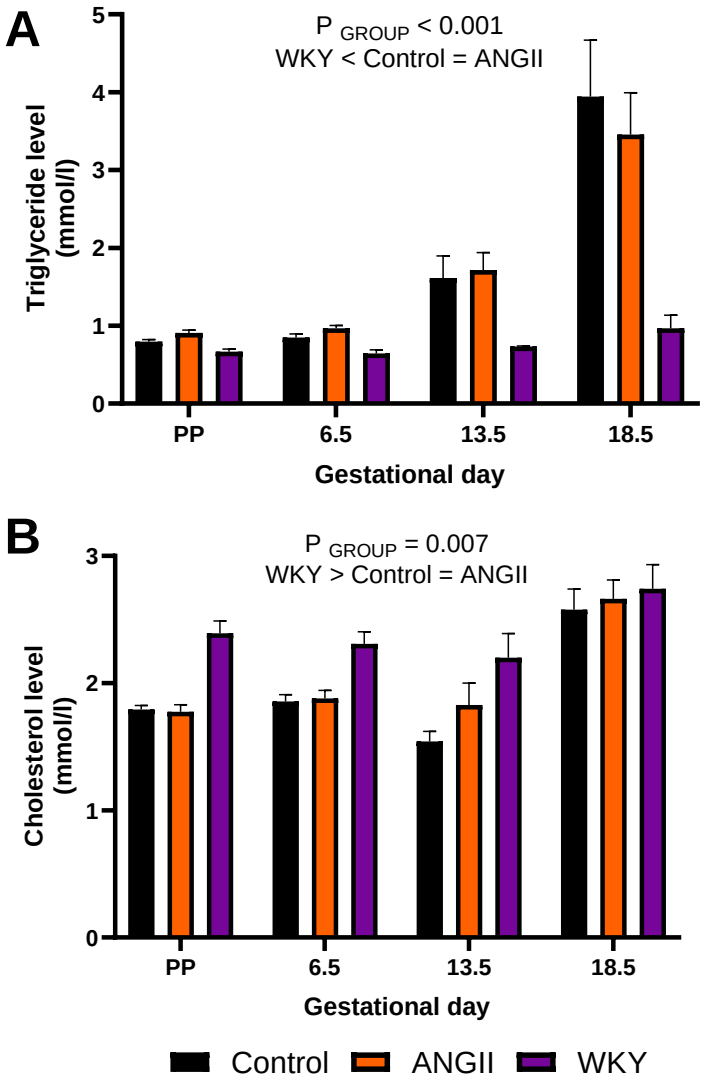

Figure 4-7. Plasma triglycerides and total cholesterol from WKY and SHRSP vehicle control and ANGII-treated females. Triglyceride (A) and cholesterol (B) content was measured from plasma collected at PP and GD 6.5, 13.5 and 18.5. Data is shown as mean ±SEM (n=8-18 per group) where individual offspring represent each data point. Data was analysed by a mixed effects model of lipid concentration vs gestational period and treatment group (P<0.05) with Tukey *post hoc* test.

4.4.6.2 Lipid composition of rat placentas

Rat placentas were harvested at GD 18.5 for lipid extraction. A lipidomic analysis of the placentas from WKY and SHRSP vehicle and ANGII dams was carried out in order to look for commonalities with the human PE phenotype. The PCA scores, loading and VIP plots are presented in Figure 4-8. PCA scores plot shows overlap between the groups which indicates minimal differences. The PCA loadings plot shows that TGs contribute to the separation in the PC1 whereas CEs and DGs contribute to the separation of the PC2. There were no VIP scores greater than 1

which means that none of the studied variables had a strong contribution to the model. However, it should be noted that the highest scoring variables belong to the CE family which suggests an important contribution to the differences between groups, although this is not important as there is no clear separation between groups and the VIP scores are less than 1.

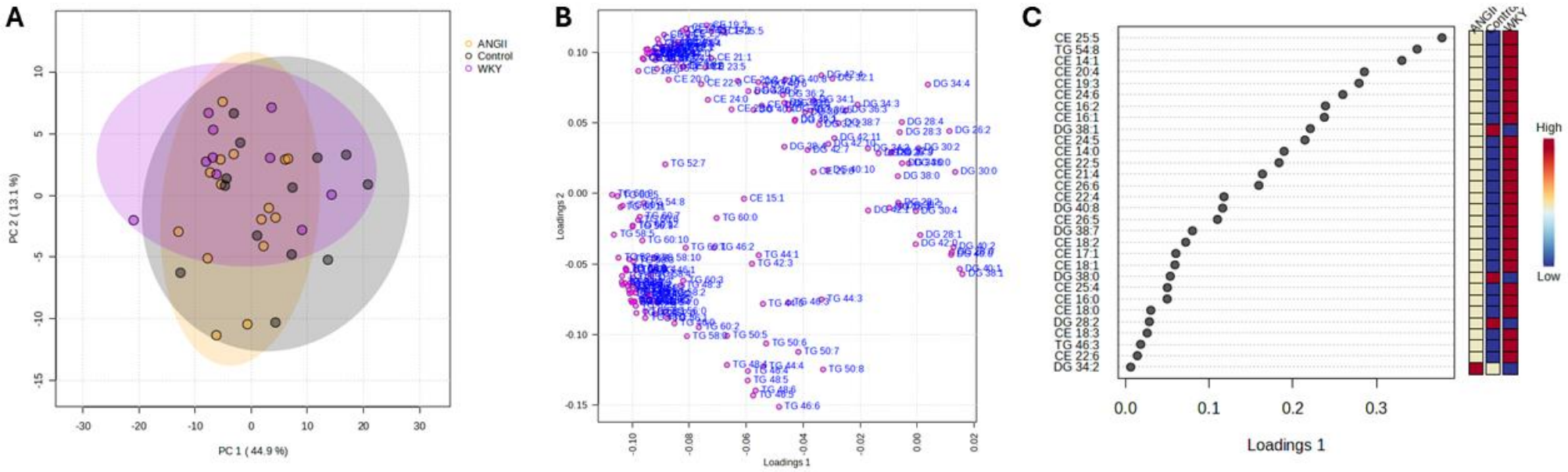

Figure 4-8. Distribution of rat lipidomics data by PCA scores and loadings plot and VIP plot of the individual contribution to group differences. (A) PCA scores plot of the SHRSP control (n=13), SHRSP ANGII (n=15) and WKY (n=10) groups. Each data point represents each individual sample and the ellipses indicate the 95 % confidence intervals. **(B)** PCA loadings plot of the different variables contributing to the differences between groups. Variables on the x axis extreme are correlated to the PC1 and variables on the y axis extreme are correlated with the PC2. **(C)** VIP plot of the top 30 contributors of the differences between groups with indication of whether these were higher or lower.

Total TG, DG and CEs were calculated from the sum of the individual lipid species from SHRSP vehicle control and ANGII and WKY placentas and represented in Figure 4-9. CEs were significantly higher in WKY placentas compared to SHRSP vehicle control (6353 ± 8050 vs 984 ± 3696 nmol/g; P=0.015) but not ANGII (2086 ± 4095 mmol/g; P=0.26). In contrast, DGs and TGs were not significantly different between groups.

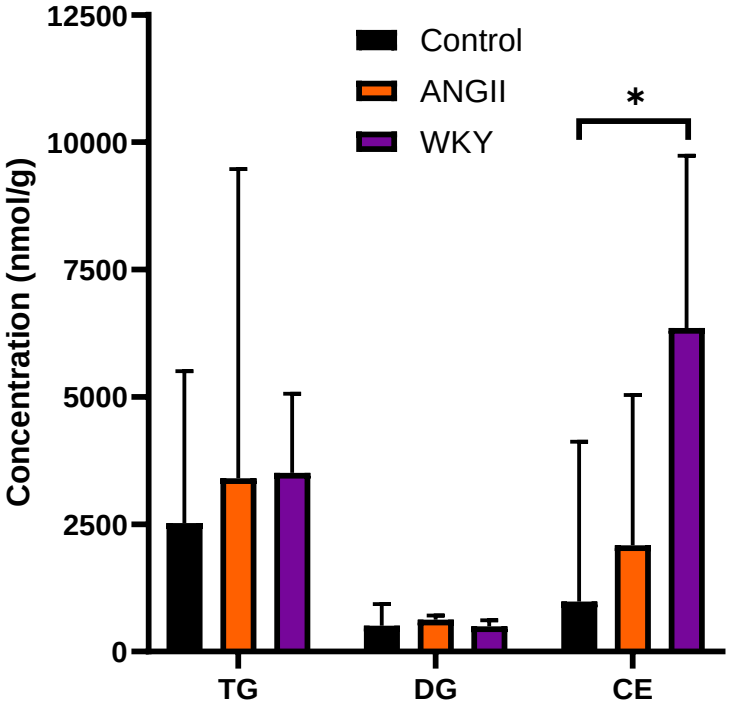

Figure 4-9. Placental composition of TG, DG and CE in SHRSP vehicle and ANGII and WKY placentas. Lipid concentration of the total TG, DG and CE in SHRSP control (n=13), SHRSP ANGII (n=15) and WKY (n=10) placentas. Data is presented as median ±IQR where individual samples represent each datapoint. Data was analysed by one-way ANOVA on log transformed data with Tukey *post hoc* test; significance at *P<0.05.

The individual TG, DG and CE species were also analysed to further investigate any differences between groups (Figure 4-10, 4-11 and 4-12). Interestingly, 79 TG, 51 DG and 66 CE species were detected in the rat placentas. There were no significant differences in the composition of the esterified fatty acids in the individual lipid species between groups (P>0.01).

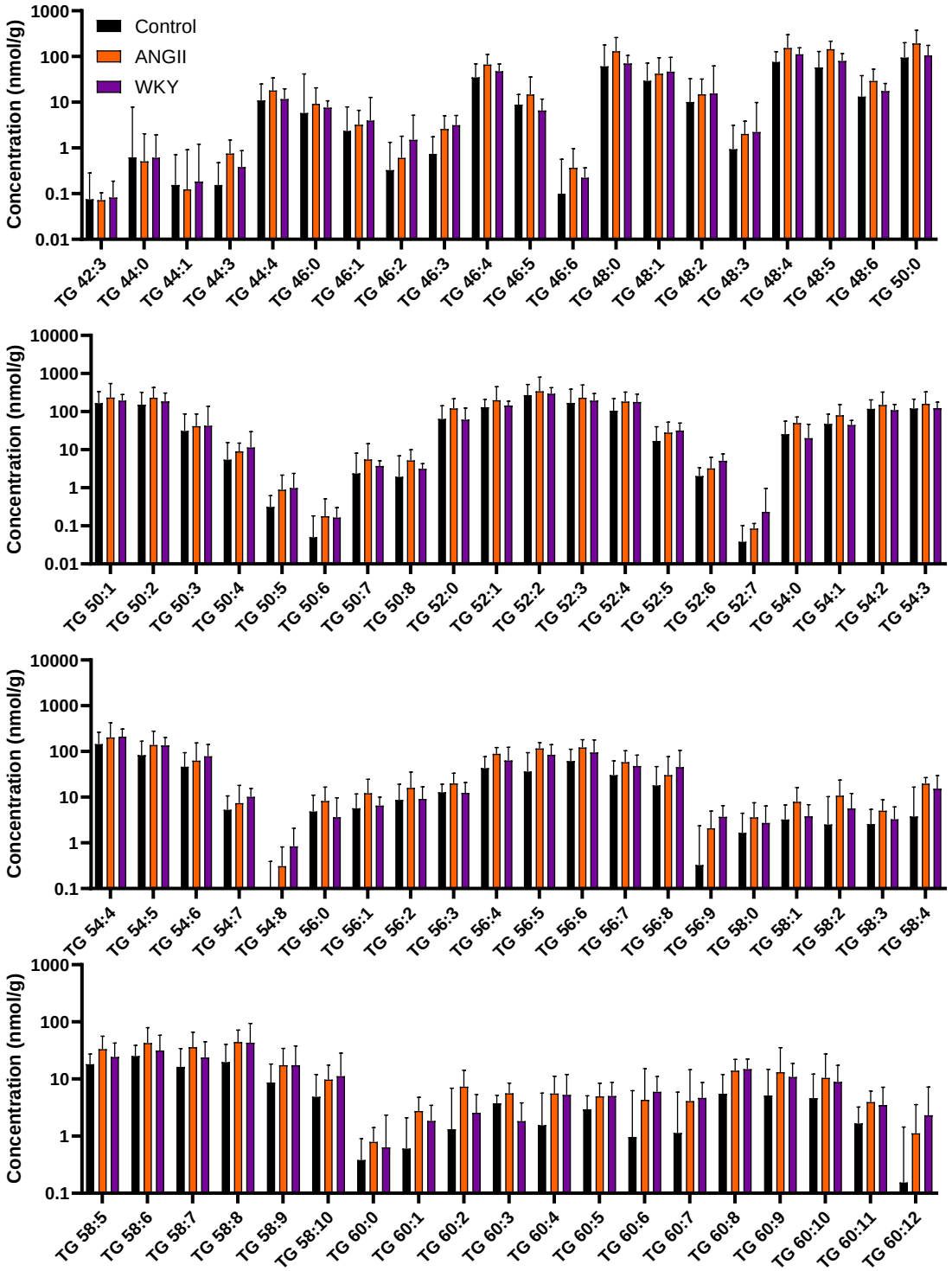

Figure 4-10. Placental composition of individual TG species in SHRSP control, SHRSP ANGII and WKY placentas. Lipid concentration of different detected TG species in SHRSP control (n=13), SHRSP ANGII (n=15) and WKY (n=10) placentas. Data is shown on a logarithmic scale to aid interpretation. Data is presented as median ±IQR where individual samples represent each datapoint. Data was analysed by a one-way ANOVA on log transformed data with *post hoc* Tukey test, significance at *P<0.01.

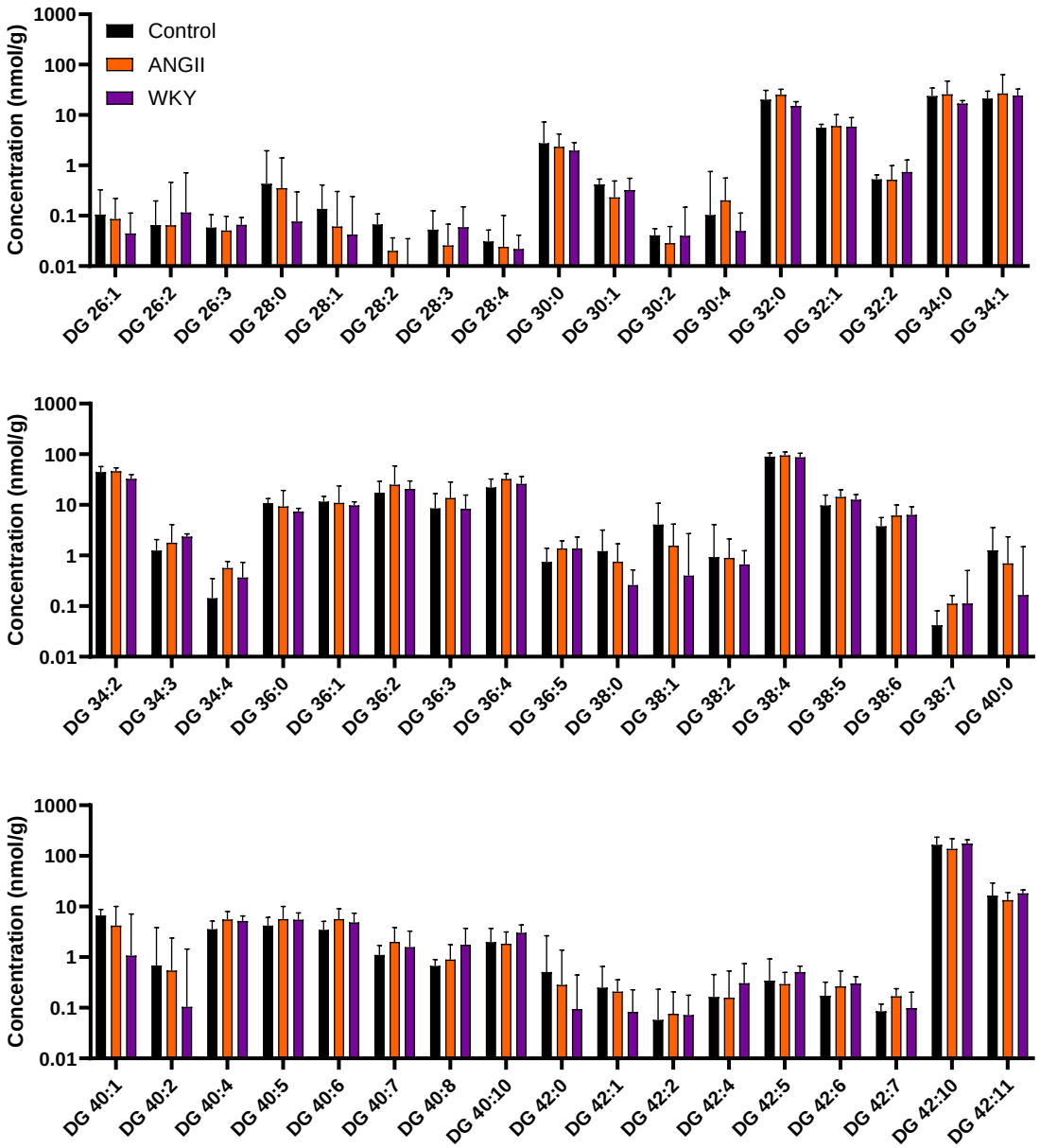

Figure 4-11. Placental composition of individual DG species in SHRSP control, SHRSP ANGII and WKY placentas. Lipid concentration of different detected DG species in SHRSP control (n=13), SHRSP ANGII (n=15) and WKY (n=10) placentas. Data is shown on a logarithmic scale to aid interpretation. Data is presented as median ±IQR where individual samples represent each datapoint. Data was analysed by a one-way ANOVA on log transformed data with *post hoc* Tukey test, significance at *P<0.01.

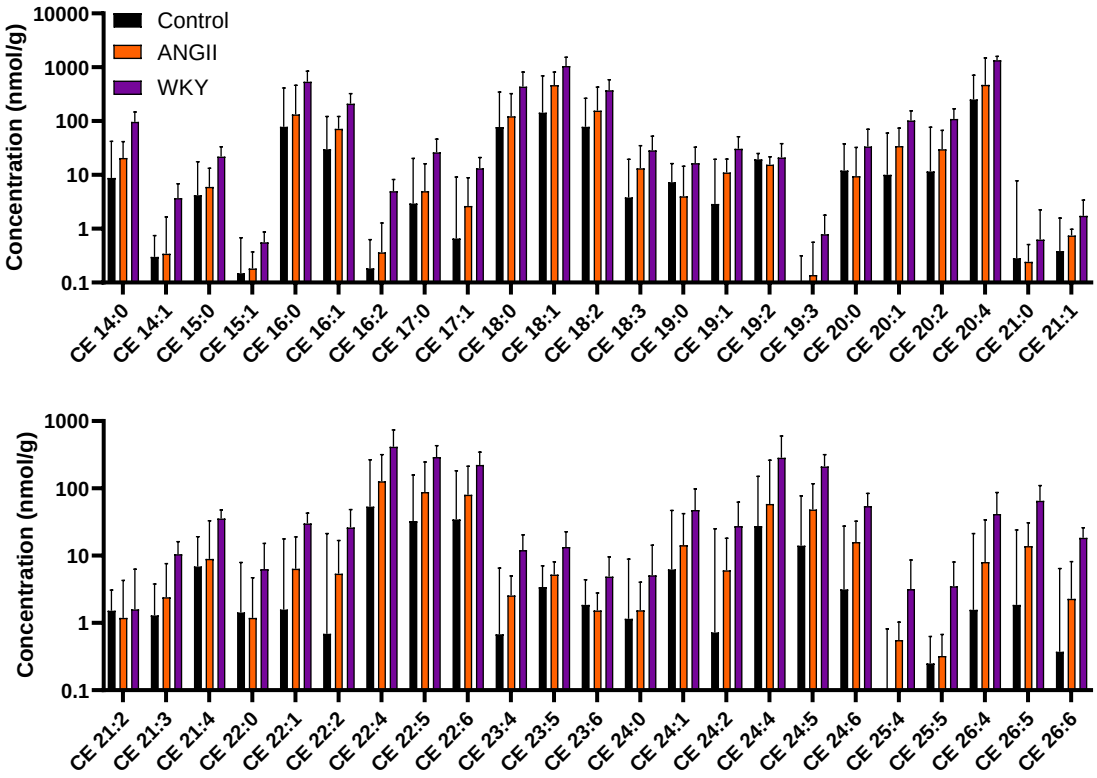

Figure 4-12. Placental composition of individual CE species in SHRSP control, SHRSP ANGII and WKY placentas. Lipid concentration of different detected CE species in SHRSP control (n=13), SHRSP ANGII (n=15) and WKY (n=10) placentas. Data is shown on a logarithmic scale to aid interpretation. Data is presented as median ±IQR where individual samples represent each datapoint. Data was analysed by a one-way ANOVA on log transformed data with *post hoc* Tukey test, significance at *P<0.01.

4.5 Discussion

The gene expression, lipidomics and histology data presented in this chapter provide additional evidence to support the proposed presence of ectopic fat on the placenta in PE. It was hypothesised that this altered placental lipid storage would also be mimicked in our ANGII rat model of superimposed PE, however, lipidomics data showed no significant differences between ANGII-exposed and vehicle control SHRSP placentas suggesting that this is not a complete model of human PE. The placental lipidomics data showed no differences in DG composition between PE and healthy or ANGII and control placentas, although subtle changes in individual DG species were observed in humans. In addition, there were no differences in total macrophage presence and activation between PE and healthy groups, although this may be explained by the low number of fields counted per image. Overall, this chapter has demonstrated important changes in the lipid storage of the placenta in humans that may contribute to the pathophysiology of PE.

Even though higher placental neutral lipid content has already been identified by the Freeman group in humans in PE, there has not been evidence showing the accumulation of these lipids in ectopic droplets. The gene expression data presented in this chapter shows the higher expression of mRNA coding for the lipid droplet-associated proteins *PLIN4* and *PLIN5* in the PE placenta. This suggests a higher amount of lipid droplets, although whether this increase in gene expression corresponds to elevated protein levels has not been confirmed. Despite their common roles in lipid droplet formation and metabolism, the five different perilipins have specific roles in different tissues. *PLIN1* is the main perilipin found in lipid droplets from mature adipocytes in WAT, whereas *PLIN2* is present in small lipid droplets from immature adipocytes and it is mainly expressed during adipocyte differentiation (Itabe et al., 2017). In addition, *PLIN2* is the major lipid droplet-associated protein in the liver and it has been suggested that it is involved in fatty liver disease (McManaman et al., 2013). Similar to *PLIN1*, *PLIN4* is associated with the late stages of human adipocyte differentiation and *PLIN5* is linked to fatty acid supply to mitochondria in muscle cells, including the heart (Itabe et al., 2017). Previous investigations on placental perilipin expression have shown that *PLIN2* plays an important role in the accumulation of lipid droplets in human trophoblasts under hypoxic conditions that mimic placental dysfunction (Bildirici et al., 2018). Out of all *PLIN* genes, only *PLIN2* and *PLIN3* have been found to be expressed in rat and human placenta (Mishima et al., 2011), although RT-PCR, and not RT-qPCR, was performed in this study. Since the expression of the other PLINs is lower compared to *PLIN2* and *PLIN3*, these authors might have missed important expression patterns by performing this technique. This shows a strength of this study, presenting the first evidence of the expression of all the perilipin genes in the human placenta and elucidating expression changes in PE. The reason behind the higher expression of these particular PLINs in placenta remains unclear, however it implies the elevated presence of ectopic placental lipid droplets in PE which was the main aim of this study.

Additionally, using lipidomics, higher TG and CE contents were observed in the PE placentas compared to healthy controls, which confirms previous findings (Brown et al., 2016). The MS method carried out in the current investigations has been upgraded from low to high-resolution tandem-MS since it was performed on these same placental samples in 2016 (Brown et al., 2016) and the analyses conducted

in this chapter corroborate the results using the low resolution method. In contrast, similar results were not found in the animal model of superimposed PE, where placental lipid content from SHRSP dams treated with ANGII did not differ from vehicle controls. These results are consistent with the circulating plasma lipid data which did not show any differences between ANGII and vehicle groups. It is important to note that higher triglycerides and lower total cholesterol were detected in SHRSP dams compared to WKY, which was also observed in the offspring (Chapter 3) and confirms strain differences. In addition, WKY placentas contained higher total CE levels which is consistent with the elevated plasma cholesterol levels in this strain. This means that the SHRSP ANGII infusion model is able to mimic the cardiovascular consequences of PE in the offspring (as discussed in Chapter 3), but it cannot imitate the insulin resistance, dyslipidaemia and placental ectopic fat accumulation in humans. Similarly, the RUPP model of PE does not show the plasma lipid abnormalities observed in humans (Gilbert et al., 2007). In contrast, the L-NAME treatment of the pregnant C57BL/6 mice mimics the metabolic lipid abnormalities observed in humans (Sun et al., 2012). The inconsistency in the metabolic impact of PE in animal models highlights the need for careful consideration when drawing conclusions from animal models.

Moreover, the present study also investigated the DG content in PE and healthy human placentas which, to our knowledge, has not been studied before and may be important in the development of the insulin resistant state. The total DG concentration was not different between PE and healthy placentas but there was lower content of some individual DG species (DG 28:0, DG 40:1 and DG 42:4) observed in PE. Despite the statistically significant results, these changes may not be biologically relevant as these lipids have not previously been identified as being involved in other human conditions. However, as this lipid class has not previously been investigated in the PE placenta, further experiments are needed to study the role of these DG species in pregnancies complicated by PE.

Elevated plasma DGs have been observed in pregnant women with PE (Hong et al., 2020), which is possibly associated with insulin resistance. This suggests an analogy with MASLD, where hepatic DGs inhibit the insulin receptor signalling through PKC (Kumashiro et al., 2011) that leads to elevated insulin resistance, increased lipolysis and lipid accumulation. However, according to the data in this

chapter, this does not seem to take place in the placenta. This was somewhat expected due to the important role of the placenta during insulin sensitive and resistant states through the secretion of placental hormones and inflammatory factors to the maternal circulation (Kampmann et al., 2019). Interestingly, recent plasma lipidomic profiling during pregnancy revealed that the TG and DG species containing 16:0, 18:0, 18:1 and 18:2 fatty acyl chains were strongly correlated with insulin resistance (Chen et al., 2023), thereby showing the importance of investigating the fatty acid chains of the studied lipids which could not be performed in this study. The challenge of analysing MS2 data for fatty acid analysis is the identification of lipids with equal (or similar) mass to charge ratios, known as isobaric interference, which cannot be discerned even when using high resolution MS techniques. This issue could be resolved by separation techniques such as liquid chromatography (LC) prior to MS which would result in added cost and time. Further investigations into the fatty acid composition of placental neutral lipids and DG are needed to reveal possible changes in the underlying composition of these lipid species in PE.

According to the results from this chapter, the elevated neutral lipids found in the PE placenta appear to accumulate in the form of lipid droplets as would be expected (Krahmer et al., 2013). It is important to note that, despite significant results, this study was powered to detect a difference using our available archival placental tissue (n=23 for PE samples) which would have allowed 80% power to detect a difference in n=17 to 23 PE placentas. Since the archival tissue was paraffin fixed, and this method was not compatible with ORO staining, further samples were collected for this experiment. The difficulty of recruiting women with PE and collecting samples during emergency C-sections limited the amount of samples obtained during this PhD. Despite this, other experiments proving the presence of lipid droplets (gene expression of PLINs and elevated CE and TG content) were powered and proved the same results.

This high ectopic fat storage and impaired lipid metabolism in the placenta may have implications in the delivery of essential fatty acids to the growing fetus, which are essential for its development, by acting as a sink for LC-PUFAs and diverting them from efflux from the placenta to the fetus. It is known that mothers and babies are deficient in LC-PUFAs during PE pregnancies (MacKay et al., 2012),

and there are several potential mechanisms that may lead to decreased fetal PUFA delivery in PE, including reduced PUFA production and/or increased PUFA storage and decreased delivery.

Regional differences have been observed in the fatty acid distribution in the healthy placenta, where AA was shown to be higher in the fetal regions compared to the maternal regions, potentially exhibiting the preferential fetal transport (rather than maternal storage) of this LC-PUFA (Rani et al., 2015). In contrast, the PE placenta in this study showed lower levels of AA in the fetal side, suggesting limited transport to the baby. In addition, this study reported lower DHA, omega-3 and higher ALA (DHA precursor) and omega-6 to omega-3 ratio (known to have proinflammatory effects) in the PE placenta compared to healthy controls (Rani et al., 2015). Although it is important to note that the pregnant women in this study were not BMI-matched and therefore this may have played a role in the different distribution of placental fatty acids, these investigations suggest that the PE placenta has impaired localisation and transport of PUFAs which may lead to the decreased levels observed in babies born after PE (MacKay et al., 2012).

The latter half of pregnancy is associated with an elevated lipid breakdown due to the development of an insulin-resistant state, and therefore it presents a source of LC-PUFAs for the growing fetus. The human placenta is responsible for the transport of maternal fatty acids to the fetus through selective uptake from the maternal circulation. MacKay et al. (2012) have found lower expression levels of Δ5- and Δ6-desaturase and very long chain fatty acid elongase (*ELOVL2*) in adipose tissue of women with PE, which are important in the synthesis of LC-PUFAs. In parallel, erythrocyte LC-PUFAs were also lower in PE compared to controls (MacKay et al., 2012). In addition, others have found lower gene expression of Δ5-desaturase and fatty acid transport proteins (*FATP*) 1 and 4 in the PE placenta vs normotensive controls (Wadhwani et al., 2014), suggesting impaired placental synthesis and transport of LC-PUFAs. These authors also reported lower DHA and total omega-3 fatty acids in placenta and cord blood in PE and found a positive correlation between the maternal and fetal levels of these fatty acids during the first trimester, thereby demonstrating the high dependence on maternal supply of LC-PUFAs. This would suggest that essential fatty acid supplementation during

pregnancy may be beneficial in PE in order to increase the maternal reservoir of LC-PUFAs, however, this is not the case.

Some studies have shown a beneficial impact of preterm LC-PUFA supplementation on the neurodevelopment of infants only during early stages of life (Hadders-Algra et al., 2007), however this has only been shown in healthy pregnancies. The benefits of LC-PUFA supplementation in preventing PE or improving neonatal neurodevelopmental outcomes are insufficient and do not provide consistent results (De Giuseppe et al., 2014). Interestingly, DHA supplementation in animal models has shown detrimental effects in cognitive and visual development due to the consequent decrease of AA (Hadders-algra, 2008), although these studies have not been carried out in models of PE. The reason behind the lack of evidence showing beneficial effects of essential fatty acid supplementation in mothers with compromised lipid metabolism may rely on the maternal excess of ectopic fat accumulation in the placenta. The elevated state of insulin resistance in PE that leads to elevated maternal plasma NEFAs and TGs (MacKay et al., 2012) may cause the ectopic lipid droplet storage in the placenta, analogous to what occurs in MASLD. During PE, the LC-PUFAs might be diverted towards storage in the placental ectopic fat rather than transport, and therefore increased levels in the mother would not translate to increased delivery to the baby. This theory is supported by the elevated amount of polyunsaturated fatty acids in the fatty acyl chains of the TGs in PE (Brown et al., 2016) and has also been suggested in animal models of PE (Gopalakrishnan et al., 2022). Others have also observed elevated LC-PUFAs in the TG fraction of the FGR placenta (Chassen et al., 2018), suggesting that this mechanism may be part of other pregnancy pathologies.

A limitation of the present study is that the levels of phospholipids could not be quantified in the placental tissue from PE and healthy patients. Experiments with radiolabelled fatty acids (including PUFAs) in pregnant women have shown that LC-PUFAs are esterified in the placenta mainly into phospholipids (Gil-Sánchez et al., 2010), which may be an important step contributing to the delivery of essential fatty acids to the fetus. Interestingly, Brown et al. (2016) found a significantly increased concentration of PC and total phospholipids in the PE placenta, which may reflect the importance of these lipids during placental alterations. Additionally, recent *omic* analyses in the PE placenta have revealed

important changes in phospholipid metabolism that contribute to the heightened inflammatory state observed in PE (Zhang et al., 2022), showing the important contribution of these lipids to this pathology.

While the activation of certain immunoregulatory factors is normal during the physiological response to pregnancy, the activation of proinflammatory markers has been observed in different complications of pregnancy, which may also be linked to changes in lipid metabolism. Macrophages and other leukocytes play important roles in healthy placentation and immune tolerance to the fetus, which require an orchestrated balance to ensure successful pregnancy, while any deviations from this normal physiological response can result in complications (True et al., 2022). Differences in the macrophage phenotype and distribution have been linked to PE, where there is an increase in the levels of pro-inflammatory macrophages and a decrease in anti-inflammatory macrophages which predominate in healthy pregnancies (Schonkeren et al., 2011). Interestingly, this study showed a higher number of total macrophages (CD14 marker) in PE compared to controls, however this difference was only present in the decidua basalis (basal placental site) and not in the decidua patietalis (fetal side). Similarly, increased macrophages (CD68 marker) in PE have been observed around the spiral arteries (Labarrere et al., 2017), suggesting that localisation within the tissue is important when drawing conclusions from macrophage IHC markers. Notably, these studies did not examine the activated macrophages in the placenta, but TNF-α (marker secreted by activated macrophages) in the PE placenta has previously been shown not to differ from healthy controls (Benyo et al., 2001), while others have found differences at both RNA and protein level (Wang and Walsh, 1996). These differences are probably due to the processing of the placenta, as the former investigations sampled eight different tissue sites, whereas the latter only sampled one. This highlights the importance of multiple random sampling for robustness when dealing with a heterogenous tissue such as placenta. The results presented in this chapter show that neither total or activated macrophages were different between PE and healthy placentas, although this could be due to the sampling of only one placental biopsy per patient as well as the imaging of selected regions of the placental slides rather than the whole stained slide. Therefore, further investigations should be carried out to further elucidate the localisation of macrophage activation in the PE placenta,

especially since the data in this chapter suggests numerically higher CSF1R+ cells in PE. In addition, it would be interesting to study the connection between macrophage activation and lipid release and accumulation in PE, as it has been reported that the high omega-6 to omega-3 ratio in the PE placenta may affect placental inflammation (Rani et al., 2015) and, in GDM, elevated NEFAs lead to increased lipid droplet accumulation and proinflammatory cytokine production in culture (Pathmaperuma et al., 2010).

In conclusion, this chapter has shown that mothers with PE present an altered fatty acid metabolism that leads to the presence of ectopic fat in the placenta, possibly as a consequence of impaired adipose tissue expansion. This may underlie the exacerbated insulin resistance state in PE pregnancies which further increases maternal lipid concentrations. The impaired metabolic profile of the mother may interfere with LC-PUFA transport to the baby, although this needs to be investigated further. For this reason, the next chapter will examine the gene expression of placental markers of fatty acid transport, lipolysis and synthesis in PE.

5 Placental lipid metabolism and transport in pregnancies complicated by preeclampsia

5.1 Introduction

Mothers with PE have an altered fatty acid metabolism. The previous chapter demonstrated elevated lipid storage in the PE placenta that may affect the delivery of essential fatty acids to the fetus. It is known that mothers and babies affected by PE have lower amounts of erythrocyte LC-PUFAs and higher amounts of plasma NEFAs (MacKay et al., 2012), which suggests lower LC-PUFA synthesis and transport and higher lipolysis rates. Previous studies have focused on maternal plasma, erythrocyte and adipose tissue lipid status and function during PE and FGR pregnancies (MacKay et al., 2012), however, placental lipid transport, lipolysis and fatty acid synthesis have not been extensively studied.

The limited ability of the fetus to synthesise LC-PUFAs requires maternal supply during pregnancy (Haggarty, 2004). During early pregnancy, there is an increase in liver lipid synthesis driven by estrogen, and lipids are accumulated in the maternal adipose tissue to be released for the fetus during the last trimester. Fatty acids, especially DHA (22:6 n-3) and AA (20:4 n-6), are essential for the neurodevelopment of the fetus and are associated with pregnancy outcomes (Al et al., 2000). DHA and AA are synthesised by the mother from the dietary intake of the precursors ALA (18:3 n-3) and LA (18:2 n-6), respectively, via Δ5 and Δ6 desaturase and very long chain FA elongase enzymes. These LC-PUFAs are released into the maternal circulation and taken up by the liver to be esterified into TGs, which are then re-released into the circulation in VLDL and transferred to the fetus by the placenta in the form of NEFAs (Herrera and Ortega-Senovilla, 2023). The placenta is responsible for the uptake of LC-PUFA by the syncytiotrophoblast layer and the selective export to the fetus. NEFAs that are transferred across the placenta are available from the lipolysis of maternal adipose tissue lipid stores, which are packaged into VLDL by the liver, and then released by LPL and other placental lipases acting on the TGs within the core of VLDL (Haggarty, 2004). Interestingly, the placenta preferentially transports DHA (compared to other LC PUFA), thereby indicating the transport preference of some LC-PUFAs to the baby (Haggarty et al., 1999). Experiments on human trophoblast (BeWo) cells have demonstrated that DHA is preferentially incorporated into TGs, which may

indicate an important role in fetal delivery (Campbell et al., 1997). In addition, the placenta is also capable of taking up LDL through a specific LDL receptor (LDLR) needed to provide cholesterol for the growing fetus (Yañez and Leiva, 2022).

It is unclear whether the impaired placentation during PE affects the fatty acid metabolising proteins responsible for the synthesis, processing and delivery of LC-PUFAs to the baby, although PE is associated with impaired delivery of LC-PUFAs to the baby. Placental fatty acid composition of healthy and PE placentas shows elevated levels of the DHA precursor ALA in the latter (Rani et al., 2015), which suggests reduced conversion to DHA in the mother. In addition, it has been shown that the adipose tissue of mothers with PE have lower expression of Δ5- and Δ6-desaturase and very long chain fatty acid elongase (*ELOVL2*) (MacKay et al., 2012), which are needed for the synthesis of LC-PUFAs from maternal dietary LA and ALA. In addition, gene expression levels of placental lipases including adipose triglyceride lipase (ATGL), hormone sensitive lipase (HSL) and LPL have been found to be lower in PE, which could suggest reduced lipolysis and availability of NEFAs for the fetus (Barrett et al., 2015). Lower expression of Δ5-desaturase and FATP1 and 4 have been found in the PE placenta compared to controls (Wadhwani et al., 2014), thereby suggesting altered synthesis of LC-PUFAs and delivery of lipids to the fetus. Others have found elevated levels of FAPB4 in the PE placenta, which may contribute to lipid accumulation (Yan et al., 2016). Moreover, lower levels of the DHA transporter major facilitator superfamily domain containing 2a (MFSD2a) have been found in the PE placenta (Toufaily et al., 2013), which may be responsible for the reduction in DHA transport to the baby. In addition, DHA levels may be correlated with folate plasma concentration status in the placenta (Umhau et al., 2006) (Figure 1-1 in Chapter 1). The release of DHA may rely on the provision of methyl groups from folate in order to convert PE to PC, as it occurs in the liver.

Lipoprotein levels are also altered in PE, where maternal HDL is lower and LDL is higher than healthy controls (Enquobahrie et al., 2004). High TG concentrations lead to elevated small, dense LDL formation which is susceptible to oxidation and may contribute to endothelial dysfunction in obese pregnancies (Jarvie et al., 2010). A similar mechanism may take place during PE, which is also associated

with high plasma TG and cholesterol concentrations and is impacted by endothelial dysfunction. Additionally, gene expression of VLDL receptor and LDLR is lower in PE placentas (Murata et al., 1996), suggesting decreased cholesterol uptake, although these experiments have not been confirmed at the protein level.

A summary of the fatty acid transport and metabolism that takes place in the physiologically healthy placenta is depicted in Figure 1-1 in Chapter 1. The alteration of fatty acid homeostasis during PE is not fully understood and the mechanisms that lead to a LC-PUFA deficiency in the baby during PE are yet to be elucidated. For this reason, this chapter will focus on investigating the placental expression of fatty acid transporters and metabolising enzymes that may be involved in this process. Gene expression experiments were carried out, rather than protein or metabolic assays, because this is a quick and efficient method to investigate changes in the metabolism of the placenta which detects genes even if their expression is low, which may be more challenging with protein-based methods. In addition, similar to the previous chapter, FGR samples were included in these analyses in order to isolate the effects specific to PE from the placental abnormalities. FGR was defined as an estimated fetal weight of less than 5th percentile for gestation.

5.2 Hypothesis and aims

It was hypothesised that placentas from pregnancies affected by PE will have an altered expression of lipid handling proteins in the context of ectopic lipid accumulation, therefore, lipid synthesis and uptake proteins will be higher, and transport and hydrolysis proteins will be lower. The main aims were:

-To investigate the expression of genes associated with lipid synthesis, transport, and hydrolysis in healthy, PE and FGR placentas.

-Should gene expression be different in PE, to study the protein levels of fatty acid transporters in PE and healthy placentas.

-To assess the localised expression of the LDLR in placentas from PE and healthy pregnancies.

5.3 Materials and methods

5.3.1 LDLR staining on paraffin sections

Archival placental paraffin sections from healthy, PE and FGR pregnancies were stained with LDLR antibody as described in section 2.6.3. Whole stained slides were imaged with a slide scanner (x40) and analysed manually by standard weighted immunohistoscoring (protocol from the Edwards lab, University of Glasgow) by one observer (with a 10 % quality check from a second observer) blinded to sample ID. A total scoring percentage (maximum 300 %) was obtained for all images and compared between groups.

5.3.2 Gene expression analysis of placental lipid metabolism and transport proteins

RNA was extracted from a random biopsy of frozen placental tissue for qRT-PCR analysis as described in Chapter 4. Archival frozen placentas from healthy, FGR and PE pregnancies were used for these experiments, collected as described in section 2.4.2. Taqman gene expression assays (Table 8) were used for qPCR analysis on the extracted placental RNA using *TOP1* as the housekeeping gene (details on assay IDs and protein names are found in Table 1 section 2.7).

Table 8. Description of function of genes associated with lipid metabolism and transport used for investigating gene expression in placenta.

	Gene symbol	Function of the protein product
Lipid synthesis and metabolism	*ACSL1*	Involved in the conversion of free LC FAs to fatty acyl-CoA esters, which can enter the lipid biosynthesis or lipid ß-oxidation pathways.
	ACSL3	Involved in the conversion of free LC FAs to fatty acyl-CoA esters, which can enter the lipid biosynthesis or lipid ß-oxidation pathways. Important in the incorporation of FAs in PC. High expression in the brain.
	ACSL5	Involved in the conversion of free LC FAs to fatty acyl-CoA esters, which can enter the lipid biosynthesis or lipid ß-oxidation pathways. High expression in uterus and spleen.
	DGAT1	Synthesis of TGs from DGs and fatty acyl CoA esters. Primarily expressed in the small intestine for fat absorption. Involved in the recycling of FAs to produce TGs.
	DGAT2	Synthesis of TGs from DGs and fatty acyl CoA esters. Involved in *de novo* lipogenesis of TGs.
	FASN	Catalyses the synthesis of palmitate (precursor to longer saturated or monounsaturated FAs).
	SCD1	Catalyses the formation of monounsaturated FAs (MUFAs) from saturated FAs.
	SREBF-1	Transcription factor that binds to the sterol regulatory element-1 (SRE-1) to promote lipid synthesis and homeostasis. Expression is regulated by insulin.
	SREBF-2	Transcription factor that binds to the sterol regulatory element-1 (SRE-1) to promote sterol synthesis and homeostasis. Involved in cholesterol regulation.
Long chain fatty acid synthesis	*ELOVL2*	Involved in fatty acid elongation to synthesise n-3 and n-6 long chain FAs.
	ELOVL5	Involved in fatty acid elongation to synthesise n-3 and n-6 long chain FAs.
	ELOVL6	Involved in fatty acid elongation to synthesise long chain saturated FAs that are used as precursors for n-3 and n-6 long chain FAs.
	FADS1	Desaturase involved in the synthesis of n-3 and n-6 long chain FAs.

	Gene symbol	Function of the protein product
Fatty acid transporters	*CD36*	Long chain fatty acid transport protein. Highly expressed in muscle, adipose tissue and gut.
	FABP1	Long chain fatty acid transport protein. Highly expressed in the liver.
	FABP2	Long chain fatty acid transport protein. Highly expressed in the gut.
	FABP3	Long chain fatty acid transport protein. Highly expressed in muscle and heart.
	FABP4	Long chain fatty acid transport protein. Highly expressed in adipocytes.
	FABP5	Long chain fatty acid transport protein. Highly expressed in the epidermis.
	FABP6	Long chain fatty acid transport protein. Highly expressed in the gut.
	FATP2	Long chain fatty acid transport protein. Highly expressed in the liver and kidneys.
	PLTP	Phospholipid transfer protein from TG-rich lipoproteins to HDL.
	27A1	Long chain fatty acid transport protein.
	27A4	Long chain fatty acid transport protein. Important FA transporter in the small intestine.
DHA transport	*MFSD2a*	Lyso-PC transporter. Mainly involved in the DHA transport and uptake into the brain.
	MTHFR	Involved in the conversion of THF to 5-Methyl THF, which is a substrate for the methylation of homocysteine to methionine.
	PEMT	Transferase involved in converting PE to PC in the liver.
Lipolysis	*Angptl4*	Regulates triglyceride lipolysis by inhibiting LPL.
	LIPC	Hepatic lipase that hydrolyses the TGs and phospholipids present in lipoproteins.
	LIPE	Hormone-sensitive lipase that preferentially hydrolyses DGs to MGs during lipolysis.
	LIPG	Endothelial lipase that hydrolyses the TGs and phospholipids present in lipoproteins.
	LPL	Lipase that hydrolyses the TGs and phospholipids present in lipoproteins.
	PNPLA2	Lipase that catalyses the first reaction of lipolysis from TGs to DGs.

5.3.3 Western blotting

Immunoblotting of FABP5 protein was performed on archival placental samples from healthy, PE and FGR pregnancies, as described in section 2.8.3. Placental tissue lysis (approximately 0.5 mg) was performed as described in section 2.8.1. HEK293 lysates were added to the gels as positive controls. Protein quantification of the lysates was carried out with a Bradford assay as in section 2.8.2. SDS-PAGE and blotting with human anti-FABP5 monoclonal antibody (1 in 8000 dilution) and 800cw donkey anti-mouse (1 in 10000 dilution) were performed as described in section 2.8.3. Imaging was carried out in the Odyssey Imaging System at 700 and 800 nm and quantified on the LI-COR Image Studio Lite software. Target protein signal was normalised to total protein LNF (detailed in section 2.8.3) and normalised signals were used for statistical analysis.

5.3.4 Statistical analysis

Results were presented as mean ±SD if parametric or median ±IQR if nonparametric after Ryan-Joiner testing. Patient characteristics are presented as mean ±SD for continuous variables and number and percentages for primiparous and fetal sex. Difference testing between continuous variables were carried out by an unpaired t-test or one-way ANOVA. Difference testing between proportions were carried out by a Fisher's exact test. A PCA was performed with the gene expression data for healthy, FGR and PE samples, however, there was no clear separation between groups and therefore individual gene expression differences are presented in this chapter instead. Gene expression data was analysed by a one-way ANOVA on log transformed data. Correlations between gene expression and neutral lipid lipidomics data were carried out using a Pearson correlation on log transformed data. FABP5 monomer results were analysed by an unpaired two sample t-test and FABP5 dimer results were analysed by a Mann-Whitney test. LDLR staining results were analysed by a nonparametric Mann-Whitney test. Statistical analyses were performed on Minitab software version 21.4.3. Statistical significance was assumed at $P<0.05$.

5.4 Results

5.4.1 Patient demographics

Patient demographics from the healthy (n=68), PE (n=23) and FGR (n=10) patients are the same as in Chapter 4, summarised in Table 7, section 4.4.1. Only a subset of samples was used for LDLR staining (Healthy: n=7 and PE: n=6) and FABP5 immunoblotting (Healthy: n=20 and PE: n=20), however, there were no differences in demographics compared to the full dataset, and PE and healthy samples were still BMI and age matched.

5.4.2 Expression of genes involved in lipid synthesis and metabolism in healthy and PE placenta

A PCA was performed with the gene expression data within the different groups (Figure 5-1). PCA scores plot shows overlap between the groups which indicates minimal differences. Despite this, individual genes were plotted in order to dissect the individual differences in the genes involved in lipid metabolism.

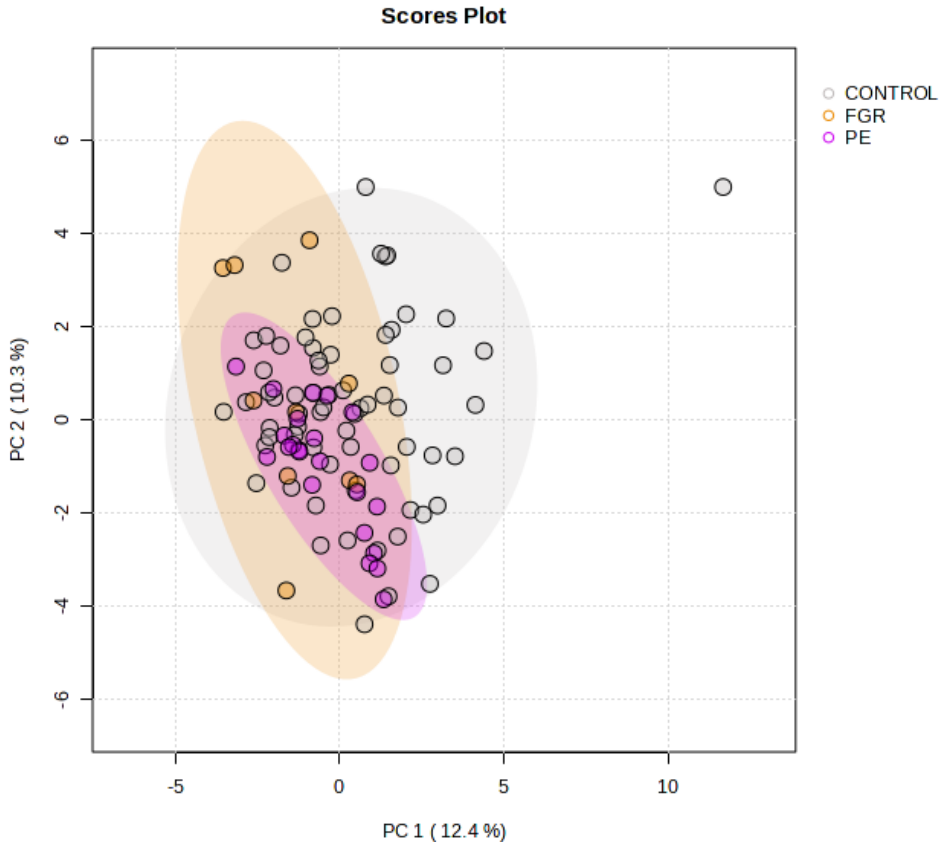

Figure 5-1. Distribution of gene expression data by PCA scores of the individual contribution to group differences. PCA scores plot of the healthy (n=68), PE (n=23) and FGR (n=10) groups. Each data point represents each individual sample and the ellipses indicate the 95 % confidence intervals.

Several genes involved in lipid biosynthesis and metabolism were investigated in healthy and PE placentas. *DGAT 1/2* are lipogenic enzymes responsible for generating TGs from DGs and *ACSL1/3/5* are involved in defining the pathway fate of the lipids. No significant differences were found in the expression of *DGAT1*, *ACSL1*, *ACSL3* and *ACSL5* between groups (P>0.05) (Figure 5-3A, C, D and E). Gene expression of placental *DGAT2* was significantly higher in PE compared to healthy controls (0.91 ± 1.08 vs 0.61 ± 0.88 %; P=0.027) (Figure 5-2B), but there were no significant differences compared to FGR (0.65 ± 0.68 %; P=0.21 (PE vs FGR) and P=0.99 (Healthy vs FGR)).

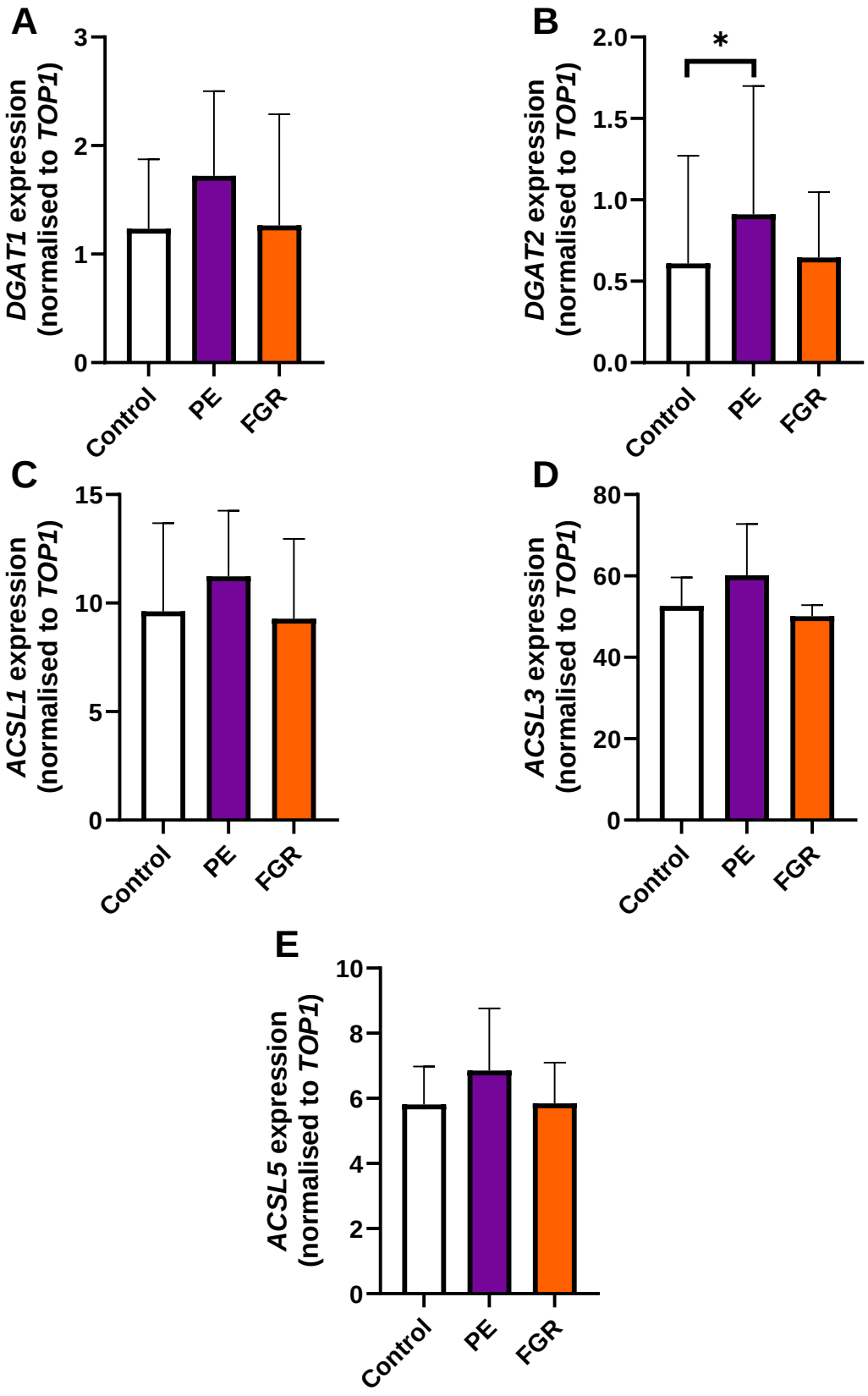

Figure 5-2. Expression of genes involved in lipid biosynthesis and pathway determination. Gene expression of *DGAT1* **(A)**, *DGAT2* **(B)**, *ACSL1* **(C)**, *ACSL3* **(D)** and *ACSL5* **(E)** was analysed by qRT-PCR and presented as a percentage of the expression of the housekeeping gene *TOP1*. Data is shown as median ±IQR where individual samples represent each data point (Healthy: n=68, PE: n=23, FGR: n=10). Data was analysed by a one-way ANOVA on log transformed data with Tukey *post hoc* test; significance at *P<0.05.

Transcription factors *SREBF-1* and *2* regulate the synthesis of cholesterol, saturated fatty acids (SA-FAs) and MUFAs carried out by *FASN* and *SCD1*. *FASN* expression was significantly higher in PE compared to healthy and FGR placentas (57.37 ± 59.49 vs 37.91 ± 26.20 and 30.59 ± 35.06 %; P=0.016 and P=0.018) (Figure 5-3A). In addition, SREBF-1 expression was significantly higher in PE compared to healthy controls (69.01 ± 33.94 vs 39.45 ± 22.52 %; P<0.001) but there were no significant differences compared to FGR (46.85 ± 23.03 %; P=0.073 (PE vs FGR) and P=0.24 (Healthy vs FGR)) (Figure 5-3C). There were no significant differences in the expression of *SCD1* and *SREBF-2* between groups (P>0.05) (Figure 5-3B and D).

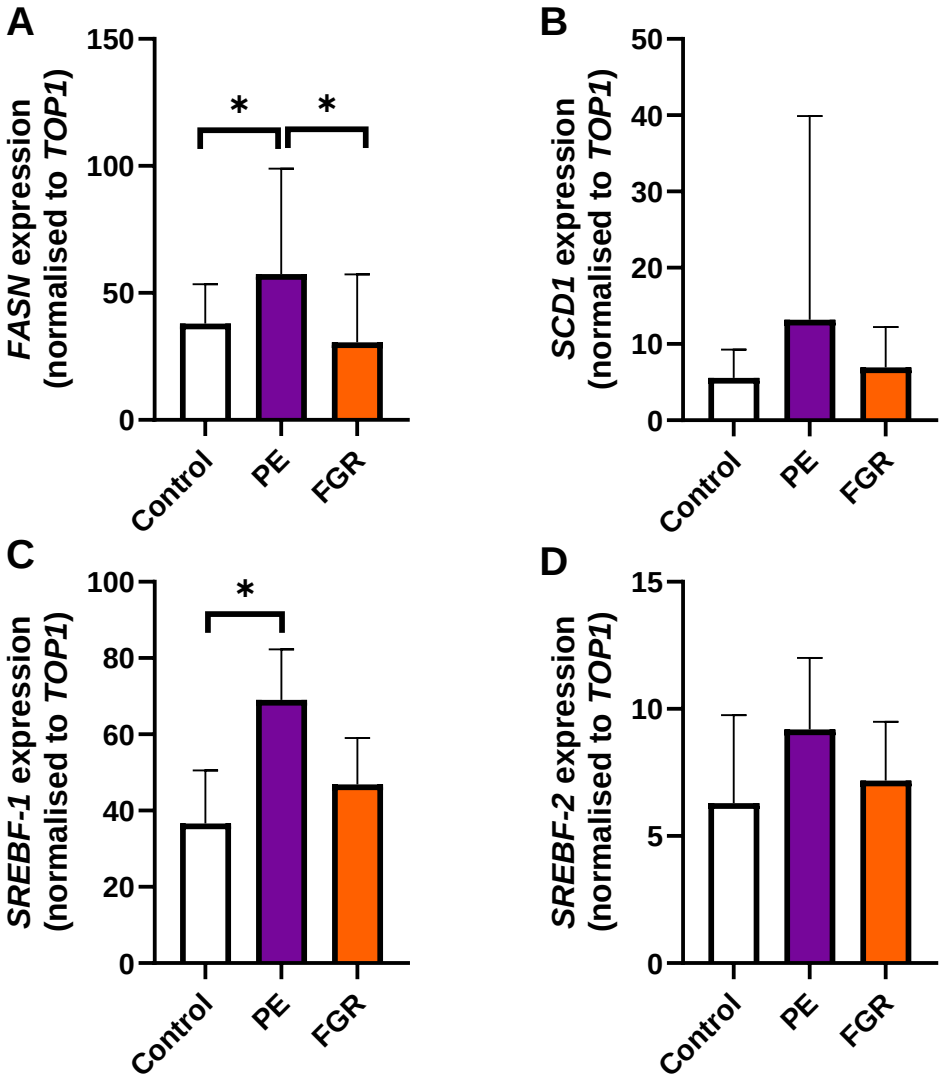

Figure 5-3. Gene expression of lipid synthesis genes. Gene expression of *FASN* **(A)**, *SCD1* **(B)**, *SREBF-1* **(C)** and *SREBF-2* **(D)** was analysed by qRT-PCR and presented as a percentage of the expression of the housekeeping gene *TOP1*. Data is shown as median ±IQR where individual samples represent each data point (Healthy: n=68, PE: n=23, FGR: n=10). Data was analysed by a one-way ANOVA on log transformed data with Tukey *post hoc* test; significance at *P<0.05.

As *FASN*, *DGAT2* and *SREBF-1* are involved in *de novo* lipogenesis, the correlation between these genes and placental neutral lipid was investigated. *FASN*, *DGAT2* and *SREBF-1* showed a statistically significant positive correlation with placental TG, CE and total neutral lipid (TG+CE) content (Figure 5-4).

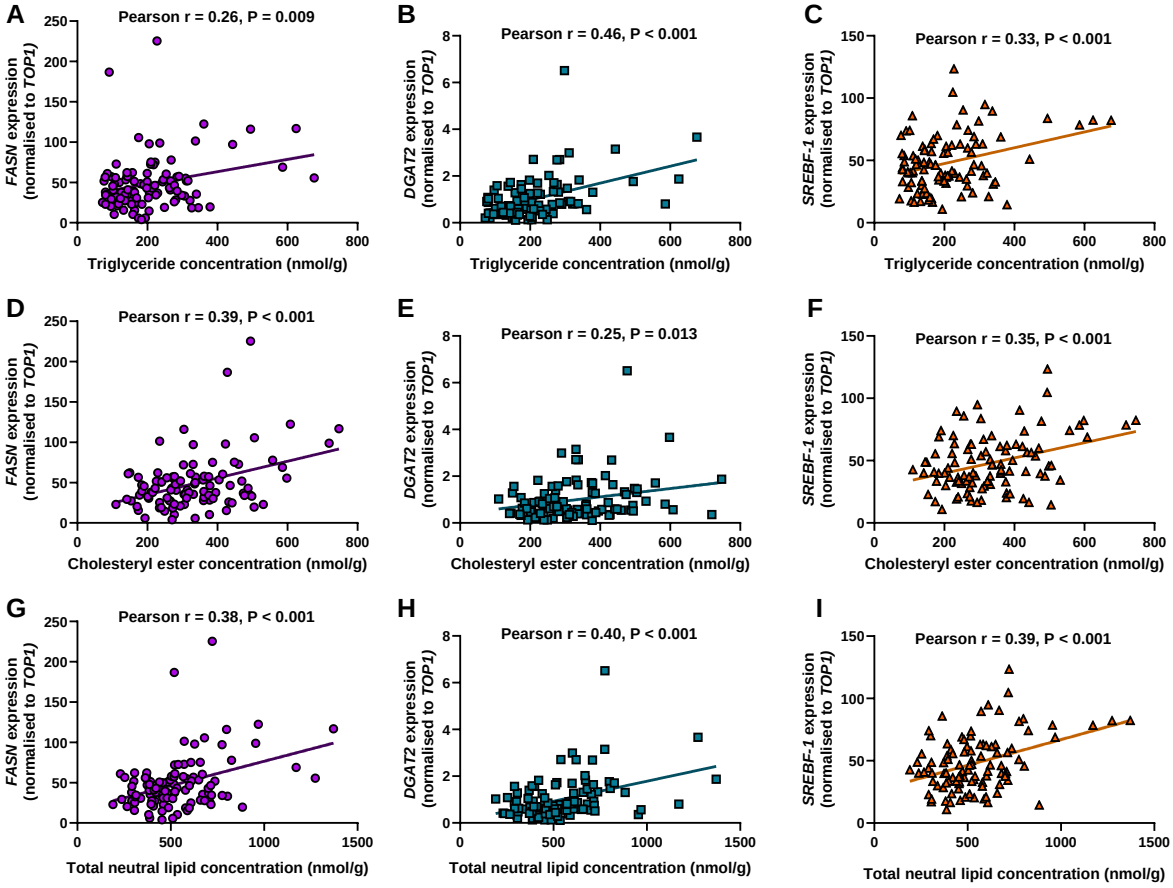

Figure 5-4. Correlation between *de novo* lipogenesis genes *FASN*, *DGAT2* and *SREBF-1* with placental neutral lipid content. Correlations between TG and *FASN* (A), *DGAT2* (B) and *SREBF-1* (C); CE and *FASN* (D), *DGAT2* (E) and *SREBF-1* (F); and total neutral lipid and *FASN* (G), *DGAT2* (H) and *SREBF-1* (I) were assessed using a Pearson correlation on log transformed data. Statistical significance was assumed at $P<0.05$.

The gene expression of elongases *ELOVL2/5/6* and the desaturase *FADS1* was investigated due to their involvement in the synthesis of long-chain fatty acids. There were no significant differences in the placental expression of any of these genes between groups ($P>0.05$) (Figure 5-5).

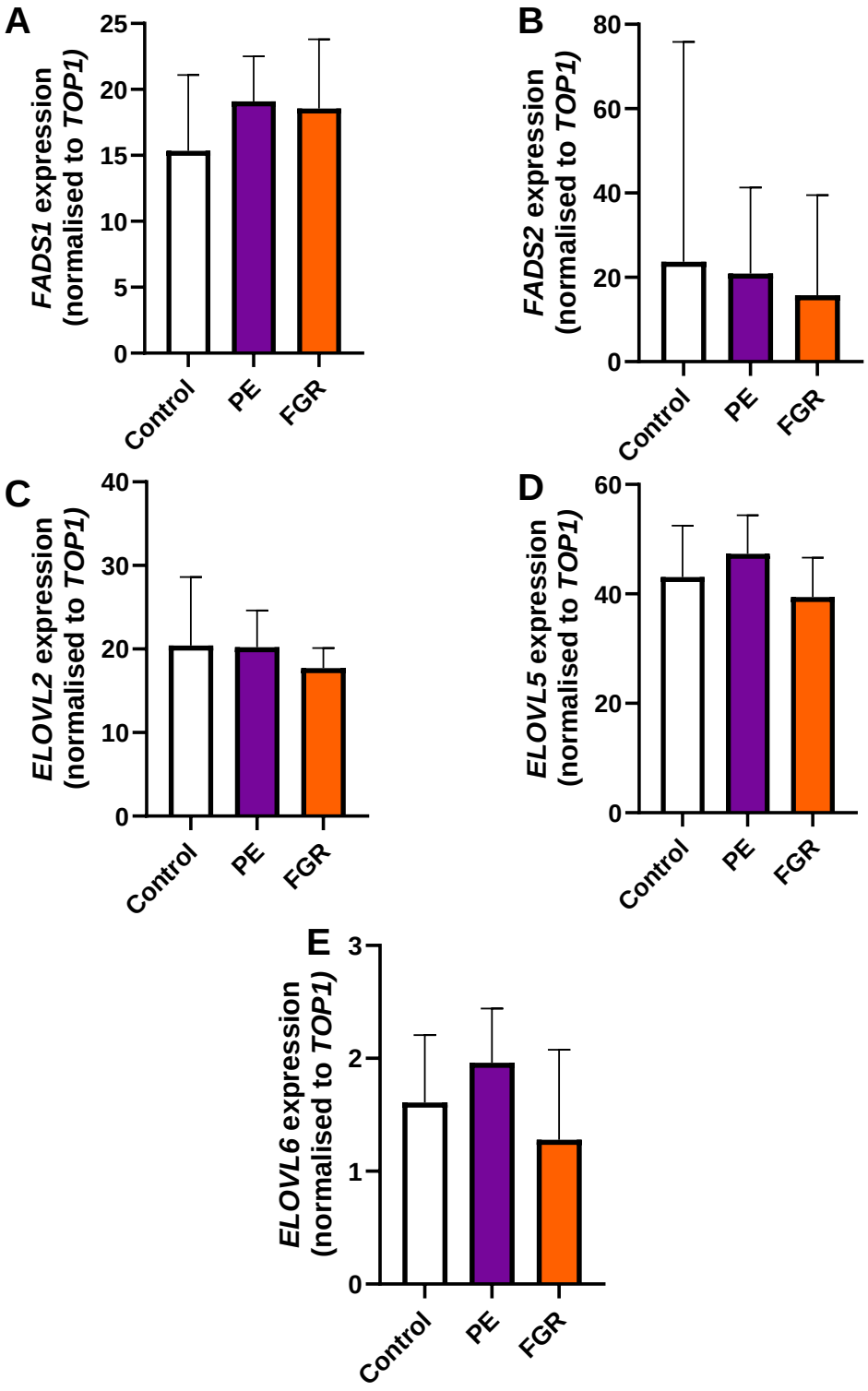

Figure 5-5. Gene expression of long-chain fatty acid synthesis genes. Gene expression of *FADS1* **(A)**, *FADS2* **(B)**, *ELOVL2* **(C)**, *ELOVL5* **(D)** and *ELOVL6* **(E)** was analysed by qRT-PCR and presented as a percentage of the expression of the housekeeping gene *TOP1*. Data is shown as median ±IQR where individual samples represent each data point (Healthy: n=68, PE: n=23, FGR: n=10). Data was analysed by a one-way ANOVA on log transformed data with Tukey *post hoc* test; significance at *P<0.05.

The gene expression of several lipid transport genes was investigated in healthy, PE and FGR placentas, including fatty acid transport proteins (*27A1*, *FATP2* and *27A4*), fatty acid translocase *CD36*, phospholipid transport protein *PLTP* and fatty acid binding proteins (*FABP3-6*). There were no significant differences in the gene expression of *27A1*, *FATP2*, *27A4*, *CD36* and *PLTP* between groups (Figure 5-6). *FABP5* expression was significantly lower in PE compared to healthy placentas (51.9 ± 30.7 vs 71.8 ± 40.6 %; P=0.012) but there were no significant differences compared to FGR (51.9 ± 31.4 %; P=0.99 (PE vs FGR) and P=0.13 (Healthy vs FGR)) (Figure 5-7C). Moreover, the expression of FABP6 was significantly lower in FGR compared to healthy controls (0.0031 ± 0.0047 vs 0.0090 ± 0.015 %; P=0.03) but there were no differences with PE (0.0075 ± 0.023 %; P=0.15 (FGR vs PE) and P=0.74 (Healthy vs PE)) (Figure 5-7D). No significant differences were found in the expression of *FABP3/4* between groups (P>0.05) (Figure 5-7A and B).

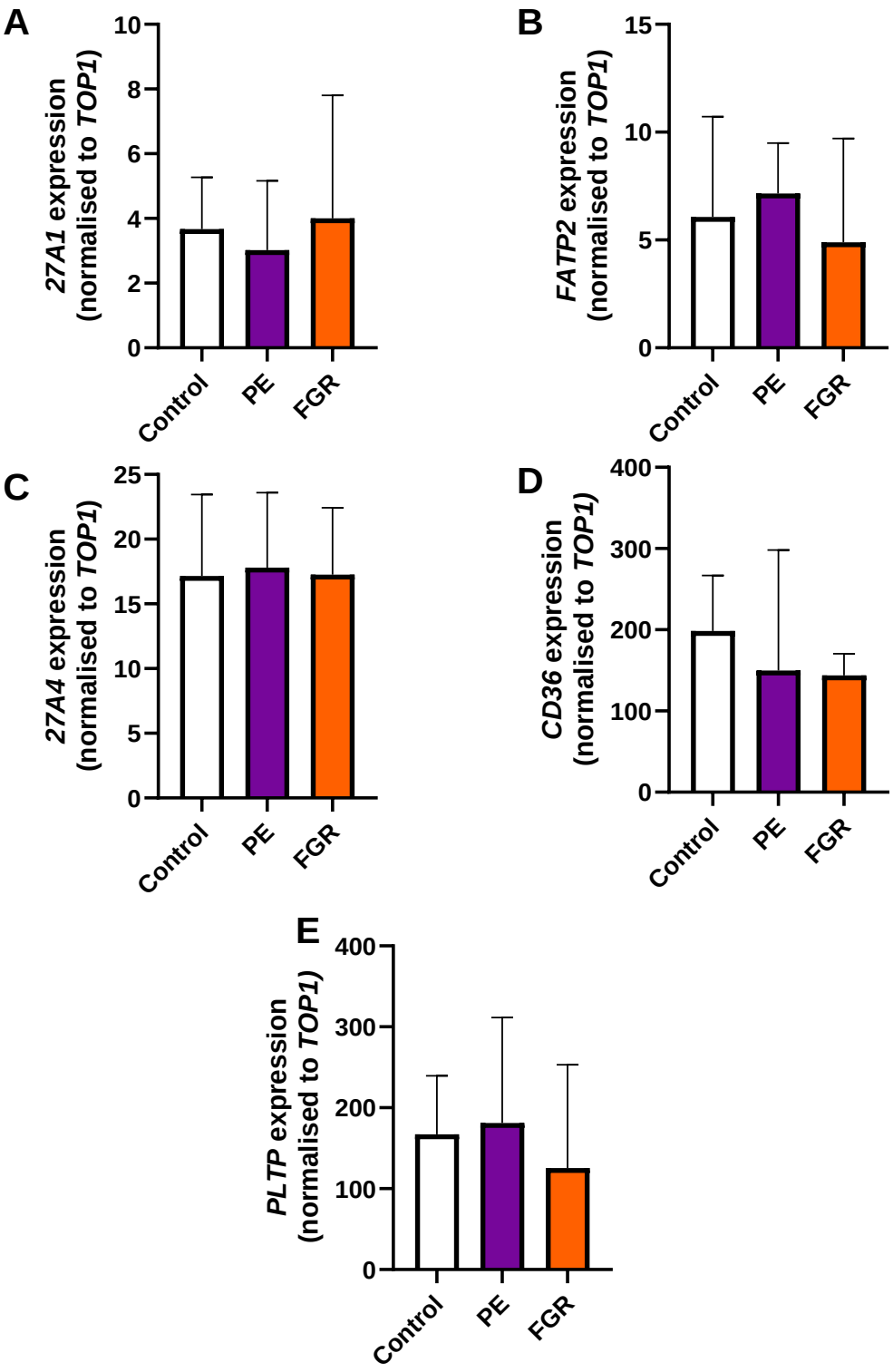

Figure 5-6. Gene expression of lipid transport genes. Gene expression of *27A1* **(A)**, *FATP2* **(B)**, *27A4* **(C)**, *CD36* **(D)** and *PLTP* **(E)** was analysed by qRT-PCR and presented as a percentage of the expression of the housekeeping gene *TOP1*. Data is shown as median ±IQR where individual samples represent each data point (Healthy: n=68, PE: n=23, FGR: n=10). Data was analysed by a one-way ANOVA on log transformed data with Tukey *post hoc* test; significance at *P<0.05.

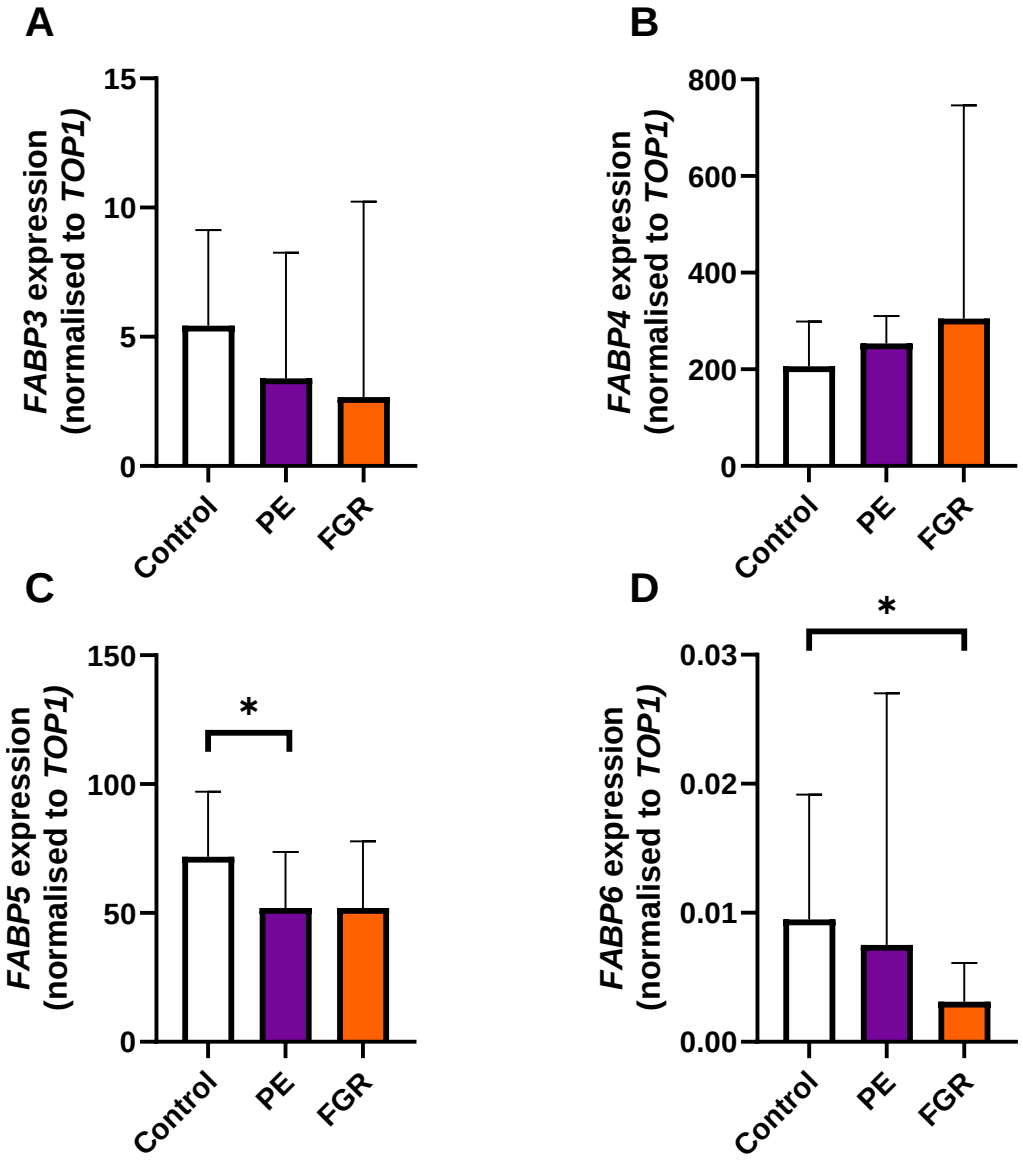

Figure 5-7. Gene expression of intracellular fatty acid transport genes. Gene expression of *FABP3* **(A)**, *FABP4* **(B)**, *FABP5* **(C)** and *FABP6* **(D)** was analysed by qRT-PCR and presented as a percentage of the expression of the housekeeping gene *TOP1*. Data is shown as median ±IQR where individual samples represent each data point (Healthy: n=68, PE: n=23, FGR: n=10). Data was analysed by a one-way ANOVA on log transformed data with Tukey *post hoc* test; significance at *P<0.05.

DHA transport was investigated in the placenta by studying the gene expression of the DHA-specific lysophospholipid transporter *MFSD2a*, the methyltransferase *PEMT* and the reductase *MTHFR* in healthy, PE and FGR placentas (Figure 5-8). There were no significant differences in the expression of the investigated genes between groups.

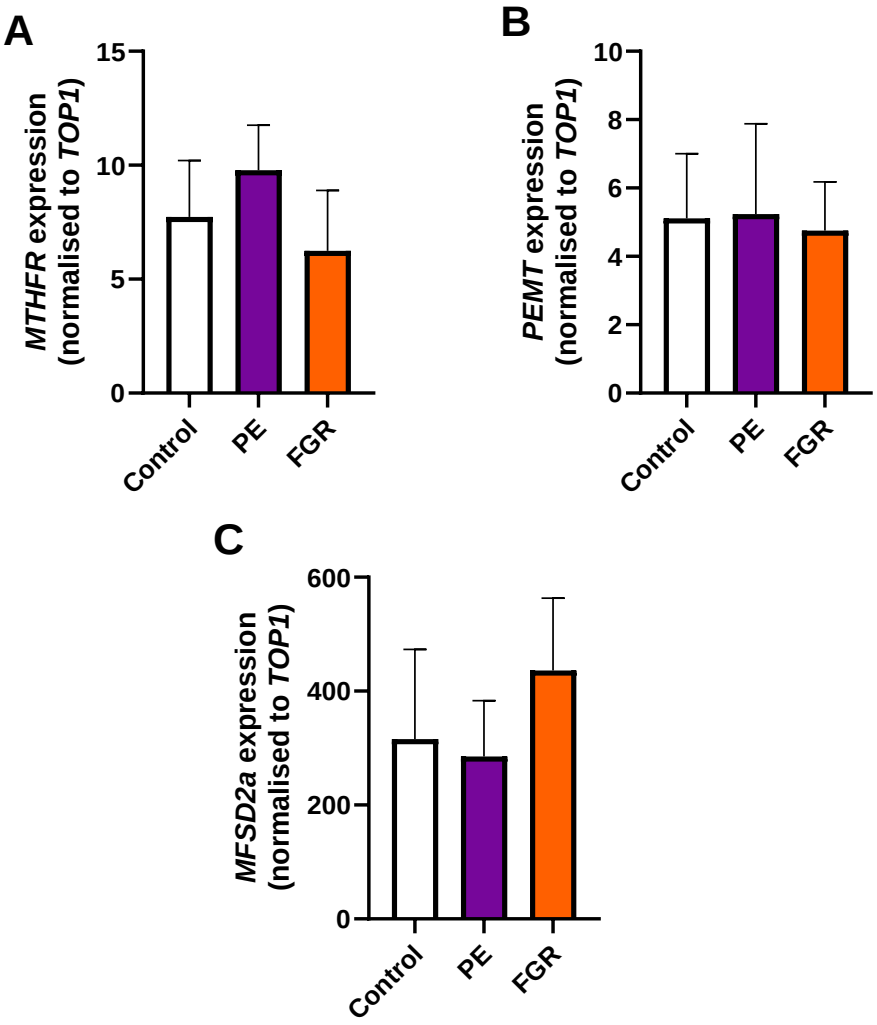

Figure 5-8. Expression of genes involved in DHA mobilisation. Gene expression of *MTHFR* **(A)**, *PEMT* **(B)** and *MFSD2a* **(C)** was analysed by qRT-PCR and presented as a percentage of the expression of the housekeeping gene *TOP1*. Data is shown as median ±IQR where individual samples represent each data point (Healthy: n=68, PE: n=23, FGR: n=10). Data was analysed by a one-way ANOVA on log transformed data with Tukey *post hoc* test; significance at *P<0.05.

The gene expression of lipolysis-associated genes was quantified in placentas from healthy, PE and FGR pregnancies, including *LPL*, hepatic lipase (*LIPC*), hormone sensitive lipase (*LIPE*), endothelial lipase (*LIPG*), adipose triglyceride lipase (*PNPLA2*) and the glycoprotein *Angptl4*, which inhibits LPL. The expression of *LIPE* was significantly higher in PE compared to healthy placentas (0.090 ± 0.074 vs 0.057 ± 0.040 %; P=0.007) but there were no significant differences compared to FGR (0.066 ± 0.038 %; P=0.63 (PE vs FGR) and P=0.46 (Healthy vs FGR)) (Figure 5-9C). The placental expression of *Angtpl4* was also significant higher in PE compared to healthy controls (182.1 ± 89.9 vs 131.5 ± 87.0 %; P=0.047) but no differences were found with the FGR group (140.0 ± 209.4 %; P=0.96 (PE vs FGR) and P=0.33 (Healthy vs FGR)) (Figure 5-9F). No differences were found in the expression of *LPL*, *LIPC*, *LIPG* and *PNPLA2* between groups (Figure 5-9A, B, D and E).

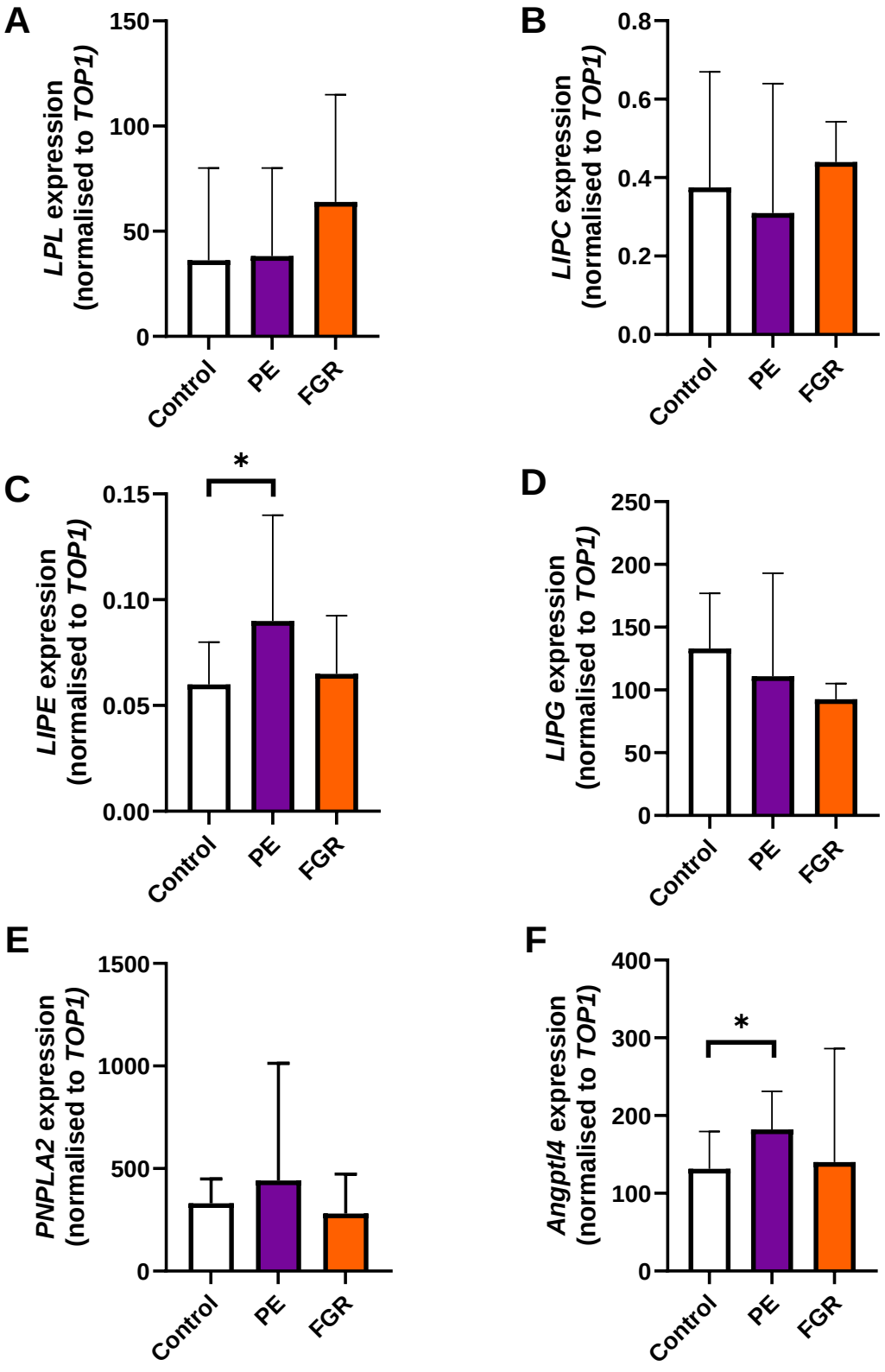

Figure 5-9. Gene expression of lipolysis-associated genes. Gene expression of *LPL* **(A)**, *LIPC* **(B)**, *LIPE* **(C)**, *LIPG* **(D)**, *PNPLA2* **(E)** and *Angptl4* **(F)** was analysed by qRT-PCR and presented as a percentage of the expression of the housekeeping gene *TOP1*. Data is shown as median ±IQR where individual samples represent each data point (Healthy: n=68, PE: n=23, FGR: n=10). Data was analysed by a one-way ANOVA on log transformed data with Tukey *post hoc* test; significance at *P<0.05.

5.4.3 FABP5 protein levels in PE and healthy placentas

Since it was observed that *FABP5* gene expression was significantly lower in healthy compared to PE placentas, immunoblotting was carried out to confirm this at the protein level. Immunoblotting experiments on healthy and PE placentas was performed on a subset of samples (healthy (n=20) and PE (n=20)) from the patients in Table 7 (Chapter 4). It was found that placental FABP5 is present as both a monomer (15 kDa) and a dimer (30 kDa) and therefore each molecular conformation was analysed separately (Figure 5-10). There were no significant differences between PE and healthy placental monomer FABP5 levels (114.7 ± 60.1 vs 101.7 ± 50.8; P=0.46) (Figure 5-10D) or dimer FABP5 levels (25.24 ± 30.32 vs 23.80 ± 7.83; P=0.23) (Figure 5-10E).

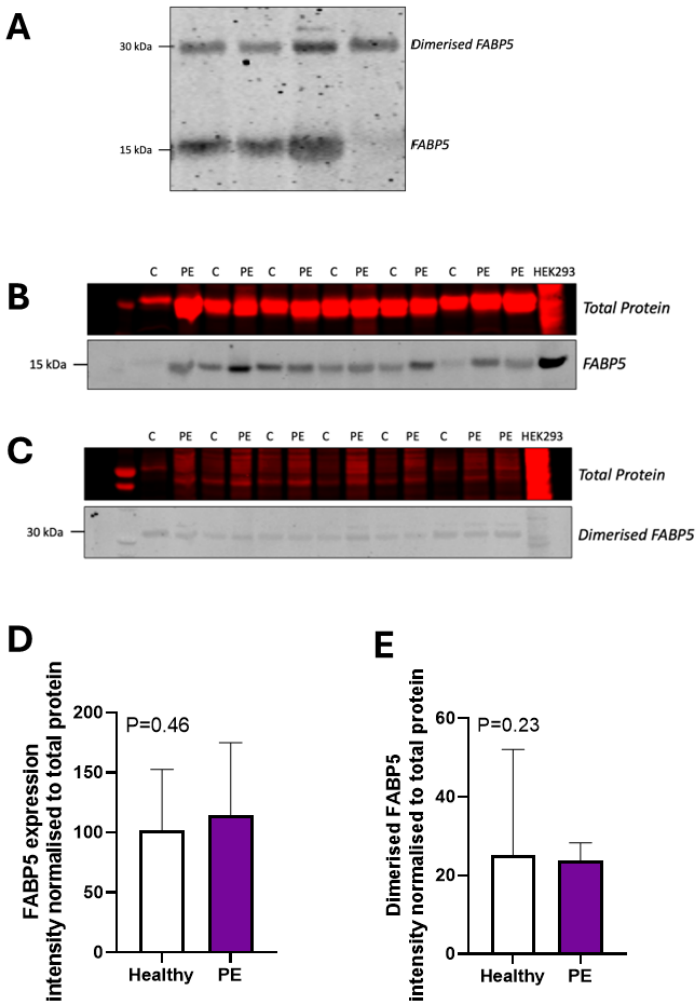

Figure 5-10. FABP5 protein levels in the healthy and PE placentas. (A) Representative immunoblot showing the monomer and dimer forms of FAPB5. **(B)** Representative FABP5 monomer (15 kDa) immunoblots with total protein reference. **(C)** Representative FABP5 dimer (30 kDa) immunoblots with total protein. **(D)** FABP5 expression intensity of the monomer normalised to total protein stain. **(E)** FABP5 expression intensity of the dimer normalised to total protein stain. Data is shown as mean ±SD (monomer data) or as median ± IQR (dimer data) where individual samples represent each data point (Healthy: n=20 and PE: n=20). Data was analysed by an unpaired t-test (monomer data) and a Mann-Whitney test (dimer data); significance at P<0.05. Representative images were kindly provided by undergraduate student Chelsea Corney.

5.4.4 LDLR immunohistochemistry of placental samples from healthy pregnancies and pregnancies complicated by PE

LDLR staining was quantified on healthy and PE placentas by histoscoring (Figure 5-11) on a subset of samples (healthy (n=7) and PE (n=6)) from the patients in Table 7 (Chapter 4). There were no significant differences between groups (Healthy: 10 ± 40 vs PE: 5 ± 12.5 %; P=0.45).

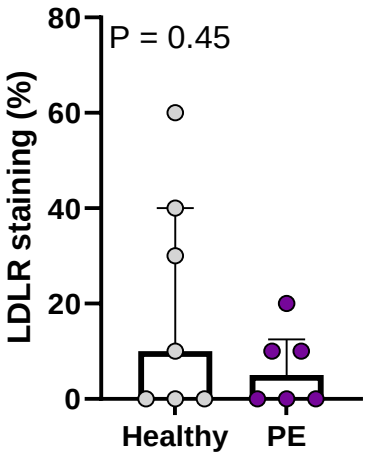

Figure 5-11. LDLR staining on placentas from healthy and PE pregnancies. Quantified LDLR staining on placental tissue by histoscoring. Data is shown as median ±IQR where individual samples represent each data point (Healthy: n=7 and PE: n=6). Data was analysed by Mann-Whitney test; significance at P<0.05.

5.5 Discussion

The previous chapter demonstrated an elevated amount of ectopic fat in the form of lipid droplets in the PE placenta. Further investigations into the lipid homeostasis of the placenta were carried out in this chapter to elucidate the contribution of placental lipid homeostasis genes to this fat accumulation and the lipid abnormalities observed in PE women. The gene expression data presented in this chapter show evidence of an altered expression of lipid metabolism genes in the PE placenta, as hypothesised. It was observed that PE placentas had higher *Angptl4*, *LIPE*, *DGAT2*, *FASN* and *SREBF-1* expression and lower *FABP5* expression compared to healthy placentas. FABP5 protein in the placenta was observed as a dimer and a monomer, which may show the importance of this conformation in the function of this transport protein, however protein expression did not differ between PE and controls. In addition, there were no differences in LDLR staining between healthy and PE placentas, although this may result from low power due to the low sample size. Overall, this chapter has demonstrated important changes

in lipolysis and lipid synthesis, regulation and transport of fatty acids, which may contribute to the altered lipid status observed in PE pregnancies.

PE placentas showed a higher expression of lipid biosynthesis-associated genes including *FASN*, *DGAT2* and the transcription factor *SREBF-1*. In addition, there was a positive correlation between TG, CE and total neutral lipid (TG+CE) concentrations from lipidomics data (Chapter 4) and the expression of *FASN*, *DGAT2* and *SREBF-1*, thereby suggesting the association of these genes and neutral lipid content in the placenta. SREBF-1 is known to regulate *de novo* lipogenesis by activating *FASN* and *SCD1*, therefore the higher expression of *FASN* could be explained by the higher expression of *SREBF-1*. Fatty acid synthase (*FASN*) is involved in *de novo* lipid synthesis by generating new saturated fatty acids. During pregnancy, *FASN* is expressed in the placenta to maintain essential functions for development, and its alteration may lead to placental abnormalities. Placental *FASN* expression is elevated in GDM pregnancies and pregnancies impacted by maternal hypercholesterolemia, indicating that the maternal metabolic profile can affect placental lipid synthesis (Marseille-Tremblay et al., 2008). Moreover, insulin is known to increase *de novo* lipogenesis in the liver even in insulin resistant states. In the liver, the activation of the SREBF-1 pathway remains responsive to insulin and, due to the high insulin levels in insulin resistance, there is an excess of lipid synthesis that leads to hypertriglyceridemia (Brown and Goldstein, 2008) as well as an increase in fat deposition in organs, which is thought to contribute to the pathology of MASLD (Xu et al., 2013). Insulin has also been observed to increase *FASN* expression in human adipocytes in culture (Claycombe et al., 1998). A similar mechanism may take place in the placenta where SREBF-1 increases the expression of *FASN* which promotes lipogenesis and lipid accumulation under the state of hyperinsulinemia and insulin resistance in PE.

Interestingly, *FASN* levels are upregulated by SREBF-1 and 2 when the intracellular concentrations of PUFAs are low (Carreras-Badosa et al., 2016). Higher erythrocyte fatty acid proportions of SA-FAs and lower unsaturated fatty acids and PUFAs have been found in maternal and cord blood during PE pregnancies compared to healthy controls (MacKay et al., 2012). In addition, lower synthesis of LC-PUFAs takes place in maternal adipose tissue during PE pregnancies which may also suggest lower liver synthesis (MacKay et al., 2012). Therefore, placental *FASN* expression may also be upregulated due to low levels of PUFAs being

incorporated from the maternal circulation. This theory is supported by the lack of differences in the placental gene expression of elongases *ELOVL2/5* and the desaturase *FADS1* between PE and healthy groups in this chapter, which means that the placenta does not compensate for the low LC-PUFAs availability from the mother and further contributes to the low LC-PUFA abundance in the placenta. Additionally, there were no differences in the expression of genes potentially involved in the mobilisation of DHA including *PEMT* and *MTHFR* even though expression was detected in the placentas, which suggests that a similar mechanism of DHA transport to that which takes place in the liver may take place in the placenta, however this does not contribute to the pathology of PE.

The gene expression of *DGAT2*, an enzyme involved in the synthesis of TGs, is also higher in PE placentas. DGAT2 has been associated with the accumulation of TGs in the liver causing hepatic steatosis, and DGAT2 inhibitors are currently being investigated as potential therapeutics to treat MASLD (Amin et al., 2019). In addition, animal studies have shown that DGAT2 is able to regulate the activation of SREBF-1, which also contributes to fat accumulation in the liver (Rong et al., 2024), thereby showing the interaction between these two proteins. DGAT2 may potentially be involved in the synthesis and accumulation of TGs in the placenta of women with PE and may be linked to ectopic lipid droplet accumulation and elevated neutral lipid content observed in the previous chapter. Unlike *DGAT1*, which is involved in the recycling of FAs to produce TGs, *DGAT2* is involved in the *de novo* lipogenesis process, thereby indicating that the elevated TGs found in the PE placenta arise from new lipid synthesis rather than from the exogenously supplied FA availability.

Furthermore, lipolysis is affected in the PE placenta by the elevated expression of *LIPE* and *Angptl4*. Lipolysis carried out by LPL is one of the main contributors to the release of NEFAs from TGs in VLDL that allows the uptake of NEFAs by the placental fatty acid transporters. LPL activity increases in the healthy placenta during the third trimester to increase fatty acid transport to the baby (Magnusson-Olsson et al., 2006). The results from this chapter show no differences in *LPL* mRNA expression in the PE placenta compared to controls, which is in concordance with previous investigations (Laivuori et al., 2006). However, *Angptl4*, known to inhibit LPL activity, was significantly higher in PE, thereby suggesting lower LPL activity at the placental surface and reduced uptake of fatty acids. This may

contribute to the lower uptake of LC-PUFAs in the PE placenta or it may be a counterregulatory mechanism to limit fatty acid uptake from the elevated circulating NEFAs. Additionally, *LIPE* expression was significantly higher in the PE group compared to controls, which may act as a regulatory mechanism to the increased storage of TGs in intracellular placental lipid droplets, similar to how fatty acids are released from lipid droplets in adipose tissue. HSL has also been involved in the mobilisation of fatty acids from lipid droplets in hepatocytes during MASLD (Reid et al., 2008), although it is unknown whether the expression of *LIPE* is changed in this pathology. In contrast, *LIPE* expression has previously been shown to be lower in PE placentas compared to healthy controls (Barrett et al., 2015), although this difference with the results from this chapter may be attributable to the use of different qPCR methods and the lower n number in Barrett et al. (2015), as well as phenotypic differences including lower BMI compared to the patients in this chapter.

Transport of long-chain fatty acids may also be disturbed in the PE placenta, as indicated by the lower expression of fatty acid transporter *FABP5*. These results were not accompanied by lower protein levels of FABP5, although this may be due to the lower n number used for immunoblotting experiments. However, a dimer conformation was found in the placenta which did not denature after boiling the samples, which suggests a strong interaction between the two monomers and its importance in the placenta. To our knowledge, there has not been previous findings on the dimer conformation of this protein, and its specific function in the placenta remains to be elucidated.

FABP5 is an intracellular transporter of long-chain fatty acids involved in regulating intracellular levels of fatty acids and delivery to specific metabolic pathways in adipocytes, macrophages and liver, among others (Storch and McDermott, 2009). The role of FABP5 in pregnancy is unclear, and studies investigating the role of FABPs in pregnancy have produced contrasting results. Animal studies have shown the link between FABP5 and insulin resistance, where FABP5 knockout mice present improved insulin sensitivity and lower circulating plasma lipids while overexpression resulted in reduced insulin sensitivity (Maeda et al., 2003). In addition, plasma FABP5 has been associated with adverse lipid profiles (including high TGs and low HDL) and high insulin levels in humans (Yeung et al., 2008). A baboon model of maternal undernutrition showed that the

elevated *FABP1* and *FABP5* gene expression and protein levels in the placenta, which suggests the presence of a regulatory mechanism to maintain fatty acid delivery to the baby (Chassen et al., 2020). These results are inconsistent with the observation of lower FABP5 in the PE placenta and it suggests no changes in protein levels as indicated by the immunoblotting results in this chapter. Other FABPs, including FABP1, 3 and 4 are increased in primary human trophoblast cells alongside elevated lipid droplet numbers under hypoxic conditions (Biron-Shental et al., 2007) and FABP4 is increased in human PE placenta which may be associated with lipid accumulation (Yan et al., 2016). Interestingly, FABP5 was not increased under hypoxic conditions (Biron-Shental et al., 2007), indicating a different role for this isoform.

There is evidence indicating the role of FABP5 as a retinoic acid (RA) transporter. RA binds to nuclear receptors to upregulate genes involved in cell growth and survival. RA is essential for normal embryonic development of several organs including the brain, heart and eye (Berenguer and Duester, 2022) and has been implicated in the decidualisation process during pregnancy (Rajakumar et al., 2020). RA (carried by FABP5) activates the peroxisome proliferator-activated receptor (PPAR) β/δ which has important roles in the development of the central nervous system and neuronal maturation (Yu et al., 2012). Previous investigations have shown that there are no differences in the placental PPAR*δ* expression between healthy, PE and FGR pregnancies, thereby suggesting that it is not implicated in the pathophysiology of PE (Rodie et al., 2005). However, it may be that FABP5 is affecting this pathway by limiting the RA binding the PPAR*δ*. The lower expression of *FAPB5* in the placenta may represent lower transport of RA and may be associated with developmental and placentation abnormalities in PE, although this needs further investigation. The results from this chapter also showed lower expression of *FABP6* in FGR placentas compared to controls. FABP6 is also known to be a retinoid-binding protein which may be involved in the placental pathology of FGR, although there is a lack of evidence supporting this.

In addition, the lower expression of *FABP5* in the PE placenta may reflect the low LC-PUFA status in the placenta. There is a preferential incorporation of DHA into the TG fraction of BeWo cells compared to CEs, DGs and phospholipids (Campbell et al., 1997), which may suggest the importance of esterification into TGs for transport to the baby and the important role of HSL for releasing DHA from lipid

droplets. The increase in placental TG during PE may be storing elevated amounts of this PUFA rather than transporting it to the baby and may be the reason why we did not observe any differences in membrane fatty acid transporters in this chapter. Therefore, the intracellular transport (carried out by FABPs), rather than the transport into the placenta, appears to be impaired in PE. Interestingly, other researchers have also reached this hypothesis in FGR placentas where several LC-PUFAs have been found to be elevated in the TG fraction compared to controls, suggesting the diversion away from efflux and towards storage, although this study did not show an elevated ectopic fat content in the FGR placentas (Chassen et al., 2018). This may be reflected by the lower *FABP6* expression in FGR since there are less intracellular LC-PUFAs to bind to this transporter, although further research is needed to elucidate this theory.

LDLR protein expression in the PE placenta was not different compared to healthy controls, although this may be due to the low sample size and therefore limited conclusions can be drawn from these results. The numeric data suggests lower LDLR staining in the PE group however the lack of power due to small sample size and the variability of the data limits the statistical significance. Previous investigations have shown lower LDLR gene expression in the PE placentas which suggests reduced cholesterol transport to the baby (Murata et al., 1996), despite higher plasma LDL levels in PE pregnancies (Enquobahrie et al., 2004). In contrast, others have not found differences in the placental expression of any lipoprotein receptor or maternal and fetal serum lipoprotein concentrations between healthy and PE placentas (Hentschke et al., 2013). Interestingly, this study also reported remarkably low expression of LDLR in the third trimester placental tissue which may indicate that LDL transport does not have an important role towards the end of the pregnancy (Hentschke et al., 2013). Nevertheless, increasing the sample size in the present study would elucidate the protein level and localisation of the LDLR in healthy and PE pregnancies and the potential impact on the baby.

In conclusion, this chapter has demonstrated that PE placentas have a dysregulated *de novo* lipogenesis pathways compared to healthy controls (Figure 5-12). Elevated *LIPE* and *Angptl4* expression indicates abnormal lipolysis patterns that may be affected by the hyperinsulinemia during PE pregnancies. High *DGAT2*, *FASN* and *SREBF-1* expression suggests greater lipid synthesis that could contribute to the ectopic fat accumulation in PE placenta observed in the previous chapter.

Due to the deleterious consequences of insulin resistance on the lipid homeostasis of the placenta in PE, it would be interesting to investigate other pathologies of pregnancy where insulin resistance is likely to have an impact. For this reason, the next chapter will focus on the lipid composition of placentas from pregnancies affected by GDM to investigate the potential fatty acid dysregulations in this condition.

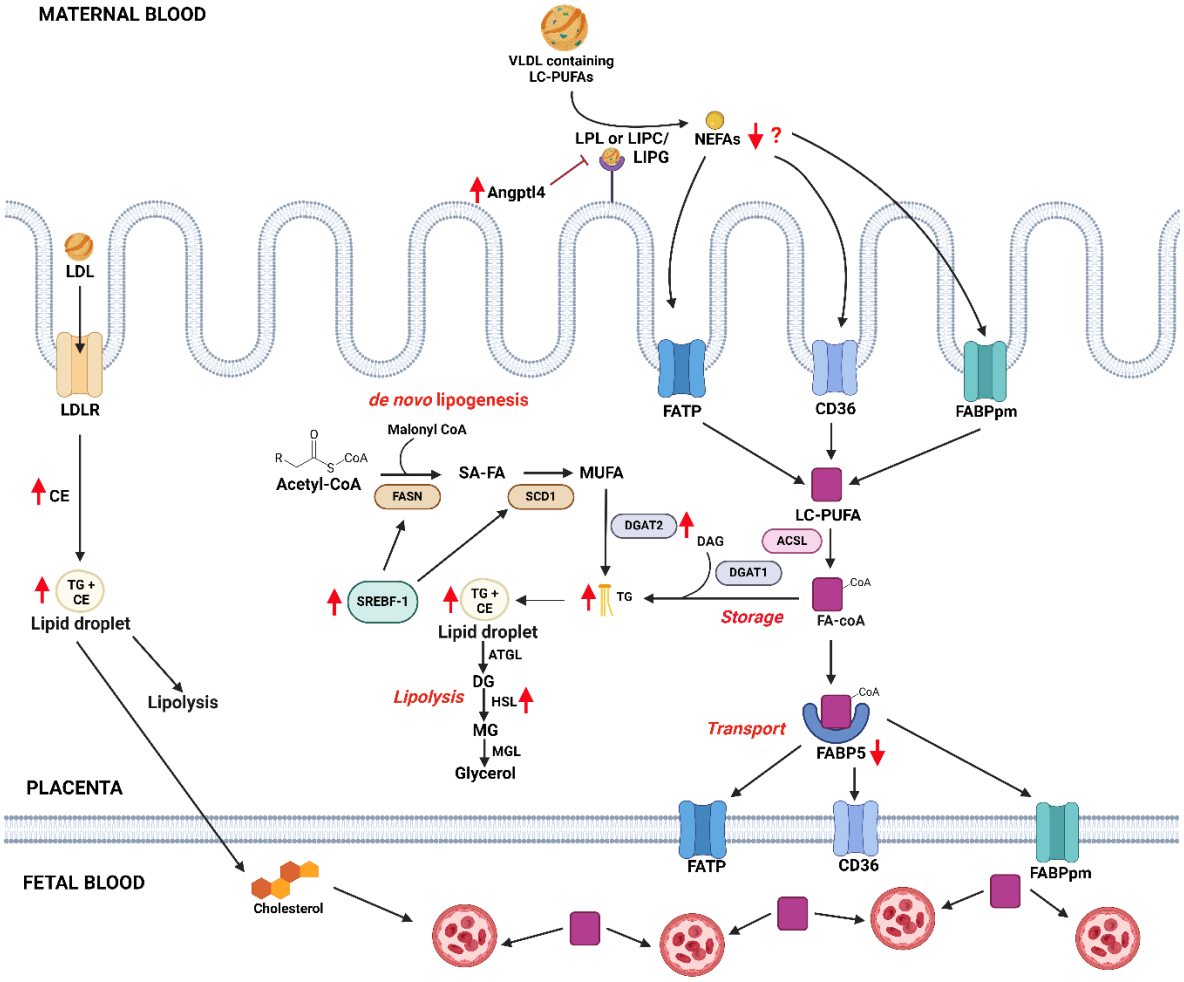

Figure 5-12. Lipid metabolism in the PE placenta. LC-PUFAs cross the placental barrier via specific LC-FA transporters. Activated FA-coA can undergo different pathways, including storage and transport. *De novo* lipogenesis is increased in PE via the elevated activation of *SREBF-1* and *FASN*. High amounts of TGs are being formed from MUFAs through the increased action of *DGAT2*. Lipoprotein release of TGs appears to be impaired in PE by the inhibition of LPL by Angptl4, which may indicate reduced uptake of LC-PUFAs. However, lipolysis of DGs is elevated by high expression of *LIPE* (HSL). High CE and TG content and lipid droplet number are elevated in the PE placenta. Intracellular transport by FABP5 is also decreased. Figure created with Biorender.com.

6 Placental lipid metabolism and storage in pregnancies complicated by gestational diabetes mellitus

6.1 Introduction

GDM is characterised by insulin resistance and hyperglycaemia during pregnancy. Women with GDM are twice as likely to develop later-life CVD compared to women with healthy pregnancies (Kramer et al., 2019), and offspring are at greater risk of obesity, increased adiposity and metabolic disorders (Bianco and Josefson, 2019). Maternal obesity increases the risk of developing GDM, and the incidence of GDM is increasing worldwide due to the rise in the numbers of older and obese mothers (Nakshine and Jogdand, 2023). Even though the link between maternal obesity and GDM is not fully understood, it is hypothesised that adipose tissue dysfunction and limited expansion capacity may play an important role (Trivett et al., 2021), however, specific mechanisms remain to be elucidated.

Despite hyperglycaemia being the primary feature of GDM, increasing evidence suggests that dyslipidaemia and adipose tissue dysfunction plays an important role in its pathophysiology. During healthy pregnancies, there is an early increase in insulin sensitivity that allows the early accumulation of lipids to sustain gestation, while the mid to late pregnancy period is characterised by an elevated rate of lipolysis and glucose production through an increase in insulin resistance. These adaptations provide energy for the mother and the baby. In contrast, women with GDM have reduced pre-pregnancy insulin sensitivity which exacerbates the response to pregnancy and results in increased lipolysis and circulating lipid concentrations (Catalano, 2010). High lipid levels can lead to endothelial dysfunction in the non-pregnant population, suggesting that elevated NEFAs during obese and GDM pregnancies may underlie the same lipotoxic effects (Jarvie et al., 2010) and may be the reason why GDM increases the risk of other pregnancy complications such as PE.

Adipose tissue from women with GDM presents with an abnormal lipid metabolism characterised by lower expression of genes involved in lipid uptake, storage and synthesis which may lead to greater fatty acid supply for placental transfer and increased fat deposition in the fetus (Lappas, 2014) and maternal organs. In

addition, obese pregnant women exhibit SAT and VAT adipocyte hypertrophy pre-pregnancy (Drolet et al., 2008), which become even more insulin-resistant during gestation. It has been hypothesised that the same dysfunction takes place in GDM, which results in fatty acid spillover and ectopic fat accumulation in to other organs including the pancreas, which may contribute to ß-cell dysfunction and insulin release (Trivett et al., 2021). Additionally, ectopic fat accumulation in the liver may also contribute to the development of insulin resistance in GDM (Lee et al., 2019). Due to this lipid dysregulation, obese women have higher TG, VLDL and lower HDL concentrations compared with lean controls and, similarly, GDM women have higher TG concentrations which may impact fetal adiposity (Catalano and Hauguel-De Mouzon, 2011).

Furthermore, maternal dyslipidaemia can affect fetal growth and later-life development. Offspring from glucose-controlled GDM pregnancies have higher lipoprotein TG enrichment compared to controls which may contribute to cardiometabolic complications later in life (Meyer et al., 2023). Interestingly, it has been suggested that elevated maternal NEFAs, rather than the hyperglycaemic environment, result in increased placental fatty acid transport and contribute to lipid esterification in fetal adipocytes and fetal macrosomia (Szabo and Szabo, 1974), which may be the reason why mothers with glucose-controlled GDM pregnancies still deliver LGA babies (Schaefer-Graf et al., 2008). Maternal TG concentrations, and not glucose levels, have been associated with neonatal weight in women with normal glucose tolerance (Cianni et al., 2005). Additionally, maternal VAT thickness is associated with birth weight which suggests limited SAT storage capacity and elevated fatty acid availability for fetal transport (Jarvie et al., 2020). In contrast, others have reported that NEFA esterification into TG in the placenta during hyperglycaemic pregnancies might be a regulatory mechanism to limit fatty acid transfer to the growing fetus (Gallo et al., 2017). This is further supported by *in vitro* human trophoblast models where culture in media with NEFAs leads to lipid droplet accumulation while incubation with glucose does not cause the same effect (Pathmaperuma et al., 2010), which would support the theory of TG accumulation in the GDM placenta. In addition, other authors have found that placentas from GDM pregnancies present upregulation of genes involved in intracellular lipid biosynthesis which contribute to TG accumulation

(Radaelli et al., 2009), thereby suggesting the presence of ectopic fat in GDM placenta.

Lipid droplet deposition in the GDM placenta has not been confirmed. A murine diet-induced GDM model has shown elevated lipid droplet ORO staining and TG, but not CE, content (Kuentzel et al., 2022). Similarly, healthy placental explants exposed to hyperglycaemic conditions show elevated TG accumulation, however, GDM placentas presented higher TG content only when GDM was concurrent with obesity (Hulme et al., 2019). High TG content in the GDM placenta has been observed in other studies, although in this case GDM was present in the absence of obesity (Visiedo et al., 2013). It is important to note that these investigations were carried out using TG quantification kits rather than lipidomics, and therefore full neutral lipid profiles were not obtained. However, others have found elevated TG in the GDM placenta, which was BMI-independent, by gas chromatography but they did not find evidence of lipid droplet accumulation (Stirm et al., 2018).

Moreover, DGs have also been involved in the pathology of GDM. Lipidomics analyses on plasma from women with GDM have revealed higher concentrations of both DG and TG (Hou et al., 2023). Elevated concentrations of DGs are linked to insulin resistance by inhibiting the activation of the insulin receptor thereby impairing insulin signalling. DGs have been associated with hepatic insulin resistance in MASLD (Kumashiro et al., 2011) and a similar mechanism may contribute to the insulin resistance observed in GDM. DGs have not previously been investigated in the GDM placenta, and as it has been observed that some changes in the DG species in the PE placenta (Chapter 4), similar patterns may also take place in GDM.

Similar to the pathology of PE, low fetal LC-PUFAs have been found in GDM pregnancies. Cord vein, but not maternal, erythrocyte AA and DHA concentrations in the phospholipid fraction are significantly lower in GDM compared to controls (Wijendran et al., 2000). Consistent with these findings, neonatal plasma from GDM pregnancies also has lower levels of AA and DHA (Thomas et al., 2005). In contrast, maternal plasma concentrations of AA and DHA have been found to be higher in women with GDM, which may indicate a fetal transport failure (Thomas et al., 2004). This may be the reason why offspring from GDM pregnancies have suboptimal behavioural and intellectual development which, interestingly, is

negatively correlated with maternal free fatty acid levels (Rizzo et al., 1991). This theory may be further supported by the elevated levels of AA and DHA in the PhE fraction of the placenta, but not the PC fraction (Uhl et al., 2015) which is known to be important for DHA mobilisation. In contrast, others have found elevated levels of DHA in both PhE and PC fractions in the GDM placenta, while there were no differences in the TG fraction (Bitsanis et al., 2006). This may also suggest that there is an increased level of LC-PUFA esterification in the placenta and therefore reduced transport, although this needs further investigation.

While insulin resistance, hyperinsulinemia and hypertriglyceridemia are common features in PE and GDM, the placental lipid regulation and neutral fat storage has not previously been investigated in the latter and may present different dysregulated mechanisms. Previous data suggests that lipids play an important role in the pathology of GDM. For this reason, this chapter will explore lipid composition and ectopic fat accumulation in the GDM placenta.

6.2 Hypothesis and aims

Similar to PE placentas, it was hypothesised that the placentas from pregnancies affected by GDM will have higher neutral lipid contents and altered levels of DGs compared to healthy placentas. The main aims were:

-To quantitate the TG, CE and DG content from GDM and healthy human placentas.

-To quantify the lipid droplet content in placentas from healthy and GDM human pregnancies.

-To investigate the expression of genes coding for proteins involved in the structure and function of lipid droplets in GDM and healthy human placentas.

6.3 Materials and methods

6.3.1 Patient recruitment

Patient recruitment of pregnant women with healthy, GDM and PE pregnancies for ORO staining, as well as GDM samples used for gene expression analysis, was carried out at the PRMU under the West of Scotland Research Ethics Service (ethics

approval: 11/AL/0017 Glasgow Royal Infirmary REC AM12) (details in section 2.4.1). The archival placental tissue from PE and healthy pregnancies used for gene expression was obtained from recruited patients at the PRMU under ethics approval 06/S070/14 Glasgow Royal Infirmary LREC1 and 01OB007 Glasgow Royal Infirmary REC (details in section 2.4.2). The archival placental tissue from GDM and matched healthy controls used for lipidomics analyses was obtained from recruited patients at delivery at the Royal Brisbane and Women's Hospital (Queensland, Australia) and at the National Health Service Greater Glasgow and Clyde maternity units under ethics approvals HREC/11/QRBW/427 (Royal Brisbane and Women's Human Research Ethics Committee), 2011/HE001301 (University of Queensland Human Research Ethics Committee) and 09/S0701/105 (West of Scotland Research Ethics Committee) (details in section 2.4.2). All recruited patients gave their informed voluntary consent.

6.3.2 Oil red O staining

ORO staining on GDM and healthy placental cryosections was carried out as described in Chapter 4 section 4.3.2. Results from each sample were calculated as a percentage of ORO staining by haematoxylin staining and an average from four placental quarters was reported.

6.3.3 Expression analysis of genes coding for lipid droplet associated proteins with qRT-PCR

RNA was extracted from frozen healthy and GDM placental tissue for qRT-PCR analysis as described in Chapter 4 section 4.3.3. Healthy archival placental samples were collected as described in section 2.4.2 and GDM samples were collected as described in section 2.4.1. Taqman gene expression assays *PLIN1*, *PLIN3*, *PLIN4* and *PLIN5* (assay IDs and gene descriptions in Table 1 section 2.8) were used for qPCR analysis on the extracted placental RNA using *TOP1* as the housekeeping gene. The fold change relative to *TOP1* was calculated with the $2^{-\Delta CT}$ formula and expressed as a percentage.

6.3.4 MTBE lipid extraction and lipidomic analysis

Lipid extractions from frozen archival human placental tissue from healthy and GDM patients were performed in part by undergraduate student Luke Bale at the

University of Wollongong. Lipids were extracted as described in Chapter 4 section 4.3.5 for human samples. Quantification of neutral lipids (TG and CE) and DG were included in this chapter. Similar to previous results, only MS1 data was included in this analysis due to difficulties in analysing MS2 data, and therefore the individual fatty acyl groups making up the different lipids could not be investigated.

6.3.5 Statistical analysis

As mentioned in Chapter 4, healthy, PE, FGR and GDM samples were included in the same analysis of gene expression and ORO area results because the same healthy placental samples were used as control for all groups. Therefore, only healthy and GDM data will be presented in this chapter. ORO area was log-transformed and analysed by a mixed effects model as described in Chapter 4 section 4.3.7. Data analysis of the averaged ORO area was performed by an unpaired t-test. Gene expression data was also analysed by an unpaired t-test.

Data cleaning for lipidomics results was carried out as in Chapter 4. Briefly, lipid species that were not detected in more than 20 % of the samples were removed from the analysis and the remaining missing results were imputed by adding the lowest value detected. Before clean-up, 194 even-chain lipid species from the TG, DG and CE families were detected in total, but only 64 remained after the “clean-up”. Total TG, DG and CE were calculated from the sum of the individual species after the clean-up and imputed values. Statistical analysis of the TG, DG and CE sum composition was carried out in Minitab on log transformed data. Statistical analysis of the individual species from lipidomics data was carried out with the web-based platform MetaboAnalyst as explained in Chapter 4. PCA loadings plot, VIP plots and sum composition from the different lipids are presented in this chapter.

Patient characteristics are presented as mean ± SD for continuous variables and number (percent) for primiparous and fetal sex. Statistical analyses were performed on Minitab software version 21.4.3. Statistical significance was assumed at $P<0.05$ for all experiments apart from lipidomics results, where statistical significance was assumed at $P<0.01$ to account for multiple testing.

6.4 Results

6.4.1 Patient demographics

Patient demographics used for the ORO analysis are summarised in Table 9. There were no significant differences in age, BMI, gestational age at delivery, birthweight, smoking status and fetal sex. There was a significantly higher proportion of primiparous births in the GDM group compared to the healthy group. It is important to note that women with a GDM diagnosis were treated following standard clinical care practices, including diet and blood glucose lowering medication (insulin and/or metformin), and therefore their glucose levels were controlled. Notably, despite using different cohorts, all GDM groups were similar in age and BMI.

Table 9. Maternal characteristics for ORO analysis. Data analysed with an unpaired t-test (*on log-transformed data). BMI: Body mass Index. Significance at P<0.05.

	Healthy (n=14)	GDM (n=10)	P-value
Age (years)	32.4 ± 3.2	32.9 ± 4.9	0.79
***Booking BMI (kg/m^2)**	25.8 ± 4.8	29.4 ± 6.5	0.16
Gestational age at delivery (days)	270 ± 10	269.5 ± 2.9	0.95
Birthweight (g)	3525 ± 469	3767 ± 570	0.29
Primiparous (n, %)	0 (0)	3 (30)	0.028
Fetal sex (male, %)	8 (57.1)	3 (30)	0.19
Smoker n (%)	2 (14.3)	0 (0)	0.24

Patient demographics used for the gene expression analysis are summarised in Table 10. There were no significant differences in age, BMI, birthweight, smoking status and fetal sex. Gestational age at delivery were significantly lower in the GDM group.

Table 10. Maternal characteristics for gene expression analysis. Data analysed with an unpaired t-test (*on log-transformed data). BMI: Body mass Index. Significance at P<0.05.

	Healthy (n=68)	GDM (n=10)	P-value
Age (years)	30.4 ± 5.1	32.9 ± 4.9	0.16
***Booking BMI (kg/m^2)**	28.9 ± 6.4	29.4 ± 6.5	0.84
Gestational age at delivery (days)	275 ± 9[a]	269.5 ± 2.9	<0.001
Birthweight (g)	3538 ± 576[a]	3767 ± 570	0.26
Primiparous (n, %)	27 (39.7)	3 (30)	0.56
Fetal sex (male, %)	32 (47.1)	3 (30)	0.26
Smoker n (%)	14 (21)	0 (0)	0.13

Patient demographics used for the lipidomics analysis are summarised in Table 11. There were no significant differences in age, BMI, gestational age at delivery, birthweight and fetal sex. Note that parity was not obtained for this dataset.

Table 11. Maternal characteristics for lipidomics analysis. Data analysed with an unpaired t-test (*on log-transformed data). BMI: Body mass Index. Significance at P<0.05. Smoking data was not available for this dataset.

	Healthy (n=17)	GDM (n=30)	P-value
Age (years)	31.1 ± 2.9	31.4 ± 5.0	0.84
***Booking BMI (kg/m^2)**	26.4 ± 5.3	26.8 ± 5.5	0.84
Gestational age at delivery (days)	280.9 ± 12.7	277.9 ± 9.8	0.42
Birthweight (g)	3371 ± 566	3574 ± 592	0.25
Fetal sex (male, %)	8 (47.1)	14 (46.7)	0.98

6.4.2 Lipid composition in the GDM placenta

PCA scores, loading and VIP plots from the healthy and GDM lipidomics results are presented in Figure 6-1. The PCA scores plot showed overlap between the groups which indicates minimal difference, although it is worth noting the large confidence interval in the GDM group which indicates high variability within the group. The PCA loadings plot shows that there are several individual TG, DG and CE species that contribute to the separation of the PC1 although the majority of species are clustered in the top right corner which indicates the contribution to the similarities between the groups. The VIP plot shows the top 30 variables that strongly contribute to the separation of the groups with VIP scores greater than 1. These are lower in GDM placentas apart from DG 28:3, DG 36:6 and DG 28:1 which are higher in GDM, and may indicate the important contribution of the DG lipid group to the model.

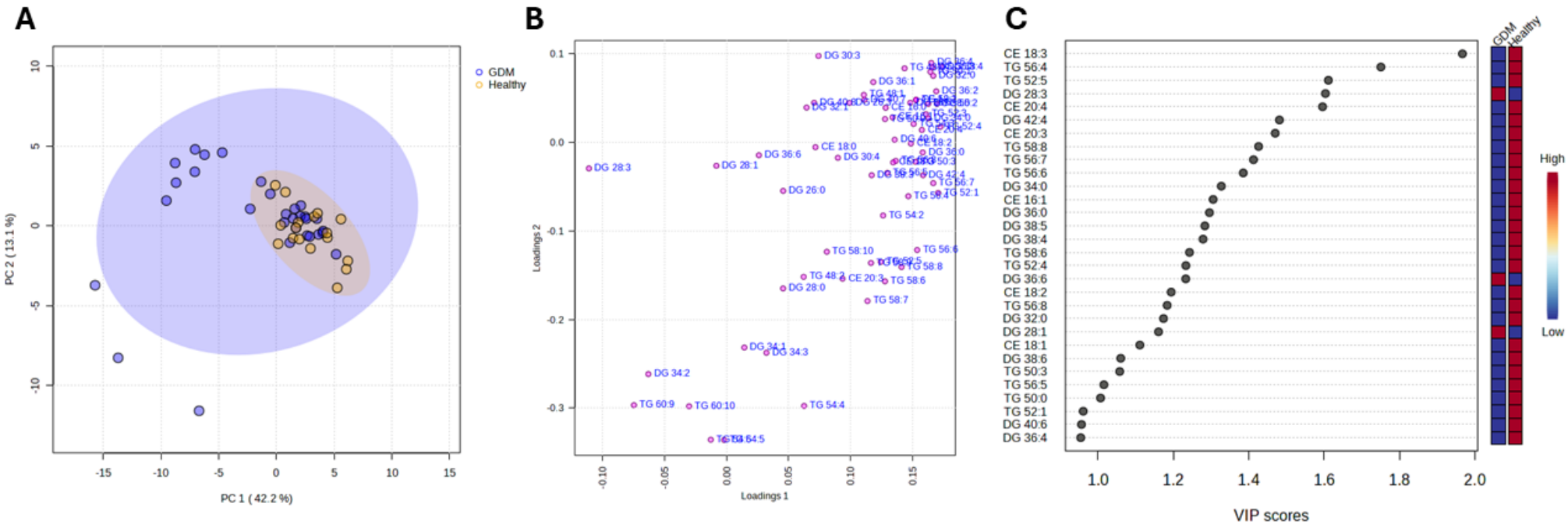

Figure 6-1. Distribution of the GDM and healthy placental lipidomics data by PCA score, loadings plot and VIP plot of the individual contribution to group differences. (A) PCA scores plot of the healthy (n=17) and GDM (n=30) groups. Each data point represents an individual sample and the ellipses indicate the 95 % confidence intervals. **(B)** PCA loadings plot of the different variables contributing to the differences between healthy and GDM groups. Variables on the x axis extreme are correlated to the PC1 and variables on the y axis extreme are correlated with the PC2. **(C)** VIP plot of the top 30 contributors to the difference between groups with indication of whether these were higher or lower.

Total TG, DG and CEs were calculated from the sum of the individual lipid species from healthy and GDM placentas and represented in Figure 6-2. TG and DGs were not significantly different between groups, however, CE was significantly lower in the GDM group compared to healthy controls (1086.1 ± 643.2 vs 1401.0 vs 800.0 nmol/g; P=0.002).

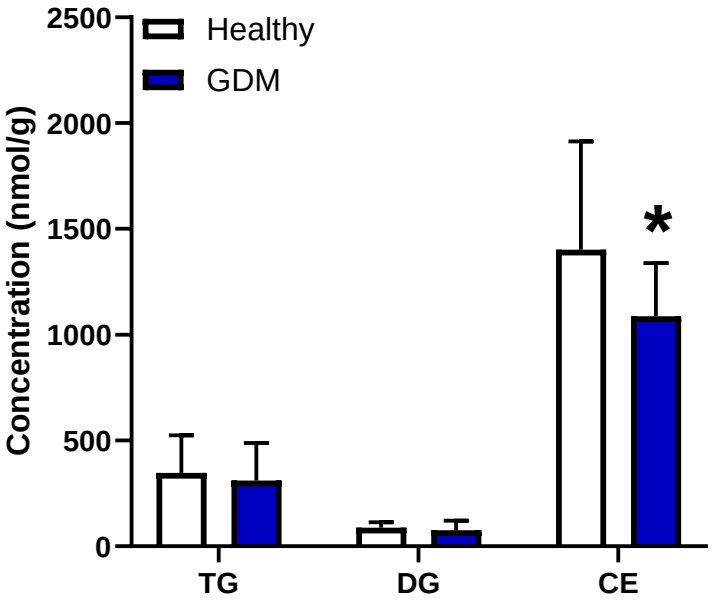

Figure 6-2. Placental composition of TG, DG and CE in healthy and GDM pregnancies. Lipid concentration of the total TG, DG and CE in healthy (n=17) and GDM (n=30) placentas. Data is presented as median ±IQR where individual samples represent each datapoint. Data was analysed by an unpaired t-test on log transformed data, significance at *P<0.05.

Differences in the individual TG, DG and CE species were investigated between healthy and GDM groups (Figure 6-3, 6-4, 6-5). Out of the 29 detected TG species, TG 52:4, TG 52:5, TG 56:4, TG 56:6, TG 56:7, TG 58:6 and TG 58:8 were significantly reduced in the GDM group compared to controls (P<0.01). Out of the 27 detected DG species, DG 28:3 and DG 36:6 were significantly higher in the GDM group whereas DG 34:0, DG 36:0, DG 38:4, DG 38:5 and DG 42:4 were significantly lower in the GDM group compared to controls (P<0.01). Out of the 8 detected CE species, CE 16:1, CE 18:3, CE 20:3 and CE 20:4 were significantly lower in the GDM group compared to controls (P<0.01).

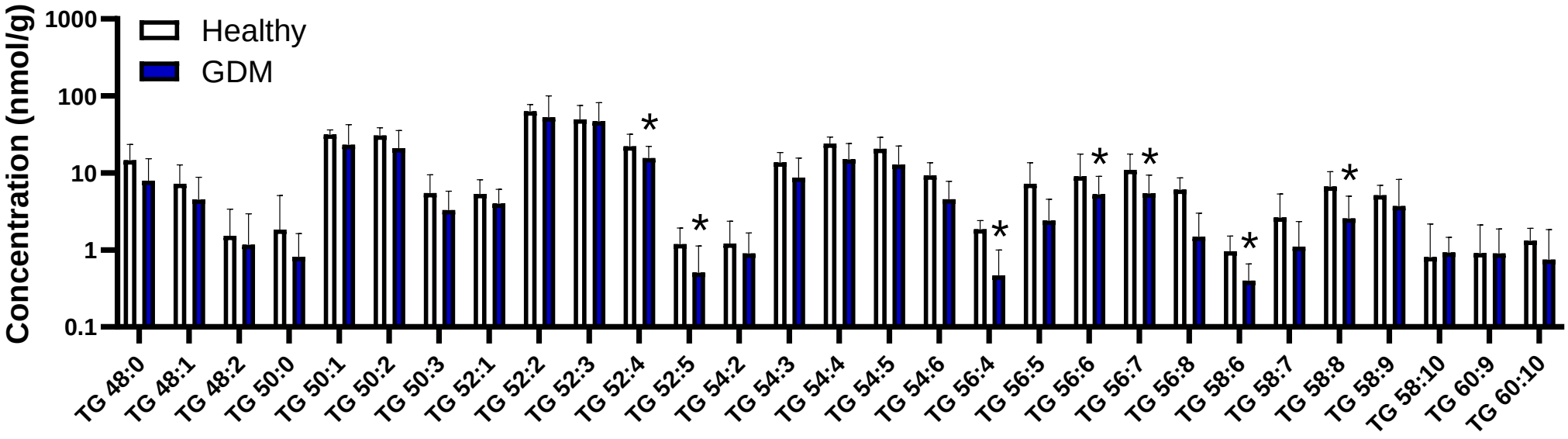

Figure 6-3. Placental composition of individual TG species in healthy and GDM pregnancies. Lipid concentration of different detected TG species in healthy (n=17) and GDM (n=30) placentas. Data is shown on a logarithmic scale to aid interpretation. Data is presented as median ±IQR where individual samples represent each datapoint. Data was analysed by an unpaired t-test on log transformed data, significance at *P<0.01.

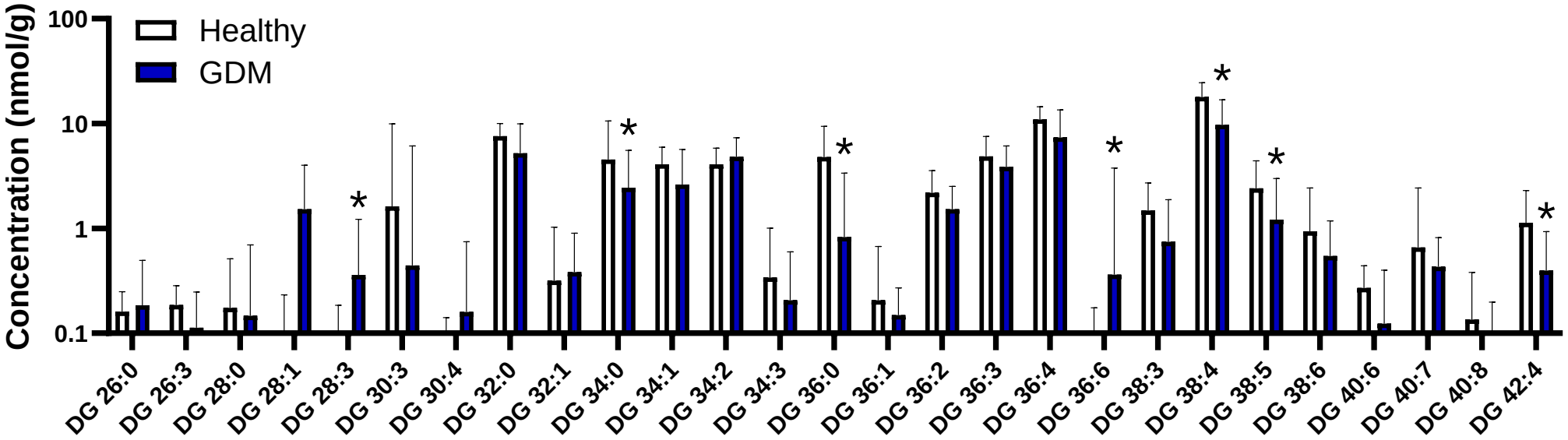

Figure 6-4. Placental composition of individual DG species in healthy and GDM pregnancies. Lipid concentration of different detected DG species in healthy (n=17) and GDM (n=30) placentas. Data is shown on a logarithmic scale to aid interpretation. Data is presented as median ±IQR where individual samples represent each datapoint. Data was analysed by an unpaired t-test on log transformed data, significance at *P<0.01.

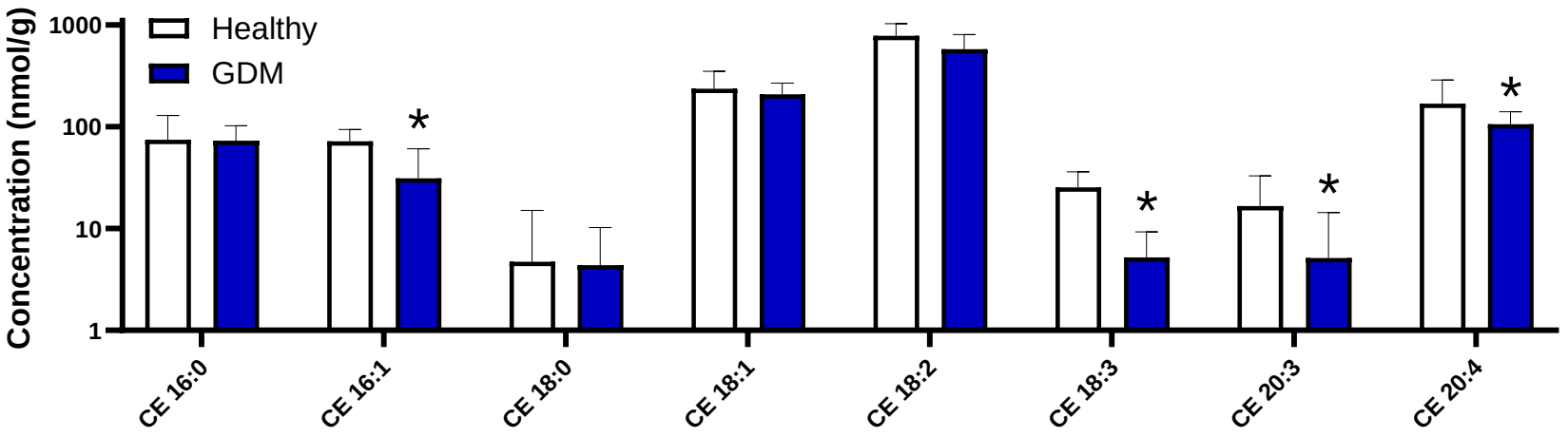

Figure 6-5 Placental composition of individual CE species in healthy and GDM pregnancies. Lipid concentration of different detected CE species in healthy (n=17) and GDM (n=30) placentas. Data is shown on a logarithmic scale to aid interpretation. Data is presented as median ±IQR where individual samples represent each datapoint. Data was analysed by an unpaired t-test on log transformed data, significance at *P<0.01.

6.4.3 Placental lipid droplet quantification

The ORO/haematoxylin stained area was quantified on placental tissue from women with GDM and healthy pregnancies (Figure 6-1). There were no significant differences between groups (Healthy: 1.94 ± 1.70 vs GDM: 2.82 ± 2.43 %; P=0.29).

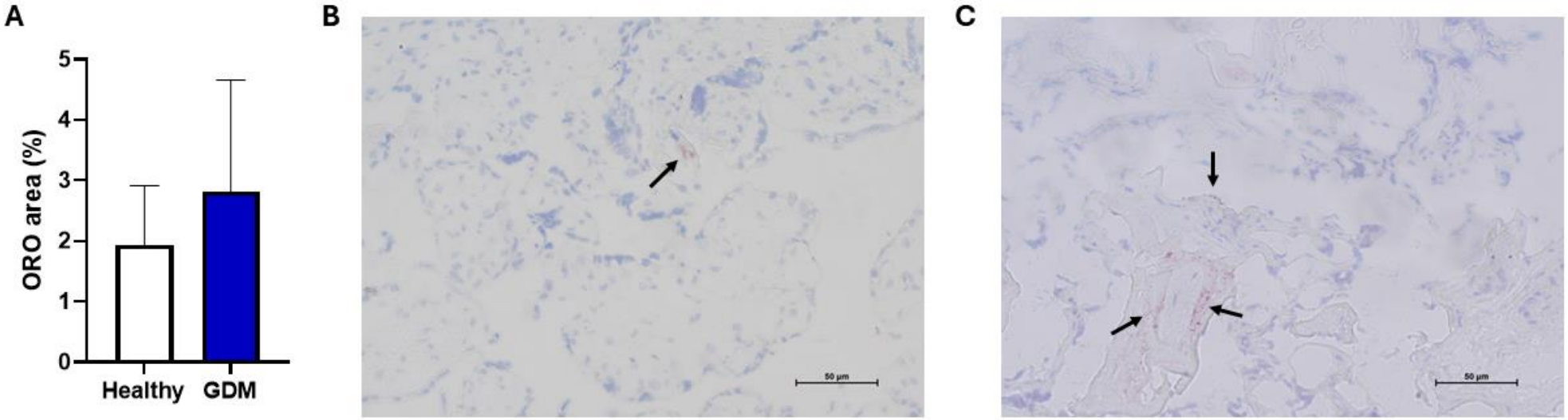

Figure 6-6. Lipid droplet quantification in healthy and GDM placentas. (A) Lipid droplet by haematoxylin area in healthy and GDM placentas. **(B)** Representative ORO image from a healthy placenta. **(C)** Representative ORO image from a GDM placenta. Data is shown as median ±IQR where individual samples represent each data point (Healthy: n=14 and GDM: n=10). Data was analysed by a one-way ANOVA (including PE group) with Tukey *post hoc* test (reported here) on log-transformed data; significance at *P<0.05.

6.4.4 Placental expression of genes coding for lipid droplet associated proteins

PLIN1, *PLIN3*, *PLIN4* and *PLIN5* were investigated in healthy and GDM placentas (Figure 6-7) as lipid droplet markers. There were no significant differences in the gene expression of these genes between groups (P>0.05).

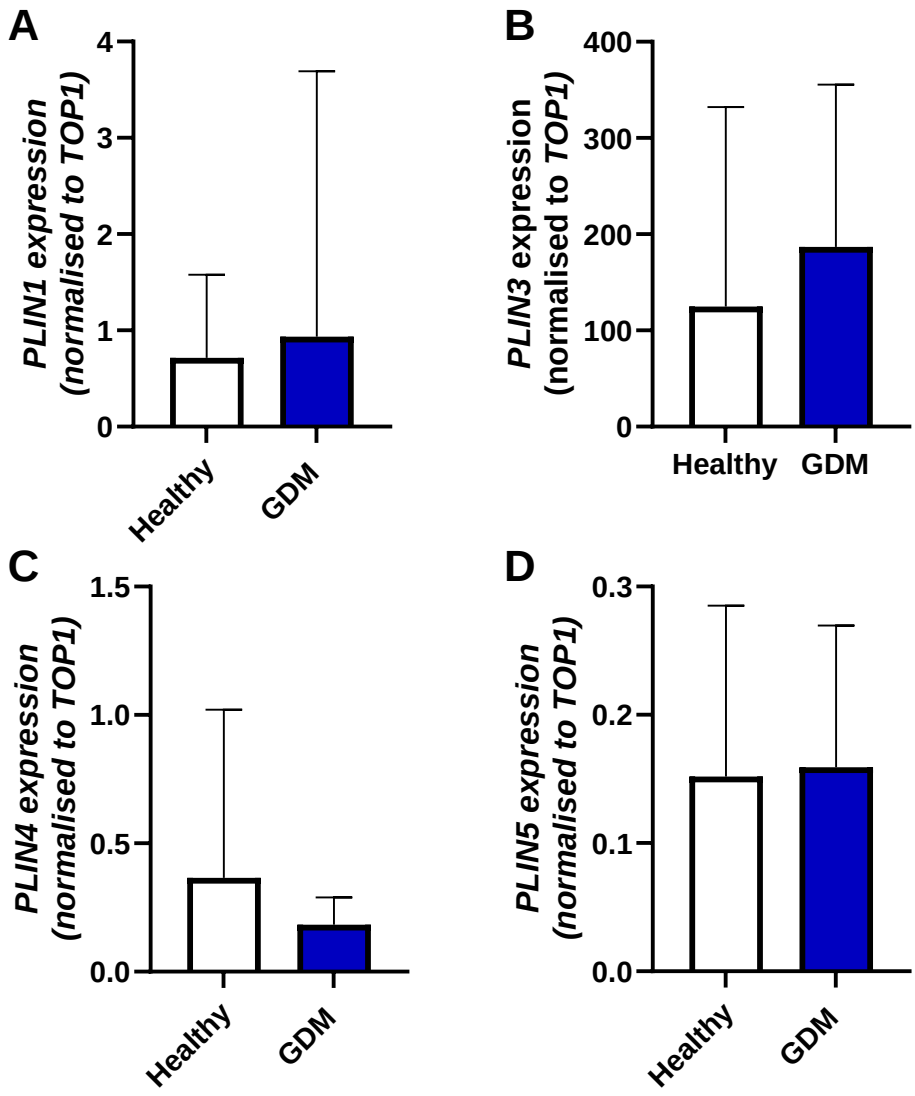

Figure 6-7. Gene expression of lipid droplet associated genes. Gene expression of *PLIN1* (A), *PLIN3* (B), *PLIN4* (C) and *PLIN5* (D) were analysed by qRT-PCR and are presented as a percentage of the expression of the housekeeping gene *TOP1*. Data is shown as median ±IQR where individual samples represent each data point (Healthy: n=68, GDM: n=9). Data was analysed by a one-way ANOVA (including PE and FGR groups) with Tukey *post hoc* test (reported here); significance at *P<0.05.

6.5 Discussion

Despite similarities with the pathophysiology of PE, the GDM placenta does not present with evidence of ectopic fat storage. It was hypothesised that, similar to PE, placentas from pregnancies complicated by GDM would have higher neutral lipid storage and altered DGs species compared to healthy placentas. The gene expression, lipidomics and histology data in this chapter showed several fatty acid differences between GDM and healthy controls, however, these changes do not appear to contribute to placental fat accumulation. Total CE content was significantly lower in GDM placentas, which may indicate altered cholesterol metabolism. Additionally, individual TG, DG and CE species were different in the GDM placenta, although the impact of these changes on the pathology of GDM remains to be elucidated.

Due to differences in treatment for glucose control and BMI among studies into patients with GDM, the pathology between studies might be markedly different, and it is challenging to draw general conclusions regarding placental fatty acid status from the available literature. Nevertheless, lipidomic and metabolomic experiments in GDM plasma have identified potential biomarkers that may aid early diagnosis, including TGs and DGs (Hou et al., 2023). These studies have highlighted the importance of lipids in the pathology of GDM, however, lipidomic experiments in the GDM placenta have not been previously reported. As shown in previous chapters, lipidomic analysis of the PE placenta can help identify potential mechanisms underlying abnormal lipid metabolism and insulin resistance. Similarly, studying lipid status in the GDM placenta is relevant in order to identify dysregulated mechanisms affecting mother and baby. The results from this chapter show that, unlike PE, there is no ectopic fat accumulation in the GDM placenta.

Adipose tissue dysfunction and lipid metabolism in GDM pregnancies

In women with additional metabolic stress, such as those with GDM and pre-existing obesity, there are alterations in adipose tissue glucose and lipid metabolism consistent with increased insulin resistance leading to elevated maternal fatty acid turnover. The limited storage capacity of adipose tissue leads to fatty acid spillover and delivery to the liver resulting in increased VLDL

secretion and plasma TG levels. Consequently, there are elevated plasma TG concentrations during GDM pregnancies, however, it is unclear whether TG is accumulated in the GDM placenta. Previous studies have reported conflicting results where TG accumulation appears to take place in the placenta during GDM, although this seems to be dependent on BMI. Higher TG content has been observed in GDM concurrent with obesity but not in non-obese women with GDM (Hulme et al., 2019). Moreover, placentas from obese women with GDM have shown upregulation of genes involved in TG and cholesterol biosynthesis pathways (Radaelli et al., 2009), which suggests increased esterification. The lipidomics results from this chapter show that there is no TG accumulation and ectopic lipid droplets in GDM placenta, although it is important to note that the patients from this study were not obese. Therefore, it may be hypothesised that pre-pregnancy BMI is an important contributor to TG accumulation in the placenta of pregnancies impacted by GDM and may explain the limited benefits of a controlled GDM pregnancy in the offspring.

Despite studies which have shown elevated TG content in the GDM placenta (Visiedo et al., 2013), there has been no evidence of increased lipid droplet content estimated by *PLIN2* expression (Stirm et al., 2018). Others have found higher expression of *PLIN1* in the GDM placenta compared to controls (Barrett, et al., 2014). In contrast, the results from this chapter showed no differences in the expression of *PLIN1*, *PLIN3*, *PLIN4* or *PLIN5* nor in ORO staining between GDM and healthy placentas, suggesting that there was no accumulation of ectopic lipid droplets. Similarly, others have not observed differences in ORO staining in the chorionic villi from GDM placentas compared to controls (Giommi et al., 2023). However, cell culture models mimicking GDM conditions have shown accumulation of lipid droplets in the placental trophoblasts, although present drawbacks as the removal and transport mechanisms are limited in *in vitro* settings. Culture of placental trophoblasts with high physiological NEFA concentration showed an increase in lipid droplet numbers (Pathmaperuma et al., 2010) and the expression of *de novo* lipogenesis genes including *SCD* (Radaelli et al., 2009). Others found elevated placental FAS protein levels in overweight insulin-treated GDM patients which were associated with elevated proinflammatory cytokines in this tissue (Marseille-Tremblay et al., 2008). This finding is consistent with metabolomics experiments where enrichment of metabolites involved in the biosynthesis of

unsaturated fatty acids was found in the GDM placenta (Yang et al., 2021). Hence, similar to PE, the increase in *de novo* lipogenesis genes may lead to the TG accumulation in GDM. Even though this is in contrast with the results from this chapter, some studies suggest that the elevated TG during GDM may be a result of the increase in dietary fat intake on top of the insulin resistant state (Ryckman et al., 2015), which highlights the important role of diet in differences between cohorts. Additionally, changes in *de novo* lipogenesis were not investigated in this chapter. A recent lipidomics study on plasma from obese women with GDM found alterations in specific TG and DG species which contained fatty acids proposed to be derived from *de novo* lipogenesis (including FA(16:0), (16:1), (18:0), and (18:1)) (Furse et al., 2022), suggesting upregulation of lipid synthesis. This finding is not surprising considering that glucose is the main substrate for *de novo* lipogenesis and it can be hypothesised that a state of chronic hyperglycaemia like GDM will have an acute impact on this process. Additionally, the insulin resistant state in GDM would further promote lipid synthesis. It is important to note that elevated levels of these *de novo* lipogenesis-related fatty acid species were also correlated with offspring adiposity (Furse et al., 2022). However, the authors in Furse et al. (2022) did not measure *de novo* lipogenesis directly due to concerns with pregnant patients and therefore the fatty acids detected may have been recycled from lipolysis. It is not clear to what extent the placenta may contribute to this lipid synthesis, however, it would be interesting to investigate the composition of the fatty acyl chains of the TG and DG species identified in this chapter by MS2 analysis, as well as the placental expression of genes involved in lipid biosynthesis, in order to investigate *de novo* lipogenesis in this tissue and compare to the PE placenta.

Several individual CE and TG species detected in this study were shown to be lower in the GDM placenta, which is in contrast with the PE placenta where most neutral lipid species were higher compared to healthy placentas (Brown et al., 2016). Moreover, despite higher DG and TG concentrations in maternal plasma from GDM pregnancies (Hou et al., 2023), this does not seem to translate to the placenta as no differences were found between GDM and controls in this chapter and only individual lipid species appear to be affected. This may suggest that the excess lipids are stored elsewhere. Data from our lab has shown that maternal GDM VAT adipocytes are hypertrophic (Zoe Lees, personal communication), which suggests

that the excess fatty acids are being stored in this compartment in GDM. VAT may act as a buffer for excess lipids in GDM and prevent accumulation in the placenta, although this requires further investigations.

Altered LC-PUFA levels in GDM

Furthermore, the highly unsaturated (four or more double bonds) TG species were lower in GDM compared to healthy placentas, which may indicate reduced LC-PUFA status although this needs to be confirmed with MS2 analysis. Similar to our results, others have found lower concentrations of TG 56:4 and TG 58:6 in plasma samples from obese women with GDM during their second trimester of gestation (Furse et al., 2019). Interestingly, several TG and DG biomarkers have also been identified to be different in plasma from women with GDM and, importantly, these differences were BMI-independent (Hou et al., 2023). Furthermore, CE 20:4, which was found to be lower in this chapter, has been positively correlated with later-life type 2 diabetes development in women with previous GDM pregnancies (Lappas et al., 2015). This evidence suggests that individual lipid biomarkers, rather than overall lipid levels, may be useful in predicting GDM and highlights the importance of lipidomic studies to understand this pathology. It is important to note that these shifts in the abundance of several lipid species in the GDM placenta may not be relevant *in vivo*, however, it is interesting that others have found differences in the abundance of TG, DG and CE species which may indicate a role in the aetiology of GDM and warrants further investigation.

Moreover, there is evidence that the LC-PUFA status is affected in mother and baby during GDM pregnancies although it remains a matter of debate. Elevated levels of AA and DHA in plasma from women with GDM have been observed compared to healthy controls, although the patients were not BMI-matched which may have an impact on the results (Thomas et al., 2004). In contrast, fetal plasma from offspring affected by GDM showed lower AA and DHA content compared to their healthy counterparts (Thomas et al., 2005), which suggests reduced transport to the baby. Nevertheless, it is important to note that glucose control and pre-pregnancy maternal BMI appear to be relevant in determining plasma AA and DHA contents, and therefore these parameters should be taken into account when drawing conclusions from the available literature. Non-obese women with GDM have lower DHA levels whereas obese women with GDM have higher DHA

levels (Wijendran et al., 1999). Similarly, plasma AA concentration is positively associated with hyperglycaemia in women with GDM (Wijendran et al., 1999). This suggests that even women with controlled GDM pregnancies will have altered levels of LC-PUFAs that may affect the transfer to the baby, which highlights the importance of investigating the placenta in GDM pregnancies. This chapter presented evidence of reduced CE 18:3 (essential dietary fatty acid) and AA in the CE fraction (CE 20:4) in the GDM placenta. These results may reflect lower essential fatty acid intake which is therefore less available for conversion to LC-PUFAs. In contrast, others have found elevated levels of these CE species in GDM plasma (Burzynska-Pedziwiatr et al., 2023), although it is important to note that this cohort had low BMI (lean) and presented with impaired glycemia whereas the cohort of women used in this chapter had higher BMI (overweight) and undertook glucose management therapy. Additionally, *in vitro* models with placental trophoblasts from GDM placentas mimicking GDM-like conditions in culture (such as high insulin and TNF-α concentrations) have shown increased uptake of AA and DHA but, interestingly, when the GDM trophoblasts were cultured under normal conditions, they showed lower LC-PUFA uptake compared to healthy trophoblasts (Araújo et al., 2013). This suggests accumulation of LC-PUFAs in the placenta under GDM conditions, which has been previously shown in placental tissue from obese pregnancies with higher omega-3 accumulation in the TG and phospholipid fraction compared to lean pregnancies (Varastehpour et al., 2006). In addition, when comparing the impact of obesity and GDM individually in the same study, only placentas from obese women have elevated LC-PUFAs in the placental phospholipid fraction compared to lean GDM and lean controls (Segura et al., 2017). This mechanism may also take place in obese GDM pregnancies and contribute to increased LC-PUFA placental accumulation and reduced transport to the baby and suggests that the environment and disease status remarkably impacts the LC-PUFA levels.

Cholesterol metabolism in GDM

The results from this chapter showed lower CE content in the GDM placenta compared to controls, which suggests disturbances in cholesterol metabolism. Cholesterol status during GDM also appears to be affected by BMI. Overweight/obese women with GDM have lower plasma cholesterol compared to

lean GDM women (Dubé et al., 2013). In addition, this study showed reduced protein levels of the fetal ABCG1 cholesterol transporter in placentas from overweight/obese women with GDM compared to lean GDM women, suggesting reduced cholesterol transport to the baby (Dubé et al., 2013). In contrast, others have found that cholesterol efflux is increased in placental fetal endothelial cells *in vitro* due to upregulated cholesterol ABC transporters (Sun et al., 2018), suggesting that increased transport, and consequently reduced placental storage of cholesterol takes place in GDM. There is an upregulated activity of CE hydrolases, but not TG hydrolases, in placentas from an animal model of GDM, suggesting increased CE turnover despite the lack of changes in total placental CE content (Kuentzel et al., 2022). Despite the inconsistencies, altogether these studies suggest that the low CE levels observed in the GDM placenta may reflect the impaired maternal cholesterol status during GDM, and further investigations need to be carried out to determine the impact on the cholesterol status of the fetus in humans during GDM.

In conclusion, this chapter has shown that mothers with GDM present an altered fatty acid metabolism that results in changes in the lipid content in the placenta, although unlike PE it does not appear to lead to ectopic fat accumulation. The impaired profile observed from placental lipidomics may present evidence of reduced accumulation of LC-PUFAs that may interfere with fetal delivery, although this needs further investigation. Overall, this chapter has demonstrated that, despite similar aetiologies, PE and GDM are different in terms of their lipid abnormalities and the impact on the placenta.

7 General discussion

Summary of main results and limitations

PE is one of the major causes of maternal complications worldwide, which impacts both mother and offspring. The number of mothers affected by PE is increasing due to the raising numbers of women at risk around child-bearing age. The associated maternal care and prematurity of the babies, as well as the extended consequences on the offspring, imposes a considerable financial burden during and after the pregnancies. The only cure for PE is the delivery of the baby, and therefore improved management and treatment during gestation must be achieved to alleviate the impact on mother and offspring. Offspring born after PE pregnancies are more likely to develop CVD later in life, however the causes leading to this remain unknown. The metabolic complications of PE in the mother are becoming increasingly relevant as it has been suggested that maternal lipid dysregulation may cause alterations in placental structure and function and may play an important role in the pathology of PE. For this reason, the main research question targeted in this thesis was whether the impaired lipid storage, transport, inflammation and hypoxia attributable to the PE phenotype contributes to the adverse cardiovascular effects on the offspring. If this proves to be right, this may be a novel way of treating mothers with PE that may improve the delivery and outcomes of the offspring. To study this, animal models of pregnancy are invaluable and provide reproducible data that allow elucidation of the underlying mechanisms and the ability to test possible treatments, although careful characterisation is needed to confirm that full phenotype is achieved in these models.

The work carried out in this thesis focused on the cardiovascular and metabolic impact of the hypertensive *in utero* stress in the offspring of an animal model of superimposed PE and compared the placental lipid metabolism between rats and humans during PE. The rat model did not show similar metabolic placental abnormalities compared to humans, which contained elevated neutral lipid content stored in lipid droplets. High human placental expression of genes involved in *de novo* lipogenesis in PE, probably as a consequence of increased insulin resistance, suggests a mechanism that could explain the excess ectopic fat in this organ. Despite some phenotypic similarities with PE, GDM did not present

an elevated lipid droplet content in the placenta, although several lipid species differences from control were identified and warrant further investigation.

It is important to note that there were some limitations in both the animal and human studies in this thesis. The high variability of the blood pressure data in the SHRSP dams treated with ANGII prevented the confirmation of the PE phenotype during this study. However, previous data from the Graham laboratory has shown elevated systolic and diastolic blood pressure in SHRSP dams treated with 750 ng/kg/min ANGII (data not published) using radiotelemetry. This technique produces data on the continuous blood pressure, heart rate and activity monitoring of the animals which provides more accurate results than the tail-cuff plethysmography method. As the mothers were not the main focus of the current study, the easier and more accessible method of tail-cuff plethysmography was used in this instance. In addition, this method may have given inaccurate readings particularly in young offspring (5 weeks of age) due to the limits of the equipment, although there was no available alternative as the radiotelemetry method is not compatible with longitudinal studies where animals are growing. Moreover, the study of the cardiovascular status of the offspring with echocardiography was impacted by the change of machines halfway through the study and the inability to compare the results from both, which impacted the accurate comparison between SHRSP and WKY offspring. The human studies were limited by the low sample sizes in the ORO staining experiments which were affected by the challenges of collecting tissue samples from pregnant women. This was particularly difficult as it was limited by having to travel to the hospital, the scepticism of the expectant mothers, and the out of hours deliveries (particularly in women with PE). Additionally, due to the restricted access to NHS data on the patients, additional information including drug treatments and smoking status was not obtained.

The cardiovascular impact PE on the offspring and potential mechanisms

This thesis hypothesised that offspring of a model of superimposed PE in SHRSP rats would present with impaired cardiac and metabolic remodelling. As described in Chapter 3, the offspring from this superimposed PE model showed signs of impaired cardiac development. This offspring study revealed that the intrauterine exposure to ANGII led to lower FS and RWT and higher E/A ratio which are

indicative of both systolic and diastolic dysfunction, respectively, which were maintained up to 17 weeks of age. The offspring of ANG-treated mothers also presented signs of impaired vascular reactivity, which may be an early sign for later-life increase in blood pressure. Therefore, this study has shown that the offspring of the ANGII-treated SHRSP model spontaneously develop cardiac defects from early development which remain up to adulthood. One of the advantages of this study was that this cardiovascular effect was not associated with birth prematurity, which allowed attribution of the cause to the intrauterine environment.

These results from the offspring study are comparable to the human data on offspring from PE pregnancies (recently reviewed in (Yang et al., 2023), including greater LV diastolic dysfunction. Children born from pregnancies affected by PE present increased left and right ventricular mass during their first months of life (Aye et al., 2020) and diastolic dysfunction during childhood (Fugelseth et al., 2011). Offspring from human PE pregnancies have higher blood pressure, smaller hearts, faster heart rates and reduced E/A ratio compared to offspring from healthy pregnancies (Yang et al., 2023), which is in contrast with the results from rats presented in this thesis. These differences may be due to several reasons, including that the human studies have only investigated specific timepoints in the offspring's lives which could indicate transient, rather than permanent, changes in the cardiac structure and function in order to adapt to the impaired cardiac development. Regardless, the similarities observed in this thesis show the translational potential of the ANGII model which is suitable for understanding the molecular mechanisms that lead to cardiovascular defects in the offspring.

Given that this thesis has shown early signs of cardiovascular defects in the offspring of a PE model that are similar to the impact observed in humans, it would be beneficial to develop strategies to monitor the risk on children and adults after PE pregnancies in order to reduce later-life impact. These may include regular echocardiography and blood pressure measurements as well as blood tests to identify markers of metabolic disturbance. This may be especially beneficial for offspring with superimposed risk for CVD, including obesity, smoking status and genetic predisposition, and therefore risk stratification may be useful for interventions and monitoring. These strategies would not only aid early

intervention but also reduce the burden of later-life cardiovascular disease as well as future PE pregnancies.

Although this study identified the impacts of PE in the offspring, the molecular mechanisms leading to the detrimental cardiovascular development were not investigated. They may be attributed to oxidative stress, hypoxia and inflammation during the development of the placenta. Phenotyping of the SHRSP dam, previously carried out by the Graham lab, did not show differences in uterine artery resistance between the vehicle control and the ANGII groups, although lower placental weight was observed. Spiral artery remodelling or placental oxidative stress were not investigated but would be useful to study in order to determine the cause of the fetal growth restriction and impaired development in the offspring. This might be done by histological staining of oxidative stress proteins including superoxide dismutase (*SOD*) and haematoxylin and eosin (H&E) stain in order to investigate structural changes in the spiral artery remodelling. In addition, other markers of endothelial dysfunction and inflammation such as vascular cell adhesion protein 1 (VCAM-1) and TNFα could be tested in these tissues by gene expression and protein analyses. Interestingly, the Graham lab has previously found signs of placental ischemia in the SHRSP model treated with 1000 and 500 ng/kg/min ANGII, and therefore future investigations should also focus on placental ischemic markers on the 750 ng/kg/min ANGII model.

Animal models of PE and the ability to mimic the human phenotype

Despite mimicking the elevated maternal blood pressure and FGR observed in the human PE phenotype, the superimposed PE animal model does not mimic the impaired lipid phenotype observed in humans. Chapter 4 showed that circulating lipids in plasma from dams exposed to ANGII were not different compared to controls. In addition, there were no differences in placental lipid content between ANGII and vehicle controls, which is in contrast to the human data whereby PE placentas present an elevated neutral lipid content (TG and CE) compared to healthy placentas. These results suggest that ANGII does not induce insulin resistance in the pregnant SHRSP dam. Similarly, other rodent models of PE, including the RUPP, also fail to imitate the metabolic phenotype of PE in humans despite manifesting the increase in blood pressure and FGR (Gilbert et al., 2007). In contrast, others have found evidence of placental ectopic fat accumulation in

a C57BL/6 mouse high-fat diet L-NAME model of PE (Sun et al., 2012). Moreover, a PE model in testosterone-treated Sprague-Dawley rats presented evidence of placental fat accumulation that leads to increased storage of LC-PUFAs and decreased delivery to the fetus (Gopalakrishnan et al., 2022). Although the authors did not report the insulin resistance status of the dams, testosterone treatment is known to be associated with insulin resistance. Based on these investigations, our model of superimposed PE may benefit from treatment with testosterone and/or high fat diet alongside ANGII in order to imitate the human metabolic syndrome of PE and fully recreate the "PE-like" symptoms. This may also contribute to mimicking the metabolic consequences of PE in the offspring, including increased adiposity, which appeared to be absent in our model.

Interestingly, other studies have demonstrated upregulation of proteins involved in hypoxia, oxidative stress and inflammation in a SHRSP placental proteomic analysis compared to WKY (Mary et al., 2021). Moreover, a transcriptomic analysis of the SHRSP uterine artery showed upregulation of proinflammatory factors, reactive oxygen species (ROS) production and RAAS genes compared to their WKY counterparts (Scott et al., 2021). These investigations are in line with the results from this thesis, as they show that the SHRSP model is able to imitate the impaired placentation involving oxidative stress and inflammation of human hypertensive pregnancies but still lacks the metabolic changes. Similarly, the placental proteome of a transgenic RAAS-activated PE-like Sprague-Dawley model showed changes associated with the RAAS and angiogenesis (Mary et al., 2021). These results further demonstrate that different animal models can only imitate certain features of the human PE pathology and that there is no ideal animal model of PE, which must be considered when investigating treatments. For instance, the SHRSP model has been used to investigate the impact of nifedipine, a common antihypertensive drug used in women with PE, during their hypertensive pregnancy and demonstrated that, despite the decrease in blood pressure, this treatment did not improve uterine artery remodelling and function (Small et al., 2016). This may be the reason why nifedipine does not improve neonatal outcomes in women with PE pregnancies despite alleviating hypertension in the mother (Winden et al., 2022). Hence, it is clear that the SHRSP model is an invaluable tool for studying certain therapies for PE and may be used to improve the detrimental cardiovascular impact on the offspring.

The metabolic impact of PE vs GDM pregnancies

The data on the presence of ectopic fat presented in this thesis provides insights on the metabolic impact of PE and GDM on the human placenta, which may be a consequence of impaired maternal adipose tissue function. The healthy physiological fat storage mechanism in adipose tissue, known as hyperplasia, consists of the generation of mature adipocytes from preadipocytes. However, some individuals have an impaired ability to produce mature adipocytes and, instead, the excess fatty acids are stored in preexisting mature adipocytes that become hypertrophic. Notably, hypertrophic adipocytes are insulin resistant which leads to elevated lipolysis rates and free fatty acid release. This fatty acid spillover leads to the diversion of fatty acids to VAT and other ectopic sites. Ectopic fat deposition is linked to the development of insulin resistance and T2DM in non-pregnant individuals. Adipose tissue plasticity is therefore involved in the development of insulin resistant states, and an analogous pathway is proposed for pregnancies that develop PE and GDM. In fact, it has been hypothesised that pregnant women with PE or GDM have a reduced capacity for hyperplasia that results in fatty acid spillover (Trivett et al., 2021), although the causes leading to this may be different in these two pathologies. Since women who develop GDM are usually overweight or obese, they may already have adipocyte hypertrophy prior to pregnancy and the metabolic stress induced post-conception may exacerbate the insulin resistance and lead to ectopic fat deposition in other organs including the pancreas which contributes to the development of diabetes. However, despite the elevated fatty acid spillover, the results in this thesis show that there is no ectopic fat deposition in the GDM placenta. Interestingly, there is data that maternal GDM VAT adipocytes are hypertrophic (Zoe Lees, personal communication), which suggests that the excess fatty acids are being stored in this compartment in GDM. There is evidence that women with GDM are more likely to develop MASLD later in life compared to women with healthy pregnancies (Forbes et al., 2011), however there is no evidence that this takes place during the pregnancy itself. This may mean that the excess circulating fatty acids and TGs in women with GDM may be stored elsewhere, such as the VAT, instead of the liver and the placenta like in PE pregnancies. After the GDM pregnancy, the exaggerated insulin resistance state improves but remains over time (Byrne et al., 1995), which may contribute to the hepatic accumulation of lipid later in life.

Following the previous theory, the VAT in women with a history of GDM may become replete over time and spill over fatty acids to other ectopic depots such as the liver.

In contrast, women with PE may have an innate insulin resistance which may also contribute to adipocyte hypertrophy and limited hyperplasia thereby leading to fatty acid spillover (Trivett et al., 2021). There is evidence that the SAT of women with PE is less reactive to insulin (Huda et al., 2014) which consequently leads to elevated lipolysis rates and circulating NEFAs and TGs (MacKay et al., 2012). However, in contrast to GDM, VAT adipocytes in PE were the same size as in BMI-matched controls (Zoe Lees, personal communication). It can be hypothesised that, as a consequence of this impaired adipose tissue expansion and elevated insulin resistance, fatty acids accumulate ectopically in other organs including liver and placenta. In fact, the link between PE and fatty liver has been observed in animal models and in humans. The dams from the L-NAME PE mouse model present fatty acid infiltration in the liver (Sun et al., 2012) and similarly, women with PE present elevated liver steatosis compared to healthy controls, as a consequence of the exaggerated insulin resistance status (Haggai et al., 2022). This evidence links PE to ectopic fat accumulation and suggests an important role in the pathology. In addition, placental neutral fat accumulation was previously observed in the PE placenta (Brown et al., 2016) and confirmed in this thesis by updated lipidomics techniques and ORO staining of lipid droplets on placental explants which showed higher droplet numbers in PE. This thesis provided additional evidence of elevated placental expression of lipid-droplet associated proteins *PLIN4* and *PLIN5*. Altogether, these investigations suggest that, although both GDM and PE are diseases with insulin resistance, the consequences of the fatty acid spillover are different potentially due to different tissue-specific responses to insulin resistance.

Mechanisms leading to placental ectopic fat accumulation in PE as potential targets for new treatments

Due to the evidence of ectopic fat accumulation observed in Chapter 4, a plethora of genes involved in fatty acid metabolism were investigated in the PE placenta in Chapter 5. It was observed that there was a higher expression of genes involved in *de novo* lipogenesis in the PE placenta, including *SREBP-1* and *FASN*, that may

contribute to the ectopic fat accumulation observed in this organ, although it should be confirmed whether these transcriptional changes translate at the protein level. Therefore, despite the original hypothesis was that the reason behind the ectopic fat deposition in the placenta was the maternal hyperlipidaemia, the results from this study suggest that the excessive insulin resistance during PE leads to increased placental fatty acid synthesis resulting from upregulation of *SREBP-1* and *FASN*. It may be hypothesised that the insulin resistance and hyperinsulinemia status in mothers with PE is triggering the *de novo* lipogenesis in the placenta as a response to this adverse environment. The placenta is sensitive to changes in the maternal environment that alter the function and structure of this organ, which consequently affects the fetus. For example, some investigators have suggested that the activation of the mammalian target of rapamycin (mTOR) (involved in insulin signal transduction) is an important placental signalling pathway that acts in response to maternal obesity and suggest that it may be a potential therapeutic target (Dimasuay et al., 2016). Similarly, the PE placenta may be responding to the maternal status and upregulating genes involved in lipogenesis. This is similar to the response of the liver during MASLD. Insulin promotes hepatic *de novo* lipogenesis during normal conditions and this is not switched off during insulin resistant states which, accompanied by hyperinsulinemia, promotes exaggerated *de novo* lipogenesis and hepatic steatosis. This thesis has presented human data on the PE placenta that suggests an analogy with the liver in MASLD. Therefore, it could be hypothesised that targeting insulin resistance and hyperlipidaemia in PE could improve the maternal environment and consequently improve placental function and transport to the fetus. Current treatments for patients with MASLD mainly aim to improve insulin sensitivity (Oseini and Sanyal, 2018) which have shown to reduce steatosis. Similar approaches may be suitable to improve placental ectopic fat accumulation in PE.

Other authors have also suggested the benefits of targeting hyperlipidaemia when treating women with GDM (Barrett, et al., 2014). The authors argue that despite the association between hyperlipidaemia and adverse maternal and neonatal outcomes, there are no routine management plans to target lipids during GDM pregnancies, although they suggest that commonly used therapies to lower TG levels in the non-pregnant population may be useful (Barrett et al., 2014).

Nevertheless, this is challenging as the impact of these treatments on the pregnancy or the health of the baby are unknown, and further research should focus on investigating this in both GDM and PE pregnancies.

LC-PUFA status in PE: future investigations

In addition to the elevated *de novo* lipogenesis in the PE placenta, Chapter 5 suggested higher LPL inhibition by the higher expression of its inhibitor *Angtptl4*, although LPL activity was not investigated due to lack of time during this PhD. LPL activity kits can be used for this purpose, although the use of frozen tissue may be challenging due to questions on the activity preservation in the tissue. If future investigations prove lower LPL activity in PE, it may indicate decreased fatty acid uptake by the placenta thereby contributing to the lower LC-PUFA status in PE. Both mother and fetus have decreased plasma LC-PUFA levels during PE (MacKay et al., 2012) which may have an impact on the later-life of the offspring as they are more likely to develop neurodevelopmental disorders such as autism and ADHD. The reasons behind this may involve low synthesis and/or impaired transport to the baby. In Chapter 4 of this thesis, it was hypothesised that LC-PUFAs may be diverted towards storage in the excess placental lipid droplets rather than transported to the fetus, which may present a cause for the lack of benefit from LC-PUFA supplementation in pregnant women. Preliminary data from Brown et al., (2016) showed elevated LC-PUFA fatty acyl chains in the TG fraction of the placenta, which would support the above hypothesis. This theory could not be tested during this thesis, although a model of placental transport was attempted to be developed in order to investigate this. The human BeWo trophoblast cell line, a commonly used *in vitro* model of the placenta, can be fused and differentiated into syncytiotrophoblast cells in order to imitate the trophoblast placental layer (Wice et al., 1990). This model has proven to have similar transport properties to the *ex vivo* perfusion placenta model, although differences in transport rate are observed which are attributable to the presence of the fetal side in the perfused placenta (Poulsen et al., 2009). The BeWo cell model is inarguably useful for the study of molecular pathways involved in placental transport, however, there is a need for the addition of the fetal endothelial barrier to optimise its applications. Other investigators have created a co-culture of BeWo and human umbilical vein endothelial cells (HUVECs) on

Transwells (permeable cell culture inserts) that is suitable for placental transport studies (Wong et al., 2020). Similarly, the creation of a co-culture model of BeWo and human neonatal microvascular endothelial cells (HMVECn) (depicted in Figure 7-1) was attempted but the COVID-19 pandemic and Brexit impeded the delivery of the HMVECn for the duration of this PhD. Preliminary data on the BeWo culture on Transwells was obtained which showed the ability of the BeWo cells to syncytialise thereby showing the suitability to mimic the human placenta. This pilot data suggests that the BeWo model may be relevant when studying transport of LC-PUFAs in PE and further experiments should be carried out in order to optimise this co-culture model and investigate transport using radio-labelled fatty acids under PE-like conditions including low oxygen and high glucose, high insulin, TG and NEFAs.

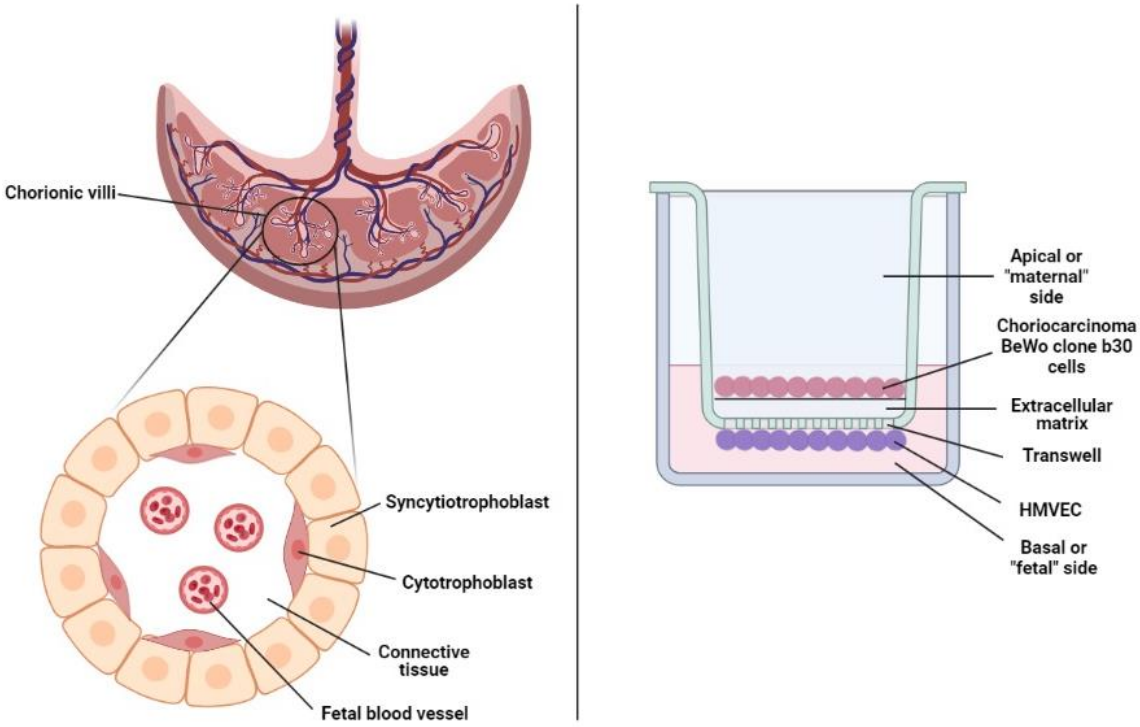

Figure 7-1. Proposed Transwell co-culture placental model. Left panel shows a molecular representation of the chorionic villi present in the placenta. Right panel represents the proposed *in vitro* model of placental transfer that imitates the chorionic villi i.e. the interface between maternal and fetal endothelium. Figure was created with BioRender.com.

The suggested entrapment of LC-PUFAs in the lipid droplets of the PE placenta may affect lipid transport to the baby which can have a deleterious impact on the neurodevelopment of the offspring. Future investigations should focus on testing this, either by MS2 lipidomics analysis or gas chromatography of *ex vivo* placental tissue from PE pregnancies in order to study the accumulation of LC-PUFAs. The use of stable radiolabelled fatty acids could also be useful for investigating the transport or storage in the placenta *in vivo*, as previous studies have used [^{13}C]-

labelled fatty acids to test placental transfer in humans by oral dose prior to delivery (Gil-Sánchez et al., 2010). To our knowledge, these studies have not been performed in pregnant women with PE and therefore this may be a useful method to prove the diversion of LC-PUFAs towards storage rather than transport. If this hypothesis is confirmed, future treatments for PE should focus on improving adipocyte storage capacity and reducing insulin resistance and fatty acid release. This could be done by lifestyle interventions such as diet and exercise, as well as treatment with statins or PPARγ agonists, which are emerging as possible treatments for PE due to their positive impact on lipid metabolism and blood pressure (Ganss, 2017), although drug safety in pregnant women remains to be tested. If the inhibition of maternal synthesis of LC-PUFAs in PE is confirmed, the above interventions could also be complemented by essential fatty acid supplementation during gestation.

In conclusion, the data presented in this thesis suggests that the dysregulation of fatty acid release and ectopic accumulation is important in the pathology of PE. Despite similarities, the pathologies of PE and GDM are different in the way the excess fatty acids are stored. In GDM, VAT appears to act as a buffer for excess fat and therefore there is no or limited spillover to the placenta, whereas in PE, the excess fatty acids are ectopically accumulated in the placenta as VAT does not store them (Figure 7-2). Placental fat accumulation in PE may be a consequence of the impaired maternal adipose tissue storage and/or the elevated lipid synthesis in the placenta as a response to the maternal insulin resistance, and therefore targeting hyperlipidaemia and insulin resistance may improve placental function and neonatal outcomes. The ANGII SHRSP model is, like many other *in vivo* models of PE, unable to mimic the insulin resistance state present in human PE, although it has shown to be useful for investigating the cardiovascular impact in the offspring. The conclusions from this thesis may impact the way the PE and GDM pathologies are considered in the healthcare system and may propose new ways for improving the health of both mother and baby. In addition, it highlights the need for the appropriate monitoring of the offspring born after these pregnancies, which could prevent the development of later-life CVD.

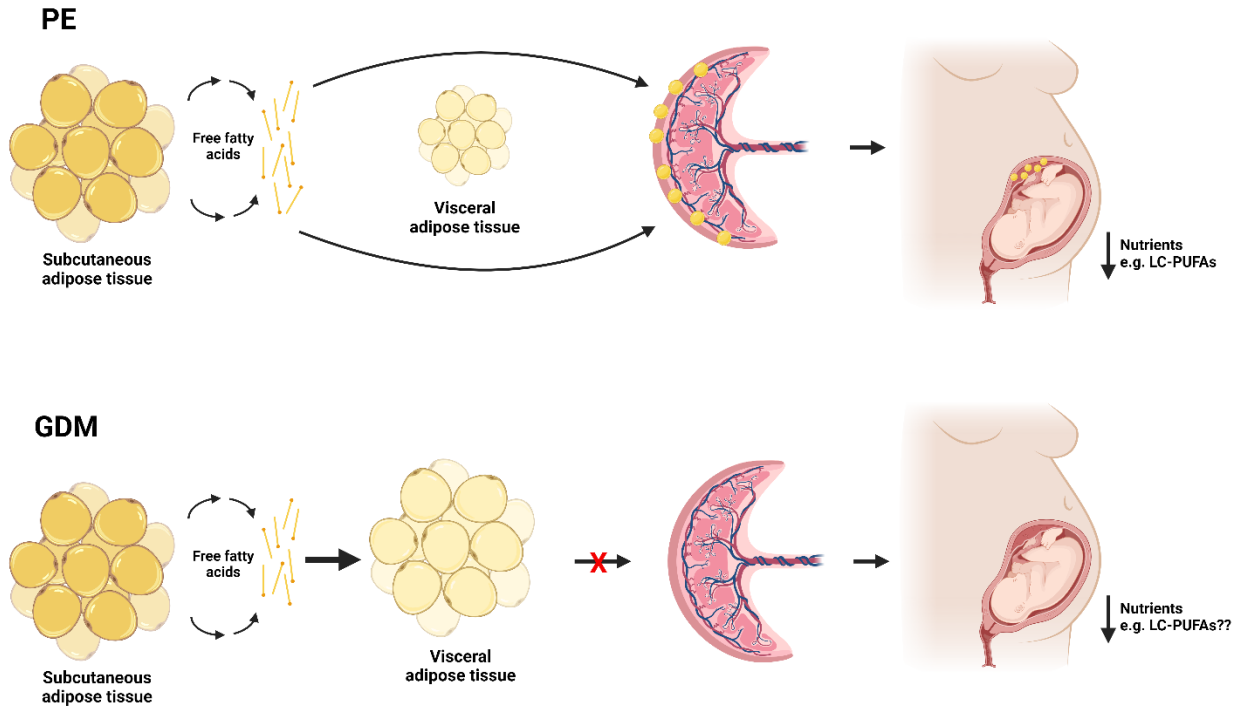

Figure 7-2. Fatty acid accumulation in PE and GDM pregnancies. In PE pregnancies, the excess fatty acids that cannot be stored in the SAT accumulate ectopically in the placenta, which potentially affects transport of essential nutrients to the baby including LC-PUFAs. In GDM pregnancies, the excess fatty acids that cannot be stored in the SAT accumulate in the VAT, which acts as a buffer for this excess. Therefore, there is no ectopic lipid droplet accumulation in the GDM placenta, although whether the transport of LC-PUFAs to the baby is affected is yet to be elucidated.

List of References

AbdAlla, S., Lother, H., El Massiery, A. and Quitterer, U. 2001. Increased AT1 receptor heterodimers in preeclampsia mediate enhanced angiotensin II responsiveness. *Nature Medicine*. **7**(9), pp.1003–1009.

Van Abeelen, A.F.M., De Rooij, S.R., Osmond, C., Painter, R.C., Veenendaal, M.V.E., Bossuyt, P.M.M., Elias, S.G., Grobbee, D.E., Van Der Schouw, Y.T., Barker, D.J.P. and Roseboom, T.J. 2011. The sex-specific effects of famine on the association between placental size and later hypertension. *Placenta*. **32**(9), pp.694–698.

Ailhaud, G., Grimaldi, P. and Négrel, R. 1992. Cellular and Molecular Aspects of Adipose Tissue Development. *Annual Review of Nutrition*. **12**, pp.207–233.

Al, M.D.M., Van Houwelingen, A.C. and Hornstra, G. 2000. Long-chain polyunsaturated fatty acids, pregnancy, and pregnancy outcome. *American Journal of Clinical Nutrition*. **71**(1 SUPPL.), pp.285S-291S.

Alexander, B.T. 2003. Placental insufficiency leads to development of hypertension in growth-restricted offspring. *Hypertension*. **41**(3), pp.457–462.

Alkemade, F.E., Gittenberger-De Groot, A.C., Schiel, A.E., VanMunsteren, J.C., Hogers, B., Van Vliet, L.S.J., Poelmann, R.E., Havekes, L.M., Van Dijk, K.W. and DeRuiter, M.C. 2007. Intrauterine exposure to maternal atherosclerotic risk factors increases the susceptibility to atherosclerosis in adult life. *Arteriosclerosis, Thrombosis, and Vascular Biology*. **27**(10), pp.2228–2235.

Alsnes, I. V, Vatten, L.J., Fraser, A., Bjørngaard, J.H., Rich-edwards, J., Romundstad, P.R., Åsvold, B.O. and Commentary, S.E. 2017. Hypertension in Pregnancy and Offspring Cardiovascular Risk in Young Adulthood. *Hypertension*. **69**, pp.591–598.

Alvarez, J.J., Montelongo, A., Iglesias, A., Lasunción, M.A. and Herrera, E. 1996. Longitudinal study on lipoprotein profile, high density lipoprotein subclass, and postheparin lipases during gestation in women. *Journal of Lipid Research*. **37**(2), pp.299–308.

Amann, K., Gharehbaghi, H., Stephan, S. and Mall, G. 1995. Hypertrophy and hyperplasia of smooth muscle cells of small intramyocardial arteries in spontaneously hypertensive rats. *Hypertension*. **25**(1), pp.124–131.

Amin, N.B., Carvajal-Gonzalez, S., Purkal, J., Zhu, T., Crowley, C., Perez, S., Chidsey, K., Kim, A.M. and Goodwin, B. 2019. Targeting diacylglycerol acyltransferase 2 for the treatment of nonalcoholic steatohepatitis. *Science Translational Medicine*. **11**(520), p.eaav9701.

Anderson, C.M., Lopez, F., Zimmer, A. and Benoit, J.N. 2006. Placental insufficiency leads to developmental hypertension and mesenteric artery dysfunction in two generations of Sprague-Dawley rat offspring. *Biology of Reproduction*. **74**(3), pp.538–544.

Araújo, J.R., Correia-Branco, A., Ramalho, C., Keating, E. and Martel, F. 2013. Gestational diabetes mellitus decreases placental uptake of long-chain polyunsaturated fatty acids: Involvement of long-chain acyl-CoA synthetase. *Journal of Nutritional Biochemistry*. **24**(10), pp.1741–1750.

Aye, C.Y.L., Lewandowski, A.J., Lamata, P., Upton, R., Davis, E., Ohuma, E.O., Kenworthy, Y., Boardman, H., Frost, A.L., Adwani, S., McCormick, K. and Leeson, P. 2020. Prenatal and postnatal cardiac development in offspring of hypertensive pregnancies. *Journal of the American Heart Association*. **9**(9), p.e014586.

Barker, D. and Osmond, C. 1988. Low birth weight and hypertension. *BMJ*.

297(6641), pp.134–135.
Barker, D.J.., Osmond, C., Winter, P.., Margetts, B. and Simmonds, S.. 1989. Weight in infancy and death from ischaemic heart disease. *The Lancet*. **334**(8663), pp.577–580.
Barker, D.J.P. 1998. In utero programming of chronic disease. *Clinical Science*. **95**(2), p.115.
Barker, D.J.P. 2007. The origins of the developmental origins theory. *Journal of Internal Medicine*. **261**(5), pp.412–417.
Barrett, H.L., Kubala, M.H., Scholz Romero, K., Denny, K.J., Woodruff, T.M., McIntyre, H.D., Callaway, L.K. and Dekker Nitert, M. 2015. Placental lipase expression in pregnancies complicated by preeclampsia: A case-control study. *Reproductive Biology and Endocrinology*. **13**(1), pp.1–9.
Barrett, H.L., Kubala, M.H., Scholz Romero, K., Denny, K.J., Woodruff, T.M., McIntyre, H.D., Callaway, L.K. and Nitert, M.D. 2014. Placental lipases in pregnancies complicated by gestational diabetes mellitus (GDM). *PLoS ONE*. **9**(8), pp.1–8.
Barrett, H.L., Nitert, M.D., McIntyre, H.D. and Callaway, L.K. 2014. Normalizing metabolism in diabetic pregnancy: Is it time to target lipids? *Diabetes Care*. **37**(5), pp.1484–1493.
Bateson, P., Barker, D., Clutton-Brock, T., Deb, D., D'Udine, B., Foley, R.A., Gluckman, P., Godfrey, K., Kirkwood, T., Lahr, M.M., McNamara, J., Metcalfe, N.B., Monaghan, P., Spencer, H.G. and Sultan, S.E. 2004. Developmental plasticity and human health. *Nature*. **430**(6998), pp.419–421.
Beckers, K.F., Gomes, V.C.L., Crissman, K.J.R., Adams, D.M., Liu, C.C., Del Piero, F., Butler, S.D. and Sones, J.L. 2021. Cardiometabolic Phenotypic Differences in Male Offspring Born to Obese Preeclamptic-Like BPH/5 Mice. *Frontiers in Pediatrics*. **9**(September), pp.1–9.
Bellos, I., Pergialiotis, V. and Papapanagiotou, A. 2020. Systematic Reviews Comparative efficacy and safety of oral antihypertensive agents in pregnant women with chronic hypertension : a network metaanalysis. *The American Journal of Obstetrics & Gynecology*. **223**(4), pp.525–537.
Benyo, D.F., Smarason, A., Redman, C.W.G., Sims, C. and Conrad, K.P. 2001. Expression of inflammatory cytokines in placentas from women with preeclampsia. *Journal of Clinical Endocrinology and Metabolism*. **86**(6), pp.2505–2512.
Benyshek, D.C., Johnston, C.S. and Martin, J.F. 2006. Glucose metabolism is altered in the adequately-nourished grand-offspring (F3 generation) of rats malnourished during gestation and perinatal life [5]. *Diabetologia*. **49**(5), pp.1117–1119.
Berenguer, M. and Duester, G. 2022. Retinoic acid, RARs and early development. *Journal of Molecular Endocrinology*. **69**(4), pp.T59–T67.
van den Berg, R.A., Hoefsloot, H.C.J., Westerhuis, J.A., Smilde, A.K. and van der Werf, M.J. 2006. Centering, scaling, and transformations: Improving the biological information content of metabolomics data. *BMC Genomics*. **7**, pp.1–15.
Bergen, W.G. and Mersmann, H.J. 2005. Comparative aspects of lipid metabolism: Impact on contemporary research and use of animal models. *Journal of Nutrition*. **135**(11), pp.2499–2502.
Bianco, M.E. and Josefson, J.L. 2019. Hyperglycemia During Pregnancy and Long-Term Offspring Outcomes. *Curr Diab Rep*. **19**(12), pp.139–148.
Bildirici, I., Schaiff, W.T., Chen, B., Morizane, M., Oh, S.Y., O'Brien, M., Sonnenberg-Hirche, C., Chu, T., Barak, Y., Nelson, D.M. and Sadovsky, Y.

2018. PLIN2 Is Essential for Trophoblastic Lipid Droplet Accumulation and Cell Survival during Hypoxia. *Endocrinology*. **159**(12), pp.3937–3949.

Biron-Shental, T., Schaiff, W.T., Ratajczak, C.K., Bildirici, I., Nelson, D.M. and Sadovsky, Y. 2007. Hypoxia regulates the expression of fatty acid-binding proteins in primary term human trophoblasts. *American Journal of Obstetrics and Gynecology*. **197**(5), 516.e1-516.e6.

Bitsanis, D., Ghebremeskel, K., Moodley, T., Crawford, M.A. and Djahanbakhch, O. 2006. Gestational diabetes mellitus enhances arachidonic and docosahexaenoic acids in placental phospholipids. *Lipids*. **41**(4), pp.341–346.

Boeldt, D. and Bird, I. 2017. Vascular adaptation in pregnancy and endothelial dysfunction in preeclampsia. *The Journal of Endocrinology*. **232**(1), pp.R27–R44.

Boneh, H.R., Pariente, G., Baumfeld, Y., Yohay, D., Rotem, R. and Weintraub, A.Y. 2022. Superimposed versus de novo pre-eclampsia: Is there a difference? *International Journal of Gynecology and Obstetrics*. **159**(2), pp.392–397.

Braunthal, S. and Brateanu, A. 2019. Hypertension in pregnancy: Pathophysiology and treatment. *SAGE Open Medicine*. **7**, pp.1–15.

Bray, G.A., Jablonski, K.A., Fujimoto, W.Y., Barrett-Connor, E., Haffner, S., Hanson, R.L., Hill, J.O., Hubbard, V., Kriska, A., Stamm, E. and Pi-Sunyer, F.X. 2008. Relation of central adiposity and body mass index to the development of diabetes in the Diabetes Prevention Program. *American Journal of Clinical Nutrition*. **87**(5), pp.1212–1218.

Bridges, J.P., Gilbert, J.S., Colson, D., Gilbert, S.A., Dukes, M.P., Ryan, M.J. and Granger, J.P. 2009. Oxidative stress contributes to soluble fms-like tyrosine kinase-1 induced vascular dysfunction in pregnant rats. *American Journal of Hypertension*. **22**(5), pp.564–568.

British Heart Foundation 2024. *Heart and Circulatory Disease Statistics 2021* [Online]. Available from: https://www.bhf.org.uk/what-we-do/our-research/heart-statistics/heart-statistics-publications/cardiovascular-disease-statistics-2021%0Ahttps://www.bhf.org.uk/what-we-do/our-research/heart-statistics/heart-statistics-publications/cardiovascular-disease-sta.

Brown, M.A., Magee, L.A., Kenny, L.C., Karumanchi, S.A., Mccarthy, F.P., Saito, S., Hall, D.R., Warren, C.E., Adoyi, G. and Ishaku, S. 2018. Hypertensive Disorders of Pregnancy. *Hypertension*. **72**, pp.24–43.

Brown, M.S. and Goldstein, J.L. 2008. Selective versus Total Insulin Resistance: A Pathogenic Paradox. *Cell Metabolism*. **7**(2), pp.95–96.

Brown, S.H.J., Eather, S.R., Freeman, D.J., Meyer, B.J. and Mitchell, W. 2016. A Lipidomic Analysis of Placenta in Preeclampsia: Evidence for Lipid Storage. *PLoS ONE*. **11**(9), pp.1–13.

Buchanan, T.A. and Xiang, A.H. 2005. Gestational diabetes mellitus. *J Clin Invest*. **115**(3), pp.485–491.

Buck, C. and Simpson, H. 1982. Infant diarrhoea and subseqeunt mortality from heart disease and cancer. *Journal of Epidemiology and Community Health*. **36**(1), pp.27–30.

Buckingham, M., Meilhac, S. and Zaffran, S. 2005. Building the mammalian heart from two sources of myocardial cells. *Nature Reviews Genetics*. **6**(11), pp.826–835.

Buelke-Sam, J., Nelson, C.J., Byrd, R.A. and Holson, J.F. 1982. Blood flow during pregnancy in the rat: I. Flow patterns to maternal organs. *Teratology*. **26**(3), pp.269–277.

Burchakov, D.I., Kuznetsova, I. V and Uspenskaya, Y.B. 2017. Omega-3 Long-Chain Polyunsaturated Fatty Acids and Preeclampsia : Trials Say “No”, but Is It the Final Word? *Nutrients*. **9**(12), p.1364.

Burzynska-Pedziwiatr, I., Dudzik, D., Sansone, A., Malachowska, B., Zieleniak, A., Zurawska-Klis, M., Ferreri, C., Chatgilialoglu, C., Cypryk, K., Wozniak, L.A., Markuszewski, M.J. and Bukowiecka-Matusiak, M. 2023. Targeted and untargeted metabolomic approach for GDM diagnosis. *Frontiers in Molecular Biosciences*. **9**(January), pp.1–14.

Byrne, M.M., O’Meara, J.S.N.M. and Polonsky, K.S. 1995. Insulin secretion in insulin-resistant women with a history of gestational diabetes. *Metabolism*. **44**(8), pp.1067–1073.

Campbell, F.M., Clohessy, A.M., Gordon, M.J., Page, K.R. and Dutta-Roy, A.K. 1997. Uptake of long chain fatty acids by human placental choriocarcinoma (BeWo) cells: Role of plasma membrane fatty acid-binding protein. *Journal of Lipid Research*. **38**(12), pp.2558–2568.

Carlos A. Labarrere, Hector L. DiCarlo, M., Bammerlin, E., Hardin, J.W., Yeon Mee Kim, M., Chaemsaithong, P., Haas, D.M., Kassab, G.S. and Romero, R. 2017. *Failure of physiologic transformation of spiral arteries, endothelial and trophoblast cell activation, and acute atherosis in the basal plate of the placenta*.

Carmiel Haggai, M., Sgayer, I., Bornstein, J., Odeh, M., Lowenstein, L. and Frank Wolf, M. 2022. Liver stiffness and steatosis in preeclampsia as shown by transient elastography–a prospective cohort study. *American Journal of Obstetrics and Gynecology*. **227**(3), 515.e1-515.e9.

Carreras-Badosa, G., Prats-Puig, A., Puig, T., Vázquez-Ruíz, M., Bruel, M., Mendoza, E., De Zegher, F., Ibáñez, L., López-Bermejo, A. and Bassols, J. 2016. Circulating Fatty Acid Synthase in pregnant women: Relationship to blood pressure, maternal metabolism and newborn parameters. *Scientific Reports*. **6**(August 2015), pp.1–8.

Catalano, P.M. 2010. The impact of gestational diabetes and maternal obesity on the mother and her offspring. *Journal of Developmental Origins of Health and Disease*. **1**(4), pp.208–215.

Catalano, P.M. 2013. Trying to understand gestational diabetes. *Diabetic Medicine*. **31**(3), pp.273–281.

Catalano, P.M. and Hauguel-De Mouzon, S. 2011. Is it time to revisit the Pedersen hypothesis in the face of the obesity epidemic? *American Journal of Obstetrics and Gynecology*. **204**(6), pp.479–487.

Catalano, P.M., Thomas, A. and Huston-presley, L. 2003. Increased fetal adiposity: A very sensitive marker of abnormal in utero development. *American Journal of Obstetrics and Gynecology*. **189**(6), pp.1698–1704.

Catalano, P.M., Tyzbir, E.D., Roman, N.M., Amini, S.B. and Sims, E.A.H. 1991. Longitudinal changes in insulin release and insulin resistance in nonobese pregnant women. *American Journal of Obstetrics and Gynecology*. **165**(6), pp.1667–1672.

Caton, A.R., Bell, E.M., Druschel, C.M., Werler, M.M., Lin, A.E., Browne, M.L., Mcnutt, L., Romitti, P.A., Mitchell, A.A. and Olney, R.S. 2009. Antihypertensive Medication Use During Pregnancy and the Risk of Cardiovascular Malformations. *Hypertension*. **54**(1), pp.63–70.

Chahoud, I. and Paumgartten, F.J.R. 2009. Influence of litter size on the postnatal growth of rat pups: is there a rationale for litter-size standardization in toxicity studies? *Environmental research*. **109**(8), pp.1021–1027.

Challier, J.C., Basu, S., Bintein, T., Minium, J., Hotmire, K., Catalano, P.M. and Mouzon, S.H. 2008. Obesity in Pregnancy Stimulates Macrophage Accumulation and Inflammation in the Placenta. *Placenta*. **29**, pp.274–281.

Chassen, S.S., Ferchaud-Roucher, V., Gupta, M.B., Jansson, T. and Powell, T.L. 2018. Alterations in placental long chain polyunsaturated fatty acid metabolism in human intrauterine growth restriction. *Clinical Science*. **132**(5), pp.595–607.

Chassen, S.S., Ferchaud-Roucher, V., Palmer, C., Li, C., Jansson, T., Nathanielsz, P.W. and Powell, T.L. 2020. Placental fatty acid transport across late gestation in a baboon model of intrauterine growth restriction. *Journal of Physiology*. **598**(12), pp.2469–2489.

Chen, L., Mir, S.A., Bendt, A.K., Chua, E.W.L., Narasimhan, K., Tan, K.M.L., Loy, S.L., Tan, K.H., Shek, L.P., Chan, J., Yap, F., Meaney, M.J., Chan, S.Y., Chong, Y.S., Gluckman, P.D., Eriksson, J.G., Karnani, N. and Wenk, M.R. 2023. Plasma lipidomic profiling reveals metabolic adaptations to pregnancy and signatures of cardiometabolic risk: a preconception and longitudinal cohort study. *BMC Medicine*. **21**(1), pp.1–24.

Chen, P., Piaggi, P., Traurig, M., Bogardus, C., Knowler, W.C., Baier, L.J. and Hanson, R.L. 2017. Differential methylation of genes in individuals exposed to maternal diabetes in utero. *Diabetologia*. **60**(4), pp.645–655.

Chung, S., Dzeja, P.P., Faustino, R.S., Perez-Terzic, C., Behfar, A. and Terzic, A. 2007. Mitochondrial oxidative metabolism is required for the cardiac differentiation of stem cells. *Nature Clinical Practice Cardiovascular Medicine*. **4**(SUPPL. 1), pp.60–67.

Cianni, G. Di, Miccoli, R., Volpe, L., Lencioni, C., Ghio, A., Giovannitti, M.G., Cuccuru, I., Pellegrini, G., Chatzianagnostou, K., Boldrini, A. and Prato, S. Del 2005. Maternal triglyceride levels and newborn weight in pregnant women with normal glucose tolerance. *Diabetes/Metabolism Research and Reviews*. **25**, pp.21–25.

Cindrova-Davies, T. and Sferruzzi-Perri, A.N. 2022. Human placental development and function. *Seminars in Cell and Developmental Biology*. **131**(April), pp.66–77.

Clark, T., Parsons, A. and Sorenson, L. 1992. Adaptation of islets of Langerhans to pregnancy increased islet cell proliferation and insulin secretion correlates with the onset of placental lactogen secretion. *Endocrinology*. **130**(3), pp.1459–1466.

Claycombe, K.J., Jones, B.H., Standridge, M.K., Guo, Y., Chun, J.T., Taylor, J.W. and Moustaïd-Moussa, N. 1998. Insulin increases fatty acid synthase gene transcription in human adipocytes. *American Journal of Physiology - Regulatory Integrative and Comparative Physiology*. **274**(5 43-5), pp.1253–1259.

Cleal, J.K., Day, P., Hanson, M.A. and Lewis, R.M. 2009. Measurement of Housekeeping Genes in Human Placenta. *Placenta*. **30**(11), pp.1002–1003.

Coetzee, E.J., Dommisse, J. and Anthony, J. 1998. A randomised controlled trial of intravenous magnesium sulphate versus placebo in the management of women with severe pre-eclampsia. *British Journal of Obstetrics and Gynaecology*. **105**, pp.300–303.

Cohen, E., Wong, F.Y., Horne, R.S.C. and Yiallourou, S.R. 2016. Intrauterine growth restriction: Impact on cardiovascular development and function throughout infancy. *Pediatric Research*. **79**(6), pp.821–830.

Collins, R.T., Yang, W., Carmichael, S.L., Bolin, E.H., Nembhard, W.N. and Shaw, G.M. 2020. Maternal dietary fat intake and the risk of congenital

heart defects in offspring. *Pediatric Research*. **88**(5), pp.804–809.
Colombo, J., Kannass, K.N., Shaddy, D.J., Kundurthi, S., Maikranz, J.M., Anderson, C.J., Blaga, O.M. and Carlson, S.E. 2004. Maternal DHA and the development of attention in infancy and toddlerhood. *Child Development*. **75**(4), pp.1254–1267.
Coutinho, T., Goel, K., Corrêa De S, D., Kragelund, C., Kanaya, A.M., Zeller, M., Park, J.S., Kober, L., Torp-Pedersen, C., Cottin, Y., Lorgis, L., Lee, S.H., Kim, Y.J., Thomas, R., Roger, V.L., Somers, V.K. and Lopez-Jimenez, F. 2011. Central obesity and survival in subjects with coronary artery disease: A systematic review of the literature and collaborative analysis with individual subject data. *Journal of the American College of Cardiology*. **57**(19), pp.1877–1886.
Crowther, N.J., Cameron, N., Trusler, J. and Gray, I.P. 1998. Association between poor glucose tolerance and rapid post natal weight gain in seven-year-old children. *Diabetologia*. **41**(10), pp.1163–1167.
Dancis, J., Jansen, V. and Kayden, H.J. 1973. Transfer Across Perfused Human Placenta. II. Free Fatty Acids. *Pediatr Res*. **7**, pp.192–197.
Davis, Esther Frances, Lazdam, M., Lewandowski, A.J., Worton, S.A., Kelly, B., Kenworthy, Y., Adwani, S., Wilkinson, A.R., McCormick, K., Sargent, I., Redman, C. and Leeson, P. 2012. Cardiovascular risk factors in children and young adults born to preeclamptic pregnancies: A systematic review. *Pediatrics*. **129**(6).
Davis, E.F., Lewandowski, A.J., Aye, C., Williamson, W., Boardman, H., Huang, R.C., Mori, T.A., Newnham, J., Beilin, L.J. and Leeson, P. 2015. Clinical cardiovascular risk during young adulthood in offspring of hypertensive pregnancies: Insights from a 20-year prospective follow-up birth cohort. *BMJ Open*. **5**(6), pp.1–8.
Davis, Esther F., Newton, L., Lewandowski, A.J., Lazdam, M., Kelly, B.A., Kyriakou, T. and Leeson, P. 2012. Pre-eclampsia and offspring cardiovascular health: Mechanistic insights from experimental studies. *Clinical Science*. **123**(2), pp.53–72.
Desoye, G. and Herrera, E. 2021. Adipose tissue development and lipid metabolism in the human fetus: The 2020 perspective focusing on maternal diabetes and obesity. *Progress in Lipid Research*. **81**, p.101082.
Dimasuay, K.G., Boeuf, P., Powell, T.L., Jansson, T., Thompson, L.P. and Jansson, T. 2016. Placental Responses to Changes in the Maternal Environment Determine Fetal Growth. . **7**(January), pp.1–9.
Drolet, R., Richard, C., Sniderman, A.D., Mailloux, J., Fortier, M., Huot, C., Rhéaume, C. and Tchernof, A. 2008. Hypertrophy and hyperplasia of abdominal adipose tissues in women. *International Journal of Obesity*. **32**(2), pp.283–291.
Dubé, E., Ethier-Chiasson, M. and Lafond, J. 2013. Modulation of cholesterol transport by insulin-treated gestational diabetes mellitus in human full-term placenta. *Biology of Reproduction*. **88**(1), pp.1–10.
Dunlop, M. and Court, J.M. 1978. Lipogenesis in Developing Fetal Tissue. *Early Human Development*. **2**(2), pp.123–130.
Duttaroy, A.K. and Basak, S. 2020. Maternal dietary fatty acids and their roles in human placental development. *Prostaglandins Leukotrienes and Essential Fatty Acids*. **155**(February), p.102080.
Duttaroy, A.K. and Basak, S. 2022. Maternal Fatty Acid Metabolism in Pregnancy and Its Consequences in the Feto-Placental Development. *Frontiers in Physiology*. **12**(January), pp.1–16.

Elahi, M.M., Cagampang, F.R., Mukhtar, D., Anthony, F.W., Ohri, S.K. and Hanson, M.A. 2009. Long-term maternal high-fat feeding from weaning through pregnancy and lactation predisposes offspring to hypertension, raised plasma lipids and fatty liver in mice. *British Journal of Nutrition*. **102**(4), pp.514–519.

Ellul, S., Ponsonby, A.L., Carlin, J.B., Collier, F., Mansell, T., Vuillermin, P., Burgner, D., Saffery, R., Allen, K., Tang, M., Ranganathan, S., Dwyer, T. and Sly, P. 2020. Sex differences in infant blood metabolite profile in association with weight and adiposity measures. *Pediatric Research*. **88**(3), pp.473–483.

Ellul, S., Wake, M., Clifford, S.A., Lange, K., Würtz, P., Juonala, M., Dwyer, T., Carlin, J.B., Burgner, D.P. and Saffery, R. 2019. Metabolomics: Population epidemiology and concordance in Australian children aged 11-12 years and their parents. *BMJ Open*. **9**, pp.106–117.

Enquobahrie, D.A., Williams, M.A., Butler, C.L., Frederick, I.O., Miller, R.S. and Luthy, D.A. 2004. Maternal plasma lipid concentrations in early pregnancy and risk of preeclampsia. *American Journal of Hypertension*. **17**(7), pp.574–581.

Eriksson, J.G., Forsén, T., Tuomilehto, J., Winter, P.D., Osmond, C. and Barker, D.J.P. 1999. Catch-up growth in childhood and death from coronary heart disease: Longitudinal study. *British Medical Journal*. **318**(7181), pp.427–431.

Erion, D.M. and Shulman, G.I. 2010. Diacylglycerol-mediated insulin resistance. *Nature Medicine*. **16**(4), pp.400–402.

Faas, M.M. and De Vos, P. 2018. Innate immune cells in the placental bed in healthy pregnancy and preeclampsia. *Placenta*. **69**(April), pp.125–133.

Fabbrini, E., Magkos, F., Mohammed, B.S., Pietka, T., Abumrad, N.A., Patterson, B.W., Okunade, A. and Klein, S. 2009. Intrahepatic fat, not visceral fat, is linked with metabolic complications of obesity. *Proceedings of the National Academy of Sciences of the United States of America*. **106**(36), pp.15430–15435.

Farrar, D., Simmonds, M., Griffin, S., Duarte, A., Lawlor, D., Sculpher, M., Fairley, L., Golder, S., Tuffnell, D., Bland, M., Dunne, F., Whitelaw, D., Wright, J. and Sheldon, T. 2016. The identification and treatment of women with hyperglycaemia in pregnancy: an analysis of individual participant data, systematic reviews, meta-analyses and an economic evaluation. *Health Technol Assess*. **20**(86), pp.47–54.

Feig, D.S. and Moses, R.G. 2011. Metformin Therapy During Pregnancy: Good for the goose and good for the gosling too? *Diabetes Care*. **34**(10), pp.2329–2330.

Firoz, T., Magee, L.A., Macdonell, K., Payne, B.A., Gordon, R., Vidler, M. and Dadelszen, P. Von 2014. Oral antihypertensive therapy for severe hypertension in pregnancy and postpartum: a systematic review. *BJOG*. **121**, pp.1210–1218.

Forbes, S., Taylor-Robinson, S.D., Patel, N., Allan, P., Walker, B.R. and Johnston, D.G. 2011. Increased prevalence of non-alcoholic fatty liver disease in European women with a history of gestational diabetes. *Diabetologia*. **54**(3), pp.641–647.

Forsdahl, A. 1977. Are poor living conditions in childhood and adolescence an important risk factor for arteriosclerotic heart disease? *British Journal of Preventive and Social Medicine*. **31**(2), pp.91–95.

Freeman, D.J., Mcmanus, F., Brown, E.A., Cherry, L., Norrie, J., Ramsay, J.E., Clark, P., Walker, I.D., Sattar, N. and Greer, I.A. 2004. Short- and Long-

Term Changes in Plasma Inflammatory Markers Associated With Preeclampsia. *Hypertension*. **44**(5), pp.708–714.
Fugelseth, D., Ramstad, H.B., Kvehaugen, A.S., Nestaas, E., Støylen, A. and Staff, A.C. 2011. Myocardial function in offspring 5-8years after pregnancy complicated by preeclampsia. *Early Human Development*. **87**(8), pp.531–535.
Fujimaki, A., Watanabe, K., Mori, T., Kimura, C., Shinohara, K. and Wakatsuki, A. 2011. Placental oxidative DNA damage and its repair in preeclamptic women with fetal growth restriction. *Placenta*. **32**(5), pp.367–372.
Furse, S., Koulman, A., Ozanne, S.E., Poston, L., White, S.L. and Meek, C.L. 2022. Altered Lipid Metabolism in Obese Women With Gestational Diabetes and Associations With Offspring Adiposity. *Journal of Clinical Endocrinology and Metabolism*. **107**(7), pp.E2825–E2832.
Furse, S., White, S.L., Meek, C.L., Jenkins, B., Petry, C.J., Vieira, M.C., Ozanne, S.E., Dunger, D.B., Poston, L. and Koulman, A. 2019. Altered triglyceride and phospholipid metabolism predates the diagnosis of gestational diabetes in obese pregnancy. *Molecular Omics*. **15**(6), pp.420–430.
Furukawa, S., Kuroda, Y. and Sugiyama, A. 2014. A comparison of the histological structure of the placenta in experimental animals. *Journal of Toxicologic Pathology*. **27**(1), pp.11–18.
Gaggini, M., Morelli, M., Buzzigoli, E., DeFronzo, R.A., Bugianesi, E. and Gastaldelli, A. 2013. Non-alcoholic fatty liver disease (NAFLD) and its connection with insulin resistance, dyslipidemia, atherosclerosis and coronary heart disease. *Nutrients*. **5**(5), pp.1544–1560.
Gallo, L.A., Barrett, H.L. and Dekker Nitert, M. 2017. Review: Placental transport and metabolism of energy substrates in maternal obesity and diabetes. *Placenta*. **54**, pp.59–67.
Ganss, R. 2017. Maternal Metabolism and Vascular Adaptation in Pregnancy: The PPAR Link. *Trends in Endocrinology and Metabolism*. **28**(1), pp.73–84.
Gatford, K.L., Andraweera, P.H., Roberts, C.T. and Care, A.S. 2020. Animal Models of Preeclampsia: Causes, Consequences, and Interventions. *Hypertension*. **75**(6), pp.1363–1381.
Gerdts, E., Izzo, R., Mancusi, C., Losi, M.A., Manzi, M.V., Canciello, G., De Luca, N., Trimarco, B. and de Simone, G. 2018. Left ventricular hypertrophy offsets the sex difference in cardiovascular risk (the Campania Salute Network). *International Journal of Cardiology*. **258**, pp.257–261.
Ghasemi, Asghar; Sajad, J.K.K. 2021. The laboratory rat: age and body weight matter. *EXCLI Journal*. **2005**(20), pp.1431–1445.
Gil-Sánchez, A., Larqué, E., Demmelmair, H., Acien, M.I., Faber, F.L., Parrilla, J.J. and Koletzko, B. 2010. Maternal-fetal in vivo transfer of [13C]docosahexaenoic and other fatty acids across the human placenta 12 h after maternal oral intake. *American Journal of Clinical Nutrition*. **92**(1), pp.115–122.
Gilbert, J., Dukes, M., LaMarca, B., Cockrell, K., Babcock, S. and Granger, J. 2007. Effects of Reduced Uterine Perfusion Pressure on Blood Pressure and Metabolic Factors in Pregnant Rats. *American Journal of Hypertension*. **20**(6), pp.686–691.
Gillis, E.E., Williams, J.M., Garrett, M.R., Mooney, J.N. and Sasser, J.M. 2015. The Dahl salt-sensitive rat is a spontaneous model of superimposed preeclampsia. *American Journal of Physiology - Regulatory Integrative and Comparative Physiology*. **309**(1), pp.R62–R70.
Giommi, C., Lombó, M., Montik, N., Paolucci, M., Notarstefano, V., Delli Carpini,

G., Ciavattini, A., Ragusa, A., Maradonna, F., Giorgini, E. and Carnevali, O. 2023. Gestational Diabetes Mellitus and Small-for-Gestational-Age: An Insight into the Placental Molecular Biomarkers. *International Journal of Molecular Sciences*. **24**(3).

De Giuseppe, R., Roggi, C. and Cena, H. 2014. n-3 LC-PUFA supplementation: Effects on infant and maternal outcomes. *European Journal of Nutrition*. **53**(5), pp.1147–1154.

Gluckman, P.D., Hanson, M.A., Cooper, C. and Thornburg, K.L. 2008. Effect of In Utero and Early-Life Conditions on Adult Health and Disease. *New England Journal of Medicine*. **359**(1), pp.61–73.

Godfrey, K.M., Costello, P.M. and Lillycrop, K.A. 2015. The developmental environment, epigenetic biomarkers and long-term health. *Journal of Developmental Origins of Health and Disease*. **6**(5), pp.399–406.

Godfrey, K.M., Sheppard, A., Gluckman, P.D., Lillycrop, K.A., Burdge, G.C., McLean, C., Rodford, J., Slater-Jefferies, J.L., Garratt, E., Crozier, S.R., Emerald, B.S., Gale, C.R., Inskip, H.M., Cooper, C. and Hanson, M.A. 2011. Epigenetic gene promoter methylation at birth is associated with child's later adiposity. *Diabetes*. **60**(5), pp.1528–1534.

Gopalakrishnan, K., Mishra, J.S., Ross, J.R., Abbott, D.H. and Kumar, S. 2022. Hyperandrogenism diminishes maternal-fetal fatty acid transport by increasing FABP4-mediated placental lipid accumulation. *Biology of Reproduction*. **107**(2), pp.514–528.

Guénard, F., Deshaies, Y., Cianflone, K., Kral, J.G., Marceau, P. and Vohl, M.C. 2013. Differential methylation in glucoregulatory genes of offspring born before vs. after maternal gastrointestinal bypass surgery. *Proceedings of the National Academy of Sciences of the United States of America*. **110**(28), pp.11439–11444.

Guglielmi, V. and Sbraccia, P. 2018. Obesity phenotypes: Depot-differences in adipose tissue and their clinical implications. *Eating and Weight Disorders*. **23**(1), pp.3–14.

Gutiérrez-Arzapalo, P.Y., Rodríguez-Rodríguez, P., Ramiro-Cortijo, D., López de Pablo, Á.L., López-Giménez, M.R., Condezo-Hoyos, L., Greenwald, S.E., González, M. del C. and Arribas, S.M. 2018. Role of fetal nutrient restriction and postnatal catch-up growth on structural and mechanical alterations of rat aorta. *Journal of Physiology*. **596**(23), pp.5791–5806.

Hadders-algra, M. 2008. Prenatal long-chain polyunsaturated fatty acid status : the importance of a balanced intake of docosahexaenoic acid and arachidonic acid. *J. Perinat. Med.* **36**, pp.101–109.

Hadders-Algra, M., Bouwstra, H., Van Goor, S.A., Dijck-Brouwer, D.A.J. and Muskiet, F.A.J. 2007. Prenatal and early postnatal fatty acid status and neurodevelopmental outcome. *Journal of Perinatal Medicine*. **35**(SUPPL. 1), pp.28–34.

Haggarty, P. 2004. Effect of placental function in fatty acid requirements during pregnancy. *European Journal of Clinical Nutrition*. **58**(12), pp.1559–1570.

Haggarty, P., Ashton, J., Joynson, M., Abramovich, D.R. and Page, K. 1999. Effect of maternal polyunsaturated fatty acid concentration on transport by the human placenta. *Biology of the Neonate*. **75**(6), pp.350–359.

Hales, C.N. and Barker, D.J.P. 1992. Type 2 (non-insulin-dependent) diabetes mellitus: the thrifty phenotype hypothesis. *Diabetologia*. **35**(7), pp.595–601.

Hayashi, M., Hoshimoto, K., Ohkura, T. and Inaba, N. 2002. Increased levels of macrophage colony-stimulating factor in the placenta and blood in preeclampsia. *American Journal of Reproductive Immunology*. **47**(1), pp.19–

24.
Heath, R.J. and Klevebro, S. 2022. Maternal and Neonatal Polyunsaturated Fatty Acid Intake and Risk of Neurodevelopmental Impairment in Premature Infants. *Int J Mol Sci*. **23**(2), p.700.
Hegewald, M.J. and Crapo, R.O. 2011. Respiratory Physiology in Pregnancy. *Clinics in Chest Medicine*. **32**(1), pp.1–13.
Henriksen, T. and Clausen, T. 2008. The fetal origins hypothesis: Placental insufficiency and inheritance versus maternal malnutrition in well-nourished populations. *Acta Obstetricia et Gynecologica Scandinavica*. **81**(2), pp.112–114.
Hentschke, M.R., Poli-De-Figueiredo, C.E., Da Costa, B.E.P., Kurlak, L.O., Williams, P.J. and Mistry, H.D. 2013. Is the atherosclerotic phenotype of preeclamptic placentas due to altered lipoprotein concentrations and placental lipoprotein receptors? Role of a small-for-gestational-age phenotype. *Journal of Lipid Research*. **54**(10), pp.2658–2664.
Herrera, E. 2002. Implications of Dietary Fatty Acids During Pregnancy on Placental, Fetal and Postnatal Development — A Review. *Placenta*. **23**, pp.S9–S19.
Herrera, E. and Ortega-Senovilla, H. 2023. Dietary Implications of Polyunsaturated Fatty Acids during Pregnancy and in Neonates. *Life*. **13**(8).
Herse, F., Dechend, R., Harsem, N.K., Wallukat, G., Qadri, F., Hering, L., Muller, D.N., Luft, F.C. and Staff, A.C. 2007. Dysregulation of the Circulating and Tissue-Based Renin – Angiotensin System in Preeclampsia. *Hypertension*. **39**(3), pp.604–611.
Hibbeln, J.R., Davis, J.M., Steer, C., Emmett, P., Rogers, I., Williams, C. and Golding, J. 2007. Maternal seafood consumption in pregnancy and neurodevelopmental outcomes in childhood (ALSPAC study): an observational cohort study. *Lancet*. **369**(9561), pp.578–85.
Hillier, T.A., Pedula, K.L., Schmidt, M.M., Mullen, J.A., Charles, M.-A. and Pettitt, D.J. 2007. Childhood Obesity and Metabolic Imprinting: The ongoing effects of maternal hyperglycemia. *Diabetes Care*. **30**(9), pp.2287–2292.
Hinchliffe, S.A., Lynch, M.R.J., Sargent, P.H., Howard, C. V. and Van Velzen, D. 1992. The effect of intrauterine growth retardation on the development of renal nephrons. *BJOG: An International Journal of Obstetrics & Gynaecology*. **99**(4), pp.296–301.
Hjort, L., Martino, D., Grunnet, L.G., Naeem, H., Maksimovic, J., Olsson, A.H., Zhang, C., Ling, C., Olsen, S.F., Saffery, R. and Vaag, A.A. 2018. Gestational diabetes and maternal obesity are associated with epigenome-wide methylation changes in children. *JCI insight*. **3**(17), pp.1–14.
Hong, X., Zhang, B., Liang, L., Zhang, Y., Ji, Y., Wang, G., Ji, H., Clish, C.B., Burd, I., Pearson, C., Zuckerman, B., Hu, F.B. and Wang, X. 2020. Postpartum plasma metabolomic profile among women with preeclampsia and preterm delivery: Implications for long-term health. *BMC Medicine*. **18**(1), pp.1–12.
Horrocks, L.A. and Yeo, Y.K. 1999. Health benefits of docosahexaenoic acid (DHA). *Pharmacological Research*. **40**(3), pp.211–225.
Hou, G., Gao, Y., Poon, L.C., Ren, Y., Zeng, C., Wen, B., Syngelaki, A., Lin, L., Zi, J., Su, F., Xie, W., Chen, F. and Nicolaides, K.H. 2023. Maternal plasma diacylglycerols and triacylglycerols in the prediction of gestational diabetes mellitus. *BJOG: An International Journal of Obstetrics and Gynaecology*. **130**(3), pp.247–256.
Huda, S.S., Forrest, R., Paterson, N., Jordan, F., Sattar, N. and Freeman, D.J.

2014. In preeclampsia, maternal third trimester subcutaneous adipocyte lipolysis is more resistant to suppression by insulin than in healthy pregnancy. *Hypertension*. **63**(5), pp.1094–1101.

Huda, S.S., Jordan, F., Bray, J., Love, G., Payne, R., Sattar, N. and Freeman, D.J. 2017. Visceral adipose tissue activated macrophage content and inflammatory adipokine secretion is higher in pre-eclampsia than in healthy pregnancy. *Clinical Science*. **131**(13), pp.1529–1540.

Hulme, C.H., Nicolaou, A., Murphy, S.A., Heazell, A.E.P., Myers, J.E. and Westwood, M. 2019. The effect of high glucose on lipid metabolism in the human placenta. *Scientific Reports*. **9**(1), pp.1–9.

Inoue, T., Masuda, T. and Kishi, K. 1989. Structural and Functional Alterations of Mesenteric Vascular Beds in Spontaneously Hypertensive Rats. *Japanese Heart Journal*. **31**(3), pp.393–403.

Inzani, I. and Ozanne, S.E. 2022. Programming by maternal obesity: a pathway to poor cardiometabolic health in the offspring. *The Proceedings of the Nutrition Society*. **81**(3), pp.227–242.

Irani, R.A. and Xia, Y. 2011. Renin Angiotensin Signaling in Normal Pregnancy and Preeclampsia. *Seminars in Nephrology*. **31**(1), pp.47–58.

Iruretagoyena, J.I., Gonzalez-Tendero, A., Garcia-Canadilla, P., Amat-Roldan, I., Torre, I., Nadal, A., Crispi, F. and Gratacos, E. 2014. Cardiac dysfunction is associated with altered sarcomere ultrastructure in intrauterine growth restriction. *American Journal of Obstetrics and Gynecology*. **210**(6), 550.e1-550.e7.

Itabe, H., Yamaguchi, T., Nimura, S. and Sasabe, N. 2017. Perilipins: a diversity of intracellular lipid droplet proteins. *Lipids in Health and Disease*. **16**(1), pp.1–11.

Jarvie, E., Hauguel-de-Mouzon, S., Nelson, S.M., Sattar, N., Catalano, P.M. and Freeman, D.J. 2010. Lipotoxicity in obese pregnancy and its potential role in adverse pregnancy outcome and obesity in the offspring. *Clinical Science*. **119**(3), pp.123–129.

Jarvie, E.M., Stewart, F.M., Ramsay, J.E., Brown, E.A., Meyer, B.J., Olivecrona, G., Griffin, B.A. and Freeman, D.J. 2020. Maternal Adipose Tissue Expansion, A Missing Link in the Prediction of Birth Weight Centile. *Journal of Clinical Endocrinology and Metabolism*. **105**(3), pp.814–825.

John C. Hauth, MD, Rebecca G. Clifton, PhD, James M. Roberts, MD, Leslie Myatt, P., Catherine Y. Spong, MD, Kenneth J. Leveno, MD, Michael W. Varner, MD, R.J., Wapner, MD, John M. Thorp Jr., MD, Brian M. Mercer, MD, Alan M. Peaceman, MD, S., M. Ramin, MD, Marshall W. Carpenter, MD, Philip Samuels, MD, Anthony Sciscione, D., Jorge E. Tolosa, MD, MSCE, George Saade, MD, Yoram Sorokin, MD, and G.D. and Anderson 2011. Maternal Insulin Resistance and Preeclampsia. *Am J Obstet Gynecol*. **204**(4), pp.e1–e6.

Jönsson, J., Renault, K.M., García-Calzón, S., Perfilyev, A., Estampador, A.C., Nørgaard, K., Lind, M.V., Vaag, A., Hjort, L., Michaelsen, K.F., Carlsen, E.M., Franks, P.W. and Ling, C. 2021. Lifestyle Intervention in Pregnant Women With Obesity Impacts Cord Blood DNA Methylation, Which Associates With Body Composition in the Offspring. *Diabetes*. **70**(4), pp.854–866.

Joss-Moore, L.A., Wang, Y., Campbell, M.S., Moore, B., Yu, X., Callaway, C.W., McKnight, R.A., Desai, M., Moyer-Mileur, L.J. and Lane, R.H. 2010. Uteroplacental insufficiency increases visceral adiposity and visceral adipose PPARγ2 expression in male rat offspring prior to the onset of obesity. *Early Human Development*. **86**(3), pp.179–185.

Kallol, S. and Albrecht, C. 2020. Materno-fetal cholesterol transport during pregnancy. *Biochemical Society Transactions*. **48**(3), pp.775–786.

Kampmann, U., Knorr, S., Fuglsang, J. and Ovesen, P. 2019. Determinants of Maternal Insulin Resistance during Pregnancy: An Updated Overview. *Journal of Diabetes Research*. **2019**(Figure 1).

Karastergiou, K. and Fried, S.K. 2013. Multiple adipose depots increase cardiovascular risk via local and systemic effects topical collection on clinical trials and their interpretations. *Current Atherosclerosis Reports*. **15**(10), p.361.

Kasture, V., Dalvi, S., Swamy, M., Kale, A. and Joshi, S. 2020. Omega-3 fatty acids differentially influences embryotoxicity in subtypes of preeclampsia. *Clinical and Experimental Hypertension*. **42**(3), pp.205–212.

Katsi, V., Papakonstantinou, I.P., Papazachou, O., Makris, T. and Tsioufis, K. 2023. Beta-Blockers in Pregnancy: Clinical Update. *Current Hypertension Reports*. **25**(2), pp.13–24.

Kaufmann, P., Black, S. and Huppertz, B. 2003. Endovascular Trophoblast Invasion: Implications for the Pathogenesis of Intrauterine Growth Retardation and Preeclampsia. *Biology of reproduction*. **69**(December), pp.1–7.

Khong, T.Y., Wolf, F.D.E., Robertson, W.B., Brosens, I. and Robertson, W.B. 1986. Inadequate maternal vascular response to placentation in pregnancies complicated by pre-eclampsia and by small-for-gestational age infants. . **93**(October), pp.1049–1059.

Koh-Tan, H.H.C., McBride, M.W., McClure, J.D., Beattie, E., Young, B., Dominiczak, A.F. and Graham, D. 2013. Interaction between chromosome 2 and 3 regulates pulse pressure in the stroke-prone spontaneously hypertensive rat. *Hypertension*. **62**(1), pp.33–40.

Koren, G. and Pariente, G. 2018. Pregnancy- Associated Changes in Pharmacokinetics and their Clinical Implications. *Pharmaceutical Research*. **35**(3).

Koulouraki, S., Paschos, V., Pervanidou, P., Christopoulos, P., Gerede, A. and Eleftheriades, M. 2023. Short- and Long-Term Outcomes of Preeclampsia in Offspring: Review of the Literature. *Children (Basel)*. **10**(5), p.826.

Krahmer, N., Farese, R. V. and Walther, T.C. 2013. Balancing the fat: Lipid droplets and human disease. *EMBO Molecular Medicine*. **5**(7), pp.973–983.

Kramer, C.K., Campbell, S. and Retnakaran, R. 2019. Gestational diabetes and the risk of cardiovascular disease in women: a systematic review and meta-analysis. *Diabetologia*. **62**(6), pp.905–914.

Kuentzel, K.B., Bradić, I., Mihalič, Z.N., Korbelius, M., Rainer, S., Pirchheim, A., Kargl, J. and Kratky, D. 2022. Dysregulation of Placental Lipid Hydrolysis by High-Fat/High-Cholesterol Feeding and Gestational Diabetes Mellitus in Mice. *International Journal of Molecular Sciences*. **23**(20).

Kulkarni, A. V, Mehendale, S.S., Yadav, H.R., Kilari, A.S., Taralekar, V.S. and Joshi, S.R. 2010. Circulating angiogenic factors and their association with birth outcomes in preeclampsia. *Hypertension Research*. **33**(February), pp.561–567.

Kulvietis, V., Zalgeviciene, V., Didziapetriene, J. and Rotomskis, R. 2011. Transport of nanoparticles through the placental barrier. *Tohoku Journal of Experimental Medicine*. **225**(4), pp.225–234.

Kumashiro, N., Erion, D.M., Zhang, D., Kahn, M., Beddow, S.A., Chu, X., Still, C.D., Gerhard, G.S., Han, X., Dziura, J., Petersen, K.F., Samuel, V.T. and Shulman, G.I. 2011. Cellular mechanism of insulin resistance in nonalcoholic

fatty liver disease. *Proceedings of the National Academy of Sciences of the United States of America*. **108**(39), pp.16381–16385.

Kvehaugen, A.S., Dechend, R., Ramstad, H.B., Troisi, R., Fugelseth, D. and Staff, A.C. 2011. Endothelial function and circulating biomarkers are disturbed in women and children after preeclampsia. *Hypertension*. **58**(1), pp.63–69.

Lain, K.Y. and Catalano, P.M. 2007. Metabolic changes in pregnancy. *Clinical Obstetrics and Gynecology*. **50**(4), pp.938–948.

Laitinen, K. 2021. Fat Requirements in Pregnancy and Infancy *In*: *Fats and Associated Compounds: Consumption and Human Health.*, pp.1–27.

Laivuori, H., Gallaher, M.J., Collura, L., Crombleholme, W.R., Markovic, N., Rajakumar, A., Hubel, C.A., Roberts, J.M. and Powers, R.W. 2006. Relationships between maternal plasma leptin, placental leptin mRNA and protein in normal pregnancy, pre-eclampsia and intrauterine growth restriction without pre-eclampsia. *Molecular Human Reproduction*. **12**(9), pp.551–556.

Lamichhane, S., Ahonen, L., Dyrlund, T.S. and Kemppainen, E. 2018. Dynamics of Plasma Lipidome in Progression to Islet Autoimmunity and Type 1 Diabetes – Type 1 Diabetes Prediction and Prevention Study (DIPP). *Scientific Reports*. **8**(July), pp.1–12.

Lappas, M. 2014. Effect of pre-existing maternal obesity, gestational diabetes and adipokines on the expression of genes involved in lipid metabolism in adipose tissue. *Metabolism: Clinical and Experimental*. **63**(2), pp.250–262.

Lappas, M., Mundra, P.A., Wong, G., Huynh, K., Jinks, D., Georgiou, H.M., Permezel, M. and Meikle, P.J. 2015. The prediction of type 2 diabetes in women with previous gestational diabetes mellitus using lipidomics. *Diabetologia*. **58**(7), pp.1436–1442.

Lau, D.C.W. 2020. Central Role of Adipose Tissue in Pregnancy and Lactation *In*: *Maternal-Fetal and Neonatal Endocrinology* [Online]. Elsevier Inc., pp.147–158. Available from: http://dx.doi.org/10.1016/B978-0-12-814823-5.00011-8.

Lawlor, D.A., MacDonald-Wallis, C., Fraser, A., Nelson, S.M., Hingorani, A., Davey Smith, G., Sattar, N. and Deanfield, J. 2012. Cardiovascular biomarkers and vascular function during childhood in the offspring of mothers with hypertensive disorders of pregnancy: Findings from the Avon Longitudinal Study of Parents and Children. *European Heart Journal*. **33**(3), pp.335–345.

Lazdam, M., De La Horra, A., Pitcher, A., Mannie, Z., Diesch, J., Trevitt, C., Kylintireas, I., Contractor, H., Singhal, A., Lucas, A., Neubauer, S., Kharbanda, R., Alp, N., Kelly, B. and Leeson, P. 2010. Elevated blood pressure in offspring born premature to hypertensive pregnancy: Is endothelial dysfunction the underlying vascular mechanism? *Hypertension*. **56**(1), pp.159–165.

Lee, S.M., Kwak, S.H., Koo, J.N., Oh, I.H., Kwon, J.E., Kim, B.J., Kim, S.M., Kim, S.Y., Kim, G.M., Joo, S.K., Koo, B.K., Shin, S., Vixay, C., Norwitz, E.R., Park, C.W., Jun, J.K., Kim, W. and Park, J.S. 2019. Non-alcoholic fatty liver disease in the first trimester and subsequent development of gestational diabetes mellitus. *Diabetologia*. **62**(2), pp.238–248.

Lennestål, R. and Olausson, P.O. 2009. Maternal use of antihypertensive drugs in early pregnancy and delivery outcome , notably the presence of congenital heart defects in the infants. *Eur J Clin Pharmacol*. **65**, pp.615–625.

Leon, D.A., Koupilova, I., Lithell, H.O., Berglund, L., Mohsen, R., Vågerö, D.,

Lithell, U.B. and McKeigue, P.M. 1996. Failure to realise growth potential in utero and adult obesity in relation to blood pressure in 50 year old Swedish men. *British Medical Journal*. **312**(7028), pp.401–406.

Lewandowski, A.J., Augustine, D., Lamata, P., Davis, E.F., Lazdam, M., Francis, J., McCormick, K., Wilkinson, A.R., Singhal, A., Lucas, A., Smith, N.P., Neubauer, S. and Leeson, P. 2013. Preterm heart in adult life: Cardiovascular magnetic resonance reveals distinct differences in left ventricular mass, geometry, and function. *Circulation*. **127**(2), pp.197–206.

Lewis, R.M., Wadsack, C. and Desoye, G. 2018. Placental fatty acid transfer. *Current Opinion in Clinical Nutrition and Metabolic Care*. **21**(2), pp.78–82.

Lim, E.L., Hollingsworth, K.G. and Aribisala, B.S. 2011. Reversal of type 2 diabetes: normalisation of beta cell function in association with decreased pancreas and liver triacylglycerol. *Diabetologia*. **54**, pp.2506–2514.

Lin, I.C., Hsu, T.Y., Tain, Y.L., Tsai, C.C., Huang, H.C., Lai, Y.J., Chou, M.H., Huang, C.F., Yu, H.R. and Huang, L.T. 2021. Coronary Dilatation and Endothelial Inflammation in Neonates Born to Mothers with Preeclampsia. *Journal of Pediatrics*. **228**, pp.58-65.e3.

Lucas, A. 1991. Programming by early nutrition in man. *Ciba Found Symp*. **156**, pp.38–50.

MacKay, V.A., Huda, S.S., Stewart, F.M., Tham, K., McKenna, L.A., Martin, I., Jordan, F., Brown, E.A., Hodson, L., Greer, I.A., Meyer, B.J. and Freeman, D.J. 2012. Preeclampsia is associated with compromised maternal synthesis of long-chain polyunsaturated fatty acids, leading to offspring deficiency. *Hypertension*. **60**(4), pp.1078–1085.

Maeda, K., Uysal, K.T., Makowski, L., Görgün, C.Z., Atsumi, G., Parker, R.A., Brüning, J., Hertzel, A.V., Bernlohr, D.A. and Hotamisligil, G.S. 2003. Role of the fatty acid binding protein mal1 in obesity and insulin resistance. *Diabetes*. **52**(2), pp.300–307.

Magee, L.A., Smith, G.N., Bloch, C., Côté, A.-M., Jain, V., Nerenberg, K., Dadelszen, P. von, Helewa, M. and Rey, E. 2022. Guideline No. 426: Hypertensive Disorders of Pregnancy: Diagnosis, Prediction, Prevention, and Management. *SOGC Clinical Practice Guideline*. **44**(5), pp.547–571.

Magnusson-Olsson, A.L., Hamark, B., Ericsson, A., Wennergren, M., Jansson, T. and Powell, T.L. 2006. Gestational and hormonal regulation of human placental lipoprotein lipase. *Journal of Lipid Research*. **47**(11), pp.2551–2561.

Maltepe, E. and Fisher, S.J. 2015. Placenta: The Forgotten Organ. *Annual Review of Cell and Developmental Biology*. **31**, pp.523–552.

Maris, M.E., Melchert, R.B., Joseph, J. and Kennedy, R.H. 2005. Gender differences in blood pressure and heart rate in spontaneously hypertensive and Wistar-Kyoto rats. *Clinical and Experimental Pharmacology and Physiology*. **32**(1–2), pp.35–39.

Marseille-Tremblay, C., Ethier-Chiasson, M., Forest, J.C., Giguère, Y., Masse, A., Mounier, C. and Lafond, J. 2008. Impact of maternal circulating cholesterol and gestational diabetes mellitus on lipid metabolism in human term placenta. *Molecular Reproduction and Development*. **75**(6), pp.1054–1062.

Martin, H., Hu, J., Gennser, G. and Norman, M. 2000. Impaired endothelial function and increased carotid stiffness in 9-year-old children with low birthweight. *Circulation*. **102**(22), pp.2739–2744.

Martin, J.F., Johnston, C.S., Han, C.T. and Benyshek, D.C. 2000. Nutritional origins of insulin resistance: A rat model for diabetes- prone human populations. *Journal of Nutrition*. **130**(4), pp.741–744.

Marventano, S., Kolacz, P., Castellano, S., Galvano, F., Buscemi, S., Mistretta, A. and Grosso, G. 2015. A review of recent evidence in human studies of n-3 and n-6 PUFA intake on cardiovascular disease, cancer, and depressive disorders: Does the ratio really matter? *International Journal of Food Sciences and Nutrition*. **66**(6), pp.611–622.

Mary, S., Small, H., Herse, F., Carrick, E., Flynn, A., Mullen, W., Dechend, R. and Delles, C. 2021. Preexisting hypertension and pregnancy-induced hypertension reveal molecular differences in placental proteome in rodents. *Physiological Genomics*. **53**(6), pp.259–268.

Mathiowetz, A.J. and Olzmann, J.A. 2024. Lipid droplets and cellular lipid flux. *Nature Cell Biology*. **26**(3), pp.331–345.

McCarthy, F.P., Kingdom, J.C., Kenny, L.C. and Walsh, S.K. 2011. Animal models of preeclampsia; Uses and limitations. *Placenta*. **32**(6), pp.413–419.

McLaren, J., Gao, X., Ghouri, N., Freeman, D.J., Richardson, J., Sattar, N. and Gill, J.M.R. 2024. Weight gain leads to greater adverse metabolic responses in South Asian compared with white European men: the GlasVEGAS study. *Nature Metabolism*. **6**(8), pp.1632–1645.

McManaman, J.L., Bales, E.S., Orlicky, D.J., Jackman, M., MacLean, P.S., Cain, S., Crunk, A.E., Mansur, A., Graham, C.E., Bowman, T.A. and Greenberg, A.S. 2013. Perilipin-2-null mice are protected against diet-induced obesity, adipose infl ammation, and fatty liver disease. *Journal of Lipid Research*. **54**(5), pp.1346–1359.

Meyer, B.J., Cortie, C., Dekker-Nitert, M., Barrett, H.L. and Freeman, D.J. 2023. Women with gestational diabetes mellitus, controlled for plasma glucose level, exhibit maternal and fetal dyslipidaemia that may warrant treatment. *Diabetes Research and Clinical Practice*. **204**(July), p.110929.

Middleton, P., Jc, G., Jf, G., Shepherd, E., Sf, O., Makrides, M., Middleton, P., Jc, G., Jf, G., Shepherd, E., Sf, O. and Makrides, M. 2018. Omega-3 fatty acid addition during pregnancy =. *Cochrane Database Syst Rev*. **11**(11).

Mishima, T., Miner, J.H., Morizane, M., Stahl, A. and Sadovsky, Y. 2011. The expression and function of fatty acid transport protein-2 and -4 in the murine placenta. *PLoS ONE*. **6**(10), pp.1–8.

Molnár, M., Sütö, T., Tóth, T. and Hertelendy, F. 1994. Prolonged blockade of nitric oxide synthesis in gravid rats produces sustained hypertension, proteinuria, thrombocytopenia, and intrauterine growth retardation. *American Journal of Obstetrics and Gynecology*. **170**(5), pp.1458–1466.

Morgan, H.L., Butler, E., Ritchie, S., Herse, F., Dechend, R., Beattie, E., McBride, M.W. and Graham, D. 2018. Modeling superimposed preeclampsia using ang II (angiotensin II) infusion in pregnant stroke-prone spontaneously hypertensive rats. *Hypertension*. **72**(1), pp.208–218.

Moritz, K.M., Mazzuca, M.Q., Siebel, A.L., Mibus, A., Arena, D., Tare, M., Owens, J.A. and Wlodek, M.E. 2009. Uteroplacental insufficiency causes a nephron deficit, modest renal insufficiency but no hypertension with ageing in female rats. *Journal of Physiology*. **587**(11), pp.2635–2646.

Morris, M.J. and Chen, H. 2009. Established maternal obesity in the rat reprograms hypothalamic appetite regulators and leptin signaling at birth. *International Journal of Obesity*. **33**(1), pp.115–122.

Murata, M., Kodama, H., Goto, K., Hirano, H. and Tanaka, T. 1996. Decreased very-low-density lipoprotein and low-density lipoprotein receptor messenger ribonucleic acid expression in placentas from preeclamptic pregnancies. *American Journal of Obstetrics and Gynecology*. **175**(6), pp.1551–1556.

Nakshine, V.S. and Jogdand, S.D. 2023. A Comprehensive Review of Gestational

Diabetes Mellitus: Impacts on Maternal Health, Fetal Development, Childhood Outcomes, and Long-Term Treatment Strategies. *Cureus*. **15**(10).

Napoli, C., D'Armiento, F.P., Mancini, F.P., Postiglione, A., Witztum, J.L., Palumbo, G. and Palinski, W. 1997. Fatty streak formation occurs in human fetal aortas and is greatly enhanced maternal, hypercholesterolemia. Intimal accumulation of low density lipoprotein and its oxidation precede monocyte recruitment into early atheroeclerotic lesions. *Journal of Clinical Investigation*. **100**(11), pp.2680–2690.

National Institute for Health and Care Excellence 2015. Diabetes in pregnancy : management from preconception to the postnatal period. *NICe*. (February), pp.2–65.

Nikawa, J. ichi, Tanabe, T., Ogiwara, H., Shiba, T. and Numa, S. 1979. Inhibitory effects of long-chain acyl coenzyme a analogues on rat liver acetyl coenzyme a carboxylase. *FEBS Letters*. **102**(2), pp.223–226.

O'Brien, K. and Wang, Y. 2023. The Placenta: A Maternofetal Interface. *Annual Review of Nutrition*. **43**, pp.301–325.

Obermann-Borst, S.A., Vujkovic, M., De Vries, J.H., Wildhagen, M.F., Looman, C.W., De Jonge, R., Steegers, E.A.P. and Steegers-Theunissen, R.P.M. 2011. A maternal dietary pattern characterised by fish and seafood in association with the risk of congenital heart defects in the offspring. *BJOG: An International Journal of Obstetrics and Gynaecology*. **118**(10), pp.1205–1215.

Odigboegwu, O., Pan, L.J. and Chatterjee, P. 2018. Use of Antihypertensive Drugs During Preeclampsia. *Front Cardiovasc Med*. **5**(May), pp.1–4.

Ojeda, N.B., Grigore, D., Robertson, E.B. and Alexander, B.T. 2007. Estrogen protects against increased blood pressure in postpubertal female growth restricted offspring. *Hypertension*. **50**(4), pp.679–685.

Oken, E., Kleinman, K.P., Olsen, S.F., Rich-Edwards, J.W. and Gillman, M.W. 2004. Associations of seafood and elongated n-3 fatty acid intake with fetal growth and length of gestation: Results from a US pregnancy cohort. *American Journal of Epidemiology*. **160**(8), pp.774–783.

Olivera, S. and Graham, D. 2023. Sex differences in preclinical models of hypertension. *Journal of Human Hypertension*. **37**(8), pp.619–625.

Ong, K.K.L., Ahmed, M.L., Dunger, D.B., Emmett, P.M. and Preece, M.A. 2000. Association between postnatal catch-up growth and obesity in childhood: Prospective cohort study. *British Medical Journal*. **320**(7240), pp.967–971.

Oseini, A. and Sanyal, A.J. 2018. Therapies In Non-Alcoholic Steatohepatitis (Nash). *Liver Int*. **37**(Suppl 1), pp.97–103.

Painter, R.C., de Rooij, S.R., Bossuyt, P.M., Simmers, T.A., Osmond, C., Barker, D.J., Bleker, O.P. and Roseboom, T.J. 2006. Early onset of coronary artery disease after prenatal exposure to the Dutch famine. *The American Journal of Clinical Nutrition*. **84**(2), pp.322–327.

Palinski, W., Nicolaides, E., Liguori, A. and Napoli, C. 2009. Influence of maternal dysmetabolic conditions during pregnancy on cardiovascular disease. *Journal of Cardiovascular Translational Research*. **2**(3), pp.277–285.

Parker, R. 2018. The role of adipose tissue in fatty liver diseases. *Liver Research*. **2**(1), pp.35–42.

Patel, H.N., Miyoshi, T., Addetia, K., Henry, M.P., Citro, R., Daimon, M., Gutierrez Fajardo, P., Kasliwal, R.R., Kirkpatrick, J.N., Monaghan, M.J., Muraru, D., Ogunyankin, K.O., Park, S.W., Ronderos, R.E., Sadeghpour, A., Scalia, G.M., Takeuchi, M., Tsang, W., Tucay, E.S., Tude Rodrigues, A.C.,

Vivekanandan, A., Zhang, Y., Schreckenberg, M., Blankenhagen, M., Degel, M., Rossmanith, A., Mor-Avi, V., Asch, F.M., Lang, R.M., Prado, A.D., Filipini, E., Kwon, A., Hoschke-Edwards, S., Afonso, T.R., Thampinathan, B., Sooriyakanthan, M., Zhu, T., Wang, Z., Wang, Y., Yin, L., Li, S., Alagesan, R., Balasubramanian, S., Ananth, R.V.A., Bansal, M., Alizadehasl, A., Badano, L., Bossone, E., Di Vece, D., Bellino, M., Nakao, T., Kawata, T., Hirokawa, M., Sawada, N., Nabeshima, Y., Yun, H.R. and Hwang, J. won 2021. Normal Values of Cardiac Output and Stroke Volume According to Measurement Technique, Age, Sex, and Ethnicity: Results of the World Alliance of Societies of Echocardiography Study. *Journal of the American Society of Echocardiography*. **34**(10), pp.1077-1085.e1.

Pathmaperuma, A.N., Maña, P., Cheung, S.N., Kugathas, K., Josiah, A., Koina, M.E., Broomfield, A., Delghingaro-Augusto, V., Ellwood, D.A., Dahlstrom, J.E. and Nolan, C.J. 2010. Fatty acids alter glycerolipid metabolism and induce lipid droplet formation, syncytialisation and cytokine production in human trophoblasts with minimal glucose effect or interaction. *Placenta*. **31**(3), pp.230–239.

Patterson, A.J. and Zhang, L. 2010. Hypoxia and Fetal Heart Development. *Current Molecular Medicine*. **10**(7), pp.653–666.

Payne, J.A., Alexander, B.T. and Khalil, R.A. 2003. Reduced Endothelial Vascular Relaxation in Growth-Restricted Offspring of Pregnant Rats With Reduced Uterine Perfusion. *Hypertension*. **42**(4), pp.768–774.

Pedersen, J. 1955. Weight and Length at Birth of Infants of Diabetic Mothers. *Acta Endocrinologica*. **18**(4), pp.5–6.

Perry, R.J., Samuel, V.T., Petersen, K.F. and Shulman, G.I. 2014. The role of hepatic lipids in hepatic insulin resistance and type 2 diabetes. *Nature*. **510**(7503), pp.84–91.

Plows, J.F., Stanley, J.L., Baker, P.N., Reynolds, C.M. and Vickers, M.H. 2018. The pathophysiology of gestational diabetes mellitus. *International Journal of Molecular Sciences*. **19**(11), pp.1–21.

Poulsen, M.S., Rytting, E., Mose, T. and Knudsen, L.E. 2009. Modeling placental transport: Correlation of in vitro BeWo cell permeability and ex vivo human placental perfusion. *Toxicology in Vitro*. **23**(7), pp.1380–1386.

Prieto-Sánchez, M.T., Ruiz-Palacios, M., Blanco-Carnero, J.E., Pagan, A., Hellmuth, C., Uhl, O., Peissner, W., Ruiz-Alcaraz, A.J., Parrilla, J.J., Koletzko, B. and Larqué, E. 2017. Placental MFSD2a transporter is related to decreased DHA in cord blood of women with treated gestational diabetes. *Clinical Nutrition*. **36**(2), pp.513–521.

Primatesta, P., Falaschetti, E. and Poulter, N.R. 2005. Birth weight and blood pressure in childhood: Results from the health survey for England. *Hypertension*. **45**(1), pp.75–79.

Radaelli, T., Lepercq, J., Varastehpour, A., Basu, S., Catalano, P.M. and Hauguel-De Mouzon, S. 2009. Differential regulation of genes for fetoplacental lipid pathways in pregnancy with gestational and type 1 diabetes mellitus. *American Journal of Obstetrics and Gynecology*. **201**(2), 209.e1-209.e10.

Rahman, L., Anwar, R. and Mose, J.C. 2024. Hypertension in Pregnancy Maternal and neonatal outcome among women with early-onset preeclampsia and late-onset preeclampsia. *Hypertension in Pregnancy*. **43**(1).

Raijmakers, M.T.M., Dechend, R. and Poston, L. 2004. Oxidative stress and preeclampsia: Rationale for antioxidant clinical trials. *Hypertension*. **44**(4), pp.374–380.

Rajakumar, A., Kane, M.A., Yu, J., Taylor, R.N. and Sidell, N. 2020. Aberrant retinoic acid production in the decidua: Implications for pre-eclampsia. *J Obstet Gynaecol Res*. **46**(7), pp.1007–1016.

Ramlakhan, K.P., Johnson, M.R. and Roos-Hesselink, J.W. 2020. Pregnancy and cardiovascular disease. *Nature Reviews Cardiology*. **17**(November), pp.718–731.

Ramos, M.P., Crespo-Solans, M.D., Del Campo, S., Cacho, J. and Herrera, E. 2003. Fat accumulation in the rat during early pregnancy is modulated by enhanced insulin responsiveness. *American Journal of Physiology - Endocrinology and Metabolism*. **285**(2 48-2), pp.318–328.

Rani, A., Chavan-gautam, P., Mehendale, S., Wagh, G. and Joshi, S. 2015. Differential regional fatty acid distribution in normotensive and preeclampsia placenta. *BBACLI*. **4**, pp.21–26.

Ravelli, G.P., Stein, Z.A. and Susser, M.W. 1976. Obesity in Young Men after Famine Exposure in Utero and Early Infancy. *N Engl J Med*. **295**(7), pp.349–353.

Redman, C.W.G., Sacks, G.P. and Sargent, I.L. 1999. Preeclampsia: An excessive maternal inflammatory response to pregnancy. *American Journal of Obstetrics and Gynecology*. **180**(2 I), pp.499–506.

Reid, B.N., Ables, G.P., Otlivanchik, O.A., Schoiswohl, G., Zechner, R., Blaner, W.S., Goldberg, I.J., Schwabe, R.F., Chua, S.C. and Huang, L.S. 2008. Hepatic overexpression of hormone-sensitive lipase and adipose triglyceride lipase promotes fatty acid oxidation, stimulates direct release of free fatty acids, and ameliorates steatosis. *Journal of Biological Chemistry*. **283**(19), pp.13087–13099.

Reister, F., Frank, H.G., Heyl, W., Kosanke, G., Huppertz, B., Schröder, W., Kaufmann, P. and Rath, W. 1999. The distribution of macrophages in spiral arteries of the placental bed in pre-eclampsia differs from that in healthy patients. *Placenta*. **20**(2–3), pp.229–233.

Resi, V., Basu, S., Haghiac, M., Presley, L., Minium, J., Kaufman, B., Bernard, S., Catalano, P. and Hauguel-de Mouzon, S. 2012. Molecular inflammation and adipose tissue matrix remodeling precede physiological adaptations to pregnancy. *American Journal of Physiology - Endocrinology and Metabolism*. **303**(7), pp.832–840.

Reynolds, I., II, R.L.P. and Boxer, R.S. 2019. Cardiovascular health and healthy aging *In*: *Coll, P. (eds) Healthy Aging.*, pp.31–51.

Rizi, S.S., Wiens, E., Hunt, J. and Ducas, R. 2024. Cardiac physiology and pathophysiology in pregnancy. *Canadian Journal of Physiology and Pharmacology*. **571**, pp.552–571.

Rizzo, T., Boyd E. Metzger, Burns, W.J. and Burns, K. 1991. Correlations between Antepartum Maternal Metabolism and Intelligence of Offspring. *The New England Journal of Medicine*. **325**(13).

Rizzoni, D., Castellano, M., Porteri, E., Bettoni, G., Muiesan, M.L. and Agabiti-Rosei, E. 1994. Vascular structural and functional alterations before and after the development of hypertension in shr. *American Journal of Hypertension*. **7**(2), pp.193–200.

Rodie, V.A., Caslake, M.J., Stewart, F., Sattar, N., Ramsay, J.E., Greer, I.A. and Freeman, D.J. 2004. Fetal cord plasma lipoprotein status in uncomplicated human pregnancies and in pregnancies complicated by pre-eclampsia and intrauterine growth restriction. *Atherosclerosis*. **176**(1), pp.181–187.

Rodie, V.A., Young, A., Sattar, N., Greer, A. and Freeman, D.J. 2005. Proliferator-Activated Receptor 0 and ’ Y Expression in Healthy Pregnancy

and in Preeclampsia and Intrauterine Growth Restriction. *The Journal of the Society for Gynecologic Investigation: JSGI*. **12**, pp.320–329.

Rodriguez-Lopez, M., Osorio, L., Acosta-Rojas, R., Figueras, J., Cruz-Lemini, M., Figueras, F., Bijnens, B., Gratacós, E. and Crispi, F. 2016. Influence of breastfeeding and postnatal nutrition on cardiovascular remodeling induced by fetal growth restriction. *Pediatric Research*. **79**(1), pp.100–106.

Rodríguez-Rodríguez, P., de Pablo, A.L.L., Condezo-Hoyos, L., Martín-Cabrejas, M.A., Aguilera, Y., Ruiz-Hurtado, G., Gutierrez-Arzapalo, P.Y., Ramiro-Cortijo, D., Fernández-Alfonso, M.S., González, M. del C. and Arribas, S.M. 2015. Fetal undernutrition is associated with perinatal sex-dependent alterations in oxidative status. *Journal of Nutritional Biochemistry*. **26**(12), pp.1650–1659.

Rodríguez-Rodríguez, P., Ramiro-Cortijo, D., Reyes-Hernández, C.G., López de Pablo, A.L., Carmen González, M. and Arribas, S.M. 2018. Implication of oxidative stress in fetal programming of cardiovascular disease. *Frontiers in Physiology*. **9**(MAY), pp.1–13.

Rong, S., Xia, M., Vale, G., Wang, S., Kim, C.W., Li, S., McDonald, J.G., Radhakrishnan, A. and Horton, J.D. 2024. DGAT2 inhibition blocks SREBP-1 cleavage and improves hepatic steatosis by increasing phosphatidylethanolamine in the ER. *Cell Metabolism*. **36**(3), pp.617-629.e7.

Roseboom, T., de Rooij, S. and Painter, R. 2006. The Dutch famine and its long-term consequences for adult health. *Early Human Development*. **82**(8), pp.485–491.

Roth, G.A., Mensah, G.A., Johnson, C.O., Addolorato, G., Ammirati, E., Baddour, L.M., Barengo, N.C., Beaton, A.Z., Benjamin, E.J., Benziger, C.P., Bonny, A., Brauer, M., Brodmann, M., Cahill, T.J. and Fuster, V. 2020. Global Burden of Cardiovascular Diseases. *JACC*. **76**(25), pp.2982–3021.

Rueda-Clausen, C.F., Dolinsky, V.W., Morton, J.S., Proctor, S.D., Dyck, J.R.B. and Davidge, S.T. 2011. Hypoxia-induced intrauterine growth restriction increases the susceptibility of rats to high-fat diet-induced metabolic syndrome. *Diabetes*. **60**(2), pp.507–516.

Rueda-Clausen, C.F., Morton, J.S. and Davidge, S.T. 2009. Effects of hypoxia-induced intrauterine growth restriction on cardiopulmonary structure and function during adulthood. *Cardiovascular Research*. **81**(4), pp.713–722.

Ryckman, K.K., Spracklen, C.N., Smith, C.J., Robinson, J.G. and Saftlas, A.F. 2015. Maternal lipid levels during pregnancy and gestational diabetes: A systematic review and meta-analysis. *BJOG: An International Journal of Obstetrics and Gynaecology*. **122**(5), pp.643–651.

Sandra Schlafke, A.C.E. 1975. Cellular Trophoblast Basis of Interaction Uterus Implantation. *Biology of Reproduction*. **65**, pp.41–65.

Sanghavi, M., Rutherford, J.D. and Chb, M.B. 2014. Cardiovascular Physiology of Pregnancy. *Circulation*. **130**(12), pp.1003–1008.

Sarr, O., Yang, K. and Regnault, T.R.H. 2012. In utero programming of later adiposity: The role of fetal growth restriction. *Journal of Pregnancy*. **2012**.

Sattar, N. and Freeman, D.J. 2012. Potential mechanisms contributing to gestational diabetes and pre-eclampsia in the obese woman *In*: *Maternal Obesity*. Cambridge University Press, pp.45–55.

Sattar, N. and Greer, I.A. 1999. Lipids and the pathogenesis of pre-eclampsia. *Current Obstetrics and Gynaecology*. **9**(4), pp.190–195.

Sattar, N., Petrie, J.R. and Jaap, A.J. 1998. The atherogenic lipoprotein phenotype and vascular endothelial dysfunction. *Atherosclerosis*. **138**(2),

pp.229–235.
Saunders, M. 2009. Transplacental transport of nanomaterials. *Wiley Interdisciplinary Reviews: Nanomedicine and Nanobiotechnology*. **1**(6), pp.671–684.
Schaefer-Graf, U.M., Graf, K., Kulbacka, I., Kjos, S.L., Dudenhausen, J., Vetter, K. and Herrera, E. 2008. Maternal lipids as strong determinants of fetal environment and growth in pregnancies with gestational diabetes mellitus. *Diabetes Care*. **31**(9), pp.1858–1863.
Scheidl, T.B., Brightwell, A.L., Easson, S.H. and Thompson, J.A. 2023. Maternal obesity and programming of metabolic syndrome in the offspring: searching for mechanisms in the adipocyte progenitor pool. *BMC Medicine*. **21**(1), pp.1–13.
Schonkeren, D., Van Der Hoorn, M.L., Khedoe, P., Swings, G., Van Beelen, E., Claas, F., Van Kooten, C., De Heer, E. and Scherjon, S. 2011. Differential distribution and phenotype of decidual macrophages in preeclamptic versus control pregnancies. *American Journal of Pathology*. **178**(2), pp.709–717.
Scott, K., Morgan, H.L., Delles, C., Fisher, S., Graham, D. and McBride, M.W. 2021. Distinct uterine artery gene expression profiles during early gestation in the stroke-prone spontaneously hypertensive rat. *Physiological Genomics*. **53**(4), pp.160–171.
Seebacher, F., Zeigerer, A., Kory, N. and Krahmer, N. 2020. Hepatic lipid droplet homeostasis and fatty liver disease. *Seminars in Cell and Developmental Biology*. **108**(April), pp.72–81.
Segura, M.T., Demmelmair, H., Krauss-Etschmann, S., Nathan, P., Dehmel, S., Padilla, M.C., Rueda, R., Koletzko, B. and Campoy, C. 2017. Maternal BMI and gestational diabetes alter placental lipid transporters and fatty acid composition. *Placenta*. **57**, pp.144–151.
Selivanova, E.K., Shvetsova, A.A., Shilova, L.D., Tarasova, O.S. and Gaynullina, D.K. 2021. Intrauterine growth restriction weakens anticontractile influence of NO in coronary arteries of adult rats. *Scientific Reports*. **11**(1), pp.1–11.
Shah, D.M. 2005. Role of the renin-angiotensin system in the pathogenesis of preeclampsia. *American Journal of Renal Physiology*. **288**, pp.614–625.
Sharkey, L.C., McCune, S.A., Yuan, O., Lange, C. and Fray, J. 2001. Spontaneous pregnancy-induced hypertension and intrauterine growth restriction in rats. *American Journal of Hypertension*. **14**(10), pp.1058–1066.
Shoelson, S.E., Herrero, L. and Naaz, A. 2007. Obesity, Inflammation, and Insulin Resistance. *Gastroenterology*. **132**(6), pp.2169–2180.
Silverman, B.L., Metzger, B.E., Cho, N.H. and Loeb, C.A. 1995. Impaired Glucose Tolerance in Adolescent Offspring of Diabetic Mothers. *Diabetes Care*. **18**(5), pp.611–617.
Sivan, E. and Boden, G. 2003. Free Fatty Acids, Insulin Resistance, and Pregnancy. *Curr Diab Rep*. **3**, pp.319–322.
Skilton, M.R., Ayer, J.G., Harmer, J.A., Webb, K., Leeder, S.R., Marks, G.B. and Celermajer, D.S. 2012. Impaired fetal growth and arterial wall thickening: A randomized trial of omega-3 supplementation. *Pediatrics*. **129**(3), pp.e698–e703.
Skilton, M.R. and Phang, M. 2016. From the α to the ω-3: Breaking the link between impaired fetal growth and adult cardiovascular disease. *Nutrition*. **32**(7–8), pp.725–731.
Słupecka-Ziemilska, M., Wychowański, P. and Puzianowska-Kuznicka, M. 2020. Gestational Diabetes Mellitus Affects Offspring's Epigenome. Is There a Way to Reduce the Negative Consequences? *Nutrients*. **12**(9), p.2792.

Small, H.Y., Morgan, H., Beattie, E., Griffin, S., Indahl, M., Delles, C. and Graham, D. 2016. Abnormal uterine artery remodelling in the stroke prone spontaneously hypertensive rat. *Placenta*. **37**, pp.34–44.

Soares M.J. and Hunt, J.S. 2006. Reduced Uterine Perfusion Pressure (RUPP) Model for Studying Cardiovascular-Renal Dysfunction in Response to Placental Ischemia *In*: *Placenta and Trophoblast. Methods in Molecular Medicine™.*, pp.383–393.

Soares, M.J., Iqbal, K. and Kozai, K. 2017. Hypoxia and Placental Development. *Birth Defects Research*. **109**(17), pp.1309–1329.

Soares, M.J., Varberg, K.M. and Iqbal, K. 2018. Hemochorial placentation: Development, function, and adaptations. *Biology of Reproduction*. **99**(1), pp.196–211.

Soma-Pillay, P., Nelson-Piercy, C., Tolppanen, H. and Mebazaa, A. 2016. Physiological changes in pregnancy. *Cardiovascular Journal of Africa*. **27**(2), pp.89–94.

Stadler, J.T., Scharnagl, H., Wadsack, C. and Marsche, G. 2023. Preeclampsia Affects Lipid Metabolism and HDL Function in Mothers and Their Offspring. *Antioxidants*. **12**(4), p.795.

Staley, J.R., Bradley, J., Silverwood, R.J., Howe, L.D., Tilling, K., Lawlor, D.A. and Macdonald-Wallis, C. 2015. Associations of blood pressure in pregnancy with offspring blood pressure trajectories during childhood and adolescence: findings from a prospective study. *Journal of the American Heart Association*. **4**(5), pp.1–12.

Stirm, L., Kovářová, M., Perschbacher, S., Michlmaier, R., Fritsche, L., Siegel-Axel, D., Schleicher, E., Peter, A., Pauluschke-Fröhlich, J., Brucker, S., Abele, H., Wallwiener, D., Preissl, H., Wadsack, C., Häring, H.U., Fritsche, A., Ensenauer, R., Desoye, G. and Staiger, H. 2018. BMI-Independent Effects of Gestational Diabetes on Human Placenta. *Journal of Clinical Endocrinology and Metabolism*. **103**(9), pp.3299–3309.

Storch, J. and McDermott, L. 2009. Structural and functional analysis of fatty acid-binding proteins. *Journal of Lipid Research*. **50**(SUPPL.), pp.S126–S131.

Sun, M. na, Yang, Z. and Ma, R. qiong 2012. Effect of high-fat diet on liver and placenta fatty infiltration in early onset preeclampsia-like mouse model. *Chinese Medical Journal*. **125**(19), pp.3532–3538.

Sun, Y., Kopp, S., Strutz, J., Gali, C.C., Zandl-Lang, M., Fanaee-Danesh, E., Kirsch, A., Cvitic, S., Frank, S., Saffery, R., Björkhem, I., Desoye, G., Wadsack, C. and Panzenboeck, U. 2018. Gestational diabetes mellitus modulates cholesterol homeostasis in human fetoplacental endothelium. *Biochimica et Biophysica Acta - Molecular and Cell Biology of Lipids*. **1863**(9), pp.968–979.

Sutton, E.F., Lob, H.E., Song, J., Xia, Y.W., Butler, S., Liu, C.C., Redman, L.M. and Sones, J.L. 2017. Adverse metabolic phenotype of female offspring exposed to preeclampsia in utero: A characterization of the BPH/5 mouse in postnatal life. *American Journal of Physiology - Regulatory Integrative and Comparative Physiology*. **312**(4), pp.R485–R491.

Swislocki, A. and Tsuzuki, A. 1993. Insulin resistance and hypertension: Glucose intolerance, hyperinsulinemia, and elevated free fatty acids in the lean spontaneously hypertensive rat. *American Journal of the Medical Sciences*. **306**(5), pp.282–286.

Szabo, A.J. and Szabo, O. 1974. Placental Free-Fatty-Acid Transfer and Fetal Adipose-Tissue Development: an Explanation of Fetal Adiposity in Infants of Diabetic Mothers. *The Lancet*. **304**(7879), pp.498–499.

Tada, Y., Kagota, S., Matsumoto, M., Naito, Y., Shibata, H., Nejime, N., Tsujino, T., Koshiba, M., Masuyama, T. and Shinozuka, K. 2010. Characterization of cardiac size and function in SHRSP.Z-Lepr fa/ izmDmcr rats, a new animal model of metabolic syndrome. *Biological and Pharmaceutical Bulletin*. **33**(12), pp.1971–1976.

Talton, O.O., Bates, K., Salazar, S.R., Ji, T. and Schulz, L.C. 2019. Lean maternal hyperglycemia alters offspring lipid metabolism and susceptibility to diet-induced obesity in mice. *Biology of Reproduction*. **100**(5), pp.1356–1369.

Tan, C.M.J. and Lewandowski, A.J. 2020. The Transitional Heart: From Early Embryonic and Fetal Development to Neonatal Life. *Fetal Diagnosis and Therapy*. **47**(5), pp.373–386.

Tanner, M.S., Malhotra, A., Davey, M.A., Wallace, E.M., Mol, B.W. and Palmer, K.R. 2022. Maternal and neonatal complications in women with medical comorbidities and preeclampsia. *Pregnancy Hypertension*. **27**(February 2021), pp.62–68.

Tchkonia, T., Tchoukalova, Y.D., Giorgadze, N., Pirtskhalava, T., Karagiannides, I., Forse, R.A., Koo, A., Stevenson, M., Chinnappan, D., Cartwright, A., Jensen, M.D. and Kirkland, J.L. 2005. Abundance of two human preadipocyte subtypes with distinct capacities for replication, adipogenesis, and apoptosis varies among fat depots. *American Journal of Physiology - Endocrinology and Metabolism*. **288**(1 51-1), pp.267–277.

Tenhola, S., Rahiala, E., Martikainen, A., Halonen, P. and Voutilainen, R. 2003. Blood pressure, serum lipids, fasting insulin, and adrenal hormones in 12-year-old children born with maternal preeclampsia. *Journal of Clinical Endocrinology and Metabolism*. **88**(3), pp.1217–1222.

Terstappen, F., Spradley, F.T., Bakrania, B.A., Clarke, S.M., Joles, J.A., Paauw, N.D., Garrett, M.R., Lely, A.T. and Sasser, J.M. 2019. Prenatal sildenafil therapy improves cardiovascular function in fetal growth restricted offspring of dahl salt-sensitive rats. *Hypertension*. **73**(5), pp.1120–1127.

Thomas, B., Ghebremeskel, K., Lowy, C., Min, Y. and Crawford, M.A. 2004. Plasma AA and DHA levels are not compromised in newly diagnosed gestational diabetic women. *European Journal of Clinical Nutrition*. **58**(11), pp.1492–1497.

Thomas, B.A., Ghebremeskel, K., Lowy, C., Offley-Shore, B. and Crawford, M.A. 2005. Plasma fatty acids of neonates born to mothers with and without gestational diabetes. *Prostaglandins Leukotrienes and Essential Fatty Acids*. **72**(5), pp.335–341.

Timpka, S., Macdonald-Wallis, C., Hughes, A.D., Chaturvedi, N., Franks, P.W., Lawlor, D.A. and Fraser, A. 2016. Hypertensive disorders of pregnancy and offspring cardiac structure and function in adolescence. *Journal of the American Heart Association*. **5**(11).

Tobi, E.W., Lumey, L.H., Talens, R.P., Kremer, D., Putter, H., Stein, A.D., Slagboom, P.E. and Heijmans, B.T. 2009. DNA methylation differences after exposure to prenatal famine are common and timing- and sex-specific. *Human Molecular Genetics*. **18**(21), pp.4046–4053.

Tobin, K.A.R., Johnsen, G.M., Staff, A.C. and Duttaroy, A.K. 2009. Long-chain Polyunsaturated Fatty Acid Transport across Human Placental Choriocarcinoma (BeWo) Cells. *Placenta*. **30**(1), pp.41–47.

Toufaily, C., Vargas, A., Lemire, M., Lafond, J., Rassart, É. and Barbeau, B. 2013. MFSD2a, the Syncytin-2 receptor, is important for trophoblast fusion. *Placenta*. **34**(1), pp.85–88.

Tracy, R.E. and Walia, P. 2002. A method to fix lipids for staining fat embolism in paraffin sections. *Histopathology*. **41**(1), pp.75–79.

Trivett, C., Lees, Z.J. and Freeman, D.J. 2021. Adipose tissue function in healthy pregnancy, gestational diabetes mellitus and pre-eclampsia. *European Journal of Clinical Nutrition*. **75**, pp.1745–1756.

True, H., Blanton, M., Sureshchandra, S. and Messaoudi, I. 2022. Monocytes and Macrophages in Pregnancy: The Good, the Bad, and the Ugly. *Immunol Rev*. **308**(1), pp.77–92.

Uhl, O., Demmelmair, H., Segura, M.T., Florido, J., Rueda, R., Campoy, C. and Koletzko, B. 2015. Effects of obesity and gestational diabetes mellitus on placental phospholipids. *Diabetes Research and Clinical Practice*. **109**(2), pp.364–371.

Umhau, J.C., Dauphinais, K.M., Patel, S.H., Nahrwold, D.A., Hibbeln, J.R., Rawlings, R.R. and George, D.T. 2006. The relationship between folate and docosahexaenoic acid in men. *European Journal of Clinical Nutrition*. **60**(3), pp.352–357.

Varastehpour, A., Radaelli, T., Minium, J., Ortega, H., Herrera, E., Catalano, P. and Hauguel-de Mouzon, S. 2006. Activation of phospholipase A2 is associated with generation of placental lipid signals and fetal obesity. *Journal of Clinical Endocrinology and Metabolism*. **91**(1), pp.248–255.

Lo Vasco, V.R., Salmaso, R., Zanardo, V., Businaro, R., Visentin, S., Trevisanuto, D. and Cosmi, E. 2011. Fetal aorta wall inflammation in ultrasound-detected aortic intima/media thickness and growth retardation. *Journal of Reproductive Immunology*. **91**(1–2), pp.103–107.

Veerbeek, J.H.W., Hermes, W., Breimer, A.Y., Rijn, B.B. Van, Koenen, S. V, Mol, B.W., Franx, A., Groot, C.J.M. De and Koster, M.P.H. 2015. Cardiovascular disease risk factors after early-onset preeclampsia, late-onset preeclampsia, and pregnancy-induced hypertension. *Hypertension*. **65**(3), pp.600–606.

Videla, L.A., Rodrigo, R., Araya, J. and Poniachik, J. 2004. Oxidative stress and depletion of hepatic long-chain polyunsaturated fatty acids may contribute to nonalcoholic fatty liver disease. *Free Radical Biology and Medicine*. **37**(9), pp.1499–1507.

Visiedo, F., Bugatto, F., Sánchez, V., Cózar-Castellano, I., Bartha, J.L. and Perdomo, G. 2013. High glucose levels reduce fatty acid oxidation and increase triglyceride accumulation in human placenta. *American Journal of Physiology - Endocrinology and Metabolism*. **305**(2), pp.205–212.

Wadhwani, N., Patil, V., Pisal, H., Joshi, A., Mehendale, S., Gupte, S., Wagh, G. and Joshi, S. 2014. Altered maternal proportions of long chain polyunsaturated fatty acids and their transport leads to disturbed fetal stores in preeclampsia. *Prostaglandins Leukotrienes and Essential Fatty Acids*. **91**(1–2), pp.21–30.

Wang, H., Li, N., Chivese, T., Werfalli, M., Sun, H., Yuen, L., Ambrosius, C., Elise, C. and Immanuel, J. 2022. IDF Diabetes Atlas : Estimation of Global and Regional Gestational Diabetes Mellitus Prevalence for 2021 by International Association of Diabetes in Pregnancy Study Group ' s Criteria. *Diabetes Research and Clinical Practice*. **183**, p.109050.

Wang, Y. and Walsh, S.W. 1996. TNFα concentrations and mRNA expression are increased in preeclamptic placentas. *Journal of Reproductive Immunology*. **32**(2), pp.157–169.

Waterland, R.A. and Jirtle, R.L. 2003. Transposable Elements: Targets for Early Nutritional Effects on Epigenetic Gene Regulation. *Molecular and Cellular Biology*. **23**(15), pp.5293–5300.

Watkins, S.M., Zhu, X. and Zeisel, S.H. 2003. Phosphatidylethanolamine-N-methyltransferase Activity and Dietary Choline Regulate Liver-Plasma Lipid Flux and Essential Fatty Acid Metabolism in Mice. *Journal of Nutrition*. **133**(11), pp.3386–3391.

Wehrens, R., Hageman, J.A., van Eeuwijk, F., Kooke, R., Flood, P.J., Wijnker, E., Keurentjes, J.J.B., Lommen, A., van Eekelen, H.D.L.M., Hall, R.D., Mumm, R. and de Vos, R.C.H. 2016. Improved batch correction in untargeted MS-based metabolomics. *Metabolomics*. **12**(5).

West, C.A. 2023. Late Pregnant Dahl Salt-Sensitive Rats from Charles River Laboratories Do Not Exhibit Superimposed Preeclampsia. *Reproductive Sciences*. **30**(8), pp.2580–2583.

West, R.C., Ming, H., Logsdon, D.M., Sun, J., Rajput, S.K., Kile, R.A., Schoolcraft, W.B., Roberts, R.M., Krisher, R.L., Jiang, Z. and Yuan, Y. 2019. Dynamics of trophoblast differentiation in peri- implantation – stage human embryos. *PNAS*. **116**(45), pp.22635–22644.

West, R.M. 2022. Best practice in statistics: The use of log transformation. *Annals of Clinical Biochemistry*. **59**(3), pp.162–165.

Wice, B., Menton, D., Geuze, H. and Schwartz, A.L. 1990. Modulators of cyclic AMP metabolism induce syncytiotrophoblast formation in vitro. *Experimental Cell Research*. **186**(2), pp.306–316.

Wijendran, V., Bendel, R.B., Couch, S.C., Philipson, E.H., Cheruku, S. and Lammi-Keefe, C.J. 2000. Fetal erythrocyte phospholipid polyunsaturated fatty acids are altered in pregnancy complicated with gestational diabetes mellitus. *Lipids*. **35**(8), pp.927–931.

Wijendran, V., Bendel, R.B., Couch, S.C., Philipson, E.H., Thomsen, K., Zhang, X. and Lammi-Keefe, C.J. 1999. Maternal plasma phospholipid polyunsaturated fatty acids in pregnancy with and without gestational diabetes mellitus: Relations with maternal factors. *American Journal of Clinical Nutrition*. **70**(1), pp.53–61.

Wilson, P.N. and Osbourn, D.F. 1960. Compensatory Growth After Undernutrition in Mammals and Birds. *Biological Reviews*. **35**(3), pp.324–361.

Winden, T.M.S. Van, Nijman, T.A.J., Kleinrouweler, C.E., Salim, R., Kashanian, M., Omari, W.R. Al, Pajkrt, E., Mol, B.W., Oudijk, M.A. and Roos, C. 2022. Tocolysis with nifedipine versus atosiban and perinatal outcome : an individual participant data meta - analysis. *BMC Pregnancy and Childbirth*., pp.1–10.

Wlodek, M.E., Westcott, K., Siebel, A.L., Owens, J.A. and Moritz, K.M. 2008. Growth restriction before or after birth reduces nephron number and increases blood pressure in male rats. *Kidney International*. **74**(2), pp.187–195.

Wojczakowski, W., Kimber-Trojnar, Ż., Dziwisz, F., Słodzińska, M., Słodziński, H. and Leszczyńska-Gorzelak, B. 2021. Preeclampsia and cardiovascular risk for offspring. *Journal of Clinical Medicine*. **10**(14), pp.1–17.

Wong, M.K., Li, E.W., Adam, M., Selvaganapathy, P.R. and Raha, S. 2020. Establishment of an in vitro placental barrier model cultured under physiologically relevant oxygen levels. *Molecular Human Reproduction*. **26**(5), pp.353–365.

Woollett, L.A. 2011. Transport of maternal cholesterol to the fetal circulation. *Placenta*. **32**, pp.S218–S221.

Xu, X., So, J.S., Park, J.G. and Lee, A.H. 2013. Transcriptional control of hepatic lipid metabolism by SREBP and ChREBP. *Seminars in Liver Disease*. **33**(4), pp.301–311.

Yallampalli, C. and Garfield, R.E. 1993. Inhibition of nitric oxide synthesis in rats during pregnancy produces signs similar to those of preeclampsia. *American Journal of Obstetrics and Gynecology*. **169**(5), pp.1316–1320.

Yamori, Y. and Horie, R. 1977. Developmental course of hypertension and regional cerebral blood flow in stroke-prone spontaneously hypertensive rats. *Stroke*. **8**(4), pp.456–461.

Yan, Y., Peng, H., Wang, P., Wang, H. and Dong, M. 2016. Increased expression of fatty acid binding protein 4 in preeclamptic Placenta and its relevance to preeclampsia. *Placenta*. **39**, pp.94–100.

Yañez, M.J. and Leiva, A. 2022. Human Placental Intracellular Cholesterol Transport: A Focus on Lysosomal and Mitochondrial Dysfunction and Oxidative Stress. *Antioxidants*. **11**(3).

Yang, C., Baker, P.N., Granger, J.P., Davidge, S.T. and Tong, C. 2023. Long-Term Impacts of Preeclampsia on the Cardiovascular System of Mother and Offspring. *Hypertension*. **80**(9), pp.1821–1833.

Yang, Y., Pan, Z., Guo, F., Wang, Huihui, Long, W., Wang, Huiyan and Yu, B. 2021. Placental metabolic profiling in gestational diabetes mellitus: An important role of fatty acids. *Journal of Clinical Laboratory Analysis*. **35**(12), pp.1–10.

Yeung, D.C.Y., Wang, Y., Xu, A., Cheung, S.C.W., Wat, N.M.S., Fong, D.Y.T., Fong, C.H.Y., Chau, M.T., Sham, P.C. and Lam, K.S.L. 2008. Epidermal fatty-acid-binding protein: A new circulating biomarker associated with cardio-metabolic risk factors and carotid atherosclerosis. *European Heart Journal*. **29**(17), pp.2156–2163.

Yogev, Y., Xenakis, E.M.J. and Langer, O. 2004. The association between preeclampsia and the severity of gestational diabetes: The impact of glycemic control. *American Journal of Obstetrics and Gynecology*. **191**(5), pp.1655–1660.

Yu, S., Levi, L., Siegel, R. and Noy, N. 2012. Retinoic acid induces neurogenesis by activating both retinoic acid receptors (RARs) and peroxisome proliferator-activated receptor β/δ (PPARβ/δ). *Journal of Biological Chemistry*. **287**(50), pp.42195–42205.

Zadoorian, A., Du, X. and Yang, H. 2023. Lipid droplet biogenesis and functions in health and disease. *Nature Reviews Endocrinology*. **19**(8), pp.443–459.

Zhang, L., Bi, S., Liang, Y., Huang, L., Li, Y., Huang, M., Huang, B., Deng, W., Liang, J., Gu, S., Chen, J., Du, L., Chen, D. and Wang, Z. 2022. Integrated Metabolomic and Lipidomic Analysis in the Placenta of Preeclampsia. *Frontiers in Physiology*. **13**(February), pp.1–11.

Zhao, J., Zheng, D.Y., Yang, J.M., Wang, M., Zhang, X.T., Sun, L. and Yun, X.G. 2016. Maternal serum uric acid concentration is associated with the expression of tumour necrosis factor-α and intercellular adhesion molecule-1 in patients with preeclampsia. *Journal of Human Hypertension*. **30**(7), pp.456–462.

Zhu, Z., Chen, X., Xiao, Y., Wen, J., Chen, J., Wang, K. and Chen, G. 2019. Gestational diabetes mellitus alters DNA methylation profiles in pancreas of the offspring mice. *Journal of Diabetes and its Complications*. **33**(1), pp.15–22.